SAND2019-11476R

# Sandia SWiFT V27 Wind Turbine Dynamic Characterization

Timothy Marinone, David Cloutier
ATA Engineering, Inc.

September 2019

Sandia National Laboratories is a multimission laboratory managed and operated by National Technology and Engineering Solutions of Sandia, LLC, a wholly owned subsidiary of Honeywell International Inc., for the U.S. Department of Energy's National Nuclear Security Administration under contract DE-NA0003525.

ATA Project No. 61178
Sandia National Laboratories RFQ No. 273252
July 18, 2013

# Executive Summary for the SNL SWIFT V27 Wind Turbine Dynamic Characterization

Prepared for

Sandia National Laboratories
P.O. Box 5800
Albuquerque, New Mexico 87123

Prepared by

ATA Engineering, Inc.
11995 El Camino Real, Suite 200
San Diego, California 92130


Prepared by:

Scanned signature - original on file ATA ENGINEERING INC

Timothy Marinone
Engineer, Test

Reviewed by:

Scanned signature - original on file ATA ENGINEERING INC

David Cloutier
Engineer, Test


CONTACTS


SNL:

| | |
|---|---|
| John White | 505-284-5400 |
| Bruce Leblanc | 505-844-1438 |
| Gil Sanchez | 505-284-4481 |

ATA:

| | |
|---|---|
| Tim Marinone | 858-480-2076 |
| Dave Cloutier | 858-480-2083 |
| Ralph Brillhart | 858-480-2082 |
| Dave Hunt | 858-480-2095 |

**ABSTRACT**

This final report summarizes ATA Engineering, Inc.'s experimental dynamic characterization of the Sandia National Laboratories (SNL) Scaled Wind Farm Technology (SWIFT) Vestas 27 (V27) wind turbine components and fully assembled turbines. Testing was performed at SNL's SWIFT facility in Lubbock, Texas, from October 2012 through June 2013. Dynamic testing consisted of modal testing of the individual blades, the towers in a free-free boundary condition, the towers bolted to the foundations, and the fully assembled wind turbines. Additionally, modal testing was performed on a hub and two nacelles to determine the mass and inertia properties of these components. Details on these tests can be found in their respective reports.

TABLE OF CONTENTS

1. INTRODUCTION AND TEST OBJECTIVES ..... 1
2. V27 BLADE VARIABILITY ..... 2
   2.1. Test Article Description and Configuration ..... 2
   2.2. Test Results ..... 3
3. HUB MASS PROPERTIES ..... 5
   3.1. Test Article Description and Configuration ..... 5
   3.2. Test Results ..... 5
4. NACELLE MASS PROPERTIES ..... 6
   4.1. Test Article Description and Configuration ..... 6
   4.2. Test Results ..... 7
5. TOWER FREE-FREE MODAL SURVEY ..... 8
   5.1. Test Article Description and Configuration ..... 8
   5.2. Test Results ..... 9
6. TOWER ON FOUNDATION MODAL SURVEY ..... 10
   6.1. Test Article Description and Configuration ..... 10
   6.2. Test Results ..... 11
7. V27 FULL TURBINE EXPERIMENTAL AND OPERATIONAL MODAL SURVEY ..... 12
   7.1. Test Article Description and Configuration ..... 12
   7.2. Experimental Modal Test Results ..... 14
   7.3. Operational Modal Test Results ..... 14
8. CONCLUSIONS ..... 16

## LIST OF TABLES

Table 2-1. V27 final global modes sorted by test frequency. ..... 4
Table 2-2. V27 final mass and inertia properties. ..... 4
Table 3-1. Mass and inertia properties of V27 hubs. ..... 5
Table 4-1. Final list of inertia properties for V27 nacelles. ..... 7
Table 5-1. Final mode list for V27 towers in free-free configuration. ..... 9
Table 6-1. Final mode list for V27 towers bolted to concrete foundation. ..... 11
Table 7-1. SNL1 and SNL2 V27 turbine final global modes sorted by test frequency. ..... 14
Table 7-2. SNL1 turbine EMA and OMA final global modes sorted by test frequency ..... 15

## LIST OF FIGURES

Figure 2-1. Bungee system used for V27 blade testing. ..... 2
Figure 2-2. V27 coordinate systems and measurement locations. ..... 3
Figure 2-3. Bifilar pendulum suspension used for V27 blade testing. ..... 3
Figure 3-1. Test setup of the V27 hub. ..... 5
Figure 4-1. V27 nacelle suspended and attached to load cells to measure mass and CG (exterior of nacelle on left and interior of nacelle on right). ..... 6
Figure 4-2. V27 nacelle mounted on air spring suspension system. ..... 7
Figure 5-1. Overall view of tower on stands (left), individual stand (right), and tower lifted on airbags (bottom). ..... 8
Figure 5-2. V27 tower and measurement locations for modal testing. ..... 9
Figure 6-1. Overall view of tower on foundation (left) and test display model (right) ..... 10
Figure 6-2. FRF comparison of base of tower and foundation. ..... 11
Figure 7-1. Overall view of V27 turbine ..... 12
Figure 7-2. V27 coordinate systems and measurement locations. ..... 13

# 1. INTRODUCTION AND TEST OBJECTIVES

Sandia National Laboratories (SNL) developed the Scaled Wind Farm Technology (SWIFT) center to enable rapid, cost-efficient testing and development of transformative wind energy technology. ATA Engineering, Inc., (ATA) was contracted as part of this effort to dynamically characterize a number of components and assemblies used at SWIFT. This executive summary provides results of the dynamic characterization of the Vestas 27 (V27) wind turbines and components. The testing was successfully completed October 2012 through June 2013. Individual blades, a hub, nacelles, towers, and full assemblies were tested in the course of this program.

The overall objective of the SWIFT V27 dynamic characterization was to obtain modal properties to use for model updating and correlation. The requirements to satisfy the overall objective were stated as follows:

1. Perform modal survey on six V27 blades.
    a. Experimentally determine primary mode shapes, frequencies, and damping.
    b. Obtain mass, center of gravity (CG), and mass moment of inertia (MOI) of the blades.
    c. Determine variability in dynamic properties of the blades.
2. Experimentally determine mass properties of hub.
3. Experimentally determine mass properties and variability of nacelles.
4. Perform modal survey on the towers in a free-free boundary condition.
    a. Experimentally determine primary mode shapes, frequencies, and damping of towers.
    b. Determine variability in dynamic properties of the towers.
5. Perform modal survey on the towers attached to the foundation.
    a. Experimentally determine primary mode shapes, frequencies, and damping; also, determine the variability of towers bolted to the foundation.
    b. Determine compliance in the tower to foundation interface.
6. Perform modal survey on the V27 full turbine assembly.
    a. Experimentally determine primary mode shapes, frequencies, and damping of turbines using both experimental and operational methods.
    b. Determine variability in dynamic properties of the turbines.

## 2. V27 BLADE VARIABILITY

This section of the report provides a brief description of the test configuration and results for the V27 modal survey and mass property measurement. The full report, titled "Final Report on SNL SWIFT V27 Modal Survey and Inertia Testing," provides additional details of this specific test effort.

### 2.1. Test Article Description and Configuration

Modal and mass testing was performed at SNL's SWIFT facility in Lubbock, Texas, on October 27–31, 2012. Modal testing was performed with the blades suspended by bungee loops, as shown in Figure 2-1. A detailed modal survey was performed on two blades, with accelerometers installed at the locations shown in Figure 2-2. A reduced set of instrumentation was used on the remaining four blades, which provided sufficient information to compare mode shapes and frequencies between blades.

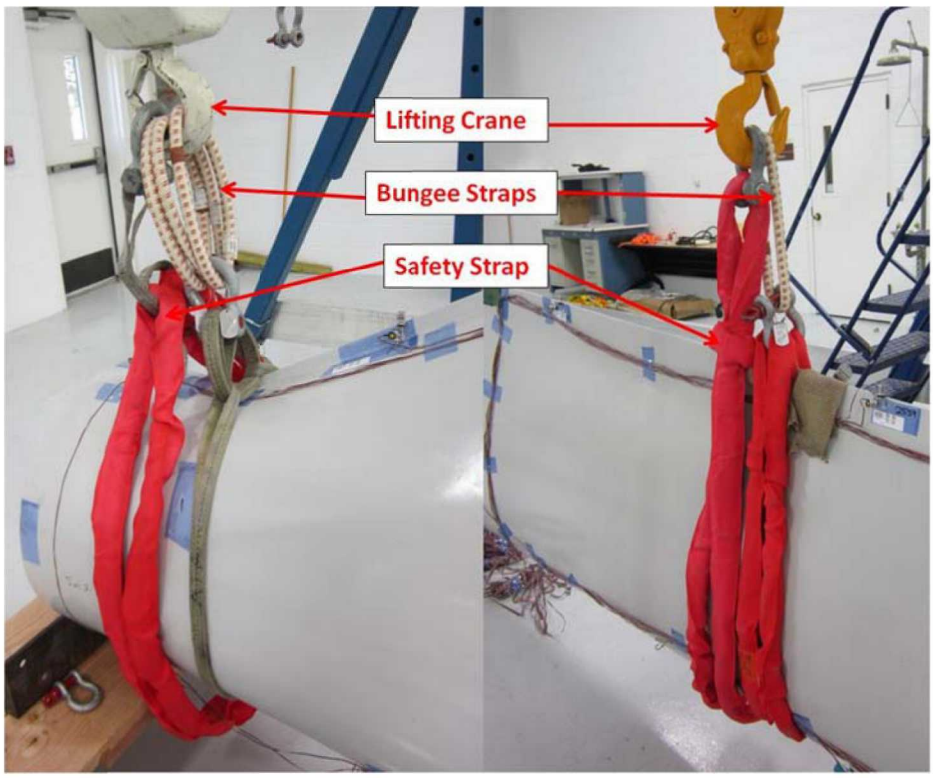


Figure 2-1. Bungee system used for V27 blade testing.

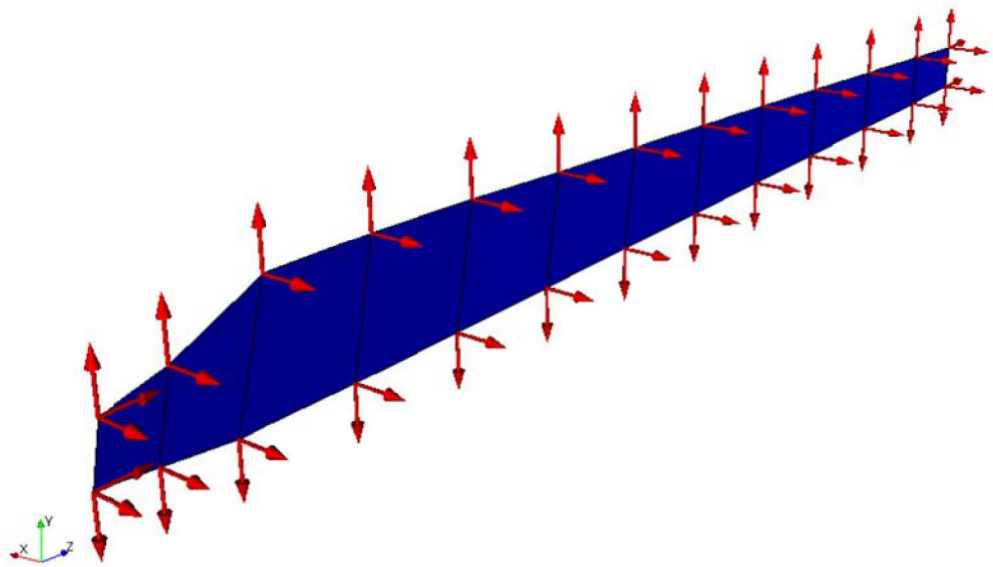


Figure 2-2. V27 coordinate systems and measurement locations.

Additionally, the blades were weighed and the mass moment of inertia about the flapwise axis determined using load cells and the bifilar pendulum technique. The test setup for mass property information is shown in Figure 2-3.

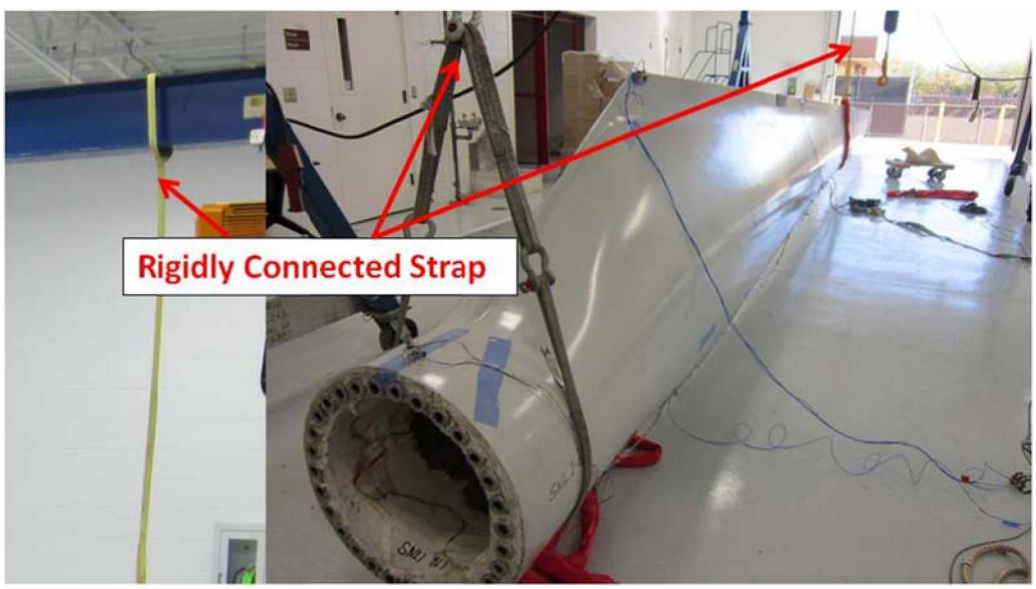


Figure 2-3. Bifilar pendulum suspension used for V27 blade testing.

## 2.2. Test Results

Table 2-1 provides the modal results up to 60 Hz for the six blades. The max frequency difference is less than 5% between all blades for the majority of modes; however, the first and second torsion modes have a greater variance, likely due to differences in blade repairs.

Table 2-1. V27 final global modes sorted by test frequency.

| Mode # | Description | Blade Frequency (Hz) | | | | | | Average (Hz) | Max Difference (%) | Priority |
|---|---|---|---|---|---|---|---|---|---|---|
| | | SNL1 - BL1 | SNL1 - BL2 | SNL1 - BL3 | SNL2 - BL1 | SNL2 - BL2 | SNL2- BL3 | | | |
| 1 | 1st Flapwise | 4.79 | 4.80 | 4.94 | 4.90 | 4.82 | 4.88 | 4.86 | 3.16 | P |
| 2 | 2nd Flapwise | 11.30 | 11.40 | 11.89 | 11.64 | 11.41 | 11.55 | 11.53 | 5.27 | P |
| 3 | 1st Edgewise | 12.35 | 12.37 | 12.67 | 12.66 | 12.29 | 12.35 | 12.45 | 3.08 | P |
| 4 | 3rd Flapwise | 21.49 | 21.40 | 21.97 | 21.54 | 21.69 | 21.29 | 21.56 | 3.19 | P |
| 5 | 2nd Edgewise | 30.10 | 29.96 | 30.86 | 31.05 | 30.59 | 30.26 | 30.47 | 3.64 | P |
| 6 | 1st Torsion | 34.70 | 30.58 | 31.08 | 33.11 | 32.40 | 32.43 | 32.38 | 13.47 | S |
| 7 | 4th Flapwise | 33.60 | 34.24 | 34.90 | 34.64 | 34.64 | 34.04 | 34.34 | 3.88 | O |
| 8 | 2nd Torsion | 50.46 | 47.75 | 48.66 | 50.02 | 51.69 | 52.53 | 50.19 | 10.01 | S |
| 9 | 3rd Edgewise | 55.36 | 55.50 | 57.74 | 56.89 | 56.10 | 55.19 | 56.13 | 4.62 | P |

Table 2-2 provides the mass property results, including weight, CG, and mass moment of inertia about the flapwise axis. Mass moment of inertia was limited to the blade flapwise term due to limits in the test setup; however, this inertia term is the most important term for model updating and correlation.

Table 2-2. V27 final mass and inertia properties.

| | SNL1_BL1 | SNL1_BL2 | SNL1_BL3 | SNL2_BL1 | SNL2_BL2 | SNL2_BL3 | Average | Max Difference (%) |
|---|---|---|---|---|---|---|---|---|
| **Weight (N)** | 6343 | 6357 | 6303 | 6552 | 6423 | 6787 | **6460.8** | **7.7** |
| **CG - X Axis (m)** | - | - | - | - | - | - | - | - |
| **CG - Y Axis (m)** | - | - | - | - | - | - | - | - |
| **CG - Z Axis (m)** | 4.18 | 4.15 | 4.19 | 4.29 | 4.16 | 4.20 | **4.20** | **3.4** |
| **Ixx (kg*m^2)** | - | - | - | - | - | - | - | - |
| **Iyy (kg*m^2)** | 5002.8 | 5466.0 | 5097.4 | 4967.0 | 5887.3 | 5796.4 | **5369.5** | **18.5** |
| **Izz (kg*m^2)** | - | - | - | - | - | - | - | - |
| * Coordinate System Origin Defined at Blade Root Center | | | | | | | | |

## 3. HUB MASS PROPERTIES

This section of the report provides a brief description of the test configuration and results for the V27 hub mass property measurement. The full report, titled "Inertia Testing of SWIFT V27 Hub," provides additional details of this specific test effort.

### 3.1. Test Article Description and Configuration

Testing of the V27 hub was conducted December 17–21, 2012, and January 6–11, 2013. Mass, CG, and moment of inertia terms were obtained for the hub. Figure 3-1 shows the test setup of the V27 hub for the modal inversion and mass line techniques.

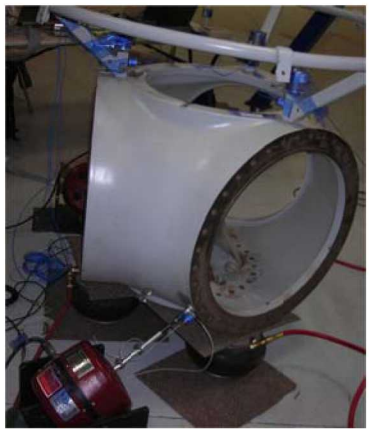

Figure 3-1. Test setup of the V27 hub.

### 3.2. Test Results

The results of the mass and inertia testing on the V27 hubs are provided in Table 3-1. The modal inversion and mass line inversion techniques were performed using the modal data and frequency response functions obtained from the shaker excitation.

Table 3-1. Mass and inertia properties of V27 hubs.

| Mass and Inertia Properties of V27 Hubs (Pitch Yaw Linkage Included) | | | | | |
|---|---|---|---|---|---|
| Property | Hub # | Load Cell | Bifilar Pendulum | Modal Inversion** | Mass Line Inversion |
| Mass (kg) | 1 | 481.7 | | 508.1 | 483.7 |
| | 2 | 474.0 | | | |
| CGx (m)* | 1 | | | -0.438 | -0.754 |
| Cgy (m)* | | | | 0.015 | 0.105 |
| CGz (m)* | | | | 0.005 | -0.143 |
| Ixx (kg*m$^2$) | | | 26.6 | 69.1 | 110.8 |
| Iyy (kg*m$^2$) | | | | 76.3 | 343.6 |
| Izz (kg*m$^2$) | | | | 86.2 | 151.6 |
| * Origin Defined at Front Face of Hub Rotor About the Center Using Rotor Csys | | | | | |
| ** Includes the Effective Mass of the Airbags | | | | | |

# 4. NACELLE MASS PROPERTIES

This section of the report provides a brief description of the test configuration and results for the V27 nacelle mass property measurement. The full report, titled "Inertia Testing of SWIFT V27 Nacelles," provides additional details of this specific test effort.

## 4.1. Test Article Description and Configuration

The V27 nacelles were tested to obtain mass and inertia properties. Each nacelle was lifted at four points with load cells to obtain the mass and CG of the structure, as shown in Figure 4-1. An effort was made to ensure that the nacelle was level with respect to the yaw bearing.

Figure 4-1. V27 nacelle suspended and attached to load cells to measure mass and CG (exterior of nacelle on left and interior of nacelle on right).

Additionally, modal testing was performed on two of the V27 nacelles to obtain all mass and inertia properties. During testing, the nacelles were supported by an airbag suspension to provide an approximate free-free boundary condition. Shakers were then attached to the nacelle to provide excitation of the six rigid body modes from which mass properties can be extracted. Figure 4-2 shows the modal test setup.

Figure 4-2. V27 nacelle mounted on air spring suspension system.

## 4.2. Test Results

The mass and inertia results are shown in Table 4-1. The masses of the nacelles were also measured independently by a crane company during transportation, and these are included for completeness. The mass and CG properties of Nacelle 3 were also obtained, but modal testing was not performed on this nacelle.

Table 4-1. Final list of inertia properties for V27 nacelles.

| Mass and Inertia Properties of V27 Nacelles | | | | |
|---|---|---|---|---|
| **Property** | **Nacelle #** | **Crane** | **Load Cell** | **Modal Inversion** |
| **Mass (kg)** | **1** | 6804 | 7038 | 5570 |
| | **2** | 6577 | 6781 | 5551 |
| | **3** | 6668 | 7203 | |
| **CGx (m)*** | **1** | | 0.67 | 0.33 |
| | **2** | | 0.61 | 0.13 |
| | **3** | | 0.65 | |
| **Cgy (m)*** | **1** | | 0.09 | 0.08 |
| | **2** | | 0.07 | -0.09 |
| | **3** | | 0.09 | |
| **CGz (m)*** | **1** | | | 0.13 |
| | **2** | | | 0.13 |
| | **3** | | | |
| **Ixx (kg*m^2)** | **1** | | | 2465 |
| | **2** | | | 2422 |
| **Iyy (kg*m^2)** | **1** | | | 12292 |
| | **2** | | | 14296 |
| **Izz (kg*m^2)** | **1** | | | 4728 |
| | **2** | | | 7192 |

## 5. TOWER FREE-FREE MODAL SURVEY

This section of the report provides a brief description of the test configuration and results for the V27 tower modal survey. The full report, titled "Modal Survey of SWIFT V27 Towers," provides additional details of this specific test effort.

### 5.1. Test Article Description and Configuration

The V27 towers were tested on specialty characterization supports designed by ATA and Sandia, shown in Figure 5-1. The stands were located approximately at the nodes of the first bending mode (4.25 and 23.1 meters from the base of the tower). Airbags (Firestone Airmount Isolators Model 19) were supported by the stands and were used to simulate a free-free boundary condition. The airbags were pressurized to approximately 90 psi at 23.1 meters from the tower base and approximately 120 psi at 4.25 meters from the tower base.

Figure 5-1. Overall view of tower on stands (left), individual stand (right), and tower lifted on airbags (bottom).

ATA created a test model representative of the tower to develop a set of test measurement degrees of freedom (DOF). The test display model (TDM), shown in Figure 5-2, is used for mode shape visualization. Accelerometers (PCB T33B) were mounted tangential to the tower to spatially filter the

response and minimize the response attributed to the breathing modes. Force was input into the structure with a calibrated modal impact hammer (PCB 086D20).

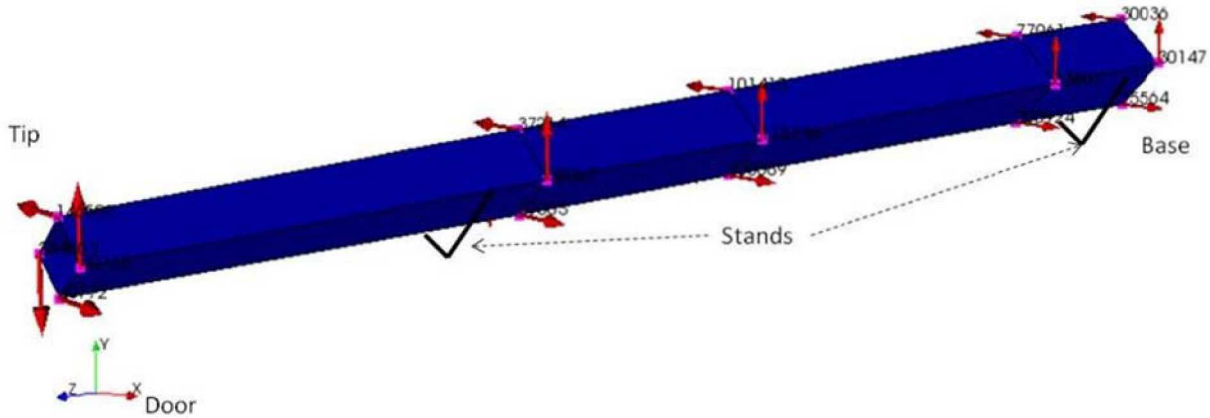


Figure 5-2. V27 tower and measurement locations for modal testing.

## 5.2. Test Results

The final list of mode shapes is included in Table 5-1. The first and second bending modes are of primary importance. Rigid body modes can be used to help correlate the model by determining the stiffness of the supports. The frequencies for Tower 1 and Tower 2 are within 5% of each other, indicating a high level of similarity between the two towers. Due to the orientation of each tower with respect to the air springs, the modes are not predominantly in the same axes. Additionally, some of the modes were able to be extracted from Tower 1 without air springs.

Table 5-1. Final mode list for V27 towers in free-free configuration.

| | Tower 1 | | Tower 2 | | Tower 1 without Air Springs | |
|---|---|---|---|---|---|---|
| | Frequency (Hz) | Damping (% Crit) | Frequency (Hz) | Damping (% Crit) | Frequency (Hz) | Damping (% Crit) |
| First Bending Mode | 10.66 | 1.47 | 10.61 | 1.10 | 10.81 | 0.81 |
| | 10.88 | 2.47 | 10.69 | 1.92 | | |
| Second Bending Mode | 28.34 | 3.06 | 28.29 | 0.85 | 26.39 | 1.10 |
| | 29.10 | 2.24 | 28.80 | 1.09 | | |
| Rigid Body Mode | 2.12 | 6.86 | 2.08 | 5.48 | 5.21 | 0.49 |

## 6. TOWER ON FOUNDATION MODAL SURVEY

This section of the report provides a brief description of the test configuration and results for the modal survey of the V27 towers bolted to the foundation. The full report, titled "Modal Survey of SWIFT V27 Towers on Foundation," provides additional details of this specific test effort.

### 6.1. Test Article Description and Configuration

The V27 towers were bolted to the concrete foundation as shown in Figure 6-1. ATA created a test model representative of the tower to develop a set of test measurement degrees of freedom (DOF). The test display model (TDM), used for mode shape visualization, is also shown in Figure 6-1. Accelerometers were mounted tangential to the tower to spatially filter the response and minimize the response attributed to the breathing modes. Force was input into the structure with a calibrated modal impact hammer. Seismic accelerometers were located on the concrete foundation and at the base of the tower in order to obtain the motion of the foundation for use in determining the impedance of the structure.

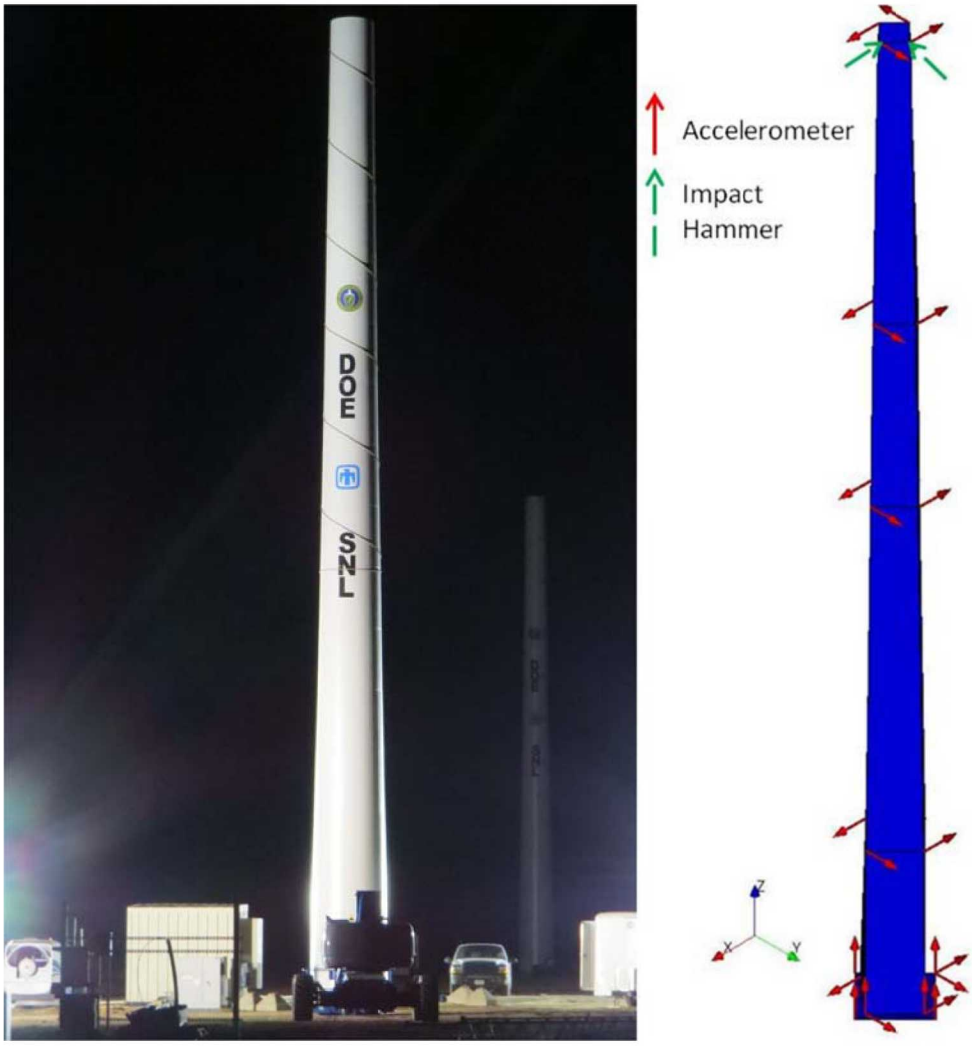


Figure 6-1. Overall view of tower on foundation (left) and test display model (right).

## 6.2. Test Results

The final list of mode shapes is included in Table 6-1. The first and second bending modes are of primary importance. The frequencies between Tower 1 and Tower 2 are within 5% of each other, indicating a high level of similarity between the two towers. The modal assurance criterion (MAC) was also computed between the two towers and shows a high level of agreement; the slightly lower values for the second bending mode are due to removing the affected channels from the mode shapes and not having sufficient high response measurements.

Table 6-1. Final mode list for V27 towers bolted to concrete foundation.

| | Axis of Motion | Tower 1 | | Tower 2 | | MAC |
|---|---|---|---|---|---|---|
| | | Frequency (Hz) | Damping (% Crit) | Frequency (Hz) | Damping (% Crit) | |
| First Bending Mode | Fore-Aft (X) | 2.70 | 0.56 | 2.61 | 0.82 | 0.95 |
| | Side-Side (Y) | 2.73 | 0.98 | 2.67 | 0.50 | 0.90 |
| Second Bending Mode | Fore-Aft (X) | 11.58 | 2.24 | 11.32 | 2.49 | 0.81 |
| | Side-Side (Y) | 11.71 | 1.76 | 11.58 | 1.57 | 0.84 |

In addition, SNL was interested in determining the stiffness between the foundation and tower due to the bolted interface. For this, the axial (Z-axis) accelerometer FRFs at the base of the tower and at the foundation are overlaid in Figure 6-2.

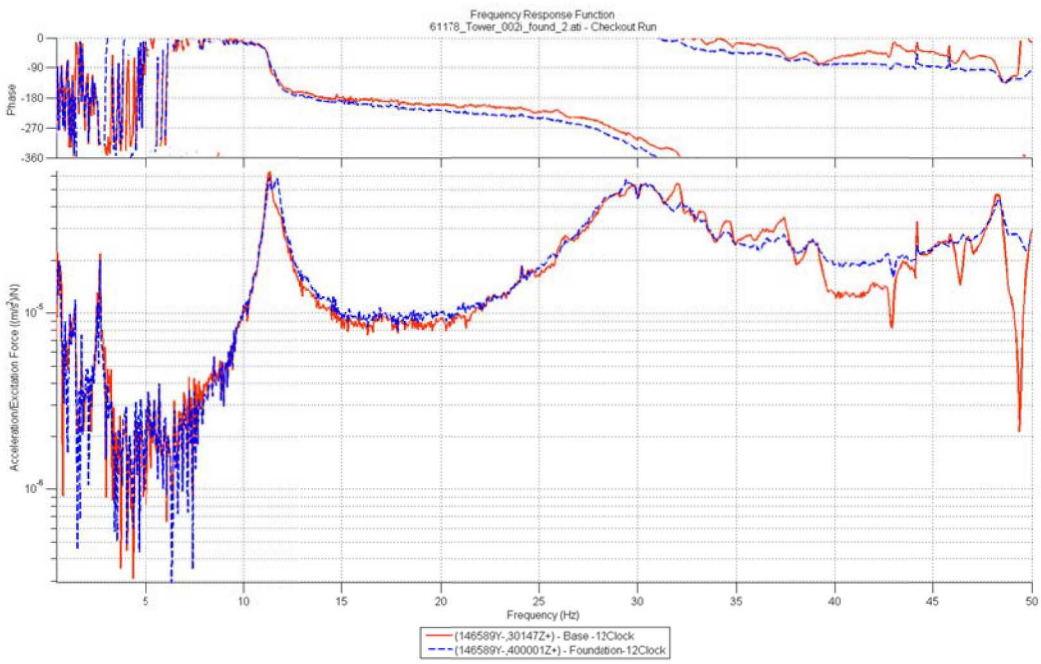


Figure 6-2. FRF comparison of base of tower and foundation.

The overlaid FRFs are almost identical, indicating that there is very minimal energy lost over the interface; therefore the interface is a very good approximation of a fixed boundary condition. There is significant motion in the foundation, however, indicating that the entire concrete foundation has relative motion with respect to ground.

# 7. V27 FULL TURBINE EXPERIMENTAL AND OPERATIONAL MODAL SURVEY

This section of the report describes the test configuration for the V27 modal survey. The full report, titled "Final Report on SNL SWIFT V27 Full Wind Turbine Experimental and Operational Modal Analysis," provides additional details of this specific test effort.

## 7.1. Test Article Description and Configuration

The V27 225 kW wind turbine has a 30 meter tower with 13 meter rotor blades. The V27 turbine is shown in Figure 7-1. The V27 was tested in a parked configuration to prevent the turbine from rotating during testing, and the turbine rotor was set to zero degrees to minimize the potential of damage due to wind.

Figure 7-1. Overall view of V27 turbine.

The final set of measurement locations totaled 80 fixed DOF at 53 node locations. The geometry and nodes were defined using one global coordinate system and four local coordinate systems. The tower and foundation DOF were located in the global coordinate system; each blade and the nacelle were in their own local coordinate systems. Figure 7-2 shows the test display model and accelerometer locations, with each arrow in the figure representing an accelerometer. In total, 81 channels counting the modal hammer

were measured during impact testing. The same channels—with the exception of the modal hammer—were measured during operational testing. Due to time constraints, only a subset of channels was measured on the second turbine for comparing natural frequencies. This included all DOF measured on SNL1 except the blades. Additional biaxial accelerometers were installed on the blades at max chord on SNL2.

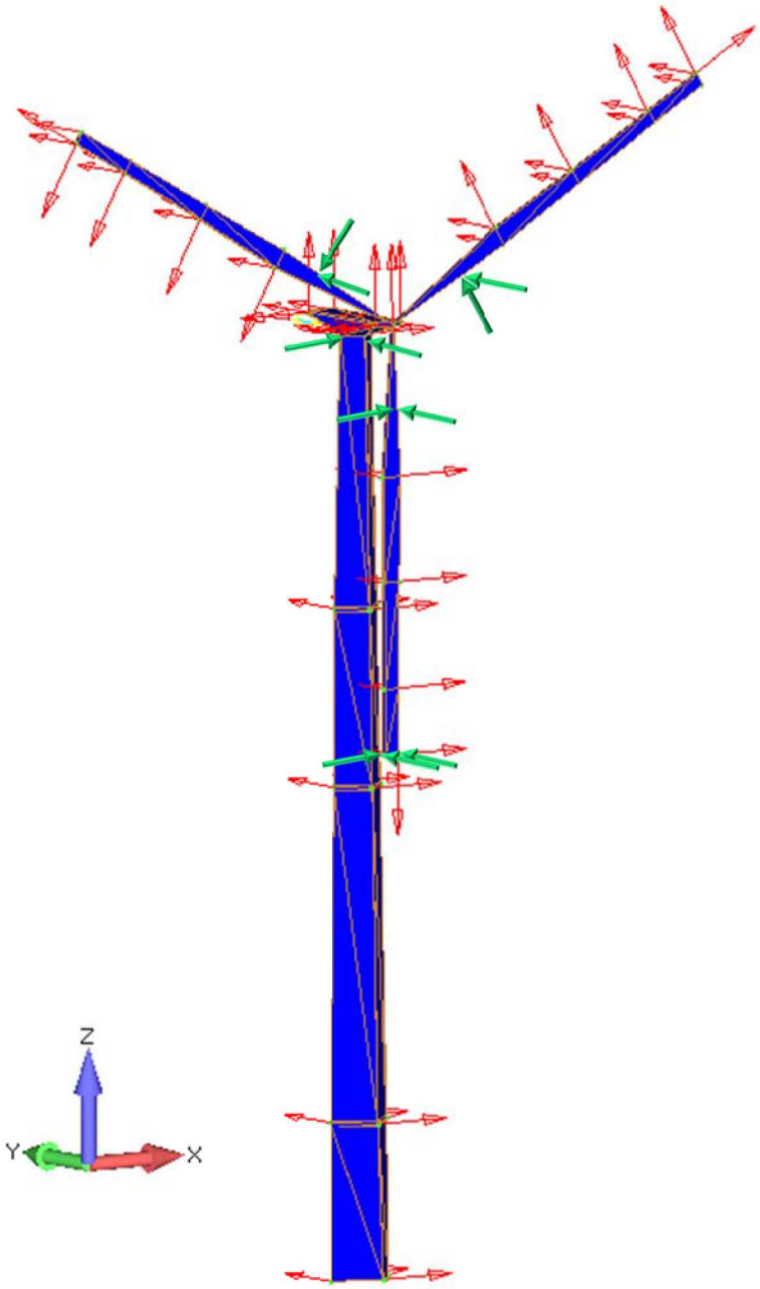


Figure 7-2. V27 coordinate systems and measurement locations.

## 7.2. Experimental Modal Test Results

The list of modes, sorted by test mode shape frequency, is provided in Table 7-1. This table lists the shape description, test frequency, and damping for the two turbines tested. Additionally, the MAC between SNL1 and SNL2 is provided for each mode. As SNL2 had a significantly reduced instrumentation set, modes were compared to SNL1 using a combination of MAC, mode shape, and comparison of PSMIF using a common sensor set. Differences in the modes between SNL1 and SNL2 are likely due to minor differences in construction and components of the turbine, as well as slight differences in rotor orientation. However, all but two modes are within a 5% difference.

Table 7-1. SNL1 and SNL2 V27 turbine final global modes sorted by test frequency.

| | SNL1 | | SNL2 | | | | |
|---|---|---|---|---|---|---|---|
| Mode | Frequency (Hz) | Damping (% Crit.) | Frequency (Hz) | Damping (% Crit.) | Diff (%) | MAC | Description |
| 1 | 1.00 | 3.39 | 0.97 | 2.66 | 3% | 96 | 1st Tower Bending Edgewise |
| 2 | 1.01 | 3.82 | 0.99 | 2.95 | 2% | 83 | 1st Tower Bending Flapwise |
| 3 | 2.02 | 2.48 | 1.88 | 2.87 | 7% | 68 | 1st Blade Flapwise Bending - Asym |
| 4 | 2.04 | 2.51 | 2.00 | 2.36 | 2% | 50 | 1st Blade Flapwise Bending - Asym |
| 5 | 2.40 | 2.13 | 2.37 | 1.59 | 1% | 82 | 1st Blade Flapwise Bending - Sym |
| 6 | 3.65 | 1.45 | | | | | 1st Blade Edgewise Bending - Asym |
| 7 | 3.73 | 1.24 | 3.75 | 0.01 | 0% | 32 | 1st Blade Edgewise Bending - Asym |
| 8 | 5.33 | 1.35 | 5.05 | 1.96 | 5% | 76 | 2nd Blade Flapwise Bending - Asym |
| 9 | 5.36 | 1.46 | 5.34 | 1.26 | 0% | 68 | 2nd Blade Flapwise Bending - Asym |
| 10 | 6.67 | 1.20 | 6.70 | 0.98 | 0% | 88 | 2nd Blade Flapwise Bending - Sym |
| 11 | 7.83 | 1.38 | 7.76 | 1.18 | 1% | 90 | 2nd Tower Bending Flapwise |
| 12 | 7.97 | 1.19 | 7.99 | 1.52 | 0% | 85 | 2nd Tower Bending Edgewise |
| 13 | 8.43 | 1.32 | 8.34 | 0.80 | 1% | 89 | 1st Tower Torsion, 2nd Blade Edgewise Bending |
| 14 | 9.67 | 1.65 | 9.99 | 1.64 | -3% | 73 | 2nd Blade Edgewise Bending - Sym |
| 15 | 11.15 | 1.19 | 11.12 | 1.29 | 0% | 83 | 3rd Blade Flapwise Bending - Asym |
| 16 | 12.52 | 3.64 | | | | | 3rd Blade Flapwise Bending - Asym |
| 17 | 12.69 | 1.70 | 12.17 | 2.68 | 4% | 84 | 2nd Blade Edgewise Bending - Asym / 3rd Blade Flap - Asym |
| 18 | 13.45 | 1.06 | 13.22 | 1.11 | 2% | 71 | 2nd Blade Edgewise Bending - Asym |
| 19 | 13.66 | 1.08 | 13.82 | 1.98 | -1% | 66 | 2nd Blade Edgewise Bending - Asym / 3rd Blade Flap -Sym |
| 20 | 13.80 | 1.04 | | | | | 3rd Blade Flapwise Bending -Sym |

## 7.3. Operational Modal Test Results

Operational modal analysis was performed on the SNL1 V27 turbine. Approximately two hours of natural wind excitation data were recorded and used for OMA. The CC-SSI algorithm in ARTeMIS was used to extract modes in the operational data.

The list of modes, sorted by test mode shape frequency, is provided in Table 7-2. This table lists the shape description, test frequency, and damping for SNL1, comparing the EMA results to OMA. Additionally, the MAC between EMA and OMA is provided for each mode. Modes were compared using a combination of MAC and visualization of the mode shape.

Table 7-2. SNL1 turbine EMA and OMA final global modes sorted by test frequency.

| | SNL1 - EMA | | SNL1 - OMA | | | | |
|---|---|---|---|---|---|---|---|
| Mode | Frequency (Hz) | Damping (% Crit.) | Frequency (Hz) | Damping (% Crit.) | Diff (%) | MAC | Description |
| 1 | 1.00 | 3.39 | | | | | 1st Tower Bending Edgewise |
| 2 | 1.01 | 3.82 | 1.00 | 0.82 | 0% | 44 | 1st Tower Bending Flapwise |
| 3 | 2.02 | 2.48 | 1.98 | 2.24 | 2% | 63 | 1st Blade Flapwise Bending - Asym |
| 4 | 2.04 | 2.51 | 2.02 | 2.45 | 1% | 98 | 1st Blade Flapwise Bending - Asym |
| 5 | 2.40 | 2.13 | 2.37 | 1.77 | 1% | 100 | 1st Blade Flapwise Bending - Sym |
| 6 | 3.65 | 1.45 | | | | | 1st Blade Edgewise Bending - Asym |
| 7 | 3.73 | 1.24 | 3.61 | 0.95 | 3% | 42 | 1st Blade Edgewise Bending - Asym |
| 8 | 5.33 | 1.35 | 5.25 | 1.40 | 2% | 73 | 2nd Blade Flapwise Bending - Asym |
| 9 | 5.36 | 1.46 | 5.31 | 1.20 | 1% | 93 | 2nd Blade Flapwise Bending - Asym |
| 10 | 6.67 | 1.20 | 6.61 | 0.97 | 1% | 100 | 2nd Blade Flapwise Bending - Sym |
| 11 | 7.83 | 1.38 | | | | | 2nd Tower Bending Flapwise |
| 12 | 7.97 | 1.19 | | | | | 2nd Tower Bending Edgewise |
| 13 | 8.43 | 1.32 | | | | | 1st Tower Torsion, 2nd Blade Edgewise Bending |
| 14 | 9.67 | 1.65 | 9.37 | 2.07 | 3% | 94 | 2nd Blade Edgewise Bending - Sym |
| 15 | 11.15 | 1.19 | 11.00 | 1.31 | 1% | 99 | 3rd Blade Flapwise Bending - Asym |
| 16 | 12.52 | 3.64 | | | | | 3rd Blade Flapwise Bending - Asym |
| 17 | 12.69 | 1.70 | | | | | 2nd Blade Edgewise Bending - Asym / 3rd Blade Flap - Asym |
| 18 | 13.45 | 1.06 | | | | | 2nd Blade Edgewise Bending - Asym |
| 19 | 13.66 | 1.08 | | | | | 2nd Blade Edgewise Bending - Asym / 3rd Blade Flap -Sym |
| 20 | 13.80 | 1.04 | 13.49 | 1.32 | 1% | 92 | 3rd Blade Flapwise Bending -Sym |

## 8. CONCLUSIONS

Modal and mass property testing was performed on several components and assemblies of SNL's SWIFT V27 wind turbines. ATA was responsible for test setup, data acquisition, data analysis, and instrumentation and hardware removal from the V27 components and assembled turbines following the test. All phases of the test program were completed and objectives met from October 2012 through June 2013.

ATA Project No. 61178
Sandia National Laboratories RFQ No. 273252
March 20, 2013

# Final Report on
# SNL SWIFT V27 Modal Survey and Inertia Testing

Prepared for

Sandia National Laboratories
P.O. Box 5800
Albuquerque, New Mexico 87123

Prepared by

ATA Engineering, Inc.
11995 El Camino Real, Suite 200
San Diego, California 92130


Prepared by:

Scanned signature - original on file ATA ENGINEERING INC

Timothy Marinone
Engineer, Test

Reviewed by:

Scanned signature - original on file ATA ENGINEERING INC

David Cloutier
Engineer, Test


CONTACTS

| | |
|---|---|
| SNL: | |
| John White | 505-284-5400 |
| Bruce Leblanc | 505-844-1438 |
| Gil Sanchez | 505-284-4481 |
| ATA: | |
| Tim Marinone | 858-480-2076 |
| Dave Cloutier | 858-480-2083 |
| Ralph Brillhart | 858-480-2082 |
| David Hunt | 858-480-2095 |

**ABSTRACT**

This final report documents ATA Engineering, Inc.'s modal survey and inertia testing of Sandia National Laboratories' Scaled Wind Farm Technology (SWIFT) Vestas 27 (V27) wind turbine blades. The modal survey was performed at SNL's SWIFT facility in Lubbock, Texas, on October 27 through October 31, 2012. Six blades were tested—two blades with a full set of instrumentation and four blades with a reduced set of instrumentation. All six blades were tested in a free-free configuration by suspending the blades with a serial bungee loop system. All six rigid body modes and the first three flexible flapwise bending modes, first three edgewise bending modes, and first torsion mode were identified as target modes. The modal survey was conducted with modal impact hammer and burst random shaker test runs, and all target modes were identified. The inertia properties of the blades were also obtained. Modal and inertia results were compared between all six blades to identify variation in the blades.

This report documents one of several different tests that were performed to characterize various components and assemblies for the SWIFT. Details on the other tests can be found in their respective reports.

TABLE OF CONTENTS

1. INTRODUCTION AND EXECUTIVE SUMMARY ..... 1
1.1. Test Objectives ..... 1
1.2. Test Performance and Results ..... 2
2. TEST CONFIGURATIONS AND PRETEST MODELING ..... 3
2.1. Test Article Description and Configuration ..... 3
2.2. Pretest Analysis ..... 6
2.3. Test Measurements and Geometry ..... 6
3. TEST DESCRIPTION ..... 9
3.1. Test Conduct ..... 9
3.1.1. Modal Survey ..... 9
3.1.2. Inertia Property Estimation Using Bifilar Pendulum ..... 12
3.2. Test Instrumentation ..... 13
3.2.1. Accelerometers ..... 15
3.2.2. Force Transducers ..... 17
3.2.3. Impact Hammer ..... 18
3.2.4. Electrodynamic Shakers ..... 20
3.2.5. DC Accelerometers ..... 21
3.2.6. Data Measurement and Recording ..... 22
3.3. Test Performance ..... 24
3.3.1. Data Quality Assessment ..... 24
3.3.2. Modal Extraction ..... 26
3.3.3. Modal Assurance Criteria ..... 27
3.3.4. Orthogonality ..... 27
4. TEST RESULTS ..... 28
4.1. V27 Final Modes ..... 28
4.2. V27 Rigid Properties ..... 32
5. CONCLUSIONS ..... 34
Appendix A On-Site Test Log and Run Log ..... A-1
Appendix B Nodes and Accelerometers Table ..... B-1
Appendix C Accelerometer Photos ..... C-1
Appendix D Shaker Configuration and Location Photos ..... D-1
Appendix E Modal Test Channel Table ..... E-1
Appendix F Test Mode Shapes ..... F-1
Appendix G Equipment Specifications ..... G-1

LIST OF TABLES

Table 1-1. Final modes, V27 wind turbine blades. ..... 2
Table 1-2. Inertia properties of V27 wind turbine blades. ..... 2
Table 2-1. V27 pseudo-orthogonality matrix. Values greater than 0.1 are yellow and those greater than 0.90 green. ..... 6
Table 2-2. Accelerometer locations (56 channels and 26 nodes, not including drive points)..... 8
Table 3-1. SNL V27 modal survey test run log. ..... 10
Table 4-1. V27 final global modes sorted by test frequency. ..... 29
Table 4-2. V27 final test modes (SNL2_BL1 and SNL2_BL3 at full instrumentation set): self-orthogonality. ..... 29
Table 4-3. V27 final test modes (all six blades at reduced instrumentation set): self-orthogonality. ..... 30
Table 4-4. V27 final mass and inertia properties. ..... 32

LIST OF FIGURES

Figure 2-1. Overall view of V27 and test facility. ..... 3
Figure 2-2. Bungee system used for V27 blade testing. ..... 4
Figure 2-3. Bifilar pendulum suspension used for V27 blade testing. ..... 5
Figure 2-4. V27 coordinate systems and measurement locations. ..... 7
Figure 3-1. Principle of bifilar pendulum. ..... 12
Figure 3-2. Data acquisition equipment and analysis workstations. ..... 13
Figure 3-3. Instrumentation cabling was routed to gather boxes where DB-50 cables were then used to connect to the data acquisition system. ..... 14
Figure 3-4. DC accelerometers were routed to DIN rails where pigtail-to-BNC cables were then used to connect to the data acquisition system. ..... 14
Figure 3-5. V27 test coordinate system transformation. ..... 15
Figure 3-6. Example accelerometer installation; note the barcode used for documenting the accelerometer location. ..... 16
Figure 3-7. PSD for both shaker inputs, MPR run 25. ..... 17
Figure 3-8. Load cells used to calculate mass and CG. ..... 18
Figure 3-9. PSD for impact hammer, run 22. ..... 19
Figure 3-10. Shaker attachment with drive point accelerometer. ..... 20
Figure 3-11. Time and spectra of DC accelerometer for bifilar pendulum test run 27. ..... 21
Figure 3-12. Data acquisition system schematic. ..... 23
Figure 3-13. FRF and coherence for impact hammer drive point 3502X–, run 22. ..... 25
Figure 3-14. Reciprocity comparison between shakers 1 and 2, run 13. ..... 26
Figure 4-1. Linearity check observing PSMIF from MPR runs 9, 10, and 11. ..... 31
Figure 4-2. FRF from MPR runs 9, 10, and 11. ..... 32

## LIST OF ABBREVIATIONS

ATA - ATA Engineering, Inc.
ASD - auto spectral density
CG - center of gravity
CMIF - complex mode-indicator function
CRS - corrected root sum
CRSS - corrected root sum square
DOF - degree of freedom
FEM - finite element model
FRF - frequency response functions
Hz - hertz
ICP™[1] - integrated circuit preamplifier
IMAT - interface between MATLAB, analysis, and test
MAC - modal assurance criteria
MMIF - multivariate mode-indicator function
MOI - moment of inertia
MPR - multiple point random
PCB - PCB Electronics, Inc.
PSD - power spectral density
PSMIF - power spectrum mode-indicator function
RMS - root mean square
SNL - Sandia National Laboratory
SWIFT - Scaled Wind Farm Technology
TEDS - transducer electronic data sheet
TAM - test analysis model
V27 - Vestas 27

[1] ICP is a registered trademark of PCB Piezotronics, Inc.

# 1. INTRODUCTION AND EXECUTIVE SUMMARY

Sandia National Laboratories (SNL) is developing the Scaled Wind Farm Technology (SWIFT) center to enable rapid, cost-efficient testing and development of transformative wind energy technology. ATA Engineering, Inc., (ATA) was contracted as part of this effort to dynamically characterize a number of components and assemblies to be used at SWIFT. This report documents the modal survey for the Vestas 27 (V27) wind turbine blades. The modal survey was successfully completed October 27–31, 2012. Six blades were tested—two with a full set of instrumentation and four with a reduced set of instrumentation. The blades were tested in a free-free configuration.

In preparation for the modal survey, SNL provided ATA with a finite element model (FEM) of the V27. ATA selected measurement locations and developed a test-analysis model (TAM) with a reduced-model mass and stiffness matrix, and a back expansion matrix for visualization of the test mode shapes. ATA used this information to plan and conduct the modal survey.

ATA conducted the test using modal impact hammer and multi-point random shaker excitation methods. ATA provided the data collection equipment and instrumentation. A bungee suspension system was used to support the V27 in order to simulate free-free boundary conditions as accurately as possible. The first flexible structural modal frequency was above the highest rigid body modal frequency. All V27 primary modes were identified up to 60 Hz, and these are presented in Table 1-1. V27 flapwise mass inertia properties were also identified and are presented in Table 1-2.

## 1.1. Test Objectives

The overall objective of the SNL V27 modal survey was to obtain modal and mass properties to use for correlation. The requirements to satisfy the overall objective were stated as follows:

1. Perform a pretest analysis, predicting the target mode shapes and frequencies.
    a. Develop a TAM for defining accelerometer locations and expanding out mode shapes.
    b. Identify modal survey excitation locations.
2. Develop a detailed test plan and procedure for conducting the modal survey. The frequency range of interest was 0–100 Hz for the V27 suspended in a simulated free-free configuration. All six rigid body modes and the first three flexible flapwise bending modes, first three edgewise bending modes, and first torsion mode were identified as target modes.
3. Experimentally define the modal parameters (frequency, damping, and shape) for all target modes of the blade.
4. Provide quick-look results on site during testing (including animated mode shapes and comparison with finite element predictions).
5. Deliver a final report detailing all tasks of the modal survey, to be included with the final project report.

## 1.2. Test Performance and Results

In preparation for the modal survey, SNL provided ATA with the measurement geometry of the V27. ATA used this information to plan, prepare for, and perform the modal survey. ATA provided the necessary data collection equipment and instrumentation.

ATA executed and completed the test using modal impact hammer excitation methods. Global blade modes were extracted from the impact hammer data runs and from the multiple-point-random data runs. All V27 primary modes were identified up to 60 Hz; they are presented in Table 1-1. The weight, CG location of the Z-axis, and the moment of inertia about the Y-axis were identified and are presented in Table 1-2; the moment of inertia in the X and Z axes were not able to be identified, as explained in the later results section. The maximum percent difference for any flexible mode aside from the torsion modes is 5.27 %.

Table 1-1. Final modes, V27 wind turbine blades.

| Mode # | Description | Blade Frequency (Hz) | | | | | | Average (Hz) | Max Difference (%) | Priority |
|---|---|---|---|---|---|---|---|---|---|---|
| | | SNL1 - BL1 | SNL1 - BL2 | SNL1 - BL3 | SNL2 - BL1 | SNL2 - BL2 | SNL2- BL3 | | | |
| 1 | 1st Flapwise | 4.79 | 4.80 | 4.94 | 4.90 | 4.82 | 4.88 | 4.86 | 3.16 | P |
| 2 | 2nd Flapwise | 11.30 | 11.40 | 11.89 | 11.64 | 11.41 | 11.55 | 11.53 | 5.27 | P |
| 3 | 1st Edgewise | 12.35 | 12.37 | 12.67 | 12.66 | 12.29 | 12.35 | 12.45 | 3.08 | P |
| 4 | 3rd Flapwise | 21.49 | 21.40 | 21.97 | 21.54 | 21.69 | 21.29 | 21.56 | 3.19 | P |
| 5 | 2nd Edgewise | 30.10 | 29.96 | 30.86 | 31.05 | 30.59 | 30.26 | 30.47 | 3.64 | P |
| 6 | 1st Torsion | 34.70 | 30.58 | 31.08 | 33.11 | 32.40 | 32.43 | 32.38 | 13.47 | S |
| 7 | 4th Flapwise | 33.60 | 34.24 | 34.90 | 34.64 | 34.64 | 34.04 | 34.34 | 3.88 | O |
| 8 | 2nd Torsion | 50.46 | 47.75 | 48.66 | 50.02 | 51.69 | 52.53 | 50.19 | 10.01 | S |
| 9 | 3rd Edgewise | 55.36 | 55.50 | 57.74 | 56.89 | 56.10 | 55.19 | 56.13 | 4.62 | P |

Table 1-2. Inertia properties of V27 wind turbine blades.

| | SNL1_BL1 | SNL1_BL2 | SNL1_BL3 | SNL2_BL1 | SNL2_BL2 | SNL2_BL3 | Average | Max Difference (%) |
|---|---|---|---|---|---|---|---|---|
| **Weight (N)** | 6343 | 6357 | 6303 | 6552 | 6423 | 6787 | **6460.8** | **7.7** |
| **CG - X Axis (m)** | - | - | - | - | - | - | - | - |
| **CG - Y Axis (m)** | - | - | - | - | - | - | - | - |
| **CG - Z Axis (m)** | 4.18 | 4.15 | 4.19 | 4.29 | 4.16 | 4.20 | **4.20** | **3.4** |
| **Ixx (kg*m^2)** | - | - | - | - | - | - | - | - |
| **Iyy (kg*m^2)** | 5002.8 | 5466.0 | 5097.4 | 4967.0 | 5887.3 | 5796.4 | **5369.5** | **18.5** |
| **Izz (kg*m^2)** | - | - | - | - | - | - | - | - |
| * Coordinate System Origin Defined at Blade Root Center | | | | | | | | |

## 2. TEST CONFIGURATIONS AND PRETEST MODELING

This section of the report describes the specific pretest activities for the V27 modal survey. The blade is described, along with pretest model preparation activities.

### 2.1. Test Article Description and Configuration

The V27 wind turbine blade is 13 meters long and is used as part of the Vestas 27 225 kW wind turbine. The V27 has a max chord of 1.3 meters and a root diameter of 0.5 meters. The V27 blade is shown in Figure 2-1.

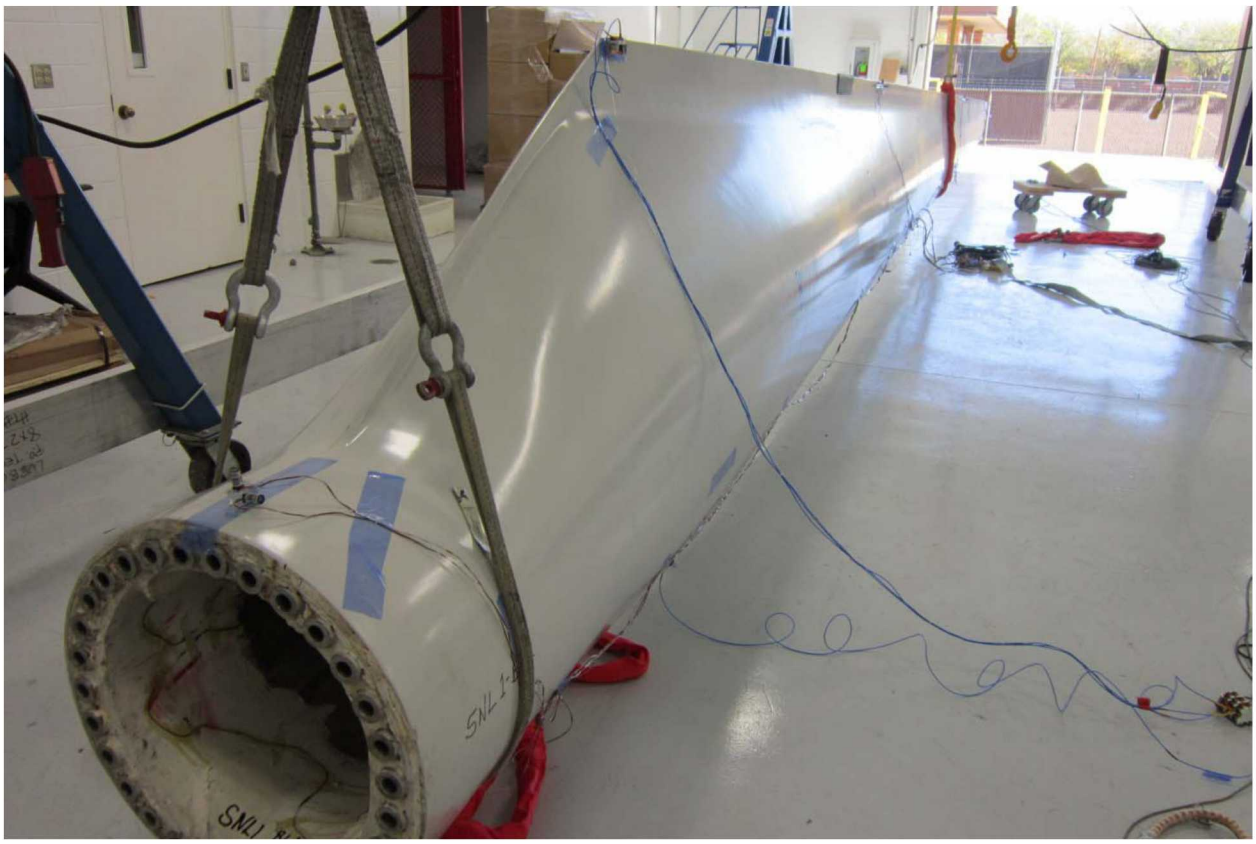

Figure 2-1. Overall view of V27 and test facility.

The V27 was tested in two different configurations to accommodate two different tests. The first configuration consisted of the blade suspended by a bungee system to separate the rigid body modes from the flexible structural modes. All rigid body modes were less than 1.8 Hz. The two support locations were at 2.40 and 10.20 meters from the root end; these locations were chosen to minimize the effect of the supports on the measurements by locating the supports at the nodes of the first flapwise bending mode. A photograph of the bungee system is shown in Figure 2-2.

The second configuration consisted of the blade rigidly suspended in order to perform a bifilar pendulum test. The two support locations were 7.80 meters from each other as defined from the modal supports but equidistant about the CG of the blade. A photograph of the bifilar pendulum suspension system is shown in Figure 2-3.

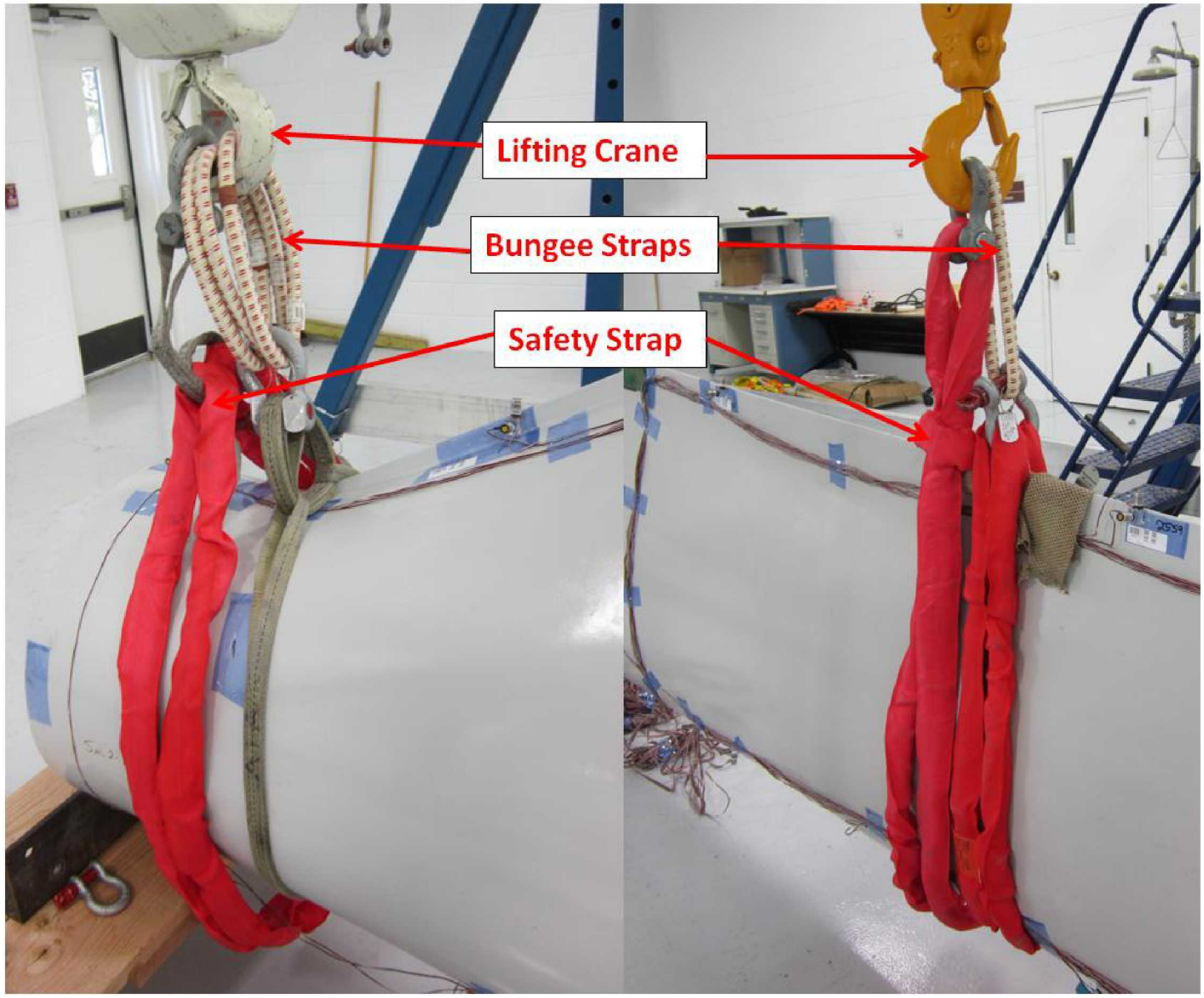


Figure 2-2. Bungee system used for V27 blade testing.

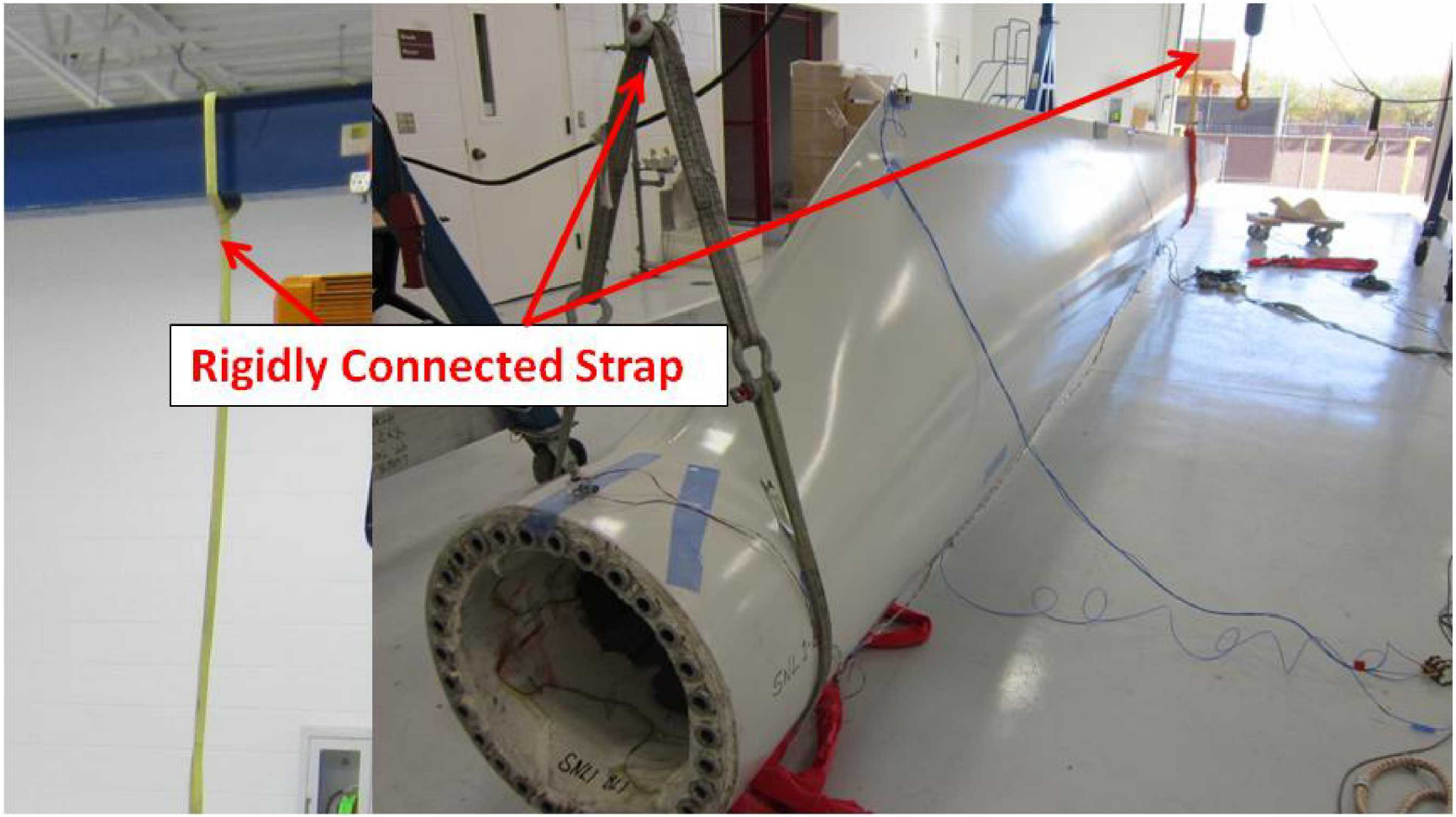


Figure 2-3. Bifilar pendulum suspension used for V27 blade testing.

## 2.2. Pretest Analysis

Pretest analysis was performed to determine accelerometer locations and calculate reduced mass, stiffness, and back-expansion matrices. The blade FEM was provided by SNL.

Table 2-1 shows the pseudo-orthogonality matrix between the FEM modes using the reduced TAM mass matrix for the blade. Details regarding the orthogonality computation are provided in Section 3.3.4. The pseudo-orthogonality computation compares the FEM modes to themselves using the reduced TAM mass matrix. Ideally, the mass for every mode is exactly captured in the TAM and the pseudo-orthogonality is an identity matrix. Practically, the difference characterizes how well the mass information is captured in the TAM, and on-diagonal values close to 1.0 with off-diagonal values close to 0.0 indicate a suitable TAM. In Table 2-1, values less than 0.1 are not displayed. Table 2-1 shows that above 27 Hz the TAM begins to lose its accuracy. This is due to the modes above this frequency having local panel flexibility. As these modes are not target modes, accurately capturing these modes was not of high priority.

Table 2-1. V27 pseudo-orthogonality matrix. Values greater than 0.1 are yellow and those greater than 0.90 green.

FEM Pseudo Orthogonality Table

| FEM shapes | | FEM shapes 1 | 2 | 3 | 4 | 5 | 6 | 7 | 8 | 9 | 10 | 11 | 12 | 13 | 14 | 15 | 16 | 17 | 18 | 19 | 20 | 21 | 22 | 23 | 24 | 25 | 26 | 27 | 28 |
|---|---|---|---|---|---|---|---|---|---|---|---|---|---|---|---|---|---|---|---|---|---|---|---|---|---|---|---|---|---|
| | POgg | 0.0 | 0.0 | 0.0 | 0.0 | 0.0 | 0.0 | 2.5 | 6.7 | 10.2 | 12.8 | 19.6 | 20.5 | 26.2 | 27.7 | 28.7 | 33.9 | 35.5 | 36.8 | 38.1 | 39.3 | 40.4 | 41.3 | 43.6 | 44.9 | 45.3 | 46.4 | 47.5 | 48.3 |
| 1 | 0.0 | 1.00 | | | | | | | | | | | | | | | | | | | | | | | | | | | |
| 2 | 0.0 | | 1.00 | | | | | | | | | | | | -0.11 | | | -0.14 | 0.23 | 0.28 | -0.47 | | 0.26 | | 0.13 | | | | |
| 3 | 0.0 | | | 1.00 | | | | | | | | | | | | | | | 0.14 | 0.30 | -0.32 | | 0.15 | | 0.15 | | | | |
| 4 | 0.0 | | | | 1.00 | | | | | | | | | | | | | | 0.10 | | -0.20 | | 0.12 | | | | | | |
| 5 | 0.0 | | | | | 1.00 | | | | | | | | | | | | | | | -0.18 | | | | | | | | |
| 6 | 0.0 | | | | | | 1.00 | | | | | | | | | | | | | | | | | | | | | | |
| 7 | 2.5 | | | | | | | 1.00 | | | | | | | 0.10 | | 0.13 | | | 0.28 | | | | | 0.10 | | | | |
| 8 | 6.7 | | | | | | | | 0.96 | | | | | | | | -0.15 | 0.11 | -0.13 | | 0.30 | | | | -0.21 | | -0.12 | | |
| 9 | 10.2 | | | | | | | | | 0.99 | | | | | | | | | | | | | | | | | | | |
| 10 | 12.8 | | | | | | | | | | 0.86 | | | | | | | | -0.15 | 0.13 | 0.22 | | | | | | | | |
| 11 | 19.6 | | | | | | | | | | | 0.76 | | | 0.17 | | | | | | 0.11 | | | | | | | | |
| 12 | 20.5 | | | | | | | | | | | | 0.77 | | | | | | | | | | | | 0.23 | | 0.11 | | |
| 13 | 26.2 | | | | | | | | | | | | | 0.91 | | | | | | | | | | | | | | | |
| 14 | 27.7 | | -0.11 | | | | | 0.10 | | | | 0.17 | | | 0.54 | | | | | 0.16 | | | | | | | | | |
| 15 | 28.7 | | | | | | | | | | | | | | | 0.49 | 0.11 | | -0.10 | | | | | | 0.15 | | | | |
| 16 | 33.9 | | | | | | | 0.13 | -0.15 | | | | | | | 0.11 | 0.17 | | | | -0.12 | | | | | | | | |
| 17 | 35.5 | | -0.14 | | | | | | 0.11 | | | | | | | | | 0.19 | | | 0.18 | | | | | | | | |
| 18 | 36.8 | | 0.23 | 0.14 | 0.10 | | | | -0.13 | | -0.15 | | | | | -0.10 | | | 0.29 | | -0.32 | -0.13 | 0.18 | | | | | | |
| 19 | 38.1 | | 0.28 | 0.30 | | | | 0.28 | | | 0.13 | | | | 0.16 | | | | | 0.63 | -0.18 | | 0.20 | | | | | | |
| 20 | 39.3 | | -0.47 | -0.32 | -0.20 | -0.18 | | | 0.30 | | 0.22 | 0.11 | | | | | -0.12 | 0.18 | -0.32 | -0.18 | 0.76 | | -0.27 | | -0.22 | | | | |
| 21 | 40.4 | | | | | | | | | | | | | | | | | | -0.13 | | | 0.19 | | | -0.13 | | | | |
| 22 | 41.3 | | 0.26 | 0.15 | 0.12 | | | | | | | | | | | | | | 0.18 | 0.20 | -0.27 | | 0.20 | | | | | | |
| 23 | 43.6 | | | | | | | | | | | | | | | | | | | | | | | 0.19 | -0.13 | | -0.11 | | |
| 24 | 44.9 | | 0.13 | 0.15 | | | | 0.10 | -0.21 | | | | 0.23 | | | 0.15 | | | | | -0.22 | -0.13 | | -0.13 | 0.43 | | 0.15 | | |
| 25 | 45.3 | | | | | | | | | | | | | | | | | | | | | | | | | 0.24 | | | 0.13 |
| 26 | 46.4 | | | | | | | | -0.12 | | | | 0.11 | | | | | | | | | | | -0.11 | 0.15 | | 0.26 | | |
| 27 | 47.5 | | | | | | | | | | | | | | | | | | | | | | | | | | | 0.17 | -0.16 |
| 28 | 48.3 | | | | | | | | | | | | | | | | | | | | | | | | | 0.13 | | -0.16 | 0.65 |

## 2.3. Test Measurements and Geometry

This section of the report provides information about the measurement locations used during the modal survey. Measurement locations were selected based on a pretest analysis. ATA created a test model representative of the V27 blade to develop a set of test measurement degrees of freedom (DOF).

The final set of measurement locations totaled 56 fixed DOF at 26 node locations. This number does not include drive point accelerometers or load cells. The geometry and nodes were defined using one global coordinate system. Figure 2-4 shows the test display model and accelerometer locations. Each arrow in the figure represents an accelerometer. Table 2-2 lists the 56 test DOF at the 26 selected model node locations, along with a description of each. Test measurements were also made at the shaker input

locations. These nodes are not included in the display model or in the table. Photos of all accelerometers are included in Appendix C. In total, 57 channels counting the modal hammer were measured during impact testing.

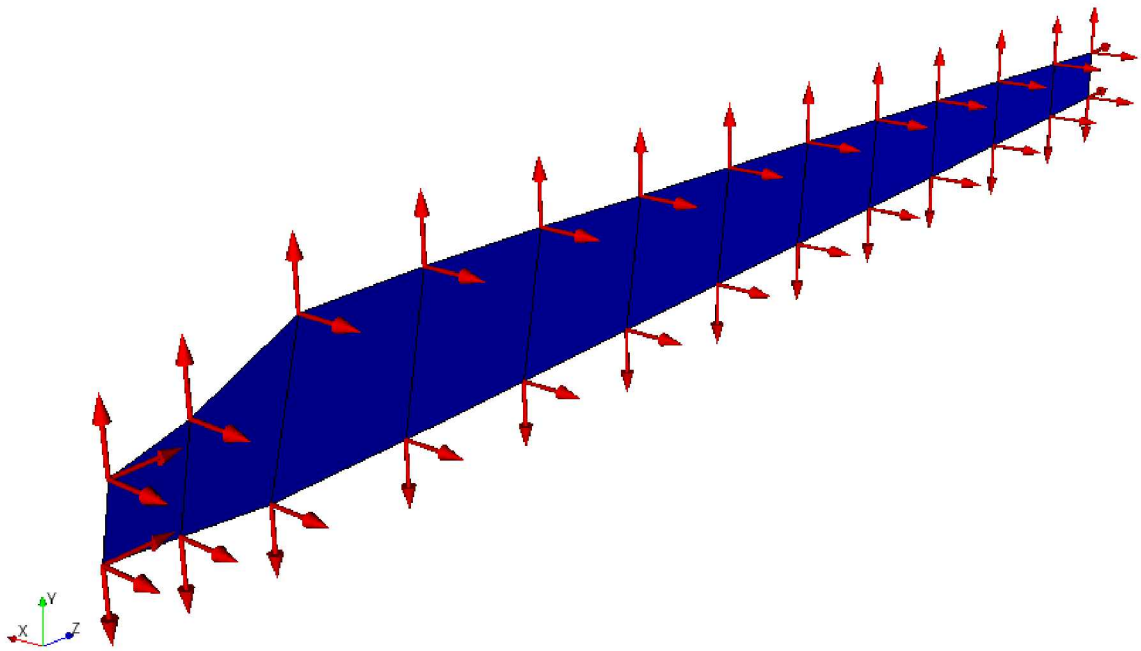


Figure 2-4. V27 coordinate systems and measurement locations.

Table 2-2. Accelerometer locations (56 channels and 26 nodes, not including drive points).

| Group Name | Node | X+ | Y+ | Z+ | Locations |
|---|---|---|---|---|---|
| Trailing | 3502 | X- | Y+ | Z+ | Trailing-1 (Tip) |
| Trailing | 3358 | X- | Y+ | | Trailing-2 |
| Trailing | 3052 | X- | Y+ | | Trailing-3 |
| Trailing | 2871 | X- | Y+ | | Trailing-4 |
| Trailing | 2559 | X- | Y+ | | Trailing-5 |
| Trailing | 2208 | X- | Y+ | | Trailing-6 |
| Trailing | 2010 | X- | Y+ | | Trailing-7 |
| Trailing | 1593 | X- | Y+ | | Trailing-8 |
| Trailing | 1359 | X- | Y+ | | Trailing-9 |
| Trailing | 878 | X- | Y+ | | Trailing-10 |
| Trailing | 488 | X- | Y+ | | Trailing-11 |
| Trailing | 242 | X- | Y+ | | Trailing-12 |
| Trailing | 76 | X- | Y+ | Z+ | Trailing-13 (Root) |
| Leading | 3537 | X- | Y- | Z+ | Leading-1 (Tip) |
| Leading | 3407 | X- | Y- | | Leading-2 |
| Leading | 3101 | X- | Y- | | Leading-3 |
| Leading | 2898 | X- | Y- | | Leading-4 |
| Leading | 2631 | X- | Y- | | Leading-5 |
| Leading | 2290 | X- | Y- | | Leading-6 |
| Leading | 2099 | X- | Y- | | Leading-7 |
| Leading | 1691 | X- | Y- | | Leading-8 |
| Leading | 1465 | X- | Y- | | Leading-9 |
| Leading | 992 | X- | Y- | | Leading-10 |
| Leading | 550 | X- | Y- | | Leading-11 |
| Leading | 296 | X- | Y- | | Leading-12 |
| Leading | 95 | X- | Y- | Z+ | Leading-13 (Root) |

| # X Entries | #Y Entries | # Z Entries |
|---|---|---|
| 26 | 26 | 4 |
| Total Number of Entries | | 56 |

# 3. TEST DESCRIPTION

The V27 modal survey involved applying and measuring external force excitations to the blade and measuring the acceleration responses at the instrumented locations. This testing allowed the measurement of frequency response functions (FRF) between the instrumented response locations and the applied shaker input forces. The FRF characterize the dynamic behavior of the structure and can be used to identify the modal parameters (frequency, damping, and shape) of the blade.

The V27 mass inertia in the Y-axis was also measured using a bifilar pendulum method.

## 3.1. Test Conduct

The following sections provide the test conduct for the modal survey and bifilar pendulum tests performed on the V27 blades. Other methods were attempted, but they yielded poor results and are not discussed further.

### 3.1.1. Modal Survey

The modal survey was performed on site at SNL's SWIFT facility in Lubbock, Texas, on October 27–31, 2012. ATA was responsible for the installation and removal of all transducers and cabling necessary for the modal survey. All DOF locations on the blade were measured and marked on the surface by ATA. The measurement locations matched those in the test display model, as selected for visualization of the primary modes. After all of the measurement locations were mapped on the blade, the accelerometers and cables were installed.

Impact testing, using an instrumented modal impact hammer, was also performed to excite the structure and perform the modal survey.

The exciter locations for the V27 modal survey were identified during the pretest analysis effort and were selected based on prior experience testing wind turbine blades. The data acquisition system measured all data channels simultaneously, allowing all data to be taken in a single pass. A complete channel table list is provided in Appendix E.

In total, 44 runs were recorded. These included check-out, impact, sine-sweep, Multi-Sine,[2] and MPR runs. The test run log is provided in Table 3-1 below. The text in the "Notes" column provides brief details on each run and any anomalies encountered. The final test mode shapes were extracted from runs 3, 22, 29, 34, 38, and 43 for blades 1–6.

[2] The products, services, and technology described here may be protected by U.S. Pat. No. 8,281,659.

Table 3-1. SNL V27 modal survey test run log.

| 61178 Project Description Test Run Log | | | | | | RMS Force level (lbs) | | | | | | |
|---|---|---|---|---|---|---|---|---|---|---|---|---|
| Run | Date | Start Time | Config† | Blade # | Exc. | 10001 | 10002 | File Name | Block | Reference Channels | Freq Range (Hz) | |
| # | (auto) | <CTRL><T> | | | Type* | | | | Size | | | Notes |
| Testing day 1 | | | | | | | | | | | | |
| Blade 1 - SNL2 BL1 | | | | | | | | | | | | |
| 1 | 10/27/2012 | 14:07 | Flap | 1 | i | - | - | 61178_V27_001i_flap_1.ati | 8192 | 3502X- | 0-100 | Impact Run - Reglued some accel blocks |
| 2 | 10/27/2012 | 14:43 | Flap | 1 | i | - | - | 61178_V27_002i_flap_1.ati | 8192 | 3502X- | 0-100 | Impact Run - Scaling looks incorrect for ch5-8 |
| 3 | 10/27/2012 | 15:15 | Flap | 1 | i | - | - | 61178_V27_003i_flap_1.ati | 8192 | 3502X-, 3537Y+,2898Y+,878X- | 0-100 | Impact Run - Changed ch 5-8 to ch 61-64 |
| 4 | 10/27/2012 | 15:55 | Flap | 1 | r | 4.77 | 1.52 | 61178_V27_004r_flap_1.ati | 1601 | 10001, 10002 | 0-78 | Shaker Checkout |
| 5 | 10/27/2012 | 19:26 | Flap | 1 | r | 4.77 | 1.52 | 61178_V27_005r_flap_1.ati | 6401 | 10001, 10002 | 0-78 | Mass Inertia Modal Method |
| Testing day 2 | | | | | | | | | | | | |
| 6 | 10/28/2012 | 7:46 | Flap | 1 | b | 0.74 | 0.66 | 61178_V27_006b_flap_1.ati | 6401 | 10001, 10002 | 0-78 | Mass Inertia Modal Method - Shaker 1 Load Cell Changed |
| 7 | 10/28/2012 | 8:11 | Flap | 1 | b | 1.29 | 1.11 | 61178_V27_007b_flap_1.ati | 6401 | 10001, 10002 | 0-78 | Mass Inertia - Level 2 |
| 8 | 10/28/2012 | 8:28 | Flap | 1 | b | 1.29 | 1.11 | 61178_V27_008b_flap_1.ati | 1601 | 10001, 10002 | 0-78 | Mass Inertia - Level 2 - Shaker 1 Pigtail and Accel Changed (36857) |
| 9 | 10/28/2012 | 8:40 | Flap | 1 | b | 4.11 | 1.11 | 61178_V27_009b_flap_1.ati | 1601 | 10001, 10002 | 0-78 | Mass Inertia - Multi Level |
| 10 | 10/28/2012 | 8:54 | Flap | 1 | b | 10.32 | 2.10 | 61178_V27_010b_flap_1.ati | 1601 | 10001, 10002 | 0-78 | Mass Inertia - High Level |
| 11 | 10/28/2012 | 9:07 | Flap | 1 | b | 0.93 | 0.86 | 61178_V27_011b_flap_1.ati | 6401 | 10001, 10002 | 0-78 | Mass Inertia - Low Level, Large Block Size |
| 12 | 10/28/2012 | 10:06 | Flap | 1 | ms | - | - | 61178_V27_012ms_flap_1.ati | 6401 | 10001, 10002 | 0-78 | Mass Inertia - Multi Sine |
| 13 | 10/28/2012 | 10:35 | Flap | 1 | ms | - | - | 61178_V27_013ms_flap_1.ati | 6401 | 10001, 10002 | 0-78 | Mass Inertia - Multi Sine - Lower Level |
| 14 | 10/28/2012 | 15:36 | Flap | 1 | man | - | - | 61178_V27_014man_flap_1.ati | 101 | - | 0-25 | Pendulum |
| 15 | 10/28/2012 | 16:02 | Flap | 1 | man | - | - | 61178_V27_015man_flap_1.ati | 101 | - | 0-25 | Bifilar Flapwise |
| Testing day 3 | | | | | | | | | | | | |
| Blade 3 SNL2 - BI3 | | | | | | | | | | | | |
| 16 | 10/29/2012 | 8:16 | Flap | 3 | man | - | - | 61178_V27_016man_flap_3.ati | 101 | - | 0-25 | Pendulum |
| 17 | 10/29/2012 | 8:43 | Flap | 3 | man | - | - | 61178_V27_017man_flap_3.ati | 101 | - | 0-25 | Bifilar Flapwise |
| 18 | 10/29/2012 | 10:10 | Flap | 3 | man | - | - | 61178_V27_018man_flap_3.ati | 101 | - | 0-25 | Axial Pendulum |
| 19 | 10/29/2012 | 11:34 | Flap | 3 | man | - | - | 61178_V27_019man_flap_3.ati | 1601 | 488 X-,Y+,Z+ | 0-78 | RB Modes Checkout |
| 20 | 10/29/2012 | 12:07 | Flap | 3 | man | - | - | 61178_V27_020man_flap_3.ati | 1601 | - | 0-78 | RB Modes Checkout - Adjusted Bungee |
| 21 | 10/29/2012 | 13:09 | Flap | 3 | man | - | - | 61178_V27_021man_flap_3.ati | 1601 | - | 0-78 | RB Modes Checkout - Moved accel |
| 22 | 10/29/2012 | 14:00 | Flap | 3 | i | - | - | 61178_V27_022i_flap_3.ati | 8192 | 3502X- | 0-100 | Impact Test |
| 23 | 10/29/2012 | 16:46 | Flap | 3 | b | 1.42 | 1.27 | 61178_V27_023b_flap_3.ati | 4096 | 10001, 10002 | 0-40 | Low Level Burst Checkout |
| 24 | 10/29/2012 | 16:46 | Flap | 3 | b | 1.20 | 1.27 | 61178_V27_024b_flap_3.ati | 4096 | 10001, 10002 | 0-20 | Low Level Burst - 0-20 Hz |
| 25 | 10/29/2012 | 16:46 | Flap | 3 | b | 1.20 | 1.27 | 61178_V27_025b_flap_3.ati | 8192 | 10001, 10002 | 0-20 | Mass Inertia - Low Level, Large Block Size |
| Testing day 4 | | | | | | | | | | | | |
| Blade 2 SNL2 - BI2 | | | | | | | | | | | | |
| 26 | 10/30/2012 | 8:36 | Flap | 2 | man | - | - | 61178_V27_026man_flap_2.ati | 101 | - | 0-25 | Pendulum |
| 27 | 10/30/2012 | 8:49 | Flap | 2 | man | - | - | 61178_V27_027man_flap_2.ati | 101 | - | 0-25 | Bifilar Flapwise |
| 28 | 10/30/2012 | 9:34 | Flap | 2 | i | - | - | 61178_V27_028i_flap_2.ati | 8192 | 488 X-,Y+,Z+ | 0-25 | RB Mode Impact |
| 29 | 10/30/2012 | 11:07 | Flap | 2 | i | - | - | 61178_V27_029i_flap_2.ati | 8192 | 3502X-, 3537Y+, | 0-100 | Impact Test |
| Blade 4 SNL1 - BI1 | | | | | | | | | | | | |
| 30 | 10/30/2012 | 14:44 | Flap | 4 | man | - | - | 61178_V27_030man_flap_4.ati | 101 | - | 0-25 | Pendulum |
| 31 | 10/30/2012 | 14:59 | Flap | 4 | man | - | - | 61178_V27_031man_flap_4.ati | 101 | - | 0-25 | Bifilar Flapwise |
| 32 | 10/30/2012 | 15:26 | Flap | 4 | i | - | - | 61178_V27_032i_flap_4.ati | 8192 | 488 X-,Y+,Z+ | 0-25 | RB Mode Impact |
| 33 | 10/30/2012 | 16:33 | Flap | 4 | i | - | - | 61178_V27_033i_flap_4.ati | 8192 | 3502X-, 3537Y+, | 0-100 | Impact Test |
| 34 | 10/30/2012 | 17:05 | Flap | 4 | i | - | - | 61178_V27_034i_flap_4.ati | 8192 | 3502X-, 3537Y+, | 0-100 | Impact Test - Corrected Channels |

Table 3-1. SNL V27 modal survey test run log (continued).

| 61178 Project Description Test Run Log | | | | | | RMS Force level (lbs) | | | | | | |
|---|---|---|---|---|---|---|---|---|---|---|---|---|
| Run | Date | Start Time | Config† | Blade # | Exc. | 10001 | 10002 | File Name | Block Size | Reference Channels | Freq Range (Hz) | |
| # | (auto) | <CTRL><T> | | | Type* | | | | | | | Notes |
| Testing day 5 | | | | | | | | | | | | |
| Blade 5 SNL1 - BI3 | | | | | | | | | | | | |
| 35 | 10/31/2012 | 8:17 | Flap | 5 | man | - | - | 61178_V27_035man_flap_5.ati | 101 | - | 0-25 | Pendulum |
| 36 | 10/31/2012 | 8:28 | Flap | 5 | man | - | - | 61178_V27_036man_flap_5.ati | 101 | - | 0-25 | Bifilar Flapwise |
| 37 | 10/31/2012 | 8:39 | Flap | 5 | i | - | - | 61178_V27_037i_flap_5.ati | 8192 | 488 X-,Y+,Z+ | 0-25 | RB Mode Impact |
| 38 | 10/31/2012 | 9:49 | Flap | 5 | i | - | - | 61178_V27_038i_flap_5.ati | 8192 | 3502X-, 3502Y+, | 0-100 | Impact Test - Pendulum Support Locations |
| 39 | 10/31/2012 | 10:49 | Flap | 5 | i | - | - | 61178_V27_039i_flap_5.ati | 8192 | 3502X-, 3502Y+, | 0-100 | Impact Test |
| Blade 6 SNL1 - BI2 | | | | | | | | | | | | |
| 40 | 10/31/2012 | 14:07 | Flap | 6 | man | - | - | 61178_V27_040man_flap_6.ati | 101 | - | 0-25 | Pendulum |
| 41 | 10/31/2012 | 14:26 | Flap | 6 | man | - | - | 61178_V27_041man_flap_6.ati | 101 | - | 0-25 | Bifilar Flapwise |
| 42 | 10/31/2012 | 14:33 | Flap | 6 | i | - | - | 61178_V27_042i_flap_6.ati | 8192 | 488 X-,Y+,Z+ | 0-25 | RB Mode Impact |
| 43 | 10/31/2012 | 15:47 | Flap | 6 | i | - | - | 61178_V27_043i_flap_6.ati | 8192 | 3502X-, 3537Y+, | 0-100 | Impact Test - Pendulum Support Locations |
| 44 | 10/31/2012 | 16:41 | Flap | 6 | i | - | - | 61178_V27_044i_flap_6.ati | 8192 | 3502X-, 3537Y+, | 0-100 | Impact Test |

| * EXCITATION TYPE | | Blade Numbering |
|---|---|---|
| i | modal impact | Blade 1 = SNL2_BL1 |
| b | modal burst random | Blade 3 = SNL2_BL3 |
| ms | multi-sine sweep | Blade 2 = SNL2_BL2 |
| man | manual excitation | Blade 4 = SNL1_BL1 |
| **Configs** | | Blade 5 = SNL1_BL3 |
| Flap | Blade Tested on Edge | Blade 6 = SNL1_BL2 |

### 3.1.2. Inertia Property Estimation Using Bifilar Pendulum

The inertia property estimation was performed on site at SNL's SWIFT facility in Lubbock, Texas, on October 27–31, 2012. ATA was responsible for proving the instrumentation and supports needed for testing. The theory used in this test, the bifilar pendulum technique, is briefly discussed below.

The bifilar pendulum technique uses a torsional pendulum located about the CG of an object to determine the mass moment of inertia, as shown in Figure 3-1.

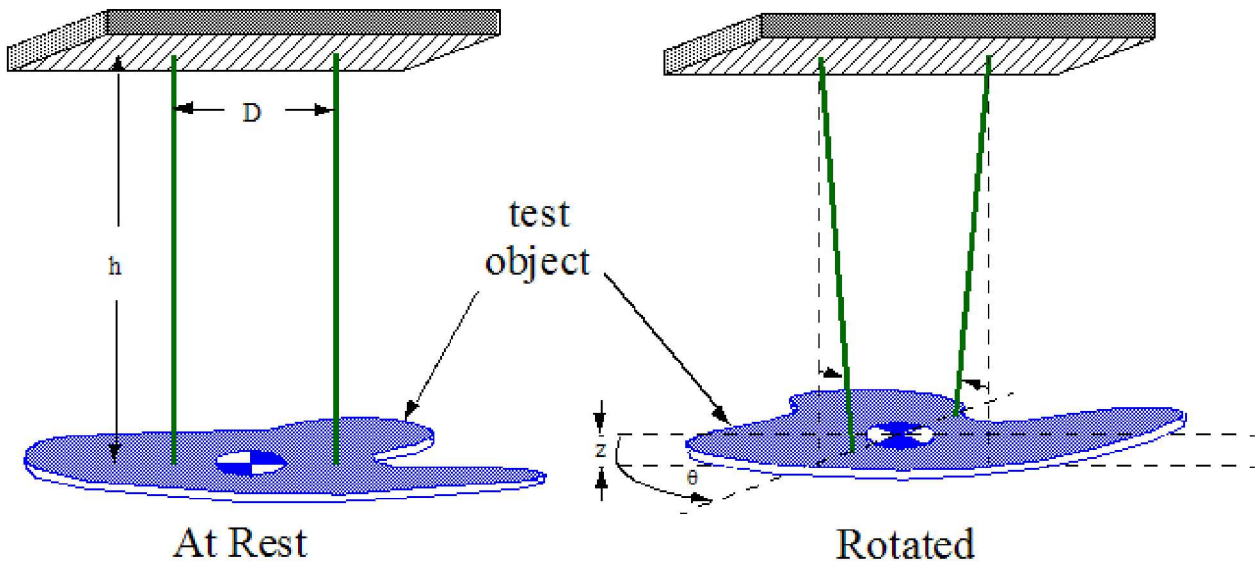


Figure 3-1. Principle of bifilar pendulum.

The key summary equation is

$$I = \frac{Mgx^2T^2}{L}\frac{1}{4\pi^2} \qquad \text{Equation 3-1}$$

where M is the mass of the object, g is the gravitational constant, x is the distance from the CG to the support, T is the period of time required to undergo one revolution, and L is the length of the pendulum. For an irregularly shaped object, this test must be completed in all three axes to obtain $I_{xx}$, $I_{yy}$ and $I_{zz}$.

### 3.2. Test Instrumentation

Modal response data were measured using accelerometers mounted on the blade, and an impact hammer with an attached load cell was used to measure the amount of force applied to the blade. Load cells were also installed between the electrodynamic shakers (used to apply the excitation force) and the blade to measure the amount of force applied. ATA provided all instrumentation required to complete the test. This included the impact hammer, shakers, shaker amplifiers, sine-sweep generator, transducer signal conditioning, data acquisition hardware, and data collection and analysis computers. SNL provided gantry cranes and the technicians to lift and move the blade.

All of the accelerometer cabling was routed and plugged into gather boxes at a central location near the data acquisition system. A photograph of ATA's workstation is shown in Figure 3-2.

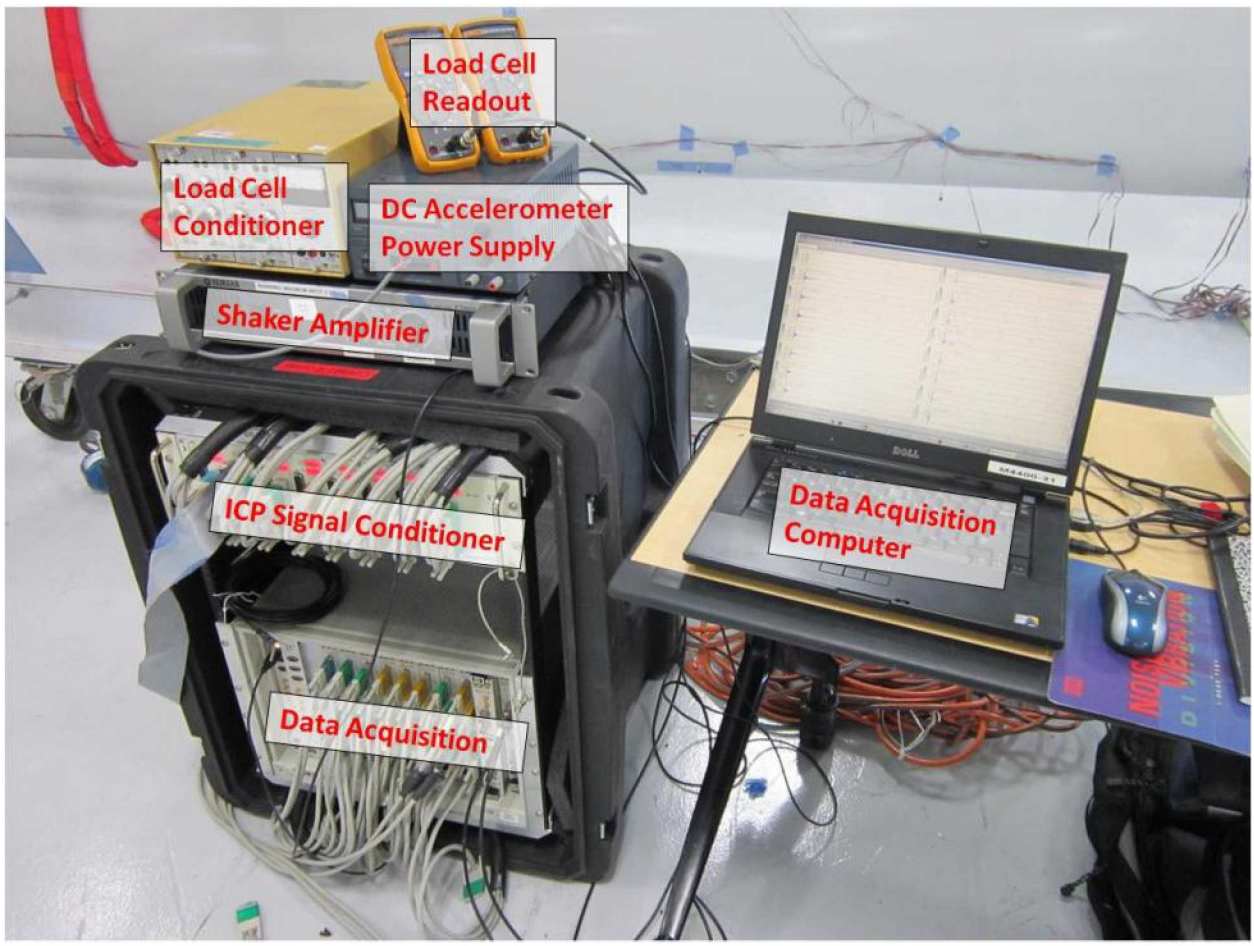


Figure 3-2. Data acquisition equipment and analysis workstations.

The DB-50 cables were then routed from the gather boxes to the data acquisition system. A photograph of the gather boxes and cabling is shown in Figure 3-3.

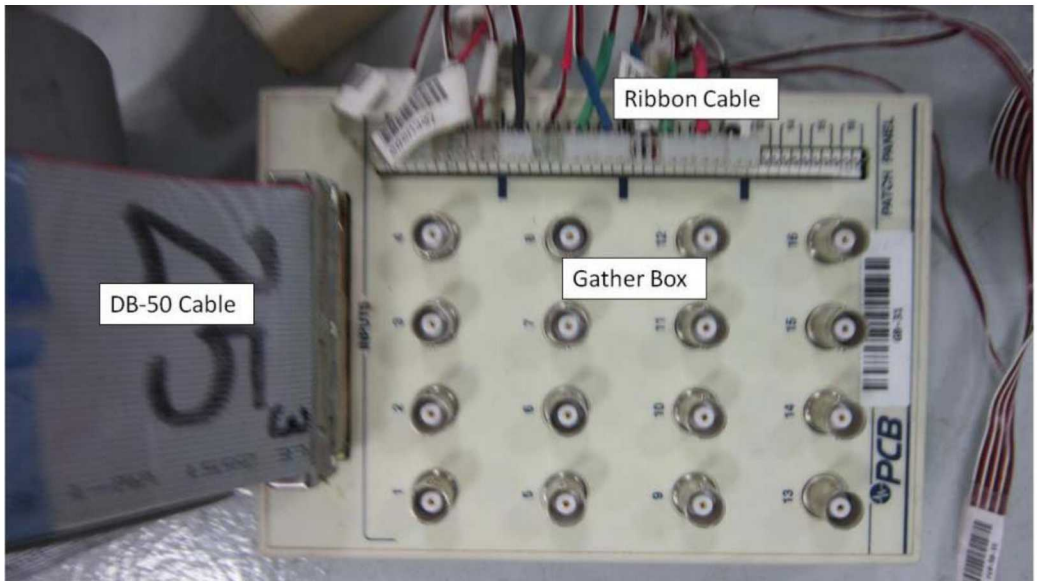


Figure 3-3. Instrumentation cabling was routed to gather boxes where DB-50 cables were then used to connect to the data acquisition system.

The DB-50 cables that connected to the VXI data acquisition system are shown in Figure 3-3. All equipment specifications are provided in Appendix G.

All of the DC accelerometers were routed to DIN rails, shown in Figure 3-4, which were powered by an external power supply. Pigtail-to-BNC cables were used to connect the DIN rails to the data acquisition system.

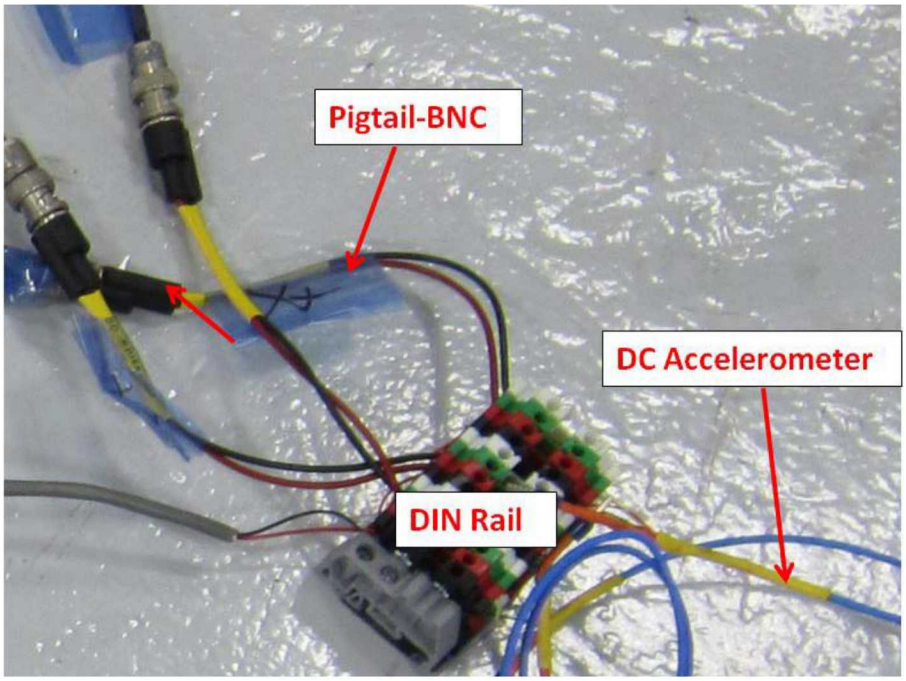


Figure 3-4. DC accelerometers were routed to DIN rails where pigtail-to-BNC cables were then used to connect to the data acquisition system.

### 3.2.1. Accelerometers

All of the accelerometers installed for the modal survey were defined using the global Cartesian coordinate system. Photos of all of the accelerometer locations are provided in Appendix C. The global coordinate system was changed after the test to comply with the standard wind turbine blade coordinate system. As a result, all accelerometer photos have an incorrect node direction. The coordinate transformation is shown in Figure 3-5.

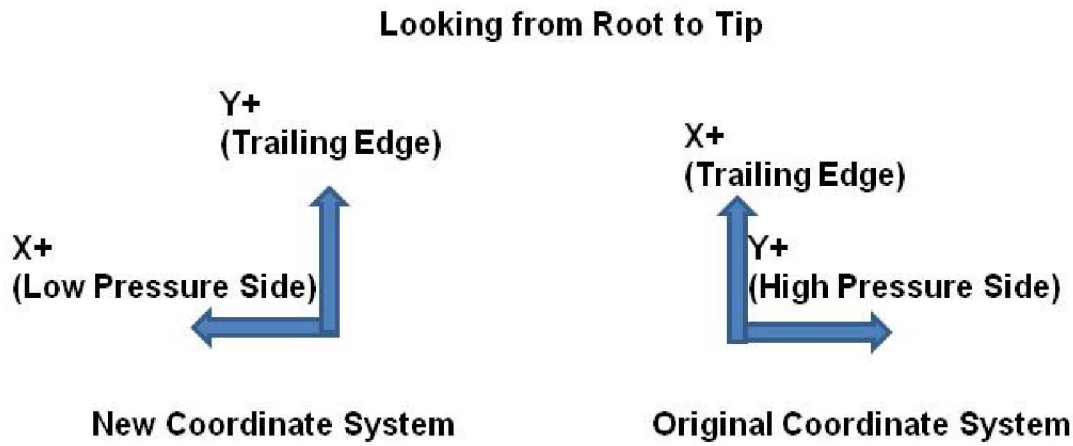


Figure 3-5. V27 test coordinate system transformation.

Accelerometers were attached as needed to mounting blocks, allowing correct alignment to the proper displacement coordinate system. Cube blocks permitted the attachment of up to three accelerometers per block and allowed tangential measurements. Semicylindrical accelerometer mounting blocks and bubble levels were used to orient some accelerometers to the coordinate system. The blocks also ensured that the accelerometers were electrically isolated from the blade. ATA provided the blocks that were used to attach accelerometers to the blade. Figure 3-6 shows an example of the accelerometer installation, including the cube and barcodes used to document the measurement location.

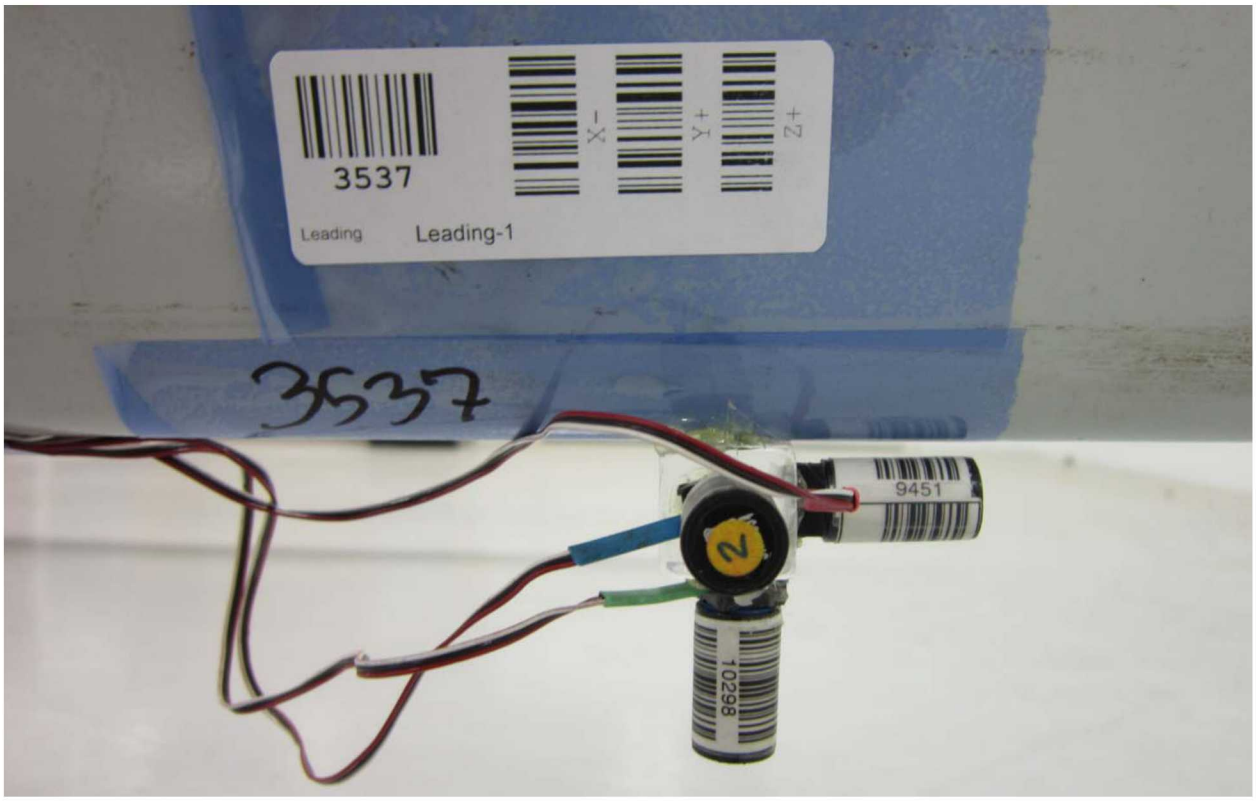


Figure 3-6. Example accelerometer installation; note the barcode used for documenting the accelerometer location.

Each accelerometer was labeled with a barcode that identified its serial number. These barcode labels were scanned with a special Palm™ handheld, which stored the information in its database. The Palm's database was then downloaded to a database on the acquisition computer, which was used to set up the channel table in the data acquisition system.

Acceleration values of 0.001 to 0.5 g (maximum) were anticipated for the modal survey. The accelerometers used for the modal survey were PCB model T333B piezoelectric, integrated circuit preamplifier (ICP®) type and were capable of measuring accelerations accurately (± 5%) from 2 to 1,000 Hz. The transducers were powered by signal-conditioning units supplied by ATA and included transducer electronic data sheet (TEDS) information, which allowed the amplifier to recognize each serial number for all of the accelerometers. Specification sheets for the accelerometers are included in Appendix G of this report. The calibrated sensitivities and calibration due dates for all accelerometers used for this test are included in Appendix E.

Acceleration values of 0.001 to 0.5 g (maximum) were anticipated for the rigid body survey. The accelerometers used for the modal survey were PCB model 3741D4HB30G, capable of measuring accelerations accurately (± 5%) from 0 to 1000 Hz. The accelerometers were powered by an external power supply producing 15 V at 0.5 A.

Test instrumentation logs were prepared and maintained to show the location of each accelerometer, along with its serial number and sensitivity.

### 3.2.2. Force Transducers

Force transducers (load cells) were provided at each of the shaker input locations. All load cell transducers were piezoelectric devices (PCB Model 208C03), each of which can measure up to 500 pounds of force in the frequency range of 1 to 36,000 Hz. The calibration values and due dates for all load cells used for this test are included in Appendix E.

The load cell measurements were used to set the open-loop excitation levels and compute the FRF for the blade. These force levels were recorded and documented using a computation of the power spectral density (PSD) and the overall root mean square (RMS) for the entire frequency band. Figure 3-7 shows the PSD for the input force of both shakers from MPR run 25.

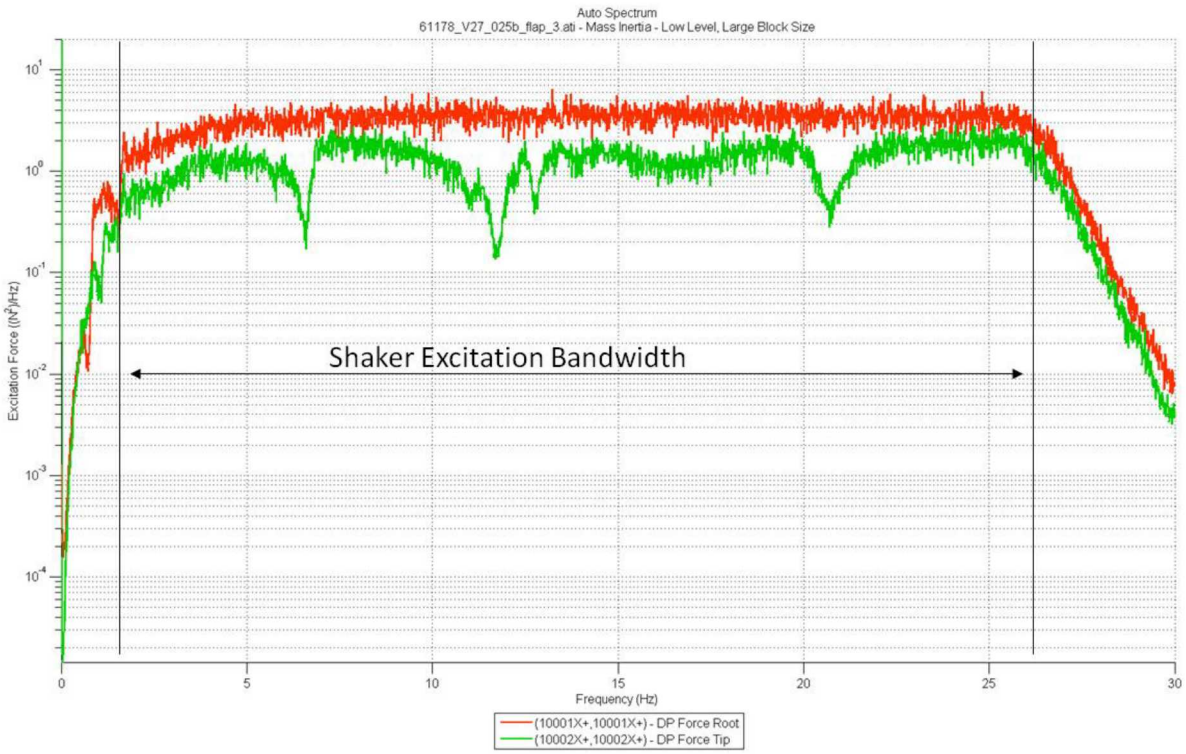


Figure 3-7. PSD for both shaker inputs, MPR run 25.

Additional static load cells (Interface Model #1210) were used to determine the mass and CG of the blade by suspending the blade at the two locations as shown in Figure 3-8; the CG was able to be determined based on the locations of the two straps and the load measured on each.

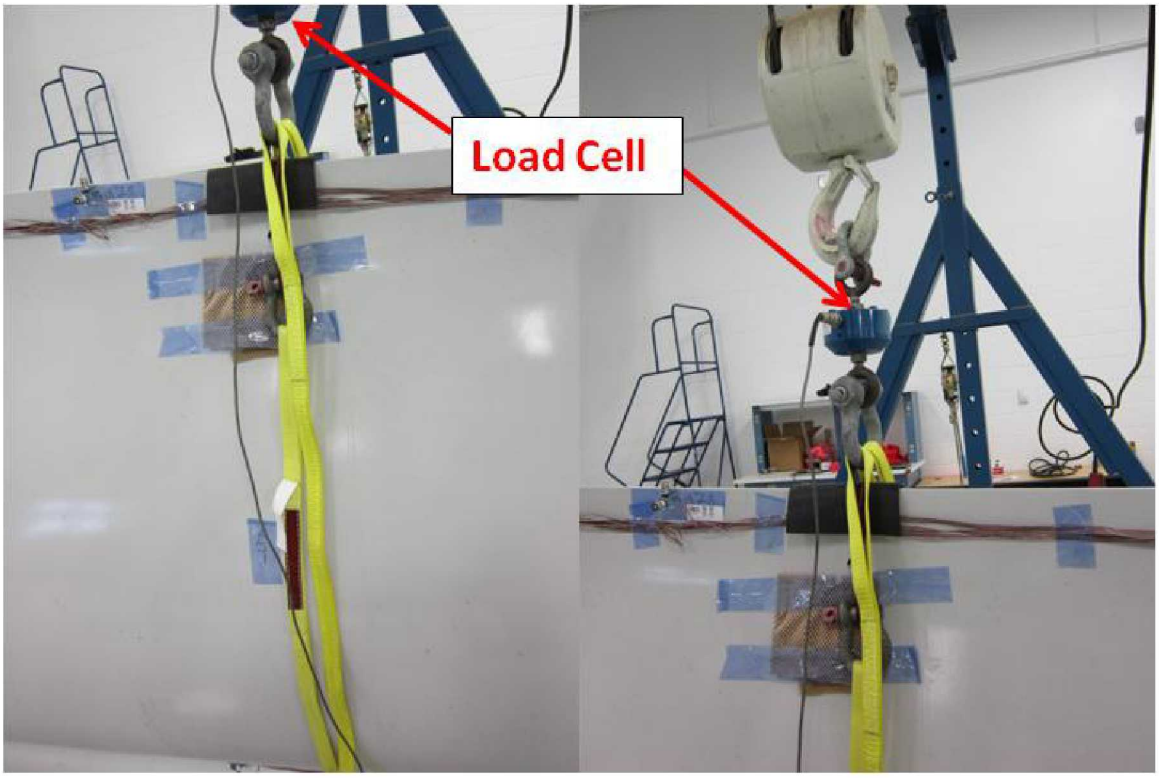


Figure 3-8. Load cells used to calculate mass and CG.

### 3.2.3. Impact Hammer

The impact hammer load cell transducer is a piezoelectric device (PCB Model 086D20) that can measure up to 5000 pounds of force in the frequency range of 1 to 12,000 Hz. The calibration values and due dates for the impact hammer used for this test are included in Appendix E. The hammer tip chosen (PCB Model 084A60) was used due to the low-frequency bandwidth excitation. The auto power spectrum for a typical impact is shown in Figure 3-9.

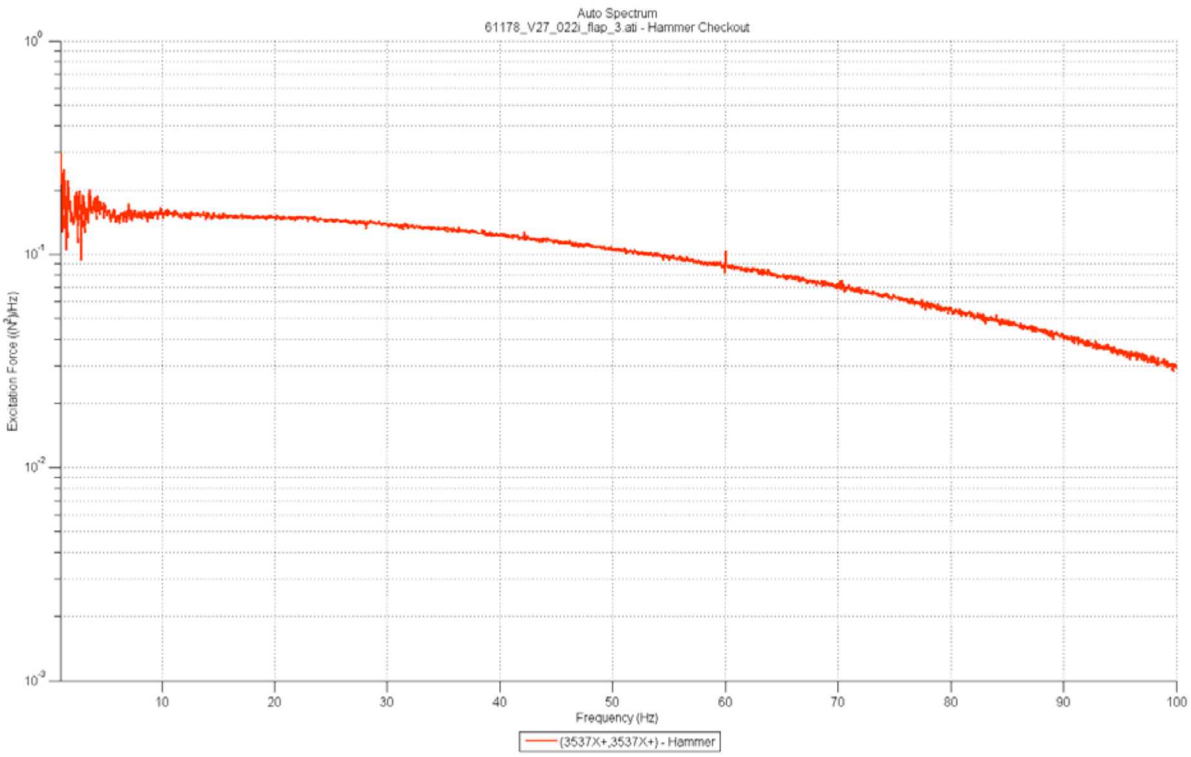


Figure 3-9. PSD for impact hammer, run 22.

### 3.2.4. Electrodynamic Shakers

The V27 modal survey required two shakers to apply simultaneous excitation during the MPR runs. ATA supplied the 110-pound MB Dynamics electrodynamic shakers. One shaker was attached at a skewed angle to the root end and the other was attached at a skewed angle to the tip. These positions provided for adequate excitation of all modes of the blade.

All shakers used plastic stingers that transmitted a direct force with minimal bending moment. The stingers are rigid enough to transmit unattenuated axial force within the frequency range of interest. Attachment between the shaker system and the blade was made through attachment blocks that were glued to the tip and root of the blade. The load cell transducers were attached to the blocks, and the stingers completed the connections between the transducers and the shakers as shown in Figure 3-10. Pictures of each shaker configuration are shown in Appendix D.

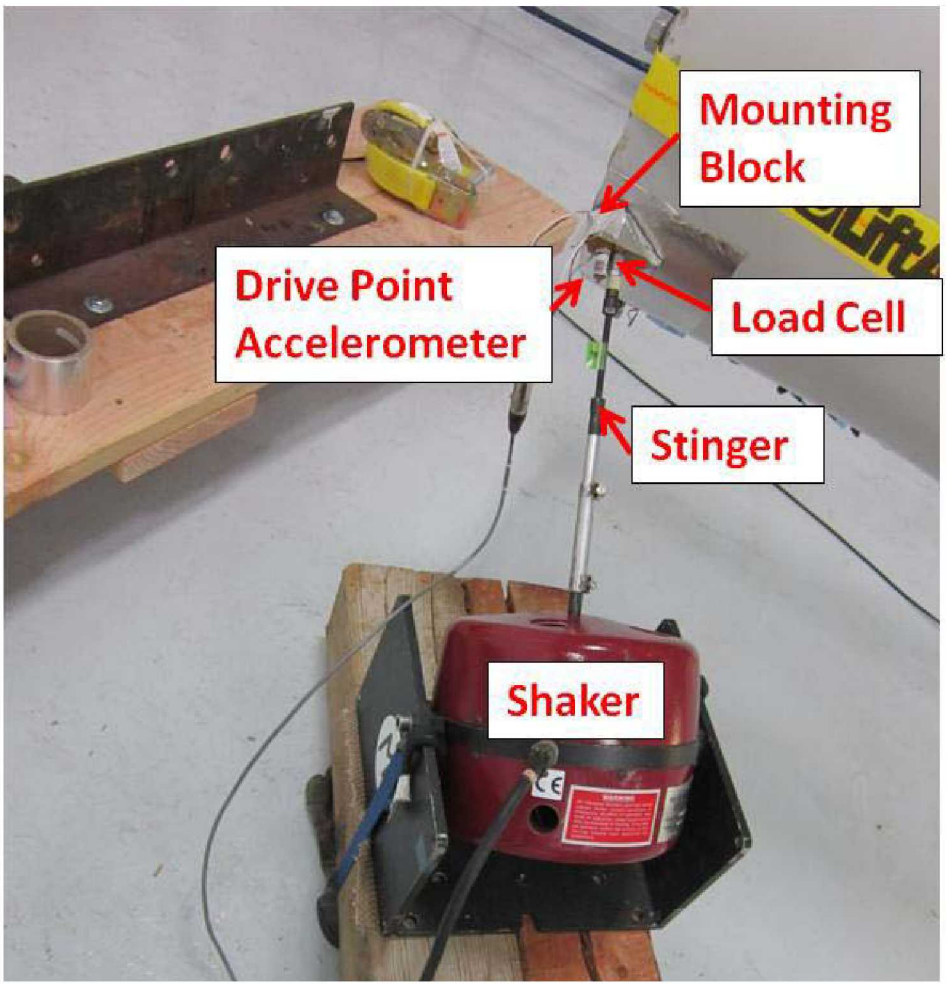


Figure 3-10. Shaker attachment with drive point accelerometer.

### 3.2.5. DC Accelerometers

The DC accelerometers were used for the bifilar pendulum testing to accurately capture the frequency of the rigid body mode. The blade was manually excited at the natural frequency of the mode and was allowed to freely oscillate and decay. A representative time and auto spectrum, shown in Figure 3-11, indicate the natural frequency of the mode due to the spike in the response at that frequency.

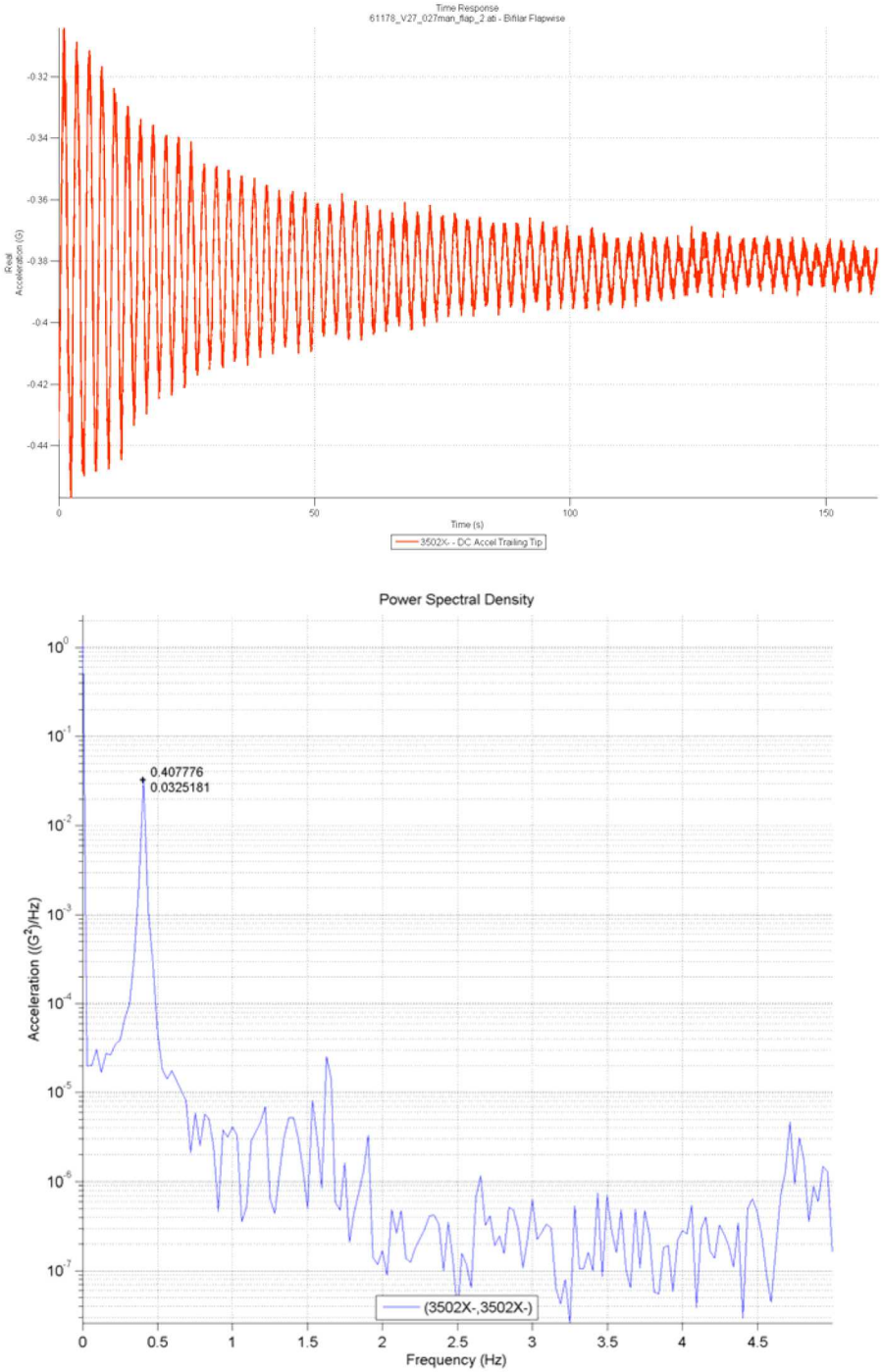


Figure 3-11. Time and spectra of DC accelerometer for bifilar pendulum test run 27.

### 3.2.6. Data Measurement and Recording

All time history, auto spectrum, coherence, and FRF data were stored on the hard disk of the data acquisition computer. All data were written to an external hard disk as a backup at the conclusion of each test day. After completion of the modal survey, the data were transferred onto the computer system at ATA's San Diego office, where the final data analysis was performed and the report written.

A schematic layout of the data collection system is shown in Figure 3-12. The system utilized a 128-channel VXI Technology digitizing front-end hardware system with 1432A analog-to-digital converter modules. The data acquisition chassis was then connected to the laptop computer through a FireWire interface card. All input forces and all response measurements were acquired simultaneously, which allowed all data to be collected in a single pass, thus reducing overall test time. The data acquisition computer was a laptop PC, and one additional computer at the test site was used for analysis and documentation. Brüel & Kjær I-deas® Test software and ATA's IMAT™ software were run on these computers to acquire and process the data. Processing included extracting the modal parameters from the FRF and evaluating the data quality and mode shapes.

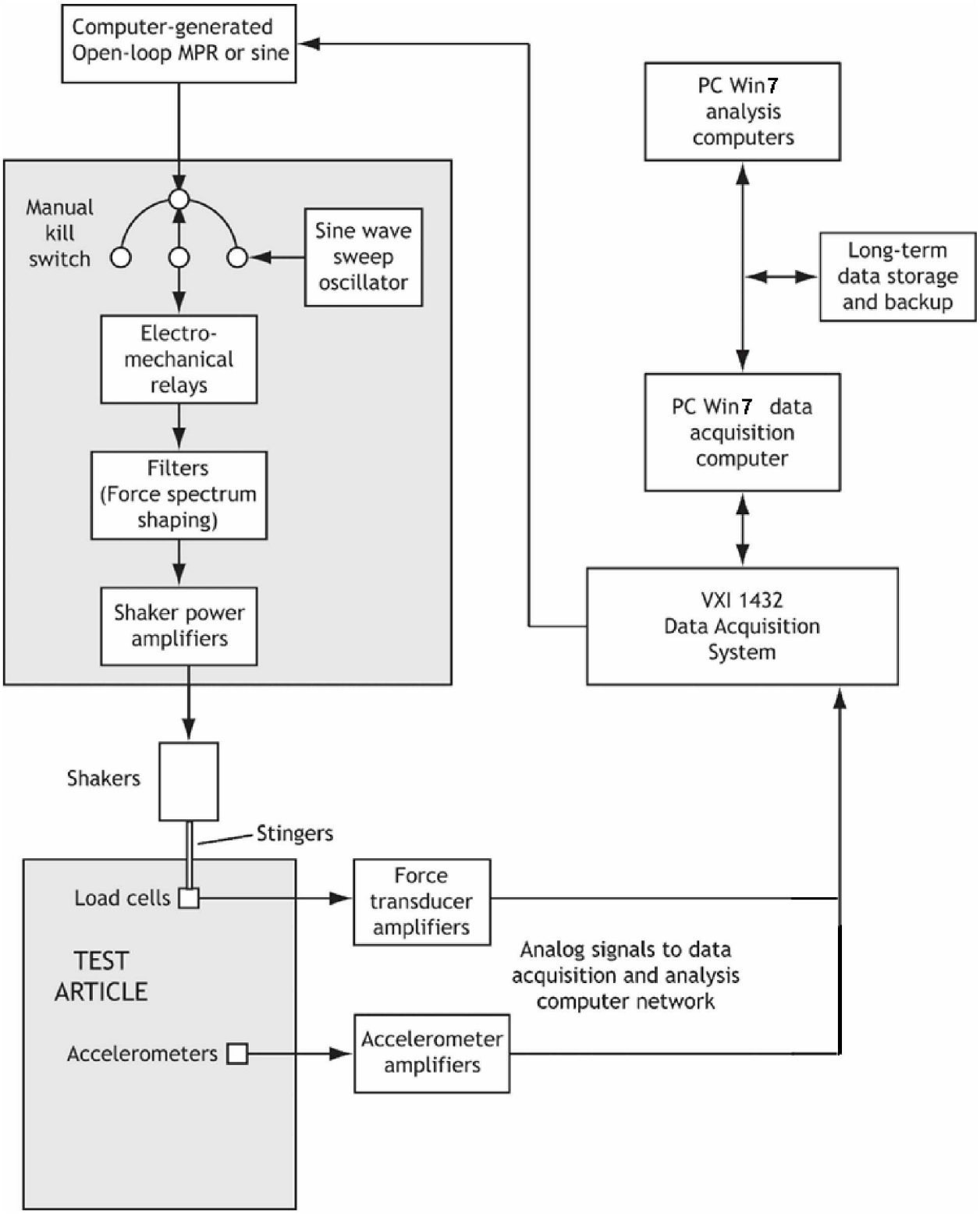


Figure 3-12. Data acquisition system schematic.

## 3.3. Test Performance

One computer was used acquire data, while the other on-site data processing computer was used to extract modal parameter information from the FRF data. The FRF data were processed to determine the resonant frequencies, mode shapes, and modal damping. Preliminary data analysis was performed as soon as the FRF were available for processing. This allowed for a quick study of the dynamic characteristics of the blade. It also allowed the data quality to be verified through the use of coherence, complex mode-indicator functions (CMIF), multivariate mode-indicator functions (MMIF), power spectrum mode-indicator functions (PSMIF), and FRF quality. Quick processing of the data into mode shapes permitted the modal assurance criteria (MAC) and self-orthogonality to be computed between the test shapes, which helped to verify the independence of the extracted modes. Back-expansion of test shapes from the measured DOF to the full test display DOF allowed visual verification that all target modes had been identified. These preliminary data were shared with SNL engineers at the test site.

### 3.3.1. Data Quality Assessment

After acquisition, processing, and on-site analysis of the test data were completed, all of the data were reviewed by ATA and SNL engineers to ensure that the test objectives and the criteria for satisfaction of the test objectives had been attained.

During the data collection process, the response signals on the acquisition computer screen were monitored continuously, and data quality was evaluated immediately after the collection of each data set by examining the force spectra (shown previously in Figure 3-7), coherence, reciprocity, and FRF quality.

Coherence functions that were computed during the acquisition process were all stored, along with the auto spectrum and FRF for each channel. In this manner, any questions about data quality could be assessed by reviewing specific coherence functions associated with a particular response measurement. Figure 3-13 shows the FRF and coherence for the drive point impact hammer location 3502X– for run 22.

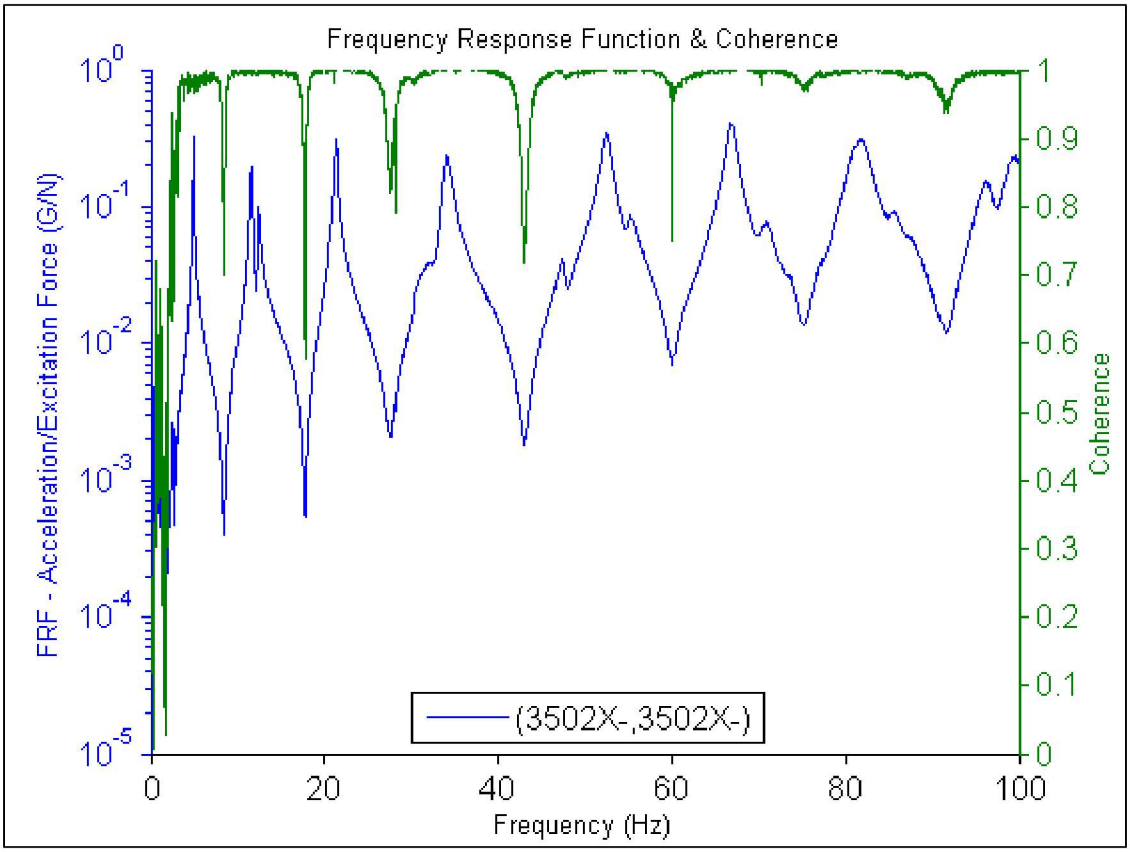


Figure 3-13. FRF and coherence for impact hammer drive point 3502X–, run 22.

In addition to the coherence review as a check of data quality, reciprocity was checked between shaker locations. Figure 3-14 shows the reciprocity comparison obtained between shakers 1 and 2 for run 13. The two functions shown indicate good reciprocity.

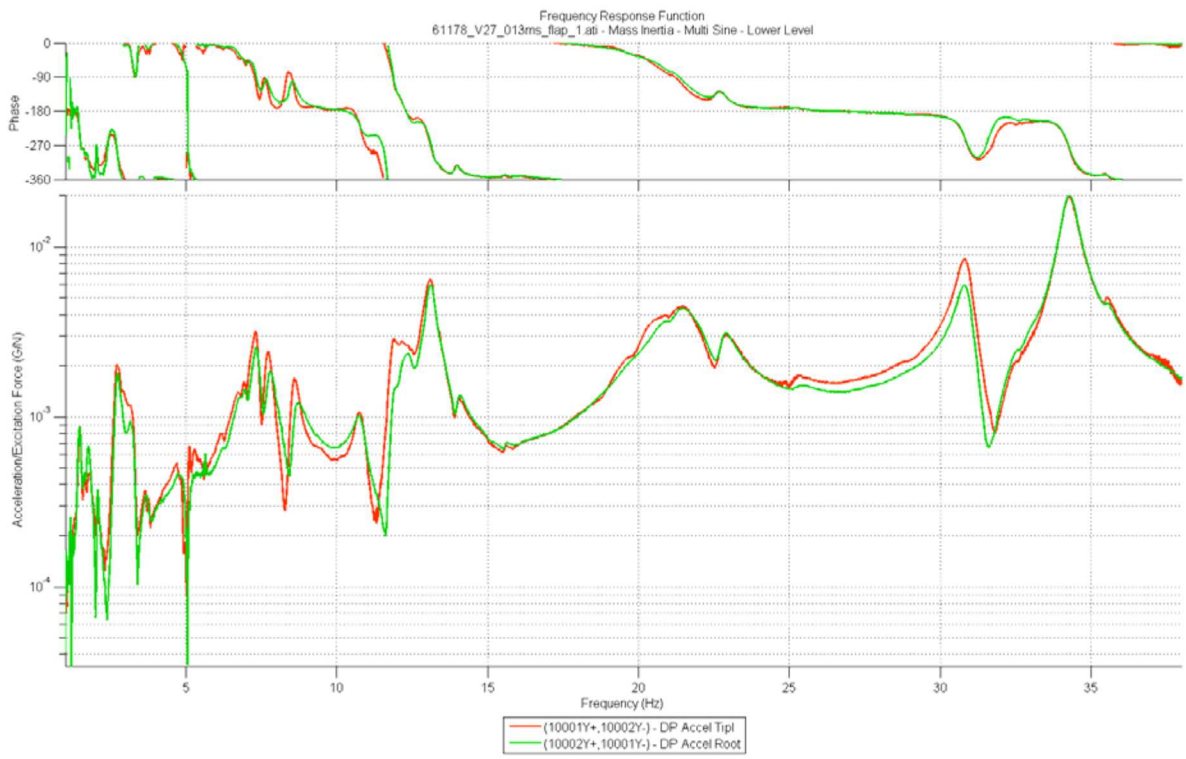


Figure 3-14. Reciprocity comparison between shakers 1 and 2, run 13.

### 3.3.2. Modal Extraction

The first indications of resonance were determined by evaluating the FRF, in particular the drive point FRF. Peaks showing dynamic amplification were tagged for documentation. Natural frequencies were verified by looking at the minimums of the MIF and MMIF, maximums of the PSMIF, and peaks indicated by the FRF. All of the modal parameters were extracted from the FRF. These modal parameters include the natural frequency, damping, and corresponding mode shapes. The modal data extracted from the FRF were evaluated while the blade was still available so that any modes that had not been clearly identified could be studied further. Data collected during MPR excitation were used to extract the final modal parameters.

The alias-free polyreference algorithm was the primary method used to extract the modal information from the test data. Real normal modes were computed directly from the test data. Damping was estimated using the same polyreference FRF curve-fitting algorithm that was used to extract the resonant frequencies. The alias-free polyreference technique in ATA's AFPoly™ IMAT toolkit employs a Laplace-domain curve-fitting algorithm capable of extracting lightly or highly damped modes in a single pass.

Data processing that was not completed during the test program was finalized at ATA following the test. Ongoing data analysis was performed at the test site as further testing was being performed. Final listings of modal frequencies, shapes, and damping estimates are provided in Section 4.

### 3.3.3. Modal Assurance Criteria

Once test modes were extracted from the data, evaluation of the modes was performed on site. This approach helped to confirm that all primary (target) modes of interest had been characterized.

The MAC was computed for the test modes to obtain an indication of the independence of the modes as directly measured. The MAC is a scalar value between zero and one representing the correlation between two mode shapes. High correlation is indicated by a value near one. The MAC value between two mode shapes is computed using the following vector inner products.

$$MAC_{12} = \frac{\left|\{\Phi_1\}^H \{\Phi_2\}\right|^2}{\{\Phi_1\}^H \{\Phi_1\}\{\Phi_2\}^H \{\Phi_2\}} \qquad \text{Equation 3-2}$$

The vectors $\Phi_1$ and $\Phi_2$ are the mode shapes being compared.

### 3.3.4. Orthogonality

Since a pretest model had been developed, the analytic mass matrix was available at the test site. This made it possible to compute orthogonality of the test modes relative to the analytic mass matrix.

The modes acquired from the test measurements were checked for orthogonality using the TAM analytical mass matrix. The orthogonality matrix $[O_{12}]$ is computed from the following matrix product.

$$[O_{12}] = [\Phi_1]^T [M_{AA}][\Phi_2] \qquad \text{Equation 3-3}$$

The terms $[\Phi_1]$ and $[\Phi_2]$ are mode shapes matrices (normalized to $[M_{AA}]$ to produce 1.0 on the $[O_{12}]$ diagonal), and $[M_{AA}]$ is the TAM analytical mass matrix. The self-orthogonality of the test mode shapes relative to the analytic mass matrix was computed from Equation 3-4 with $[\Phi_1] = [\Phi_2]$.

An additional orthogonality check was performed as a measure of correlation between test and analytical modes. This cross-orthogonality check is expressed in Equation 3-5, where $[\Phi_1]$ are test mode shapes and $[\Phi_2]$ are analysis mode shapes. Cross-orthogonality was evaluated during the test to assess whether the test had defined the predicted modes of the structure. The result, however, was not used as a criterion for acceptance of test data.

Ideally, an acquired mode will be perfectly orthogonal with respect to all of the other modes, and the modal coefficients for each DOF will contain only the contribution of the mode of interest. However, the various practical limitations in actual testing that render the attainment of perfect modal orthogonality nearly impossible include the following:

1. Extremely high modal density (several modes close in frequency)
2. Any inaccuracy or insufficiency of the acquired data
3. The possibility of the exciter location being at or near a node point of the target mode
4. Any inaccuracy of the mass matrix used for orthogonality checks
5. Any interference of uninstrumented and nonstructural component modes

# 4. TEST RESULTS

This section of the report documents the results of the V27 modal survey program. The summary tables include the modal parameters identified from the experimental data. As discussed previously, the modes of interest were all six rigid body modes, the first three flexible flapwise bending modes, the first three edgewise bending modes, and the first torsion mode. Most of the parameter estimation effort was focused on identifying these modes. All flexible target modes were extracted successfully, as were the mass, CG, and moment of inertia about the Y-axis.

Test self-MAC and orthogonality calculations, along with visual inspection of the shapes, were used to verify the uniqueness of modes reported for each configuration. The MAC and orthogonality values presented were calculated using all of the test DOF.

Test-to-analysis MACs and orthogonality matrices (cross-MAC and cross-orthogonality) are also included in this section. The test target modes demonstrated poor compatibility with the pretest analysis modes due to known correlation issues with the FEM. More details regarding modal extraction are provided in the following sections.

A back-expansion matrix was used to fill in the unmeasured DOF at each test node to improve the ability to visualize the mode shapes. For example, an accelerometer measured DOF 1465X– and Y– but not the accelerations in the corresponding Z direction. The back-expansion uses the TAM constraint matrix to interpolate these missing DOF for purposes of visualization only. The mode shapes presented in Appendix F include the back-expanded DOF. The MAC and orthogonality calculations did not use the back-expanded shapes.

This section of the report also documents the results of the V27 mass inertia testing. The summary tables include the mass and inertia parameters identified from the experimental data. As discussed previously, CG, mass, and inertia were the key items of interest, and the CG in the Z-axis, mass, and moment of inertia about the Y-axis were obtained successfully.

## 4.1. V27 Final Modes

A single V27 configuration was tested to obtain the modal results: the V27 blade mounted suspended by bungees at two locations (the nodes of the first flap bending mode). All target modes of this configuration were identified. Two excitation methods were used during testing, and the majority of the modes were successfully extracted from impact hammer test runs 3, 22, 29, 34, 38, and 43 for blades 1–6. The test run number corresponds to the test run log presented in Table 3-1.

The list of modes, sorted by test mode shape frequency, is provided in Table 4-1. This table lists the shape description, priority, test frequency, and damping for all six blades tested. Mode shape plots are provided in Appendix F.

Table 4-1. V27 final global modes sorted by test frequency.

| Mode # | Description | Blade Frequency (Hz) | | | | | | Average (Hz) | Max Difference (%) | Priority |
|---|---|---|---|---|---|---|---|---|---|---|
| | | SNL1 - BL1 | SNL1 - BL2 | SNL1 - BL3 | SNL2 - BL1 | SNL2 - BL2 | SNL2- BL3 | | | |
| 1 | 1st Flapwise | 4.79 | 4.80 | 4.94 | 4.90 | 4.82 | 4.88 | 4.86 | 3.16 | P |
| 2 | 2nd Flapwise | 11.30 | 11.40 | 11.89 | 11.64 | 11.41 | 11.55 | 11.53 | 5.27 | P |
| 3 | 1st Edgewise | 12.35 | 12.37 | 12.67 | 12.66 | 12.29 | 12.35 | 12.45 | 3.08 | P |
| 4 | 3rd Flapwise | 21.49 | 21.40 | 21.97 | 21.54 | 21.69 | 21.29 | 21.56 | 3.19 | P |
| 5 | 2nd Edgewise | 30.10 | 29.96 | 30.86 | 31.05 | 30.59 | 30.26 | 30.47 | 3.64 | P |
| 6 | 1st Torsion | 34.70 | 30.58 | 31.08 | 33.11 | 32.40 | 32.43 | 32.38 | 13.47 | S |
| 7 | 4th Flapwise | 33.60 | 34.24 | 34.90 | 34.64 | 34.64 | 34.04 | 34.34 | 3.88 | O |
| 8 | 2nd Torsion | 50.46 | 47.75 | 48.66 | 50.02 | 51.69 | 52.53 | 50.19 | 10.01 | S |
| 9 | 3rd Edgewise | 55.36 | 55.50 | 57.74 | 56.89 | 56.10 | 55.19 | 56.13 | 4.62 | P |

The orthogonality matrices for the V27 final modes are provided in Table 4-2 for the two full sets of instrumentation blades (SNL2_BL1 and SNL2_BL3) and in Table 4-3 for all six blades For the test self-orthogonality displayed in Table 4-2 and Table 4-3, high diagonal values and low off-diagonal values were obtained, indicating good mode uniqueness and high correlation between the different blades.

Table 4-2. V27 final test modes (SNL2_BL1 and SNL2_BL3 at full instrumentation set): self-orthogonality.

| Test Self Orthogonality Table | | | | | | | | | | | | | | | | | | | |
|---|---|---|---|---|---|---|---|---|---|---|---|---|---|---|---|---|---|---|---|
| | | Test Shapes | | | | SNL2_BL1 | | | | | | | | SNL2_BL3 | | | | | |
| | | | 1 | 2 | 3 | 4 | 5 | 6 | 7 | 8 | 9 | 10 | 11 | 12 | 13 | 14 | 15 | 16 | 17 | 18 |
| | | Ott | 4.9 | 11.6 | 12.7 | 21.5 | 31.1 | 33.1 | 34.6 | 50.0 | 56.9 | 4.9 | 11.5 | 12.3 | 21.3 | 30.3 | 32.4 | 34.0 | 52.5 | 55.2 |
| Test Shapes | 1 | 4.9 | 1.00 | | | | | | | | | 0.99 | | | | | | | | |
| | 2 | 11.6 | | 1.00 | | | | | | | | | 0.99 | | | | | | | |
| | 3 | 12.7 | | | 1.00 | | | | | | | | | 0.99 | | | | | | |
| | 4 | 21.5 | | | | 1.00 | | | | | | | | | 0.97 | | | | | |
| | 5 | 31.1 | | | | | 1.00 | | | | | | | | | 0.87 | | | | |
| SNL2_BL1 | 6 | 33.1 | | | | | | 1.00 | 0.56 | | | | | | | | 0.98 | 0.69 | | |
| | 7 | 34.6 | | | | | | 0.56 | 1.00 | | | | | | | | | 0.98 | | |
| | 8 | 50.0 | | | | | | | | 1.00 | | | | | | | | | 0.98 | 0.52 |
| | 9 | 56.9 | | | | | | | | | 1.00 | | | | | | | | | 0.95 |
| | 10 | 4.9 | 0.99 | | | | | | | | | 1.00 | | | | | | | | |
| | 11 | 11.5 | | 0.99 | | | | | | | | | 1.00 | | | | | | | |
| | 12 | 12.3 | | | 0.99 | | | | | | | | | 1.00 | | | | | | |
| | 13 | 21.3 | | | | 0.97 | | | | | | | | | 1.00 | | | | | |
| SNL2_BL3 | 14 | 30.3 | | | | | 0.87 | | | | | | | | | 1.00 | | | | |
| | 15 | 32.4 | | | | | | 0.98 | | | | | | | | | 1.00 | 0.61 | | |
| | 16 | 34.0 | | | | | | 0.69 | 0.98 | | | | | | | | 0.61 | 1.00 | | |
| | 17 | 52.5 | | | | | | | | 0.98 | | | | | | | | | 1.00 | 0.51 |
| | 18 | 55.2 | | | | | | | | 0.52 | 0.95 | | | | | | | | 0.51 | 1.00 |

Table 4-3. V27 final test modes (all six blades at reduced instrumentation set): self-orthogonality.

Test Self Orthogonality Table

| | | | Test Shapes | SNL1_BL1 | | | | | | | | | SNL1_BL2 | | | | | | | | | | SNL1_BL3 | | | | | | | | | | SNL2_BL1 | | | | | | | | | | SNL2_BL2 | | | | | | | | | | SNL2_BL3 | | | | | |
|---|---|---|---|---|---|---|---|---|---|---|---|---|---|---|---|---|---|---|---|---|---|---|---|---|---|---|---|---|---|---|---|---|---|---|---|---|---|---|---|---|---|---|---|---|---|---|---|---|---|---|---|---|---|---|---|---|---|---|---|---|
| | | | | 1 | 2 | 3 | 4 | 5 | 6 | 7 | 8 | 9 | 10 | 11 | 12 | 13 | 14 | 15 | 16 | 17 | 18 | 19 | 20 | 21 | 22 | 23 | 24 | 25 | 26 | 27 | 28 | 29 | 30 | 31 | 32 | 33 | 34 | 35 | 36 | 37 | 38 | 39 | 40 | 41 | 42 | 43 | 44 | 45 | 46 | 47 | 48 | 49 | 50 | 51 | 52 | 53 | 54 |
| | | | Ott | 4.8 | 11.3 | 12.3 | 21.5 | 30.1 | 33.6 | 34.7 | 50.5 | 55.4 | 4.8 | 11.4 | 12.4 | 21.4 | 30.0 | 30.6 | 34.2 | 47.8 | 55.5 | 4.9 | 11.9 | 12.7 | 22.0 | 30.9 | 31.1 | 34.9 | 48.7 | 57.7 | 4.9 | 11.6 | 12.7 | 21.5 | 31.1 | 33.1 | 34.6 | 50.0 | 56.9 | 4.8 | 11.4 | 12.3 | 21.7 | 30.6 | 32.4 | 34.6 | 51.7 | 56.1 | 4.9 | 11.5 | 12.3 | 21.3 | 30.3 | 32.4 | 34.0 | 52.5 | 55.2 |
| Test Shapes | 1 | 4.8 | | 1.00 | | | 0.91 | | | | 0.53 | | 0.96 | | | 0.90 | | | | | | 0.98 | | | 0.95 | | | | 0.55 | | 0.99 | | | 0.93 | | | | | | 0.98 | | | 0.82 | | | 0.56 | | 0.98 | | | 0.94 | | | | | |
| | 2 | 11.3 | | | 1.00 | | | | | | | 0.66 | | 1.00 | | | | | | | 0.61 | | 0.99 | | | | | | | 0.53 | | 0.99 | | | | | | | 0.64 | | 0.96 | | | 0.52 | | | | 0.52 | | 0.99 | | | | | | | 0.64 |
| | 3 | 12.3 | | | | 1.00 | | | | | | | | | 0.99 | | | | | | 0.55 | | | 0.99 | | | | | | 0.61 | | | 1.00 | | | | | | 0.51 | | | 0.98 | | | | | | | | 0.99 | | | | | | 0.58 |
| | 4 | 21.5 | 0.91 | | | | 1.00 | | 0.73 | 0.70 | 0.64 | | 0.92 | | | 1.00 | | | 0.67 | | | 0.90 | | | 0.99 | | | 0.72 | 0.65 | | 0.91 | | | 0.99 | | | 0.69 | | | 0.85 | | | 0.91 | | 0.52 | 0.76 | | | 0.88 | | | 0.98 | | 0.64 | 0.62 | | |
| | 5 | 30.1 | | | | | | 1.00 | | | | 0.89 | | 0.55 | | | 0.98 | | | | 0.91 | | | | | 0.97 | 0.81 | | | 0.79 | | | | | 1.00 | | | | 0.88 | | | | | 0.99 | | | | | 0.88 | | | | | 1.00 | | | | 0.91 |
| SNL1_BL1 | 6 | 33.6 | | | | | 0.73 | | 1.00 | 0.91 | 0.60 | | | | | 0.72 | | | 0.94 | | | | | | 0.68 | | | 0.98 | 0.56 | | | | | 0.71 | | | 0.96 | | | | | | 0.73 | | 0.58 | 0.90 | | | | | | 0.69 | | 0.76 | 0.90 | | |
| | 7 | 34.7 | | | | | 0.70 | | 0.91 | 1.00 | 0.64 | 0.57 | | | | 0.72 | | | 0.90 | 0.53 | 0.55 | | | | 0.65 | | | 0.87 | 0.58 | 0.53 | | | | 0.66 | | | 0.91 | | 0.58 | | | | 0.62 | | 0.50 | 0.87 | | 0.53 | | | | 0.64 | | 0.64 | 0.84 | | 0.59 |
| | 8 | 50.5 | 0.53 | | | | 0.64 | | 0.60 | 0.64 | 1.00 | | 0.53 | | | 0.66 | | | 0.66 | 0.86 | | 0.51 | | | 0.63 | | | 0.65 | 0.98 | | 0.52 | | | 0.64 | | | 0.66 | 0.94 | | | | | 0.64 | | | 0.66 | 0.68 | | 0.52 | | | 0.66 | | | 0.67 | 0.83 | |
| | 9 | 55.4 | | | 0.66 | | | 0.89 | | 0.57 | | 1.00 | | 0.71 | | | 0.87 | | | | 0.99 | | 0.60 | 0.50 | | 0.84 | 0.75 | | | 0.73 | | 0.58 | 0.51 | | 0.87 | | | | 1.00 | | | 0.58 | | 0.88 | | | | | 0.96 | | 0.62 | 0.53 | | 0.87 | | | | 0.98 |
| | 10 | 4.8 | 0.96 | | | | 0.92 | | | | 0.53 | | 1.00 | | | 0.92 | | | | | | 0.98 | | | 0.94 | | | | 0.55 | | 0.97 | 0.50 | | 0.93 | | | | | | 0.92 | | | 0.85 | | | 0.54 | | | 0.95 | | | 0.94 | | | | | |
| | 11 | 11.4 | | 1.00 | | | | 0.55 | | | | 0.71 | | 1.00 | | | 0.53 | | | | 0.67 | | 0.98 | | | | | | | 0.57 | | 0.97 | | | 0.52 | | | | 0.70 | | 0.94 | | | 0.59 | | | | 0.58 | | 0.98 | | | | 0.52 | | | | 0.70 |
| | 12 | 12.4 | | | | 0.99 | | | | | | | | | 1.00 | | | | | | | | | 0.98 | | | | | | 0.53 | | | 0.99 | | | | | | | | | 0.95 | | | | | | | | | 0.98 | | | | | | |
| | 13 | 21.4 | 0.90 | | | | 1.00 | | 0.72 | 0.72 | 0.66 | | 0.92 | | | 1.00 | | | 0.67 | | | 0.88 | | | 0.98 | | | 0.71 | 0.66 | | 0.90 | | | 0.98 | | | 0.69 | 0.50 | | 0.84 | | | 0.90 | | | 0.76 | | | 0.87 | | | 0.97 | | 0.61 | 0.62 | | |
| SNL1_BL2 | 14 | 30.0 | | | | | | 0.98 | | | | 0.87 | | 0.53 | | | 1.00 | | | | 0.89 | | | | | 0.90 | 0.90 | | | 0.75 | | | | | 0.97 | | | | 0.87 | | | 0.52 | | 0.98 | | | | | 0.87 | | | | | 0.99 | | | | 0.90 |
| | 15 | 30.6 | | | | | | | | | | | | | | | | 1.00 | | | | | | | | | | | | | | | | | | 0.86 | | | | | | | | | | 0.90 | | | | | | | | 0.85 | | | | |
| | 16 | 34.2 | | | | | 0.67 | | 0.94 | 0.90 | 0.66 | | | | | 0.67 | | | 1.00 | | | | | | 0.62 | | | 0.97 | 0.64 | | | | | 0.64 | | | 0.99 | | | | | | 0.70 | | | 0.89 | | | | | | 0.63 | | 0.53 | 0.98 | | |
| | 17 | 47.8 | | | | | | | | 0.53 | 0.86 | | | | | | | | | 1.00 | | | | | | | | | 0.80 | | | | | | | | | 0.82 | | | | | | | | | | 0.50 | | | | | | | | | 0.73 | |
| | 18 | 55.5 | | | 0.61 | 0.55 | | 0.91 | | 0.55 | | 0.99 | | 0.67 | | | 0.89 | | | | 1.00 | | 0.55 | 0.57 | | 0.87 | 0.75 | | | 0.79 | | 0.52 | 0.57 | | 0.90 | | | | 0.99 | | | 0.64 | | 0.91 | | | | | 0.95 | | 0.56 | 0.59 | | 0.90 | | | | 0.99 |
| | 19 | 4.9 | 0.98 | | | | 0.90 | | | | 0.51 | | 0.98 | | | 0.88 | | | | | | 1.00 | | | 0.94 | | | | 0.55 | | 0.99 | | | 0.93 | | | | | | 0.96 | | | 0.86 | | | 0.54 | | | 0.99 | | | 0.94 | | | | | |
| | 20 | 11.9 | | 0.99 | | | | | | | | 0.60 | | 0.98 | | | | | | | 0.55 | | 1.00 | | | | | | | | | 0.99 | | | | | | | 0.58 | | 0.98 | | | | | | | | | | 1.00 | | | | | | | 0.57 |
| | 21 | 12.7 | | | 0.99 | | | | | | | 0.50 | | | 0.98 | | | | | | 0.57 | | | 1.00 | | | | | | 0.60 | | | 1.00 | | | | | | 0.52 | | | 0.98 | | 0.50 | | | | | | | 0.99 | | | | | | 0.59 |
| SNL1_BL3 | 22 | 22.0 | 0.95 | | | | 0.99 | | 0.68 | 0.65 | 0.63 | | 0.94 | | | 0.98 | | | 0.62 | | | 0.94 | | | 1.00 | | | 0.69 | 0.65 | | 0.96 | | | 1.00 | | | 0.65 | 0.51 | | 0.92 | | | 0.92 | | | 0.74 | | | 0.94 | | | 1.00 | | 0.59 | 0.59 | | |
| | 23 | 30.9 | | | | | | 0.97 | | | | 0.84 | | | | | 0.90 | | | | 0.87 | | | | | 1.00 | 0.64 | | | 0.80 | | | | | 0.98 | | | | 0.83 | | | | | 0.94 | | | | | 0.84 | | | | | 0.95 | | | | 0.86 |
| | 24 | 31.1 | | | | | | 0.81 | | | | 0.75 | | | | | 0.90 | | | | 0.75 | | | | | 0.64 | 1.00 | | | 0.55 | | | | | 0.76 | 0.65 | | | 0.75 | | | | | 0.83 | | | | | 0.74 | | | | | 0.83 | | | | 0.76 |
| | 25 | 34.9 | | | | | 0.72 | | 0.98 | 0.87 | 0.65 | | | | | 0.71 | | | 0.97 | | | | | | 0.69 | | | 1.00 | 0.63 | | | | | 0.71 | | | 0.98 | | | | | | 0.77 | | | 0.91 | | | | | | 0.71 | | 0.64 | 0.96 | | |
| | 26 | 48.7 | 0.55 | | | | 0.65 | | 0.56 | 0.58 | 0.98 | | 0.55 | | | 0.66 | | | 0.64 | 0.80 | | 0.55 | | | 0.65 | | | 0.63 | 1.00 | | 0.56 | | | 0.66 | | | 0.65 | 0.94 | | 0.51 | | | 0.67 | | | 0.68 | 0.67 | | 0.56 | | | 0.68 | | | 0.67 | 0.86 | |
| | 27 | 57.7 | | 0.53 | 0.61 | | | 0.79 | | 0.53 | | 0.73 | | 0.57 | 0.53 | | 0.75 | | | | 0.79 | | | 0.60 | | 0.80 | 0.55 | | | 1.00 | | | 0.61 | | 0.79 | | | | 0.72 | | | 0.67 | | 0.78 | | | | 0.67 | | | 0.59 | | 0.79 | | | | 0.83 |
| | 28 | 4.9 | 0.99 | | | | 0.91 | | | | 0.52 | | 0.97 | | | 0.90 | | | | | | 0.99 | | | 0.96 | | | | 0.56 | | 1.00 | | | 0.94 | | | | | | 0.98 | | | 0.84 | | | 0.56 | | | 0.99 | | | 0.95 | | | | | |
| | 29 | 11.6 | | 0.99 | | | | | | | | 0.58 | 0.50 | 0.97 | | | | | | | 0.52 | | 0.99 | | | | | | | | | 1.00 | | | | | | | 0.56 | | 0.99 | | | | | | | | | | 1.00 | | | | | | 0.55 |
| | 30 | 12.7 | | | 1.00 | | | | | | | 0.51 | | | 0.99 | | | | | | 0.57 | | | 1.00 | | | | | | 0.61 | | | 1.00 | | | | | | 0.52 | | | 0.98 | | 0.51 | | | | | | | 1.00 | | 0.51 | | | | 0.60 |
| SNL2_BL1 | 31 | 21.5 | 0.93 | | | | 0.99 | | 0.71 | 0.66 | 0.64 | | 0.93 | | | 0.98 | | | 0.64 | | | 0.93 | | | 1.00 | | | 0.71 | 0.66 | | 0.94 | | | 1.00 | | | 0.67 | 0.51 | | 0.90 | | | 0.93 | | 0.50 | 0.76 | | | 0.93 | | | 1.00 | | 0.61 | 0.61 | | |
| | 32 | 31.1 | | | | | | 1.00 | | | | 0.87 | | 0.52 | | | 0.97 | | | | 0.90 | | | | | 0.98 | 0.76 | | | 0.79 | | | | | 1.00 | | | | 0.87 | | | 0.50 | | 0.98 | | | | | 0.87 | | | | | 0.99 | | | | 0.90 |
| | 33 | 33.1 | | | | | | | | | | | | | | | | 0.86 | | | | | | | | | 0.65 | | | | | | | | | 1.00 | | | | | | | | | | 0.90 | | | | | | | | 0.87 | | | | |
| | 34 | 34.6 | | | | | 0.69 | | 0.96 | 0.91 | 0.66 | | | | | 0.69 | | | 0.99 | | | | | | 0.65 | | | 0.98 | 0.65 | | | | | 0.67 | | | 1.00 | | | | | | 0.73 | | | 0.90 | | | | | | 0.66 | | 0.55 | 0.98 | | |
| | 35 | 50.0 | | | | | | | | | 0.94 | | | | | 0.50 | | | | 0.82 | | | | | 0.51 | | | | 0.94 | | | | | 0.51 | | | | 1.00 | | | | | 0.52 | | | 0.51 | 0.79 | | | | | 0.53 | | | 0.52 | 0.92 | |
| | 36 | 56.9 | | | 0.64 | 0.51 | | 0.88 | | 0.58 | | 1.00 | | 0.70 | | | 0.87 | | | | 0.99 | | 0.58 | 0.52 | | 0.83 | 0.75 | | | 0.72 | | 0.56 | 0.52 | | 0.87 | | | | 1.00 | | | 0.60 | | 0.88 | | | | | 0.96 | | 0.60 | 0.55 | | 0.87 | | | | 0.98 |
| | 37 | 4.8 | 0.98 | | | | 0.85 | | | | | | 0.92 | | | 0.84 | | | | | | 0.96 | | | 0.92 | | | | 0.51 | | 0.98 | | | 0.90 | | | | | | 1.00 | | | 0.76 | | | 0.53 | | | 0.99 | | | 0.91 | | | | | |
| | 38 | 11.4 | | 0.96 | | | | | | | | | | 0.94 | | | | | | | | | 0.98 | | | | | | | | | 0.99 | | | | | | | | | 1.00 | | | | | | | | | | 0.98 | | | | | | |
| SNL2_BL2 | 39 | 12.3 | | | 0.98 | | | | | | | 0.58 | | | 0.95 | | 0.52 | | | | 0.64 | | | 0.98 | | | | | | 0.67 | | | 0.98 | | 0.50 | | | | 0.60 | | | 1.00 | | 0.57 | | | | | | | 0.98 | | 0.54 | | | | 0.67 |
| | 40 | 21.7 | 0.82 | | | | 0.91 | | 0.73 | 0.62 | 0.64 | | 0.85 | | | 0.90 | | | 0.70 | | | 0.86 | | | 0.92 | | | 0.77 | 0.67 | | 0.84 | | | 0.93 | | | 0.73 | 0.52 | | 0.76 | | | 1.00 | | | 0.68 | | | 0.85 | | | 0.93 | | 0.55 | 0.71 | | |
| | 41 | 30.6 | | | 0.52 | | | 0.99 | | | | 0.88 | | 0.59 | | | 0.98 | | | | 0.91 | | | 0.50 | | 0.94 | 0.83 | | | 0.78 | | | 0.51 | | 0.98 | | | | 0.88 | | | 0.57 | | 1.00 | | | | | 0.84 | | | 0.54 | | 0.99 | | | | 0.91 |
| | 42 | 32.4 | | | | | 0.52 | | 0.58 | 0.50 | | | | | | | | 0.90 | | | | | | | | | | | | | | | | 0.50 | | 0.90 | | | | | | | | | | 1.00 | | | | | | | | 0.94 | | | | |
| | 43 | 34.6 | 0.56 | | | | 0.76 | | 0.90 | 0.87 | 0.66 | | 0.54 | | | 0.76 | | | 0.89 | | | 0.54 | | | 0.74 | | | 0.91 | 0.68 | | 0.56 | | | 0.76 | | | 0.90 | 0.51 | | 0.53 | | | 0.68 | | | 1.00 | | | 0.55 | | | 0.76 | | 0.54 | 0.88 | | |
| | 44 | 51.7 | | | | | | | | | 0.68 | | | | | | | | | 0.50 | | | | | | | | | 0.67 | | | | | | | | | 0.79 | | | | | | | | | 1.00 | | | | | | | | | 0.79 | |
| | 45 | 56.1 | | 0.52 | | | | 0.88 | | 0.53 | | 0.96 | | 0.58 | | | 0.87 | | | | 0.95 | | | | | 0.84 | 0.74 | | | 0.67 | | | | | 0.87 | | | | 0.96 | | | | | 0.84 | | | | | 1.00 | | | | | 0.86 | | | | 0.93 |
| | 46 | 4.9 | 0.98 | | | | 0.88 | | | | 0.52 | | 0.95 | | | 0.87 | | | | | | 0.99 | | | 0.94 | | | | 0.56 | | 0.99 | | | 0.93 | | | | | | 0.99 | | | 0.85 | | | 0.55 | | | 1.00 | | | 0.94 | | | | | |
| | 47 | 11.5 | | 0.99 | | | | | | | | 0.62 | | 0.98 | | | | | | | 0.56 | | 1.00 | | | | | | | | | 1.00 | | | | | | | 0.60 | | 0.98 | | | | | | | | | | 1.00 | | | | | | 0.59 |
| | 48 | 12.3 | | | 0.99 | | | | | | | 0.53 | | | 0.98 | | | | | | 0.59 | | | 0.99 | | | | | | 0.59 | | | 1.00 | | | | | | 0.55 | | | 0.98 | | 0.54 | | | | | | | 1.00 | | 0.53 | | | | 0.62 |
| SNL2_BL3 | 49 | 21.3 | 0.94 | | | | 0.98 | | 0.69 | 0.64 | 0.66 | | 0.94 | | | 0.97 | | | 0.63 | | | 0.94 | | | 1.00 | | | 0.71 | 0.68 | | 0.95 | | | 1.00 | | | 0.66 | 0.53 | | 0.91 | | | 0.93 | | | 0.76 | | | 0.94 | | | 1.00 | | 0.56 | 0.62 | | |
| | 50 | 30.3 | | | | | | 1.00 | | | | 0.87 | | 0.52 | | | 0.99 | | | | 0.90 | | | | | 0.95 | 0.83 | | | 0.79 | | | 0.51 | | 0.99 | | | | 0.87 | | | 0.54 | | 0.99 | | | | | 0.86 | | | 0.53 | | 1.00 | | | | 0.90 |
| | 51 | 32.4 | | | | | 0.64 | | 0.76 | 0.64 | | | | | | 0.61 | | 0.85 | 0.53 | | | | | | 0.59 | | | 0.64 | | | | | | 0.61 | | 0.87 | 0.55 | | | | | | 0.55 | | 0.94 | 0.54 | | | | | | 0.56 | | 1.00 | | | |
| | 52 | 34.0 | | | | | 0.62 | | 0.90 | 0.84 | 0.67 | | | | | 0.62 | | | 0.98 | | | | | | 0.59 | | | 0.96 | 0.67 | | | | | 0.61 | | | 0.98 | 0.52 | | | | | 0.71 | | | 0.88 | | | | | | 0.62 | | | 1.00 | | |
| | 53 | 52.5 | | | | | | | | | 0.83 | | | | | | | | | 0.73 | | | | | | | | | 0.86 | | | | | | | | | 0.92 | | | | | | | | | 0.79 | | | | | | | | | 1.00 | |
| | 54 | 55.2 | | 0.64 | 0.58 | | 0.91 | | 0.59 | | | 0.98 | | 0.70 | | | 0.90 | | | | 0.99 | | 0.57 | 0.59 | | 0.86 | 0.76 | | | 0.83 | | 0.55 | 0.60 | | 0.90 | | | | 0.98 | | | 0.67 | | 0.91 | | | | | 0.93 | | 0.59 | 0.62 | | 0.90 | | | | 1.00 |

A linearity check was performed using multiple levels of excitation. The overall structure was relatively linear over the frequency range of interest (2–80 Hz). The power spectrum mode indicator function (PSMIF) is shown in Figure 4-1 for three different levels of MPR excitation. Because the PSMIF is the summation of all FRF multiplied by each FRF conjugate, it is an ideal function to allow a global study of nonlinearity. The PSMIF plotted in Figure 4-1 are summed from both references (shakers 1 and 2), and they demonstrate good linearity in both frequency and magnitude with increasing force input. Figure 4-2 presents three FRF in total: one drive point FRF each from runs 9, 10, and 11. Good blade linearity is demonstrated in this plot as well, and the modal peaks are visible for each of the six target modes.

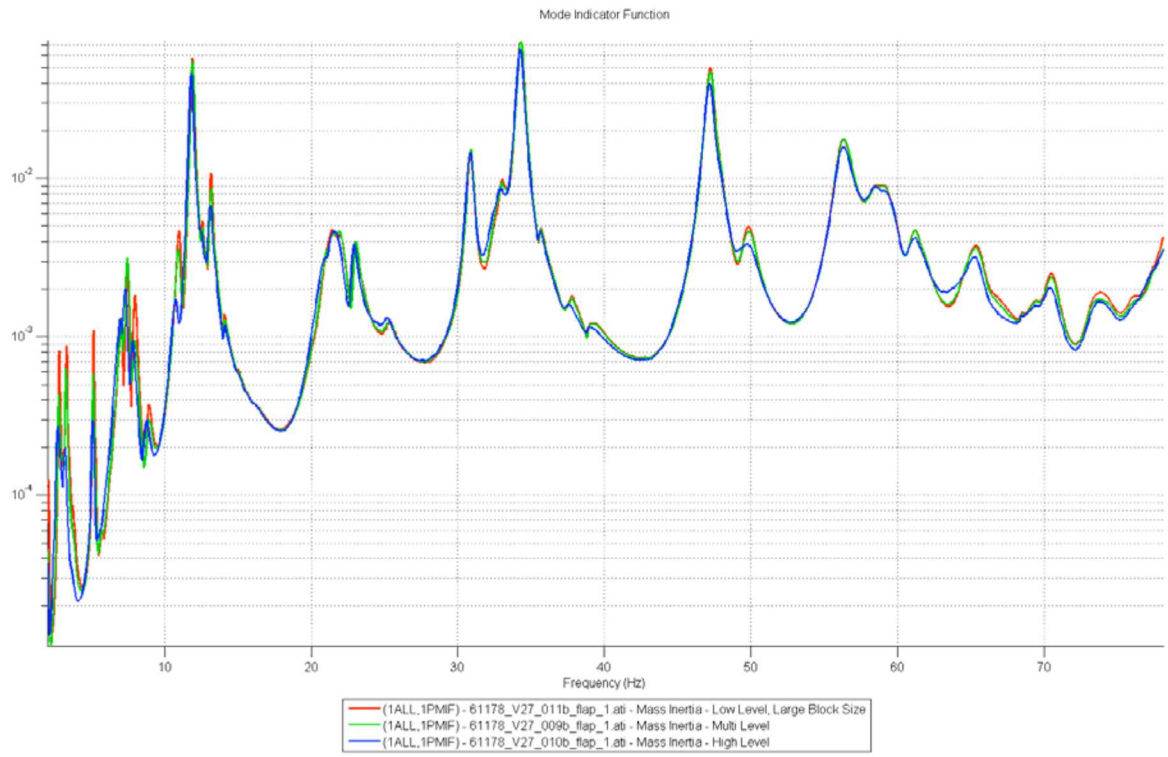


Figure 4-1. Linearity check observing PSMIF from MPR runs 9, 10, and 11.

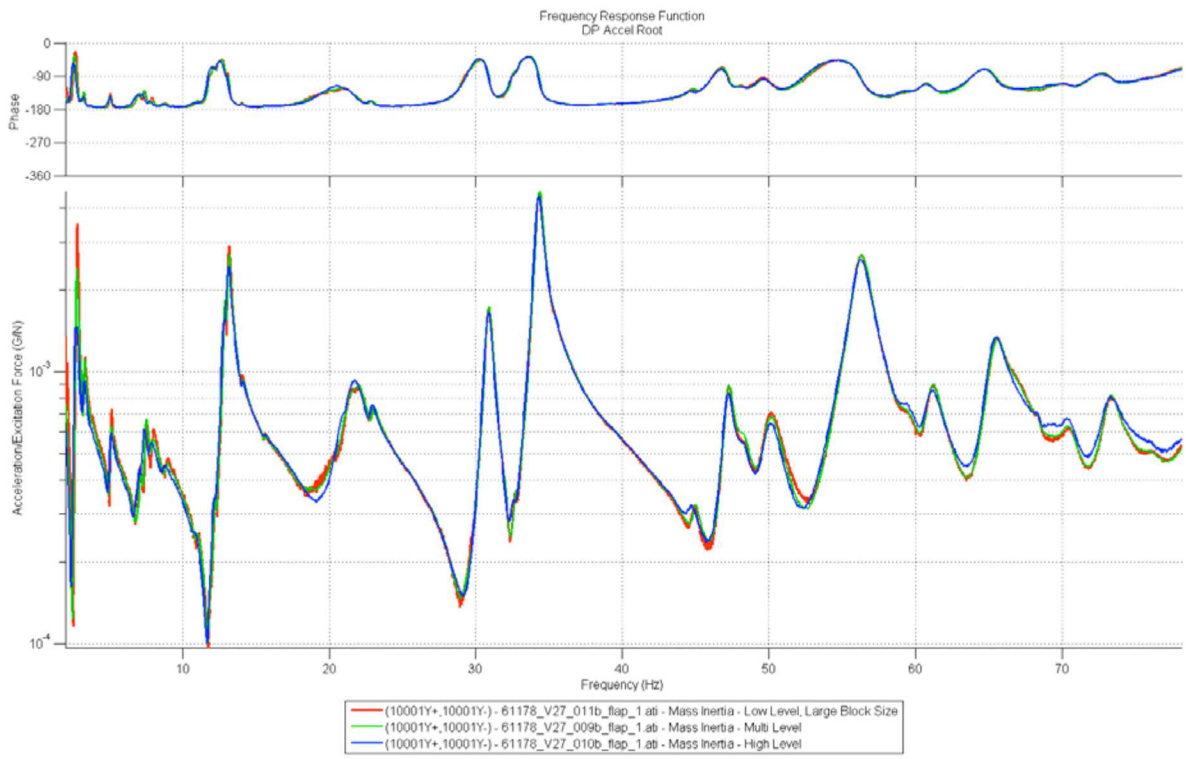


Figure 4-2. FRF from MPR runs 9, 10, and 11.

## 4.2. V27 Rigid Properties

The mass, CG, and moment of inertia about the Y-axis are shown in Table 4-4. The mass and CG of all six blades were measured using two load cells at the two support locations described previously. The moment of inertia about the Y-axis was measured using the bifilar pendulum technique described previously.

Table 4-4. V27 final mass and inertia properties.

| | SNL1_BL1 | SNL1_BL2 | SNL1_BL3 | SNL2_BL1 | SNL2_BL2 | SNL2_BL3 | Average | Max Difference (%) |
|---|---|---|---|---|---|---|---|---|
| **Weight (N)** | 6343 | 6357 | 6303 | 6552 | 6423 | 6787 | **6460.8** | **7.7** |
| **CG - X Axis (m)** | - | - | - | - | - | - | - | - |
| **CG - Y Axis (m)** | - | - | - | - | - | - | - | - |
| **CG - Z Axis (m)** | 4.18 | 4.15 | 4.19 | 4.29 | 4.16 | 4.20 | **4.20** | **3.4** |
| **Ixx (kg*m^2)** | - | - | - | - | - | - | - | - |
| **Iyy (kg*m^2)** | 5002.8 | 5466.0 | 5097.4 | 4967.0 | 5887.3 | 5796.4 | **5369.5** | **18.5** |
| **Izz (kg*m^2)** | - | - | - | - | - | - | - | - |
| * Coordinate System Origin Defined at Blade Root Center | | | | | | | | |

The CGs of all six blades were relatively close to one another, indicating the similarity between the blades. The weight of the blades and the mass moment of inertia showed higher variation, likely due to rework done on the blades.

The bifilar pendulum was not able to be used to obtain the moments of inertia about the X or Z axes, as the X-axis would have required a saddle to prevent crushing of the trailing edge and the Z-axis would have required suspending the blade vertically. The test setup prevented either of those tests from occurring.

Effort was made to use the other techniques described in the report to obtain the missing inertia and CG terms but, due to significant blade interaction with the support structure, further examination and processing of the data did not yield information of a sufficient quality to obtain the missing terms.

## 5. CONCLUSIONS

A modal survey was successfully performed on six V27 blades. A global modal survey for a single test configuration was conducted, and all primary flexible target modes were identified. The mass, CG, and moment of inertia about the Y-axis were also obtained. The modal parameters were successfully extracted, recorded, and shared with SNL engineers at the test site in a preliminary test report. ATA was responsible for test setup, data acquisition, data analysis, and instrumentation and hardware removal from the V27 blade following the test. All phases of the test program were completed October 27–31, 2012.

Modal parameters were extracted from MPR and modal impact hammer runs, and the uniqueness of the final mode shapes was verified through visual inspection and the test self-orthogonality. The self-orthogonality demonstrated that the extracted flexible mode shapes were unique, and all target modes were clearly identified with shape visualization. Finally, the V27 exhibited linear behavior, evidenced by MPR runs performed with input forces of approximately 1, 4, and 10 lbf RMS.

# Appendix A

## On-Site Test Log and Run Log

| 61178 Project Description Test Run Log | | | | | | RMS Force level (lbs) | | | | | | |
|---|---|---|---|---|---|---|---|---|---|---|---|---|
| Run # | Date (auto) | Start Time <CTRL><T> | Config† | Blade # | Exc. Type* | 10001 | 10002 | File Name | Block Size | Reference Channels | Freq Range (Hz) | Notes |
| Testing day 1 | | | | | | | | | | | | |
| Blade 1 - SNL2 BL1 | | | | | | | | | | | | |
| 1 | 10/27/2012 | 14:07 | Flap | 1 | i | - | - | 61178_V27_001i_flap_1.ati | 8192 | 3502X- | 0-100 | Impact Run - Reglued some accel blocks |
| 2 | 10/27/2012 | 14:43 | Flap | 1 | i | - | - | 61178_V27_002i_flap_1.ati | 8192 | 3502X- | 0-100 | Impact Run - Scaling looks incorrect for ch5-8 |
| 3 | 10/27/2012 | 15:15 | Flap | 1 | i | - | - | 61178_V27_003i_flap_1.ati | 8192 | 3502X-, 3537Y+,2898Y+,878X- | 0-100 | Impact Run - Changed ch 5-8 to ch 61-64 |
| 4 | 10/27/2012 | 15:55 | Flap | 1 | r | 4.77 | 1.52 | 61178_V27_004r_flap_1.ati | 1601 | 10001, 10002 | 0-78 | Shaker Checkout |
| 5 | 10/27/2012 | 19:26 | Flap | 1 | r | 4.77 | 1.52 | 61178_V27_005r_flap_1.ati | 6401 | 10001, 10002 | 0-78 | Mass Inertia Modal Method |
| Testing day 2 | | | | | | | | | | | | |
| 6 | 10/28/2012 | 7:46 | Flap | 1 | b | 0.74 | 0.66 | 61178_V27_006b_flap_1.ati | 6401 | 10001, 10002 | 0-78 | Mass Inertia Modal Method - Shaker 1 Load Cell Changed |
| 7 | 10/28/2012 | 8:11 | Flap | 1 | b | 1.29 | 1.11 | 61178_V27_007b_flap_1.ati | 6401 | 10001, 10002 | 0-78 | Mass Inertia - Level 2 |
| 8 | 10/28/2012 | 8:28 | Flap | 1 | b | 1.29 | 1.11 | 61178_V27_008b_flap_1.ati | 1601 | 10001, 10002 | 0-78 | Mass Inertia - Level 2 - Shaker 1 Pigtail and Accel Changed (36857) |
| 9 | 10/28/2012 | 8:40 | Flap | 1 | b | 4.11 | 1.11 | 61178_V27_009b_flap_1.ati | 1601 | 10001, 10002 | 0-78 | Mass Inertia - Multi Level |
| 10 | 10/28/2012 | 8:54 | Flap | 1 | b | 10.32 | 2.10 | 61178_V27_010b_flap_1.ati | 1601 | 10001, 10002 | 0-78 | Mass Inertia - High Level |
| 11 | 10/28/2012 | 9:07 | Flap | 1 | b | 0.93 | 0.86 | 61178_V27_011b_flap_1.ati | 6401 | 10001, 10002 | 0-78 | Mass Inertia - Low Level, Large Block Size |
| 12 | 10/28/2012 | 10:06 | Flap | 1 | ms | - | - | 61178_V27_012ms_flap_1.ati | 6401 | 10001, 10002 | 0-78 | Mass Inertia - Multi Sine |
| 13 | 10/28/2012 | 10:35 | Flap | 1 | ms | - | - | 61178_V27_013ms_flap_1.ati | 6401 | 10001, 10002 | 0-78 | Mass Inertia - Multi Sine - Lower Level |
| 14 | 10/28/2012 | 15:36 | Flap | 1 | man | - | - | 61178_V27_014man_flap_1.ati | 101 | - | 0-25 | Pendulum |
| 15 | 10/28/2012 | 16:02 | Flap | 1 | man | - | - | 61178_V27_015man_flap_1.ati | 101 | - | 0-25 | Bifilar Flapwise |
| Testing day 3 | | | | | | | | | | | | |
| Blade 3 SNL2 - BI3 | | | | | | | | | | | | |
| 16 | 10/29/2012 | 8:16 | Flap | 3 | man | - | - | 61178_V27_016man_flap_3.ati | 101 | - | 0-25 | Pendulum |
| 17 | 10/29/2012 | 8:43 | Flap | 3 | man | - | - | 61178_V27_017man_flap_3.ati | 101 | - | 0-25 | Bifilar Flapwise |
| 18 | 10/29/2012 | 10:10 | Flap | 3 | man | - | - | 61178_V27_018man_flap_3.ati | 101 | - | 0-25 | Axial Pendulum |
| 19 | 10/29/2012 | 11:34 | Flap | 3 | man | - | - | 61178_V27_019man_flap_3.ati | 1601 | 488 X-,Y+,Z+ | 0-78 | RB Modes Checkout |
| 20 | 10/29/2012 | 12:07 | Flap | 3 | man | - | - | 61178_V27_020man_flap_3.ati | 1601 | - | 0-78 | RB Modes Checkout - Adjusted Bungee |
| 21 | 10/29/2012 | 13:09 | Flap | 3 | man | - | - | 61178_V27_021man_flap_3.ati | 1601 | - | 0-78 | RB Modes Checkout - Moved accel |
| 22 | 10/29/2012 | 14:00 | Flap | 3 | i | - | - | 61178_V27_022i_flap_3.ati | 8192 | 3502X- | 0-100 | Impact Test |
| 23 | 10/29/2012 | 16:46 | Flap | 3 | b | 1.42 | 1.27 | 61178_V27_023b_flap_3.ati | 4096 | 10001, 10002 | 0-40 | Low Level Burst Checkout |
| 24 | 10/29/2012 | 16:46 | Flap | 3 | b | 1.20 | 1.27 | 61178_V27_024b_flap_3.ati | 4096 | 10001, 10002 | 0-20 | Low Level Burst - 0-20 Hz |
| 25 | 10/29/2012 | 16:46 | Flap | 3 | b | 1.20 | 1.27 | 61178_V27_025b_flap_3.ati | 8192 | 10001, 10002 | 0-20 | Mass Inertia - Low Level, Large Block Size |
| Testing day 4 | | | | | | | | | | | | |
| Blade 2 SNL2 - BI2 | | | | | | | | | | | | |
| 26 | 10/30/2012 | 8:36 | Flap | 2 | man | - | - | 61178_V27_026man_flap_2.ati | 101 | - | 0-25 | Pendulum |
| 27 | 10/30/2012 | 8:49 | Flap | 2 | man | - | - | 61178_V27_027man_flap_2.ati | 101 | - | 0-25 | Bifilar Flapwise |
| 28 | 10/30/2012 | 9:34 | Flap | 2 | i | - | - | 61178_V27_028i_flap_2.ati | 8192 | 488 X-,Y+,Z+ | 0-25 | RB Mode Impact |
| 29 | 10/30/2012 | 11:07 | Flap | 2 | i | - | - | 61178_V27_029i_flap_2.ati | 8192 | 3502X-, 3537Y+, | 0-100 | Impact Test |
| Blade 4 SNL1 - BI1 | | | | | | | | | | | | |
| 30 | 10/30/2012 | 14:44 | Flap | 4 | man | - | - | 61178_V27_030man_flap_4.ati | 101 | - | 0-25 | Pendulum |
| 31 | 10/30/2012 | 14:59 | Flap | 4 | man | - | - | 61178_V27_031man_flap_4.ati | 101 | - | 0-25 | Bifilar Flapwise |
| 32 | 10/30/2012 | 15:26 | Flap | 4 | i | - | - | 61178_V27_032i_flap_4.ati | 8192 | 488 X-,Y+,Z+ | 0-25 | RB Mode Impact |
| 33 | 10/30/2012 | 16:33 | Flap | 4 | i | - | - | 61178_V27_033i_flap_4.ati | 8192 | 3502X-, 3537Y+, | 0-100 | Impact Test |
| 34 | 10/30/2012 | 17:05 | Flap | 4 | i | - | - | 61178_V27_034i_flap_4.ati | 8192 | 3502X-, 3537Y+, | 0-100 | Impact Test - Corrected Channels |

| 61178 Project Description Test Run Log | | | | | | RMS Force level (lbs) | | | | | | |
|---|---|---|---|---|---|---|---|---|---|---|---|---|
| Run | Date | Start Time | Config† | Blade # | Exc. | 10001 | 10002 | File Name | Block Size | Reference Channels | Freq Range (Hz) | |
| # | (auto) | <CTRL><T> | | | Type* | | | | | | | Notes |
| Testing day 5 | | | | | | | | | | | | |
| Blade 5 SNL1 - BI3 | | | | | | | | | | | | |
| 35 | 10/31/2012 | 8:17 | Flap | 5 | man | - | - | 61178_V27_035man_flap_5.ati | 101 | - | 0-25 | Pendulum |
| 36 | 10/31/2012 | 8:28 | Flap | 5 | man | - | - | 61178_V27_036man_flap_5.ati | 101 | - | 0-25 | Bifilar Flapwise |
| 37 | 10/31/2012 | 8:39 | Flap | 5 | i | - | - | 61178_V27_037i_flap_5.ati | 8192 | 488 X-,Y+,Z+ | 0-25 | RB Mode Impact |
| 38 | 10/31/2012 | 9:49 | Flap | 5 | i | - | - | 61178_V27_038i_flap_5.ati | 8192 | 3502X-, 3502Y+, | 0-100 | Impact Test - Pendulum Support Locations |
| 39 | 10/31/2012 | 10:49 | Flap | 5 | i | - | - | 61178_V27_039i_flap_5.ati | 8192 | 3502X-, 3502Y+, | 0-100 | Impact Test |
| Blade 6 SNL1 - BI2 | | | | | | | | | | | | |
| 40 | 10/31/2012 | 14:07 | Flap | 6 | man | - | - | 61178_V27_040man_flap_6.ati | 101 | - | 0-25 | Pendulum |
| 41 | 10/31/2012 | 14:26 | Flap | 6 | man | - | - | 61178_V27_041man_flap_6.ati | 101 | - | 0-25 | Bifilar Flapwise |
| 42 | 10/31/2012 | 14:33 | Flap | 6 | i | - | - | 61178_V27_042i_flap_6.ati | 8192 | 488 X-,Y+,Z+ | 0-25 | RB Mode Impact |
| 43 | 10/31/2012 | 15:47 | Flap | 6 | i | - | - | 61178_V27_043i_flap_6.ati | 8192 | 3502X-, 3537Y+, | 0-100 | Impact Test - Pendulum Support Locations |
| 44 | 10/31/2012 | 16:41 | Flap | 6 | i | - | - | 61178_V27_044i_flap_6.ati | 8192 | 3502X-, 3537Y+, | 0-100 | Impact Test |

| * EXCITATION TYPE | | Blade Numbering |
|---|---|---|
| i | modal impact | Blade 1 = SNL2_BL1 |
| b | modal burst random | Blade 3 = SNL2_BL3 |
| ms | multi-sine sweep | Blade 2 = SNL2_BL2 |
| man | manual excitation | Blade 4 = SNL1_BL1 |
| **Configs** | | Blade 5 = SNL1_BL3 |
| Flap | Blade Tested on Edge | Blade 6 = SNL1_BL2 |

# Appendix B

## Nodes and Accelerometers Table

Full Set of Instrumentation

| Group Name | Node | X+ | Y+ | Z+ | Locations |
|---|---|---|---|---|---|
| Trailing | 3502 | X- | Y+ | Z+ | Trailing-1 |
| Trailing | 3358 | X- | Y+ | | Trailing-2 |
| Trailing | 3052 | X- | Y+ | | Trailing-3 |
| Trailing | 2871 | X- | Y+ | | Trailing-4 |
| Trailing | 2559 | X- | Y+ | | Trailing-5 |
| Trailing | 2208 | X- | Y+ | | Trailing-6 |
| Trailing | 2010 | X- | Y+ | | Trailing-7 |
| Trailing | 1593 | X- | Y+ | | Trailing-8 |
| Trailing | 1359 | X- | Y+ | | Trailing-9 |
| Trailing | 878 | X- | Y+ | | Trailing-10 |
| Trailing | 488 | X- | Y+ | | Trailing-11 |
| Trailing | 242 | X- | Y+ | | Trailing-12 |
| Trailing | 76 | X- | Y+ | Z+ | Trailing-13 |
| Leading | 3537 | X- | Y- | Z+ | Leading-1 |
| Leading | 3407 | X- | Y- | | Leading-2 |
| Leading | 3101 | X- | Y- | | Leading-3 |
| Leading | 2898 | X- | Y- | | Leading-4 |
| Leading | 2631 | X- | Y- | | Leading-5 |
| Leading | 2290 | X- | Y- | | Leading-6 |
| Leading | 2099 | X- | Y- | | Leading-7 |
| Leading | 1691 | X- | Y- | | Leading-8 |
| Leading | 1465 | X- | Y- | | Leading-9 |
| Leading | 992 | X- | Y- | | Leading-10 |
| Leading | 550 | X- | Y- | | Leading-11 |
| Leading | 296 | X- | Y- | | Leading-12 |
| Leading | 95 | X- | Y- | Z+ | Leading-13 |

| # X Entries | #Y Entries | # Z Entries |
|---|---|---|
| 26 | 26 | 4 |
| Total Number of Entries | | 56 |

Reduced Set of Instrumentation

| Group Name | Node | X+ | Y+ | Z+ | Locations |
|---|---|---|---|---|---|
| Trailing | 3502 | X- | Y+ | | Trailing-1 |
| Trailing | 2871 | X- | Y+ | | Trailing-4 |
| Trailing | 1593 | X- | Y+ | | Trailing-8 |
| Trailing | 76 | X- | Y+ | | Trailing-13 |
| Leading | 3537 | X- | | | Leading-1 |
| Leading | 2898 | X- | | | Leading-4 |
| Leading | 1691 | X- | | | Leading-8 |
| Leading | 95 | X- | | | Leading-13 |

| # X Entries | #Y Entries | # Z Entries |
|---|---|---|
| 8 | 4 | 0 |
| Total Number of Entries | | 12 |

# Appendix C

# Accelerometer Photos

Due to coordinate system change after the test was completed, the node directions listed in the following pictures are different than those listed in the report.

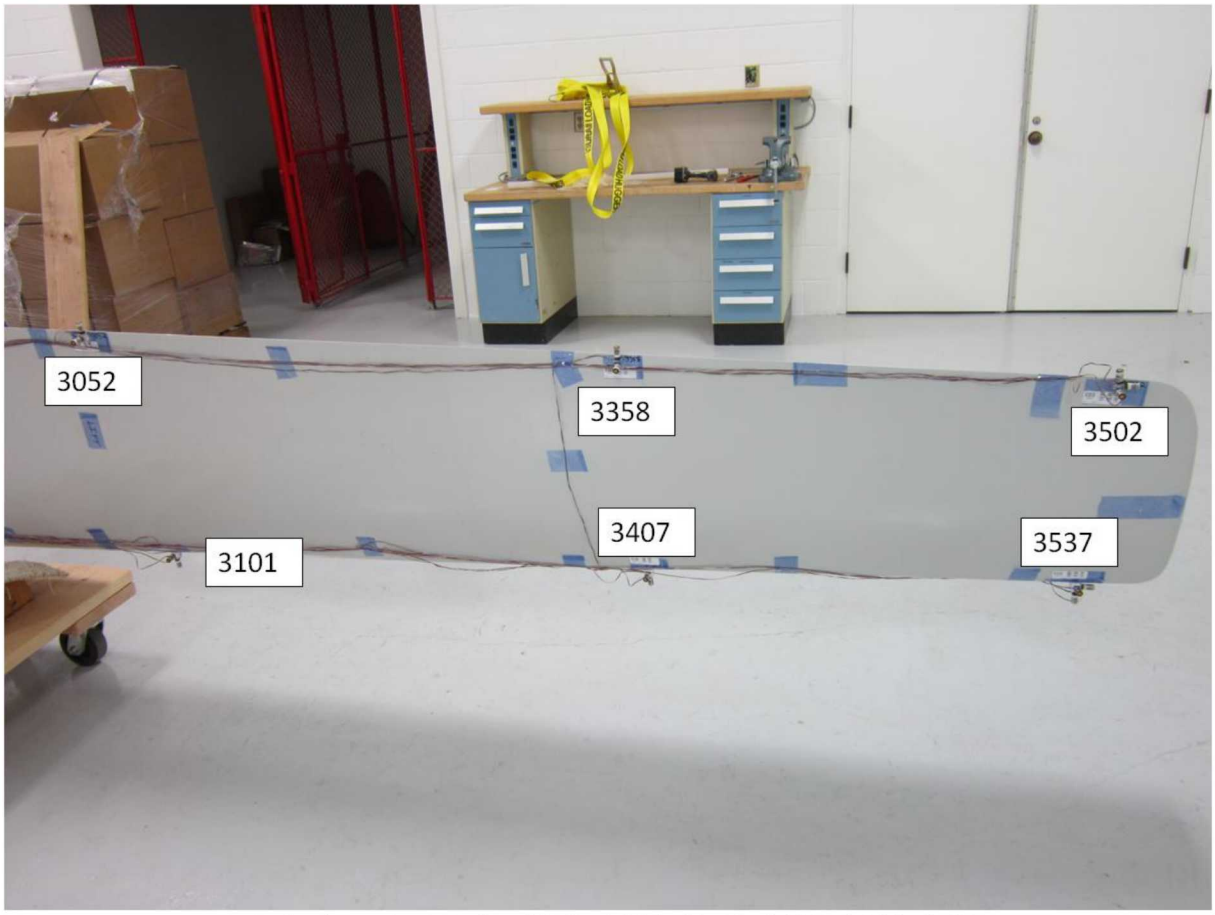


Blade Area 1 – Nodes 3052, 3101, 3358, 3407, 3502, 3537

Blade Area 2 – Nodes 2208, 2290, 2559, 2631, 2871, 2808

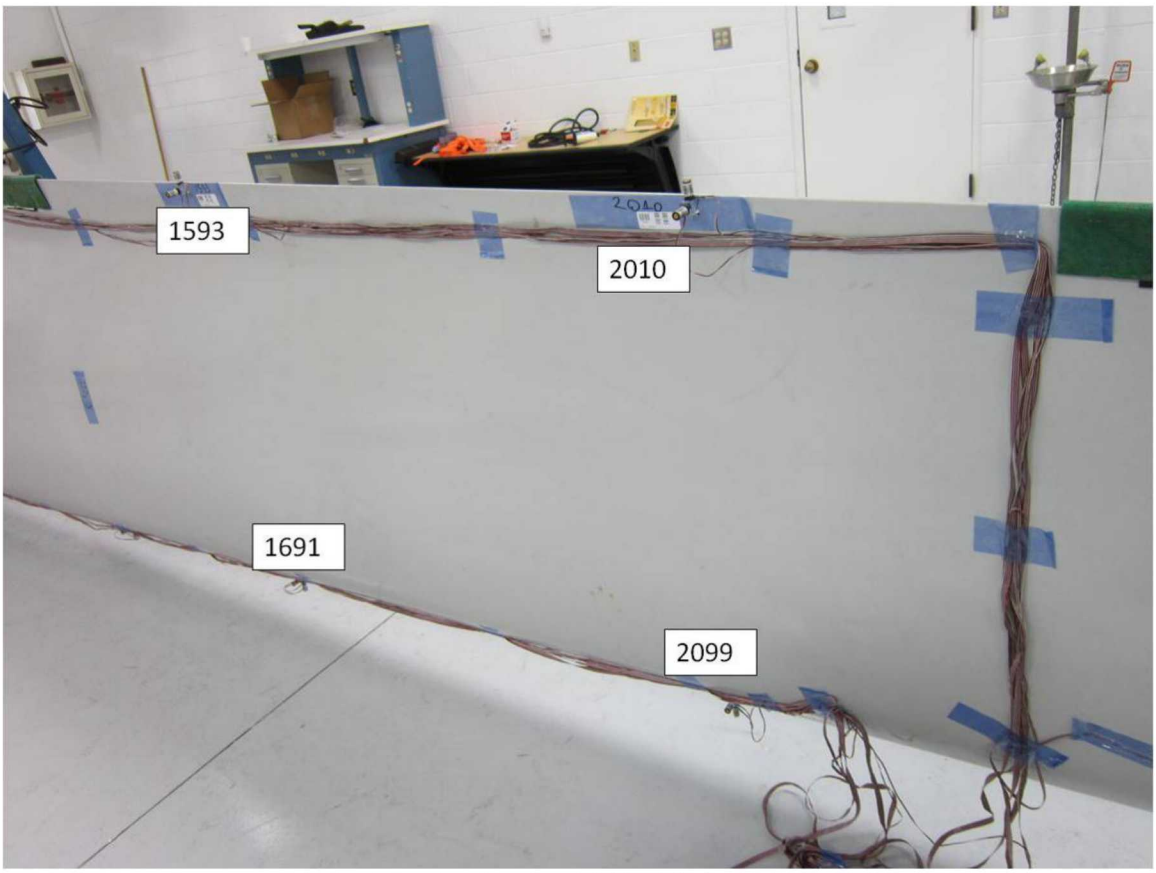


Blade Area 3 – Nodes 1593, 1691, 2010, 2099

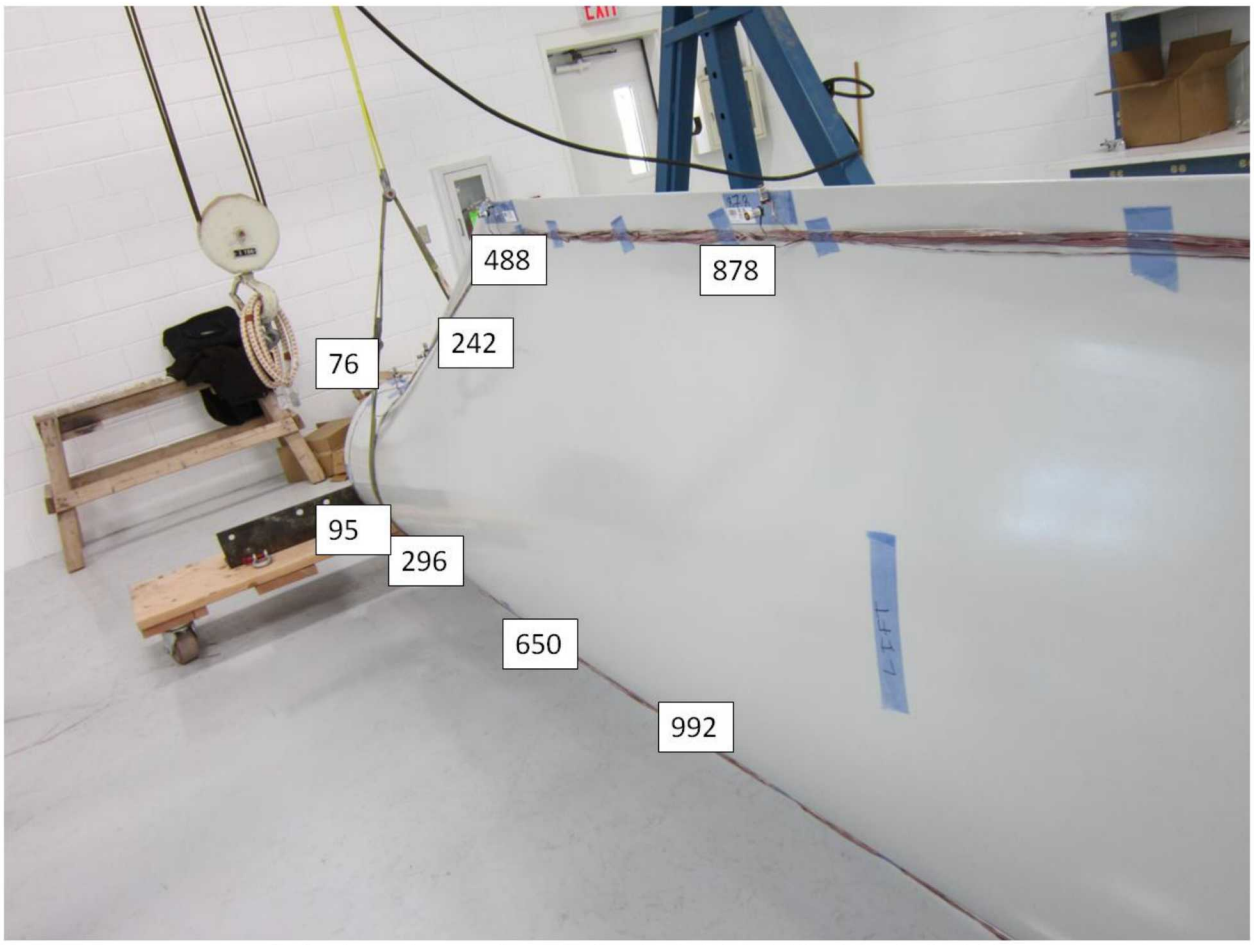


Blade Area 4 – Nodes 76, 95, 242, 296, 488, 650, 878, 992

| | |
|---|---|
| 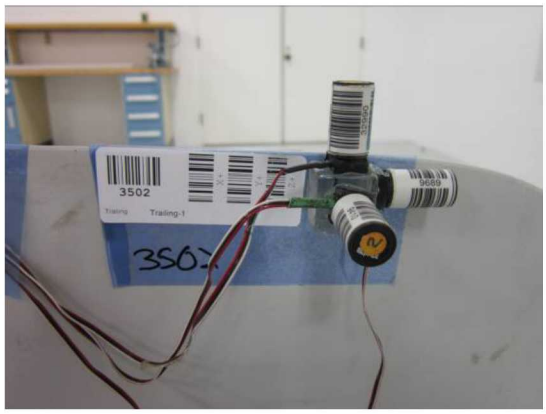 | |
| Node: 3502 Group: Trailing Dir: X+ Y+ Z+ | Node: 3358 Group: Trailing Dir: X+ Y+ |

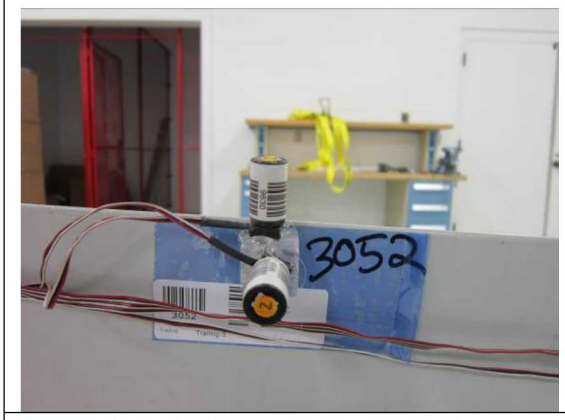


Node: 3052 Group: Trailing Dir: X+ Y+

Node: 2871 Group: Trailing Dir: X+ Y+

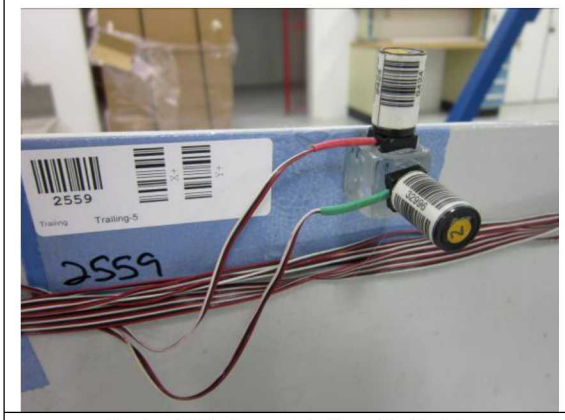


Node: 2559 Group: Trailing Dir: X+ Y+

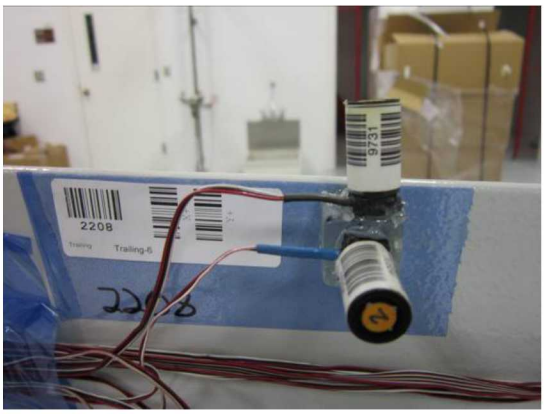


Node: 2208 Group: Trailing Dir: X+ Y+

Node: 2010 Group: Trailing Dir: X+ Y+

Node: 1593 Group: Trailing Dir: X+ Y+

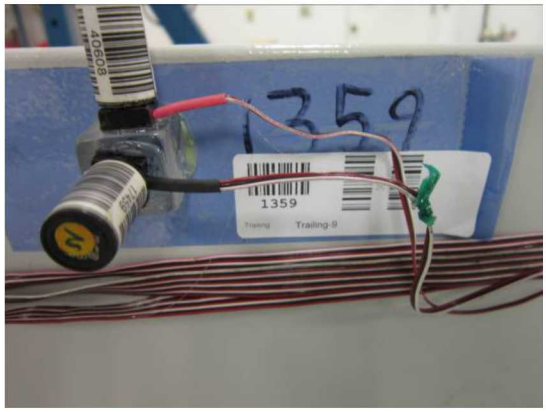


Node: 1359 Group: Trailing Dir: X+ Y+

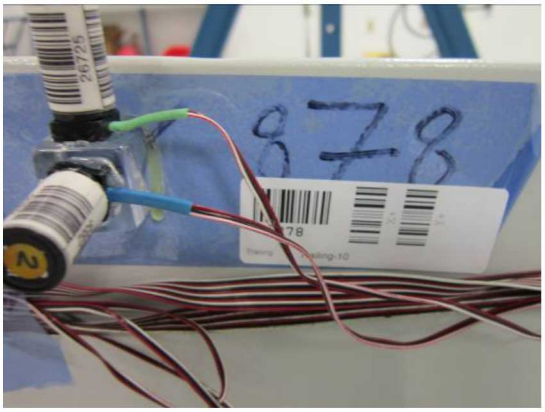


Node: 878 Group: Trailing Dir: X+ Y+

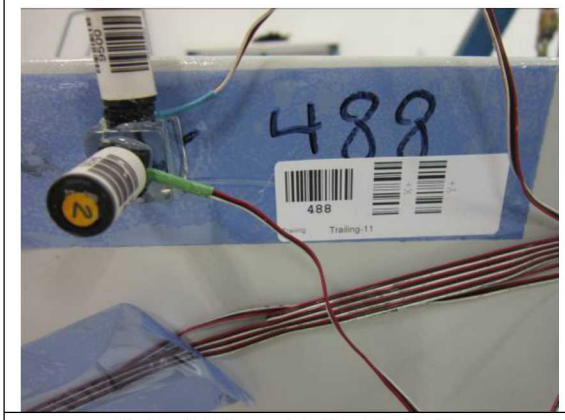


Node: 488 Group: Trailing Dir: X+ Y+

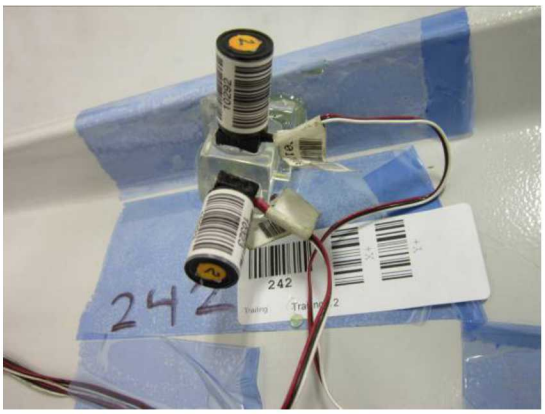


Node: 242 Group: Trailing Dir: X+ Y+

Node: 76 Group: Trailing Dir: X+ Y+ Z+

Node: 3537 Group: Leading Dir: X- Y+ Z+

Node: 3407 Group: Leading Dir: X- Y+

Node: 3101 Group: Leading Dir: X- Y+

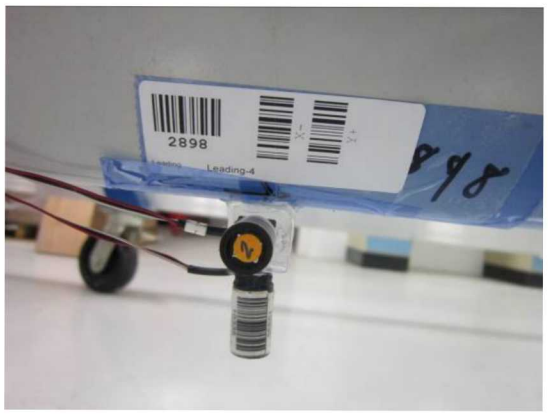


Node: 2898 Group: Leading Dir: X- Y+

Node: 2631 Group: Leading Dir: X- Y+

Node: 2290 Group: Leading Dir: X- Y+

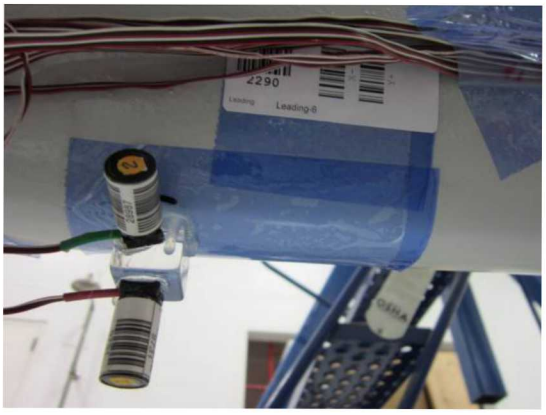


Node: 2990 Group: Leading Dir: X- Y+

Node: 1691 Group: Leading Dir: X- Y+

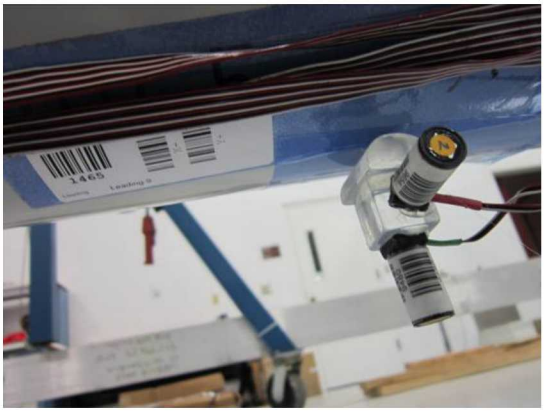


Node: 1465 Group: Leading Dir: X- Y+

Node: 992 Group: Leading Dir: X- Y+

Node: 550 Group: Leading Dir: X- Y+

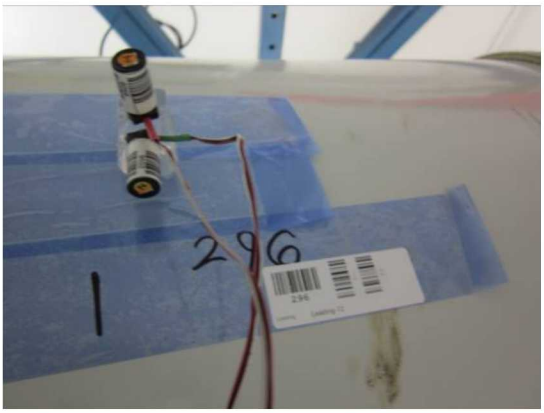


Node: 296 Group: Leading Dir: X- Y+

Node: 95 Group: Leading Dir: X- Y+ Z+

# Appendix D

## Shaker Configuration and Location Photos

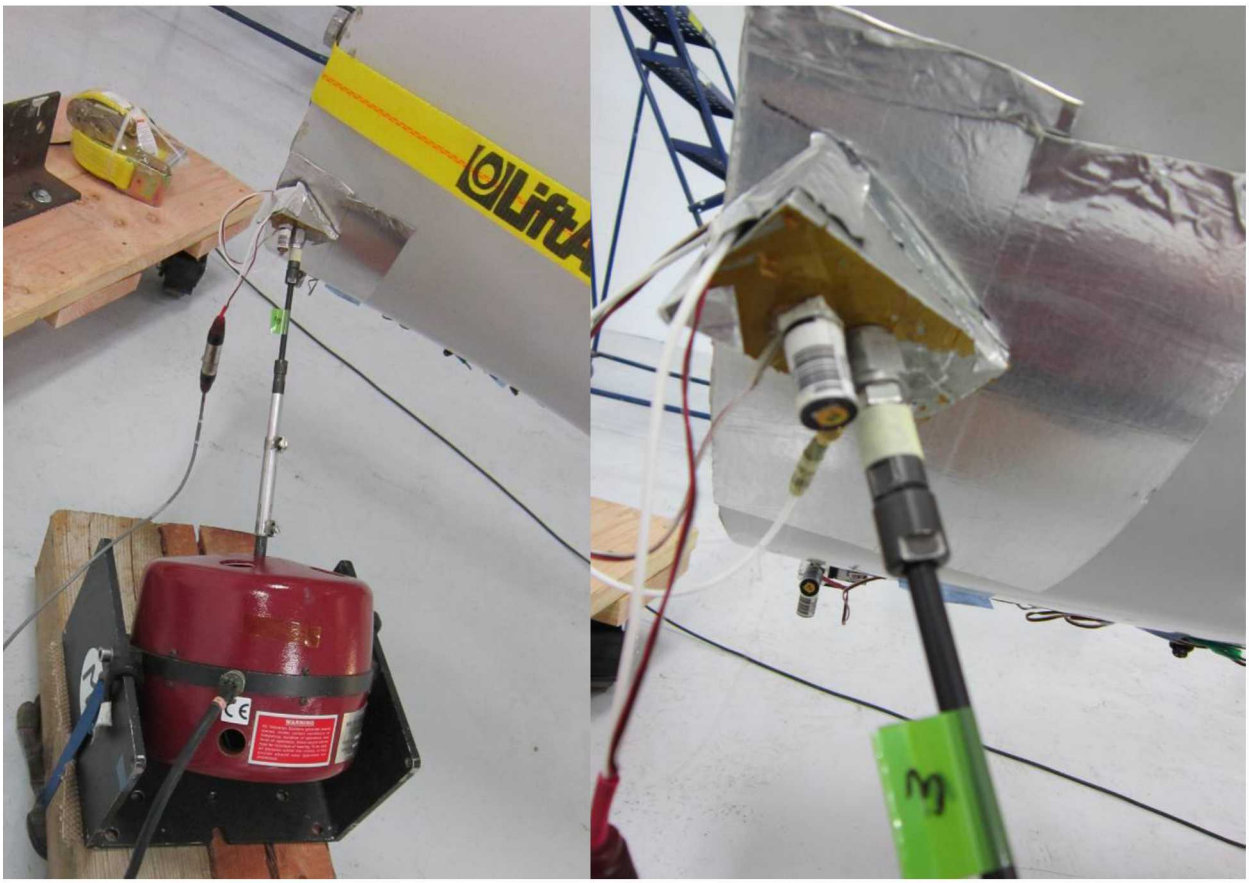

Shaker 1 – Root a) location and b) attachment

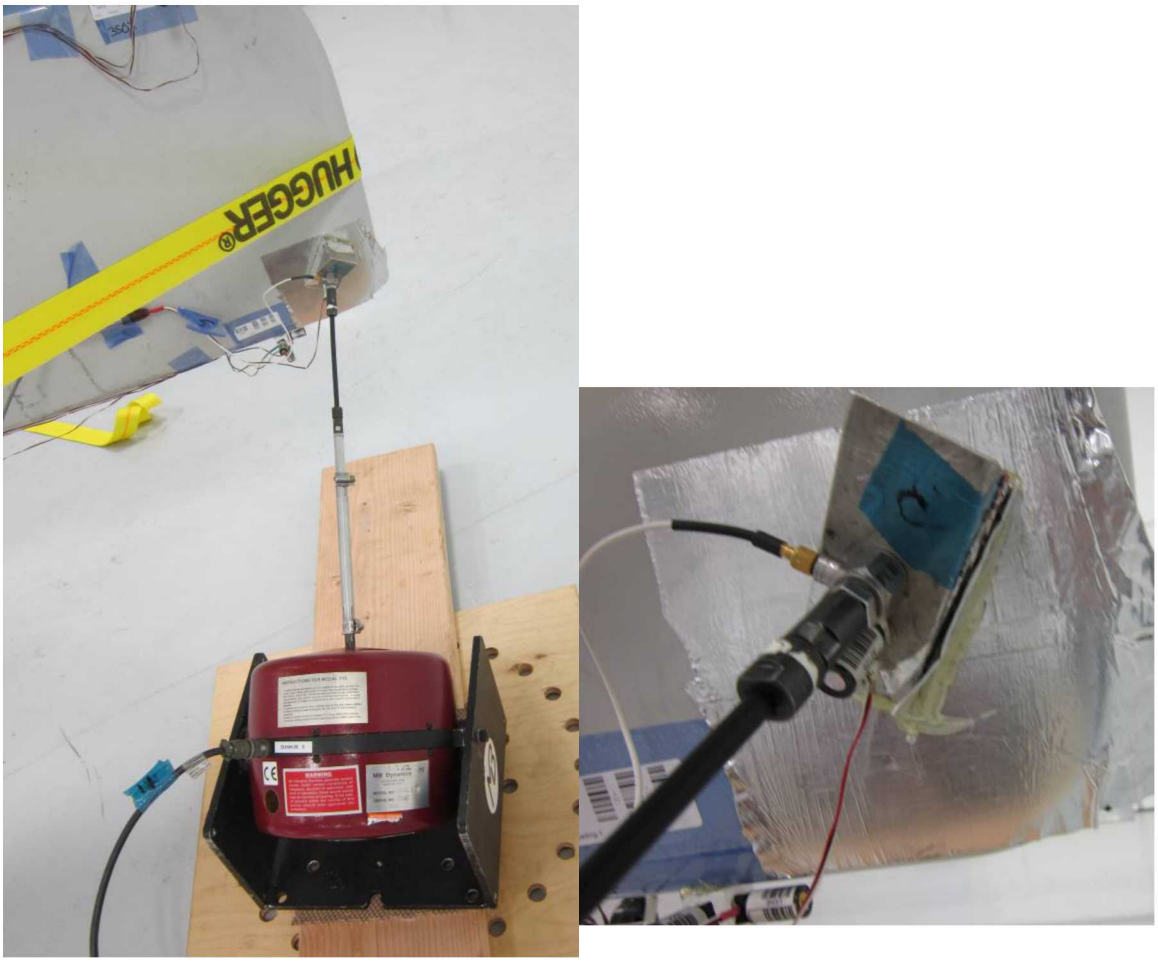


Shaker 2 – Tip a) location and b) attachment

# Appendix E

# Modal Test Channel Table

Only the channel setup for SNL2_BL1 is shown, the other blades were setup the same but contained different accelerometers at each node.

| SN | Node | DIR | Data Type | EU | Cal mV/EU | Channel Description | CAL DUE DATE |
|---|---|---|---|---|---|---|---|
| 25539S | 1 | X+ | 13 | 7 | 1.133 | Hammer | 07-Jun-13 |
| 9473 | 1691 | X- | 12 | 11 | 103.28 | Leading-8 | 17-Aug-13 |
| 9212 | 1691 | Y+ | 12 | 11 | 96.3224 | Leading-8 | 17-Aug-13 |
| 9654 | 1465 | Y+ | 12 | 11 | 102.3447 | Leading-9 | 17-Aug-13 |
| 9480 | 1465 | X- | 12 | 11 | 99.8854 | Leading-9 | 17-Aug-13 |
| 10292 | 242 | X+ | 12 | 11 | 108.8477 | Trailing-12 | 17-Aug-13 |
| 9500 | 488 | X+ | 12 | 11 | 93.1801 | Trailing-11 | 17-Aug-13 |
| 9430 | 488 | Y+ | 12 | 11 | 81.6732 | Trailing-11 | 17-Aug-13 |
| 10323 | 242 | Y+ | 12 | 11 | 93.6905 | Trailing-12 | 17-Aug-13 |
| 9385 | 2010 | Y+ | 12 | 11 | 100.0472 | Trailing-7 | 17-Aug-13 |
| 28987 | 2010 | X+ | 12 | 11 | 88.9211 | Trailing-7 | 17-Aug-13 |
| 10318 | 1593 | Y+ | 12 | 11 | 86.9038 | Trailing-8 | 17-Aug-13 |
| 28961 | 1593 | X+ | 12 | 11 | 89.368 | Trailing-8 | 17-Aug-13 |
| 28933 | 3052 | Y+ | 12 | 11 | 89.6398 | Trailing-3 | 17-Aug-13 |
| 9717 | 2871 | X+ | 12 | 11 | 90.7541 | Trailing-4 | 17-Aug-13 |
| 9658 | 3052 | X+ | 12 | 11 | 83.4838 | Trailing-3 | 17-Aug-13 |
| 9562 | 2871 | Y+ | 12 | 11 | 101.3014 | Trailing-4 | 17-Aug-13 |
| 20661 | 76 | X+ | 12 | 11 | 90.3599 | Trailing-13 | 17-Aug-13 |
| 9408 | 76 | Z+ | 12 | 11 | 99.5236 | Trailing-13 | 17-Aug-13 |
| 9438 | 76 | Y+ | 12 | 11 | 100.6007 | Trailing-13 | 17-Aug-13 |
| 40608 | 1359 | X+ | 12 | 11 | 85.1676 | Trailing-9 | 17-Aug-13 |
| 9382 | 878 | Y+ | 12 | 11 | 88.8745 | Trailing-10 | 17-Aug-13 |
| 17459 | 1359 | Y+ | 12 | 11 | 79.8151 | Trailing-9 | 17-Aug-13 |
| 26725 | 878 | X+ | 12 | 11 | 85.6211 | Trailing-10 | 17-Aug-13 |
| 9396 | 95 | Z+ | 12 | 11 | 102.8144 | Leading-13 | 17-Aug-13 |
| 9737 | 2290 | X- | 12 | 11 | 83.6883 | Leading-6 | 17-Aug-13 |
| 20663 | 2990 | Y+ | 12 | 11 | 90.8111 | Leading-7 | 17-Aug-13 |
| 9715 | 2990 | X- | 12 | 11 | 98.4429 | Leading-7 | 17-Aug-13 |
| 28966 | 2290 | Y+ | 12 | 11 | 93.9675 | Leading-6 | 17-Aug-13 |
| 9222 | 2898 | X- | 12 | 11 | 90.7832 | Leading-4 | 17-Aug-13 |
| 27440 | 2898 | Y+ | 12 | 11 | 85.8724 | Leading-4 | 17-Aug-13 |
| 10322 | 2631 | X- | 12 | 11 | 80.0196 | Leading-5 | 17-Aug-13 |
| 9709 | 2631 | Y+ | 12 | 11 | 105.3984 | Leading-5 | 17-Aug-13 |
| 9593 | 3358 | X+ | 12 | 11 | 96.2132 | Trailing-2 | 17-Aug-13 |
| 9410 | 3502 | Y+ | 12 | 11 | 101.5418 | Trailing-1 | 17-Aug-13 |
| 9689 | 3502 | Z+ | 12 | 11 | 85.3983 | Trailing-1 | 17-Aug-13 |
| 32990 | 3502 | X+ | 12 | 11 | 94.8144 | Trailing-1 | 17-Aug-13 |
| 10334 | 2208 | Y+ | 12 | 11 | 97.9161 | Trailing-6 | 17-Aug-13 |
| 32996 | 2559 | Y+ | 12 | 11 | 82.0173 | Trailing-5 | 17-Aug-13 |
| 9424 | 2559 | X+ | 12 | 11 | 97.5336 | Trailing-5 | 17-Aug-13 |
| 9731 | 2208 | X+ | 12 | 11 | 83.7423 | Trailing-6 | 17-Aug-13 |
| 9687 | 3358 | Y+ | 12 | 11 | 80.239 | Trailing-2 | 17-Aug-13 |
| 9451 | 3537 | Z+ | 12 | 11 | 98.4928 | Leading-1 | 17-Aug-13 |
| 10298 | 3537 | X- | 12 | 11 | 86.3401 | Leading-1 | 17-Aug-13 |
| 9554 | 3537 | Y+ | 12 | 11 | 85.1508 | Leading-1 | 17-Aug-13 |
| 9730 | 3407 | Y+ | 12 | 11 | 108.3291 | Leading-2 | 17-Aug-13 |
| 9509 | 3407 | X- | 12 | 11 | 110.356 | Leading-2 | 17-Aug-13 |
| 9630 | 3101 | X- | 12 | 11 | 90.8782 | Leading-3 | 17-Aug-13 |
| 10335 | 3101 | Y+ | 12 | 11 | 88.0383 | Leading-3 | 17-Aug-13 |
| 9549 | 992 | Y+ | 12 | 11 | 94.8765 | Leading-10 | 17-Aug-13 |
| 28942 | 992 | X- | 12 | 11 | 88.5929 | Leading-10 | 17-Aug-13 |
| 9660 | 550 | X- | 12 | 11 | 108.1925 | Leading-11 | 17-Aug-13 |
| 20647 | 550 | Y+ | 12 | 11 | 85.3179 | Leading-11 | 17-Aug-13 |
| 10326 | 95 | Y+ | 12 | 11 | 111.3768 | Leading-13 | 17-Aug-13 |
| 9645 | 296 | X- | 12 | 11 | 100.7877 | Leading-12 | 17-Aug-13 |
| 9713 | 95 | X- | 12 | 11 | 97.7486 | Leading-13 | 17-Aug-13 |
| 9556 | 296 | Y+ | 12 | 11 | 102.3795 | Leading-12 | 17-Aug-13 |

# Appendix F

# Test Mode Shapes

The shapes below are only for SNL2_BL1; the other shapes are similar and are not included for brevity.

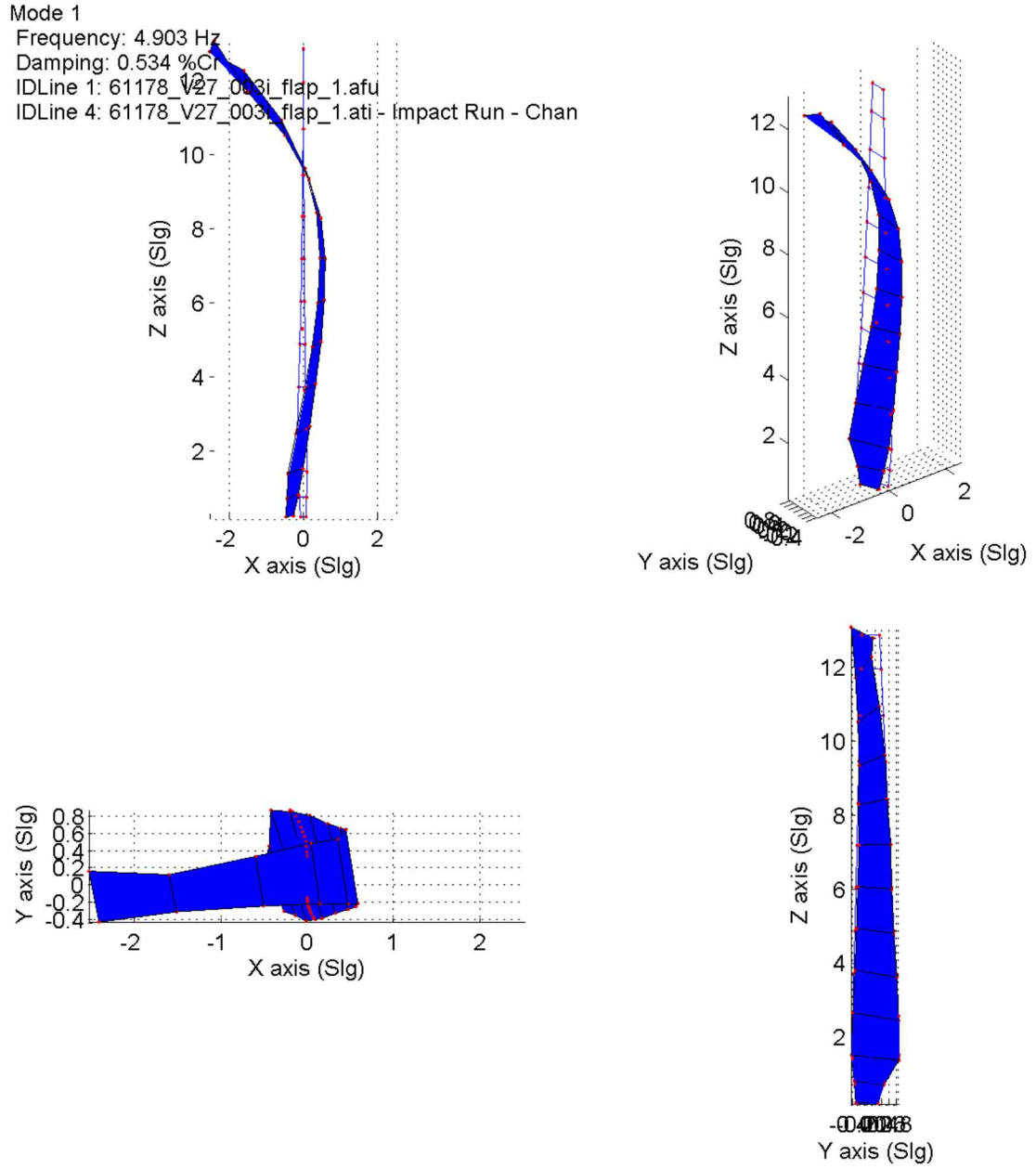

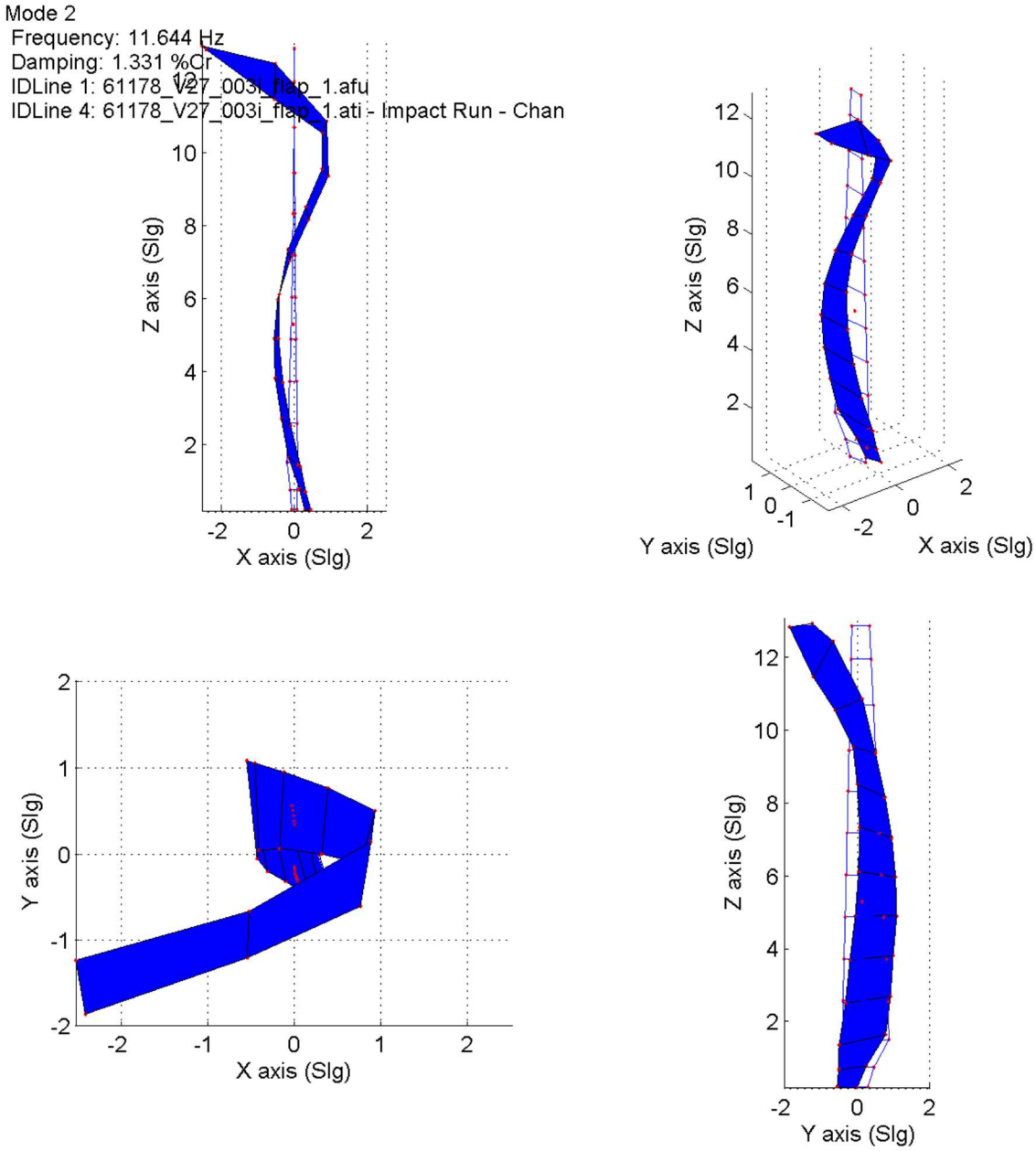
Mode 2
Frequency: 11.644 Hz
Damping: 1.331 %Cr
IDLine 1: 61178_V27_003i_flap_1.afu
IDLine 4: 61178_V27_003i_flap_1.ati - Impact Run - Chan
Z axis (Slg)
X axis (Slg)
Y axis (Slg)

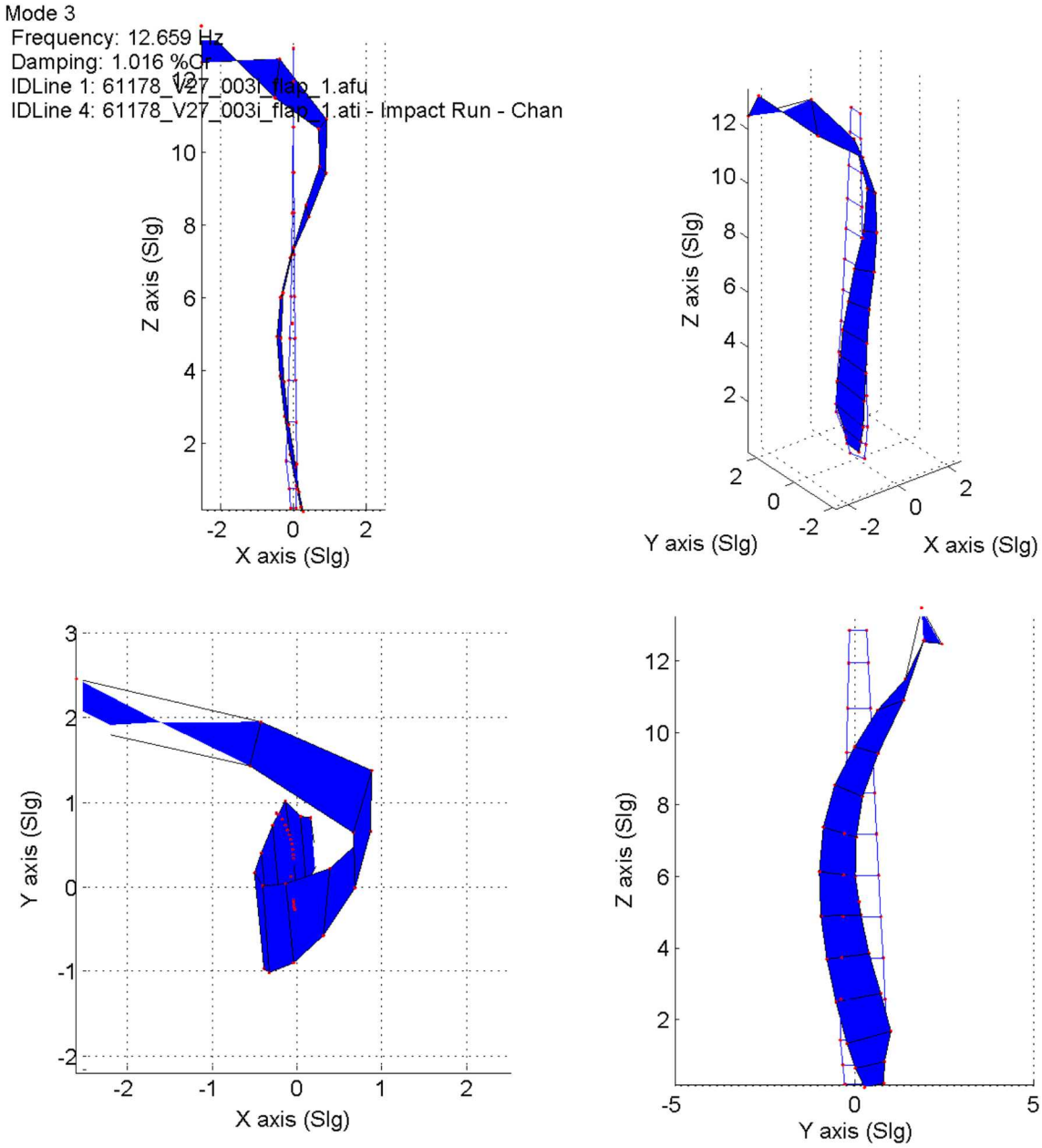
Mode 3
Frequency: 12.659 Hz
Damping: 1.016 %Cr
IDLine 1: 61178_V27_003i_flap_1.afu
IDLine 4: 61178_V27_003i_flap_1.ati - Impact Run - Chan
Z axis (Slg)
X axis (Slg)
Y axis (Slg)

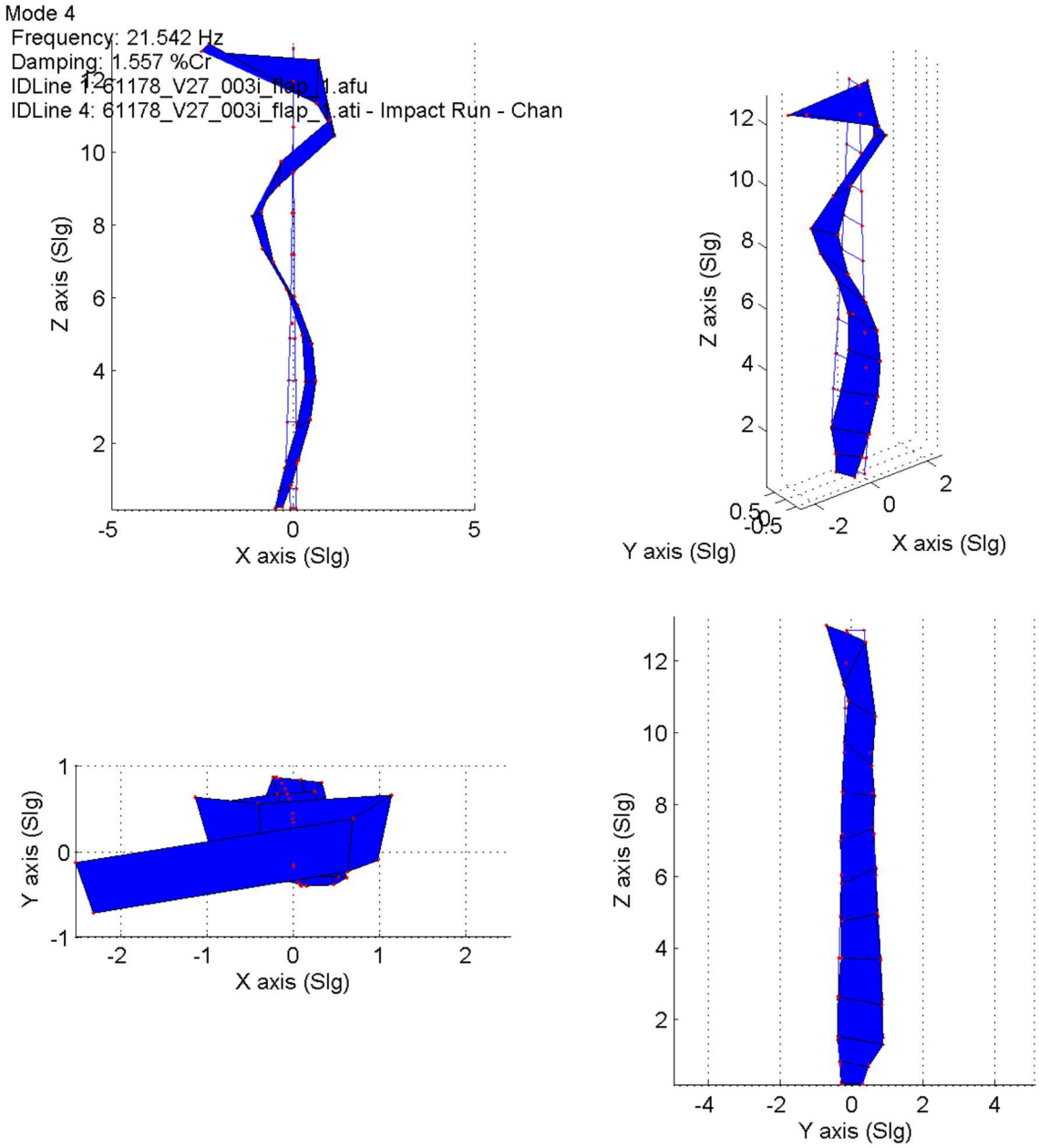
Mode 4
Frequency: 21.542 Hz
Damping: 1.557 %Cr
IDLine 1: 61178_V27_003i_flap_1.afu
IDLine 4: 61178_V27_003i_flap_1.ati - Impact Run - Chan
Z axis (Slg)
X axis (Slg)
Y axis (Slg)

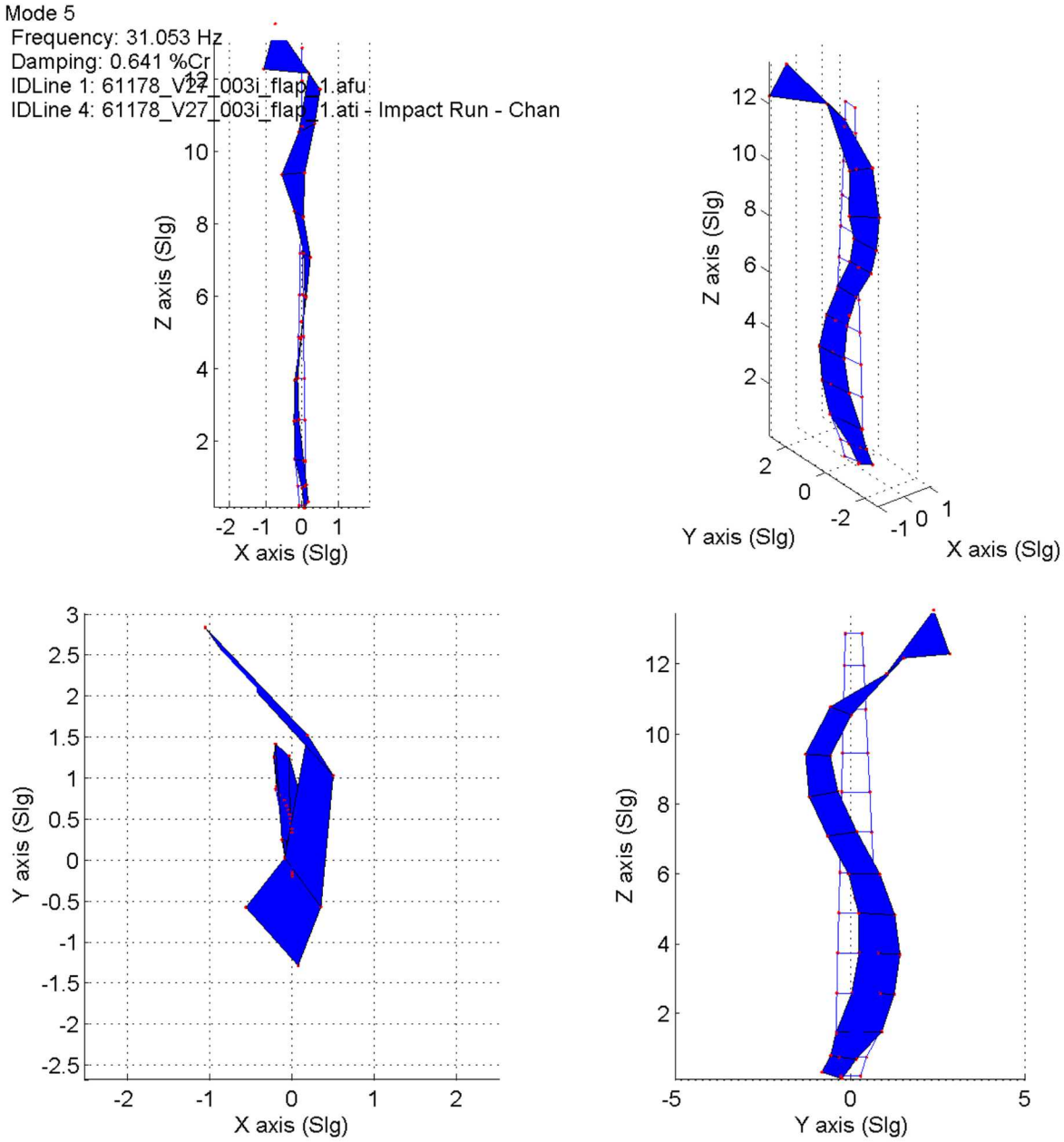
Mode 5
Frequency: 31.053 Hz
Damping: 0.641 %Cr
IDLine 1: 61178_V27_003i_flap_1.afu
IDLine 4: 61178_V27_003i_flap_1.ati - Impact Run - Chan
Z axis (Slg)
X axis (Slg)
Y axis (Slg)

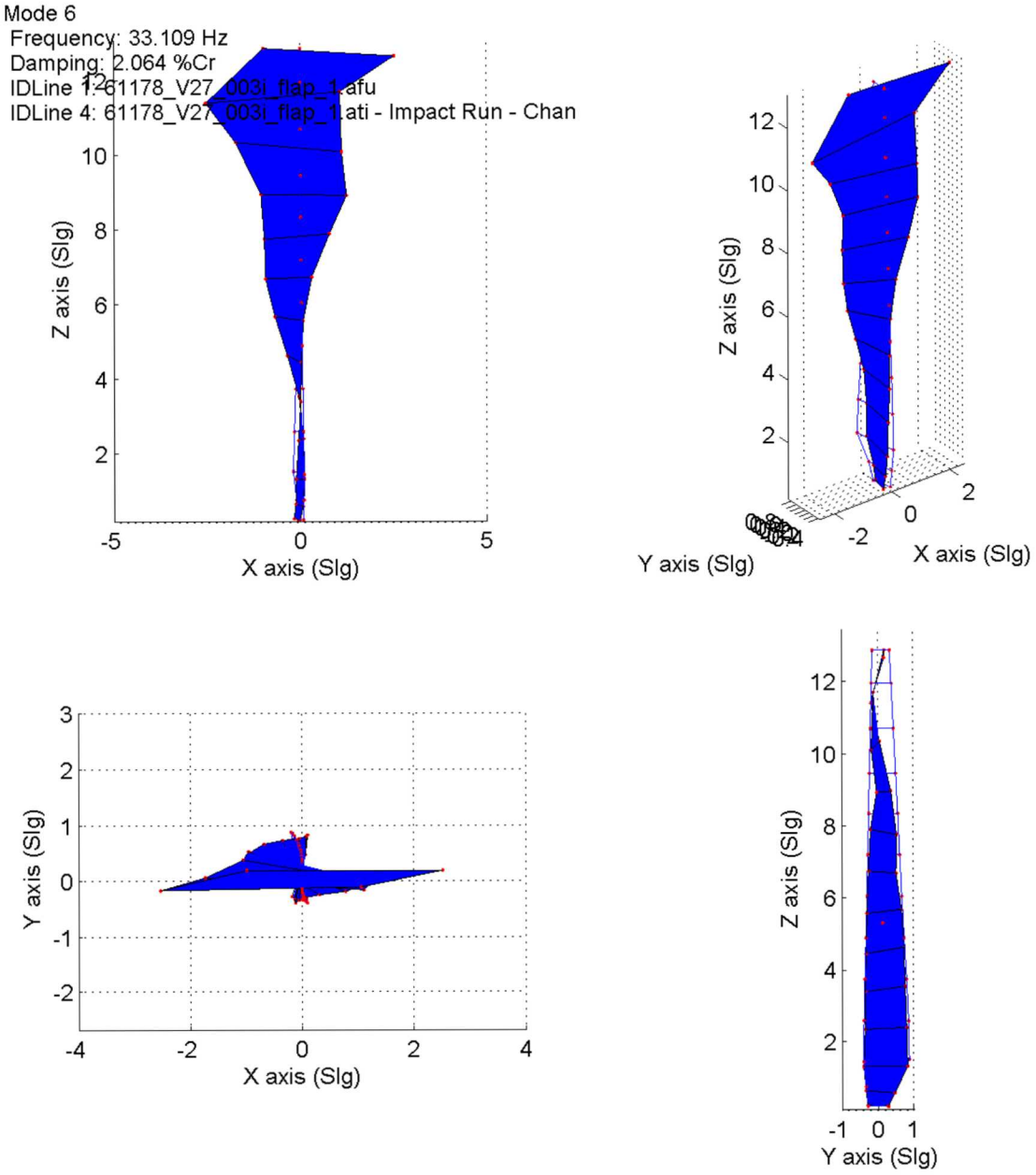
Mode 6
Frequency: 33.109 Hz
Damping: 2.064 %Cr
IDLine 1: 61178_V27_003i_flap_1.afu
IDLine 4: 61178_V27_003i_flap_1.ati - Impact Run - Chan
Z axis (Slg)
X axis (Slg)
Y axis (Slg)

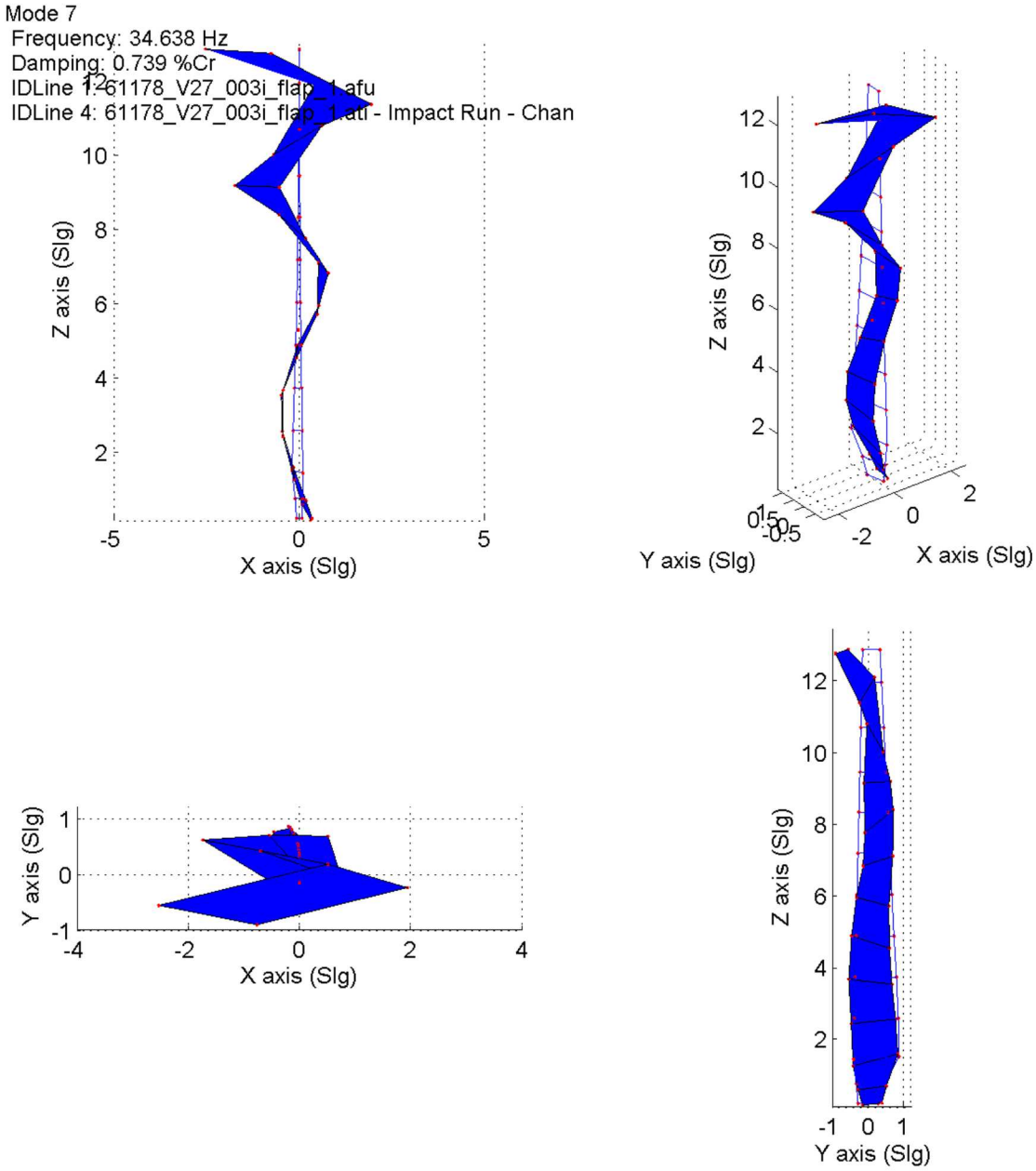
Mode 7
Frequency: 34.638 Hz
Damping: 0.739 %Cr
IDLine 1: 61178_V27_003i_flap_1.afu
IDLine 4: 61178_V27_003i_flap_1.atr - Impact Run - Chan
Z axis (Slg)
X axis (Slg)
Y axis (Slg)

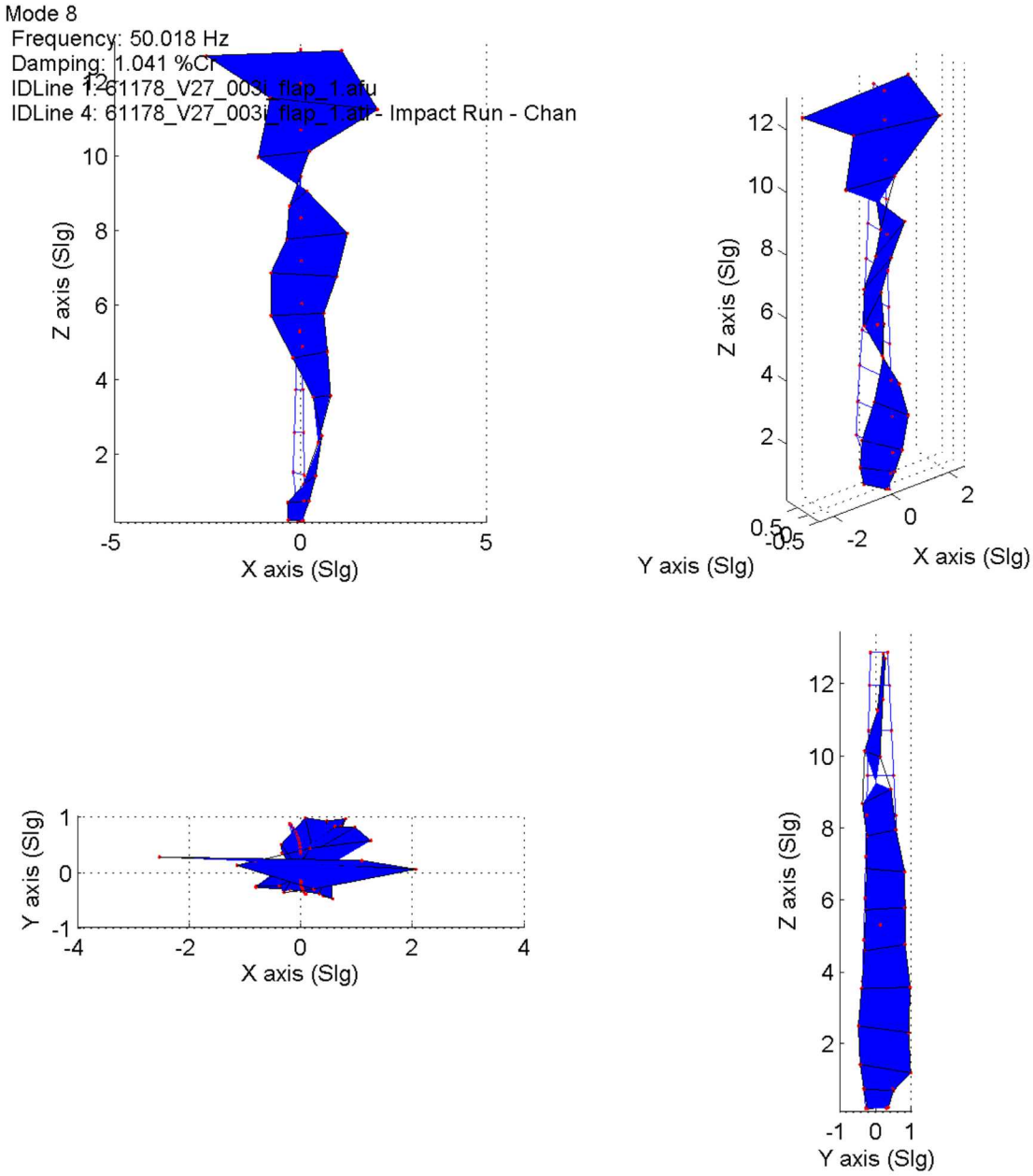
Mode 8
Frequency: 50.018 Hz
Damping: 1.041 %Cr
IDLine 1: 61178_V27_0031_flap_1.afu
IDLine 4: 61178_V27_0031_flap_1.atr - Impact Run - Chan
Z axis (Slg)
X axis (Slg)
Y axis (Slg)

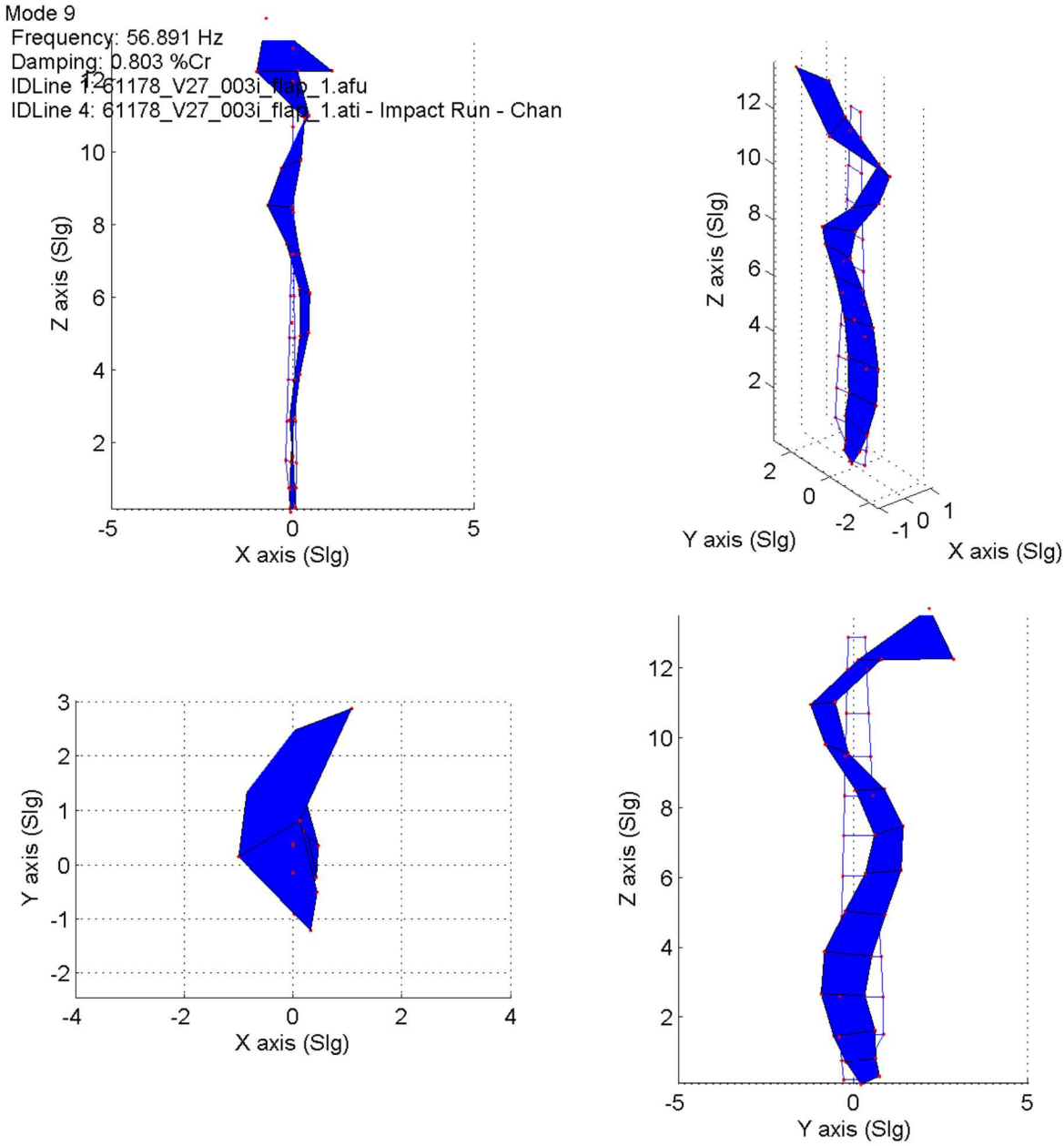
Mode 9
Frequency: 56.891 Hz
Damping: 0.803 %Cr
IDLine 1: 61178_V27_003i_flap_1.afu
IDLine 4: 61178_V27_003i_flap_1.ati - Impact Run - Chan
Z axis (Slg)
X axis (Slg)
Y axis (Slg)

# Appendix G

# Equipment Specifications

# MODAL 110

Exciter System

- ***MB's Modal family has a new addition with a new look! Unveiling the MODAL 110 – longer – lighter – stronger – and RED!***
- ***MB MODAL EXCITERS are the #1 selling exciters in the world – over 1000 in use in over 18 countries!***

The new MODAL 110 delivers 110 lbs force (500N) and 1.5" stroke pk-pk; has twice the force and 50% more stroke than the MODAL 50.

- **Long Stroke**
- **Light moving element mass**
- **Low longitudinal stiffness**
- **Stiff radial stiffness**
- **Neodymium magnets**
- **Much lighter exciter weight**
- **Thru-hole to attach stinger**

| MODAL 110 EXCITER SPECS | MB750VCF AMPLIFIER SPECS |
|---|---|
| ❖ Force: 110 lbf peak (500 N) forced-air cooled; 55 lbf pk (250 N) convection<br>❖ Force: 75 lbf RMS (350 N) forced-air cooled; 40 lbf RMS (175 N) convection<br>❖ Stroke: 1.5" (38 mm) p-p; 1.6" (41 mm) between stops<br>❖ Bandwidth: DC-5000 Hz<br>❖ Moving element: 0.9 lbs (0.4 kg)<br>❖ Longitudinal stiffness; 30 lb/in (5.2N/mm)<br>❖ Shaker weight: <48 lbs (22 kg)<br>❖ Shaker cooling: shop air, with integral air coupling; aux. fan cooling package<br>❖ Clearance hole through armature for stinger<br>❖ Compression and piano wire stingers, secured with collets and chuck nuts<br>❖ Overtravel protection<br>❖ Current limiting shutdown<br>❖ Options: Accessory Kit & Cooling Unit<br>❖ CE Mark | ❖ Linear amplifier design<br>❖ Frequency range; DC-10,000 Hz<br>❖ AC or DC coupled, separate BNCs<br>❖ Current feedback and voltage feedback, external switch selectable<br>❖ 75 VRMS max. output voltage<br>❖ 10 ARMS max. output current<br>❖ Output current measurement, BNC<br>❖ Shaker overtravel shutdown<br>❖ Programmable current limiting<br>❖ Input power: 100, 120, 208, 220, 240V; 50/60 Hz (1.5 kVA)<br>❖ Sig. IN for max OUT: 1, 3, 10 Vpk<br>❖ Phase shift between output current and BNC value: <1 degree<br>❖ 19" rack mount x 7"H x 12"D (178 mm H x 305 mm D)<br>❖ Weight: 45 lbs (20 kg)<br>❖ CE Mark |

MB Dynamics Inc • 25865 Richmond Road • Cleveland OH 44146 USA • 216.292.5850 • sales@mbdynamics.com

**High-speed Digitizers**
**VT1432B**

- 8 input ranges including a 100mV range allows use of low sensitivity transducers
- True balanced differential inputs
- On-board user-programmable DSP greatly improves total system performance
- User programmable digital anti-alias filters, with API controllable FIR and Bessel filter
- FIR digital anti-alias filter provides linear phase response for accurate single and cross channel measurements
- Multiple breakout box options with built-in signal conditioning including charge inputs, simplify tests and reduce cost
- Optional arbitrary source or dual input tachometer
- 32 MB on card FIFO memory plus optional local bus allows data records up to 146 GB with the VT2216A VXI data disk, and larger data files to external SCSI disks

**16-CHANNEL 102.4KSA/S 24-BIT DIGITIZER PLUS DSP**

## Agilent E1434A 4-Channel 65kSa/s Arbitrary Source

The Agilent Technologies E1434A four-channel arbitrary source is a C-size, one-slot, VXI module that provides stimulus for mechanical, acoustical, and electrical testing. Its versatile waveform types, performance, and tight integration with the E1432A and E1433A digitizers make it the ideal source for multi-channel measurements. Built-in sine and random noise waveforms save development time and offload computation and data movement chores from the host computer.

A single-channel version of the E1434A is available as an internal option (1D4) to the E1432A and E1433A digitizers.

▼ **More info on this product**

Downloads
Table 1

**Yamaha Shaker Amplifier**

# Specifications

## ■ General Specifications

| | | P7000S | P5000S | P3500S | P2500S |
|---|---|---|---|---|---|
| Power Output Level (Rated Power) | 8 Ω/STEREO | 750 W × 2 | 525 W × 2 | 390 W × 2 | 275 W × 2 |
| 1 kHz | 4 Ω/STEREO | 1100 W × 2 | 750 W × 2 | 590 W × 2 | 390 W × 2 |
| THD + N = 1% | 8 Ω/BRIDGE | 2200 W × 1 | 1500 W × 1 | 1180 W × 1 | 780 W × 1 |
| | 8 Ω/STEREO | 700 W × 2<br>650 W × 2 (European Model) | 500 W × 2 | 350 W × 2 | 250 W × 2 |
| 20 Hz – 20 kHz | 4 Ω/STEREO | 950 W × 2 | 700 W × 2 | 450 W × 2 | 310 W × 2 |
| THD + N = 0.1% | 8 Ω/BRIDGE | 1900 W × 1 | 1400 W × 1 | 900 W × 1 | 620 W × 1 |
| 1 kHz | 2 Ω/STEREO | 1600 W × 2 | 1300 W × 2 | 1000 W × 2 | 650 W × 2 |
| 20 ms non-clip | 4 Ω/BRIDGE | 3200 W × 1 | 2600 W × 1 | 2000 W × 1 | 1300 W × 1 |
| Power Bandwidth | Half Power | 10 Hz – 40 kHz (THD + N = 0.5 %) | | | |
| Total Harmonic Distortion (THD + N)<br>20 Hz – 20 kHz, Half Power | 4 Ω – 8 Ω/STEREO<br>8 Ω/BRIDGE | ≦ 0.1 % | | | |
| Frequency Response | RL = 8 Ω, Po = 1 W | 0 dB, +0.5 dB, –1 dB f = 20 Hz – 50 kHz | | | |
| Intermodulation distortion (IMD)<br>60 Hz:7 kHz, 4:1, Half Power | 4 Ω – 8 Ω/STEREO<br>8 Ω/BRIDGE | ≦ 0.1 % | | | |
| Channel Separation<br>Vol. max | Half Power RL = 8 Ω 1 kHz<br>input 600 Ω shunt | ≧ 70 dB | | | |
| Residual Noise Vol. min. | 20 Hz – 20 kHz (DIN AUDIO) | ≦ –70 dBu | | | |
| SN Ratio | 20 Hz – 20 kHz (DIN AUDIO) | 104 dB | 103 dB | 102 dB | 100 dB |
| Damping Factor | RL = 8 Ω, 1 kHz | ≧ 350 | | ≧ 200 | |
| Sensitivity (Vol. max.) Rated Power 8 Ω | | +8 dBu | +6 dBu | +4 dBu | +3 dBu |
| Voltage Gain (Vol. max.) | | 32.1 dB | | | |
| Input Impedance | | 30 kΩ/balanced, 15 kΩ/unbalanced | | | |
| Controls | Front Panel | POWER switch (Push on/Push off)<br>Two 31-step Volume control knobs (one per ch) | | | |
| | Rear Panel | MODE switch (STEREO/PARALLEL/BRIDGE)<br>Two FILTER switches (SUBWOOFER/LOW CUT/OFF)<br>Two fc knobs (25 to 150 Hz)<br>YS Processing switch (ON/OFF) | | | |
| Connectors | INPUT | XLR-3-31 jacks (one per ch)<br>1/4-inch TRS phone jacks (one per ch) | | | |
| | OUTPUT | Speakon jacks (one per ch)<br>5-way binding posts<br>1/4-inch phone jacks (one per ch) | | | |
| Indicators | POWER | × 1 (Green) | | | |
| | PROTECTION | × 1 (Red) | | | |
| | TEMP | × 1 (Red) (heatsink temp ≧ 85°C) | | | |
| | CLIP | × 2 (Red) | | | |
| | SIGNAL | × 2 (Green) | | | |
| | YS Processing | × 1 (Yellow) | | | |
| Load protection | | POWER switch ON/OFF muting | | | |
| | | DC-fault power supply shutdown | | DC detection | |
| Amp. protection | | Temp. detection (heat sink temp ≧ 90°C), VI limiter (RL ≦ 1 Ω) | | | |
| Limiter | | Comp: THD ≧ 0.5 % | | | |
| Cooling | | Dual variable-speed fan | | Single variable-speed fan | |
| Power Requirements | United States & Canada | 120 V, 60 Hz | | | |
| | Europe | 230 V, 50 Hz | | | |
| | Australia | 240 V, 50 Hz | | | |
| Power Consumption | Idling | 35 W | 35 W | 30 W | 25 W |
| | 1/8 output power, 4 Ω | 700 W | 550 W | 450 W | 320 W |
| | Maximum output, 4 Ω | 4000 W | 3000 W | 2000 W | 1600 W |
| Dimensions (W × H × D) | | 480 × 88 × 456 mm | | | |
| Weight | | 12 kg | 12 kg | 15 kg | 14 kg |
| Included Accessories | | Security cover (with a hex wrench), Owner's Manual | | | |

0 dBu=0.775 Vrms, Half Power=1/2 Power Output Level (Rated Power)

Specifications and descriptions in this owner's manual are for information purposes only. Yamaha Corp. reserves the right to change or modify products or specifications at any time without prior notice. Since specifications, equipment or options may not be the same in every locale, please check with your Yamaha dealer.

European models
Purchaser/User Information specified in EN55103-1 and EN55103-2

## Accelerometers

PCB PIEZOTRONICS INC.

**Model 333B**

**Product Type:** Accelerometer

Modal array, ceramic shear ICP® accel., 100 mV/g, 2 to 1000 Hz, 3-pin socket connector mounting

There is no product photo available at this time.

| PERFORMANCE | ENGLISH | SI | |
|---|---|---|---|
| Sensitivity (±20 %) | 100 mV/g | 10.2 mV/(m/s²) | |
| Measurement Range | ±50 g pk | ±490 m/s² pk | |
| Frequency Range (±5 %) | 2 to 1000 Hz | 2 to 1000 Hz | |
| Resonant Frequency | 5 kHz | 5 kHz | |
| Phase Response (±5 °) | 2 to 1000 Hz | 2 to 1000 Hz | |
| Broadband Resolution (1 to 10000 Hz) | 0.00007 g rms | 0.0007 m/s² rms | [1] |
| Non-Linearity | 1 % | 1 % | [2] |
| Transverse Sensitivity | 5 % | 5 % | [3] |
| **ENVIRONMENTAL** | | | |
| Overload Limit (Shock) | ±3500 g pk | ±34300 m/s² pk | |
| Temperature Range | 0 to 150 °F | -18 to +66 °C | |
| Temperature Response | 0.15 %/°F | 0.27 %/°C | [1] |
| **ELECTRICAL** | | | |
| Excitation Voltage | 18 to 30 VDC | 18 to 30 VDC | |
| Constant Current Excitation | 2 to 20 mA | 2 to 20 mA | |
| Output Impedance | 100 ohms | 100 ohms | |
| Output Bias Voltage | 8 to 12 VDC | 8 to 12 VDC | |
| Discharge Time Constant | 0.7 to 1.3 sec | 0.7 to 1.3 sec | |
| Settling Time (within 10% of bias) | <5 sec | <5 sec | |
| Spectral Noise (1 Hz) | 20 g/ Hz | 196 ( m/s²)/ Hz | [1] |
| Spectral Noise (10 Hz) | 4.3 g/ Hz | 42.1 ( m/s²)/ Hz | [1] |
| Spectral Noise (100 Hz) | 1.3 g/ Hz | 12.8 ( m/s²)/ Hz | [1] |
| Spectral Noise (1 kHz) | 0.6 g/ Hz | 5.9 ( m/s²)/ Hz | [1] |
| **PHYSICAL** | | | |
| Sensing Element | Ceramic | Ceramic | |
| Sensing Geometry | Shear | Shear | |
| Housing Material | Polymer | Polymer | |
| Sealing | Hermetic | Hermetic | |
| Size (Height x Diameter) | 0.84 in x 0.48 in | 21.4 mm x 12.2 mm | |
| Weight | 0.2 oz | 5.6 gm | [1] |
| Electrical Connector | 3-Pin Socket | 3-Pin Socket | |

**SUPPLIED ACCESSORIES:**

Model ACS-2 NIST Traceable single point (100 Hz) sensitivity. (1)

**OPTIONAL VERSIONS**

**T** - TEDS Capable of Digital Memory and Communication Compliant with IEEE P1451.4

**TLA** - TEDS LMS International - Free Format

**TLB** - TEDS LMS International - Automotive Format

**TLC** - TEDS LMS International - Aeronautical Format

*All specifications are at room temperature unless otherwise specified.*

**NOTES:**

[1] Typical.

[2] Zero-based, least-squares, straight line method.

[3] Transverse sensitivity is typically <= 3%.

**In the interest of constant product improvement, we reserve the right to change specifications without notices.**

## DC Accelerometer

| Model Number 3741D4HB30G | DC ACCELEROMETER | Revision E ECN #: 26946 |
|---|---|---|

| Performance | ENGLISH | SI | |
|---|---|---|---|
| Sensitivity (±5 %) | 66.7 mV/g | 6.80 mV/(m/s²) | [6] |
| Measurement Range | ±30 g pk | ±294.2 m/s² pk | |
| Frequency Range (±5 %) | 0 to 1000 Hz | 0 to 1000 Hz | |
| Frequency Range (±10 %) | 0 to 2000 Hz | 0 to 2000 Hz | |
| Resonant Frequency | >3 kHz | >3 kHz | |
| Phase Response (100 Hz) | <4 ° | <4 ° | |
| Phase Response (200 Hz) | <7 ° | <7 ° | |
| Damping Method | Gas | Gas | |
| Damping Ratio (±0.25) | 0.65 | 0.65 | |
| Broadband Resolution (0.5 to 100 Hz) | 2.5 mg rms | 0.0245 m/s² rms | [2] |
| Non-Linearity | ≤1 % FS | ≤1 % FS | [7] |
| Transverse Sensitivity | ≤3 % | ≤3 % | |
| **Environmental** | | | |
| Overload Limit (Shock) | ±10000 g pk | ±98100 m/s² pk | |
| Temperature Range (Operating) | -65 to 250 °F | -53.9 to 121 °C | |
| Temperature Range (Storage) | -65 to 250 °F | -53.9 to 121 °C | |
| Temperature Coefficient of Sensitivity | ±3.0 % | ±3.0 % | [4] |
| Zero g Offset Temperature Coefficient | ±2.0 %FSO | ±2.0 %FSO | [5][4] |
| Base Strain Sensitivity (Measured at 250 με) | 0.01 g/με | 0.10 (m/s²)/με | |
| **Electrical** | | | |
| Excitation Voltage | 6 to 30 VDC | 6 to 30 VDC | |
| Current Consumption | ≤7.5 mA | ≤7.5 mA | |
| Output Impedance | ≤100 ohm | ≤100 ohm | |
| Offset Voltage (0 g) | ±50 mVDC | ±50 mVDC | [1] |
| Common Mode Voltage (±0.1 VDC) | +2.5 VDC | +2.5 VDC | |
| Spectral Noise (1 to 1000 Hz) | 387 μg/√Hz | 3796 (μm/s²)/√Hz | [2] |
| Electrical Isolation (Base) | $>10^8$ | $>10^8$ | [3] |
| **Physical** | | | |
| Housing Material | Anodized Aluminum | Anodized Aluminum | |
| Sealing | Epoxy | Epoxy | |
| Size (Height x Length x Width) | 0.30 in x 1.00 in x .85 in | 7.62 mm x 25.4 mm x 21.6 mm | |
| Weight (without cable) | 0.35 oz | 9.92 gm | [2] |
| Electrical Connector | Integral Cable | Integral Cable | |
| Electrical Connection Position | Side | Side | |
| Cable Termination | Pigtail Ends | Pigtail Ends | |
| Cable Type | 010 4-cond Shielded | 010 4-cond Shielded | |
| Cable Length | 10 ft | 3 m | |
| Mounting | Through Holes (2) | Through Holes (2) | |

CE[8]

*All specifications are at room temperature unless otherwise specified.*
In the interest of constant product improvement, we reserve the right to change specifications without notice.
ICP® is a registered trademark of PCB group, Inc.

**Optional Versions** (Optional versions have identical specifications and accessories as listed for standard model except where noted below. More than one option maybe used.)

**Notes**

[1] Offset tolerance is based on manufacturers supplied cable length.
[2] Typical.
[3] Case and shield to mounting surface or cable leads.
[4] -65 to +250 °F, ref. 75 °F (-54 to +121 °C, ref. 24 °C)
[5] FSO = Full Scale Output over the Measurement Range (4VDC).
[6] Measured at 100 Hz, 1 grms.
[7] Zero-based, least-squares, straight line method.
[8] See PCB Declaration of Conformance PS027 for details.

**Optional Accessories**
080A208 Triaxial mounting block ()

**Supplied Accessories**
081A103 Mounting screw (2)
ACS-84 (1)
M081A103 Mounting screw and washer, M3 x 0.5 thread (2)

| Entered: BLS | Engineer: TCJ | Sales: RJL | Approved: BAM | Spec Number: |
|---|---|---|---|---|
| Date: 08/07/2007 | Date: 07/27/2007 | Date: 07/31/2007 | Date: 07/30/2007 | **30070** |

PCB PIEZOTRONICS VIBRATION DIVISION
3425 Walden Avenue
Depew, NY 14043
UNITED STATES
Phone: 888-684-0013
Fax: 716-685-3886
E-mail: vibration@pcb.com
Web site: www.pcb.com

UNIVERSAL, LOW-IMPEDANCE, VOLTAGE-MODE

# QUARTZ FORCE TRANSDUCER

with built-in amplifier Series 208A

PCB PIEZOTRONICS

FORCE

- measures tension, compression and impact
- measures incremental forces at any level
- high-level (10V), low-impedance (100 ohm) output
- static calibration; short-term static response
- rigidity nearly that of solid steel

For measuring compression, tension, impact, reaction and actuation forces in testing, vibrating, tensioning, balancing, striking, welding, rolling, cutting, coining, forming, pressing, machining and punching operations. Adaptable to controlling, monitoring, adjusting, calibrating, counting, sorting, indicating, warning, etc. Applications include vibration exciters, machine tools, aerodynamic models, materials testing and mechanical-impedance testing.

Model 208A03 quartz force transducer measures dynamic and short term static forces from 1.0 to 500 pounds (.001 to 10,000 lb optional) at any tare level within this range. In constant temperature environments, this medium-range model follows transient events lasting a few percent (~20 sec) of the discharge time constant and automatically eliminates static (tare) signal components in about 5 time constants. Optional lower range models more quickly eliminate static signal components.

The structure of this transducer contains two thin quartz disks or plates operating in a thickness-compression mode and capped by hardened steel cylindrical members. The exceptional stiffness of this design, which approaches that of a solid steel cylinder, has little effect on the rigidity of most test structures or test objects.

Quartz force transducers install by clamping precision mounting surfaces in intimate contact, usually with an elastic berryillium-copper stud or bolt. Since forces are transmitted through these interfaces, it is important that mating surfaces be precision machined and ground extremely flat and parallel, like those on the transducer. Series 208A transducers, incorporating a separate outer case and an integral metal flexure, withstand moderate torque and tranverse loads, but for high accuracy measurements, the force ought to be centrally and axially applied. A detachable impact plate and pad is supplied with the transducer.

When connected to a PCB power unit, self-amplifying PCB transducers generate a high-level, low-impedance analog output signal proportional to the measurand and compatible with most readout instruments. The simple power unit circuit powers the transducer over the signal lead (coaxial or 2-wire), eliminates bias on the output and monitors normal or faulty operation. Signal quality is almost independent of cable, length, condition and motion.

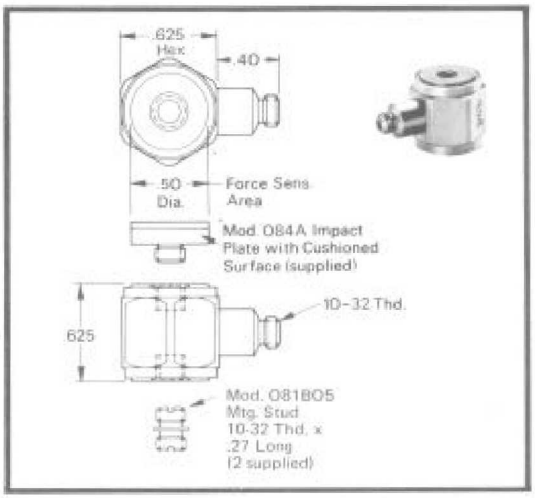


| SPECIFICATIONS: | Model No. | 208A03 |
|---|---|---|
| Range, Tension & Compression (5V out) | lb | ±500 |
| Maximum Compression | lb | 5,000 |
| Maximum Tension | lb | 750 |
| Resolution (200 μV p-p noise) | lb | 0.02 |
| Stiffness | lb/μin | 10 |
| Sensitivity | mV/lb | 10 |
| Resonant Frequency (no load) | Hz | 70,000 |
| Rise Time | μsec | 10 |
| Discharge Time Constant (T.C.) | sec | 2,000 |
| Low-Frequency (−5%) | Hz | 0.0003 |
| Linearity, B.S.L. | % | 1 |
| Output Impedance | ohms | 100 |
| Excitation (thru C.C. diode) | VDC/mA | +18 to 24/2 to 20 |
| Temperature Coefficient | %/°F | 0.03 |
| Temperature Range | °F | −100 to +250 |
| Shock (no load)/Vibration | g | 10,000/2,000 |
| Weight | gm | 25 |
| **Model No.** (Optional Ranges) | | |
| −500 + 5,000 lb (10,000 max) | 1 mV/lb | 208A05 |
| −500 + 1,000 lb (7,000 max) | 5 mV/lb | 208A04 |
| ±100 lb (+2,000 max) (500 sec T.C.) | 50 mV/lb | 208A02 |
| ±10 lb (+200 max) (50 sec T.C.) | 500 mV/lb | 208A |
| Charge-Mode | 20 pC/lb | 218A |

Note: One lbf = 4.448N (kg·m·s$^{-2}$) = 0.4536 kgf (kp)

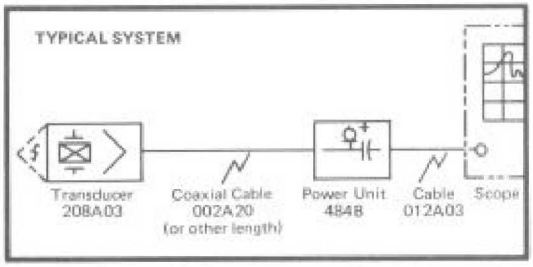

## Signal Conditioner

Model Number
**442B119**

### 16 CHANNEL ICP® SENSOR SIGNAL CONDITIONER

Revision: -B-
ECN #: ECN-64

**PERFORMANCE**

| | | |
|---|---|---|
| Frequency Response (±5% Amplitude) | Hz | 0.125 to 30k |
| Frequency Response (±5° Phase) | Hz | 0.3 to 10k |
| Broadband Noise (1 to 27.5k Hz) | µVrms | <100 |
| Signal Gain (±1%) | V/V | x1 |
| Sensor Excitation Voltage (±0.5) | VDC | 22 |
| Constant Current Sensor Excitation | mA | 2 to 10 (Preset @ 4mA) |
| Ouput Range | Vpk | ±10 |
| Output Impedance (±10%) | Ω | 1000 |
| Typical Spectral Noise | µVrms/Hz$^{1/2}$ | 15 @ 1 Hz<br>5 @ 10 Hz<br>0.4 @ 100 Hz<br>0.2 @ 1,000 Hz |

**DIGITAL COMMUNICATION**

| | | |
|---|---|---|
| Module Control | Type | Via PCB 440 Series RS-485 Backplane Network |
| TEDS Sensor Control | Type | IEEE P1451.4 |

**ENVIRONMENTAL**

| | | |
|---|---|---|
| Operating Temperature Range | °F (°C) | 32 to 120 (0 to 50) |

**ELECTRICAL**

| | | | |
|---|---|---|---|
| Power Consumption | mAmps @ 28VDC | 94 | [1] |
| | mAmps @ 5VDC | 165 | |
| | mAmps @ 15VDC | 85 | |
| | mAmps @ -15VDC | 60 | |

**MECHANICAL**

| | | | |
|---|---|---|---|
| Input Connector | Type | DB-50 Female | |
| Output Connector | Type | Quad Agilent E1432 Compatible | |
| Size (H x W) | inches (mm) | 5.05 x 1.8 (128,3 x 45,7) | [2] |
| Mass | lb (kg) | 0.69 (0,31) | |

**NOTES:**
[1] All Power Consumption Values Rated At Factory Set 4mA Constant Current Sensor Excitation
[2] Conforms to PCB 440 Series Modular System Form Factor (Single Slot)

**SUPPLIED ACCESSORIES:**
PCB 440 Series Control Software

*All specifications are at room temperature unless otherwise specified.*

ICP® is a registered trademark of PCB Group, Inc.
*In the interest of constant product improvement, specifications may change without notice.*

| Engineer: | Sales: | Approved: | Spec Number: |
|---|---|---|---|
| Date: | Date: | Date: | PS-0010 |

THE MODAL SHOP
TMS
A PCB GROUP CO.

*3149 East Kemper Rd*
*Cincinnati, OH 45241*

*800-860-4867* *Fax (513)458-2172* *sales@modalshop.com*

ENG-F011REV. NR 1/19/Y2K

## Kapton Blue Tape



800-343-1076
VentureTape
Insulation HVAC Shielding Industrial Stained Glass Glazing Optical Medical Construction Splicing Automotive

**981**

**1 mil (25 micron) Polyester Film**

Very thin, strong, polyester film with a high temperature resistant silicone adhesive. Exceptional quality, high performance. Excellent adhesion to silicone treated materials at elevated temperatures. Available in blue, yellow, black and clear.
Splicing silicone treated casting papers and release liners.

| | |
|---|---|
| **Substrate Thickness:** | |
| **Adhesive Thickness:** | |
| **Total Thickness:** | |
| **Peel Adhesion:** | 25 oz/in width (7.9 N/2.5 cm) |
| **Shear Strength:** | 2.2 psi 24+ hrs. (15.2 kPa) |
| **Elongation:** | 100% |
| **Tensile Strength:** | 18 lb/in width (81.5 N/2.5 cm) |
| **Temperature Resistance:** | -50°F to 500°F (-46°C to 260°C) |
| **Minium Application Temperature:** | 0°F (-18°C) |
| **Release Liner:** | N/A |
| **Adhesive Type:** | Silicone |

< Return to listing

## Load Cell

### SPECIFICATIONS

| PARAMETERS | MODEL 1210 | 1210 | 1220 | 1232 | 1240 |
|---|---|---|---|---|---|
| | CAPACITY | | | | |
| U.S. Models (lbf) | 300, 500, 1K, 2K | 5K, 10K | 25K, 50K | 100K | 200K |
| Metric Models (kN) | 1.5, 2.5, 5, 10 | 25, 50 | 100, 250 | 450 | 900 |
| **ACCURACY – (MAX ERROR)** | | | | | |
| Static Error Band–% FS | ± 0.04 | ± 0.05 | ± 0.05 | ± 0.06 | ± 0.07 |
| Nonlinearity–% FS | ± 0.04 | ± 0.05 | ± 0.05 | ± 0.05 | ± 0.07 |
| Hysteresis–% FS | ± 0.03 | ± 0.05 | ± 0.06 | ± 0.06 | ± 0.07 |
| Nonrepeatability–% RO | ± 0.01 | ± 0.01 | ± 0.01 | ± 0.01 | ± 0.01 |
| Creep, in 20 min–% | ± 0.025 | ± 0.025 | ± 0.025 | ± 0.025 | ± 0.025 |
| Side Load Sensitivity–% | ± 0.25 | ± 0.25 | ± 0.25 | ± 0.25 | ± 0.25 |
| Eccentric Load Sensitivity–%/in | ± 0.25 | ± 0.25 | ± 0.25 | ± 0.25 | ± 0.25 |
| **TEMPERATURE** | | | | | |
| Compensated Range–˚F | 15 to 115 | 15 to 115 | 15 to 115 | 15 to 115 | 15 to115 |
| Compensated Range–˚C | -10 to 45 | -10 to 45 | -10 to 45 | -10 to 45 | -10 to 45 |
| Operating Range–˚F | -65 to 200 | -65 to 200 | -65 to 200 | -65 to 200 | -65 to 200 |
| Operating Range–˚C | -55 to 90 | -55 to 90 | -55 to 90 | -55 to 90 | -55 to 90 |
| Effect on Zero–%RO/˚F – MAX | ± 0.0008 | ± 0.0008 | ± 0.0008 | ± 0.0008 | ± 0.0008 |
| Effect on Zero–%RO/˚C – MAX | ± 0.0015 | ± 0.0015 | ± 0.0015 | ± 0.0015 | ± 0.0015 |
| Effect on Output–%/˚F – MAX | ± 0.0008 | ± 0.0008 | ± 0.0008 | ± 0.0008 | ± 0.0008 |
| Effect on Output–%/˚C – MAX | ± 0.0015 | ± 0.0015 | ± 0.0015 | ± 0.0015 | ± 0.0015 |
| **ELECTRICAL** | | | | | |
| Rated Output–mV/V (Nominal) | 2.0 | 4.0 | 4.0 | 4.0 | 4.0 |
| Excitation Voltage–VDC – MAX | 20 | 20 | 20 | 20 | 20 |
| Bridge Resistance–Ohm (Nominal) | 350 | 350 | 350 | 350 | 350 |
| Zero Balance–% RO | ± 1.0 | ± 1.0 | ± 1.0 | ± 1.0 | ± 1.0 |
| Insulation Resistance–Megohm | 5000 | 5000 | 5000 | 5000 | 5000 |
| **MECHANICAL** | | | | | |
| Safe Overload–% CAP | ± 150 | ± 150 | ± 150 | ± 150 | ± 150 |
| Deflection @ RO–inch | 0.001 | 0.002 | 0.002 | 0.003 | 0.004 |
| Deflection @ RO–mm | 0.03 | 0.05 | 0.05 | 0.08 | 0.10 |
| Optional Base–P/N | B101 | B102 | B103 | B112 | B105 |
| Natural Frequency–kHz | 3.9, 5.0, | 6.6, 9.4 | 6.5, 7.0 | 5.8 | 4.9 |
| | 6.9, 9.8 | | | | |
| Weight–lb | 1.5 | 3.3 | 9.5 | 26 | 68 |
| Weight–kg | 0.7 | 1.5 | 4.3 | 11.8 | 30.9 |
| Connector | PC04E-10-6P | PC04E-10-6P | PC04E-10-6P | PC04E-10-6P | PC04E-10-6P |
| Calibration | T & C | T & C | T & C | T & C | T & C |

### OPTIONS*

Base (recommended)
Compression overload protection
Integral 10 ft cable
Bayonet Connector
Multiple bridge
Standardized output
Connector protection

### ACCESSORIES*

Mating connector
Instrumentation
Loading hardware

* *See appendix for more technical information*

### STANDARD CONFIGURATIONS

- 10 ft Integral Cable (12xxAJ-nn)
<or> PC04E-10-6P Standard Connector (12xxAF-nn)
<or> PT02E-10-6P Bayonet Connector (12xxACK-nn)
- Installed Base (-B suffix)

*Shown with optional base*

Interface Force Measurements Ltd., Crowthorne Business Estate, 'O' Wing, Old Wokingham Road, Crowthorne, Berks., RG45 6XE
www.interface.uk.com · email: info@interface.uk.com · Telephone: (+44) 01344 776666 · Fax:. (+44) 01344 774765

05/00

March 13, 2013

Mr. Bruce LeBlanc
Sandia National Laboratories
P.O. Box 5800
Albuquerque, NM 87123

Subject: ATA Report No. 61178, "Inertia Testing of SWIFT V27 Hub"

Dear Bruce:

This report documents ATA Engineering's inertia testing of one hub that is to be installed as part of the Sandia National Laboratories (SNL) Scaled Wind Farm Technology (SWIFT). Testing was conducted December 17–21, 2012, and January 6–11, 2013. Mass, CG, and moment of inertia terms were obtained for the hub. The testing procedure and results are documented below.

## Introduction

Sandia National Laboratories (SNL) is developing the Scaled Wind Farm Technology (SWIFT) center to enable rapid, cost-efficient testing and development of transformative wind energy technology. ATA Engineering, Inc., (ATA) was contracted as part of this effort to dynamically characterize a number of components and assemblies to be used at SWIFT. This report documents the inertia testing for one Vestas 27 (V27) hub. The testing was successfully completed December 17–21, 2012, and January 6–11, 2013. One hub was tested in a free-free configuration.

## Technical Approach

One Vestas 27 (V27) hub was tested to obtain mass and inertia properties. The weight of the hub was measured using a calibrated load cell; the weight of the yaw pitch linkage was included, as it was already mounted to the hub. The hub was then suspended from the gantry frame at two points to create a bifilar pendulum as shown in Figure 1. The frequency of rotation about the yaw axis was measured and used to calculate the moment of inertia term about the yaw axis.

Figure 1. Hub bifilar setup mounted to frame (left) and to hub (right).

The hub was then suspended by air springs (Firestone Airmount Isolators Model 19) in order to approximate a free-free boundary condition as shown in Figure 2. To ensure high-quality drive point measurements, a cylindrical coordinate system was used when mounting the seismic accelerometers (PCB 393B04). ATA created a test model representative of the hub to develop a set of test measurement degrees of freedom (DOF). The test display model (TDM), shown in Figure 3, was used for mode shape visualization.

Figure 2. V27 hub suspended on air springs.

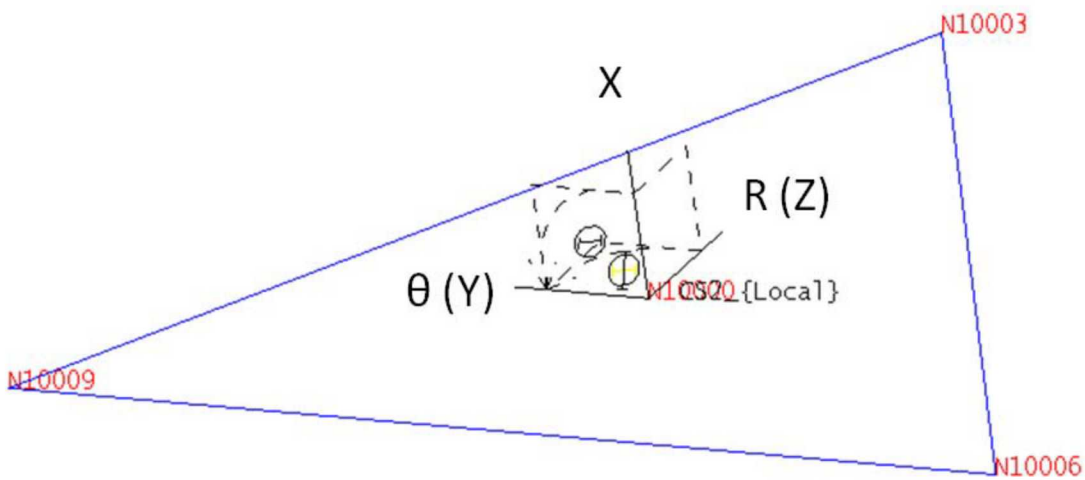


Figure 3. Hub TDM using rotor global coordinate system but with cylindrical testing coordinate system.

Two different methods for calculating the inertia properties were used.

The first method, modal inversion, involves obtaining high-quality rigid body mode shapes. This was performed by using shakers to excite all six rigid body modes in the same data run. Figure 4 shows the locations of the shakers.

Figure 4. Two shakers used to excite V27 hub.

Figure 5 shows the power spectrum mode-indicator function (PSMIF) for the test run with two shakers. The PSMIF is the summation of all FRFs multiplied by each FRF conjugate and is an ideal function to visualize the overall response of the structure. As seen, all six rigid body modes can be seen in the peaks of the response (the fifth and sixth mode are closely spaced about 11 Hz, but they are two distinct modes). To evaluate the quality of the rigid body modes obtained, the PSMIF was then synthesized using only the six rigid body modes. The synthesized PSMIF shows a high level of correlation with the test data (though the fit degrades slightly due to the close spacing of modes 5 and 6). As a result, there is confidence that the extracted rigid body modes will accurately describe the inertia properties of the hub.

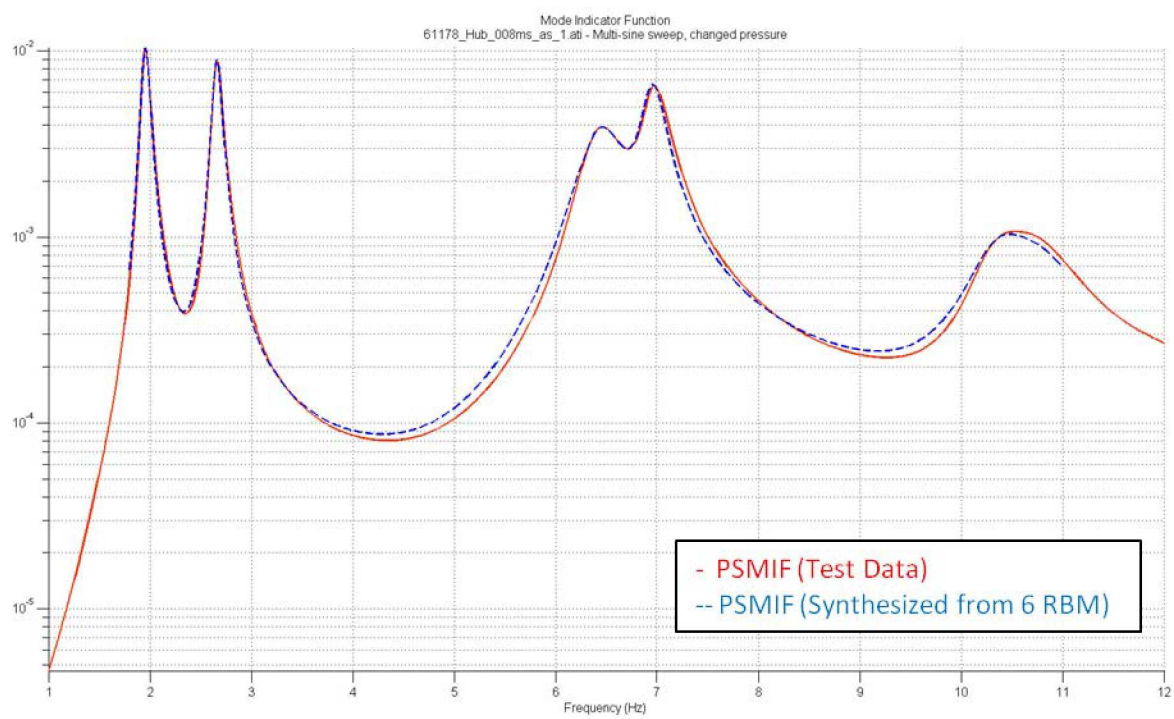


Figure 5. Test vs. synthesized PSMIF from shaker runs showing all six rigid body modes.

The second method for calculating the inertia properties, mass line estimation, involves measuring the mass line of FRFs. This was performed by using an impact hammer (PCB 086D20) to obtain high-quality FRFs by fully populating the FRF matrix, including drive points at every DOF. Figure 6

shows the drive point measurements for all of the DOFs where the six rigid body modes are evident in the peaks seen in the responses. There are clear mass lines from 20 to 50 Hz, showing good separation between the rigid body and flexible modes. As seen in the zoomed-in portion, however, there is a small but noticeable oscillation in some of the mass lines. As a result, there is expected to be some error involved in the estimation of the terms using this method.

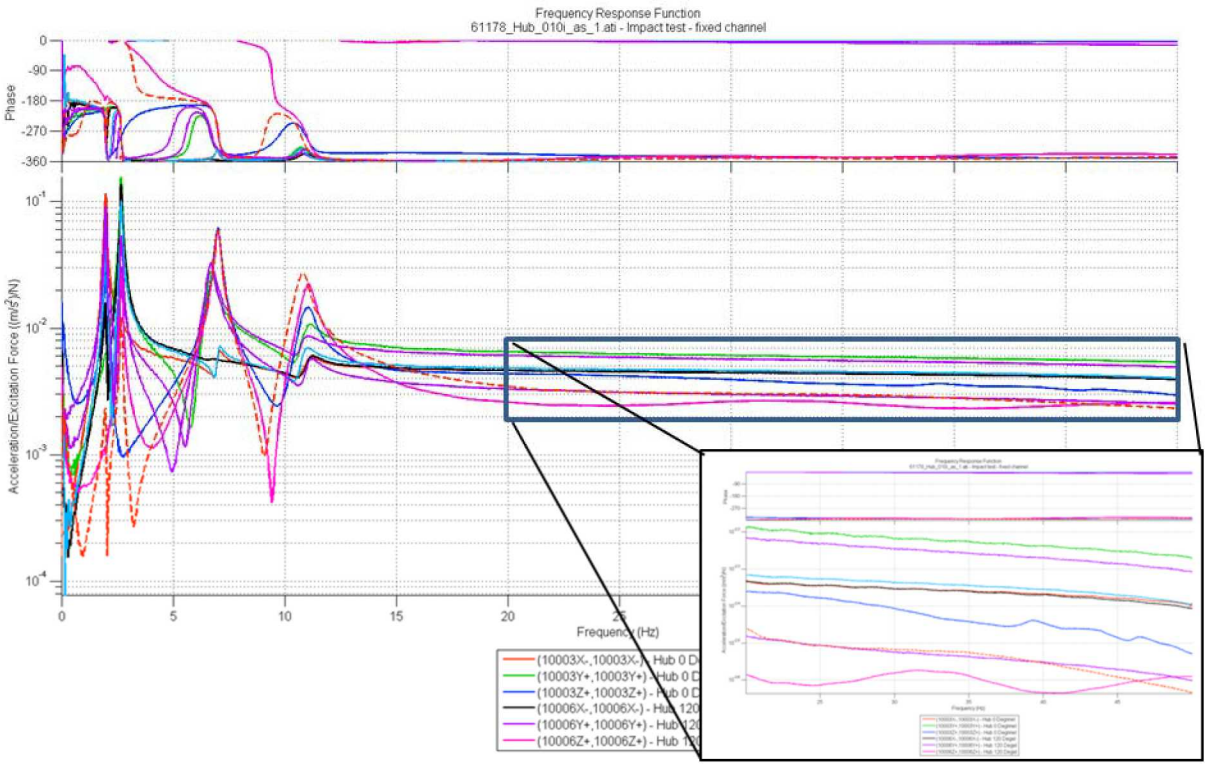


Figure 6. Drive point FRFs from impact runs showing mass lines.

Both methods were used to calculate the rigid body mass matrix as described in the Summary of Mass and Inertia Approaches. The resulting terms were compared to the mass obtained from the load cell and the inertia term obtained from the bifilar pendulum approach. Table 1 lists the various terms obtained from all of the methods used.

Table 1. Extracted inertia properties for V27 hub.

| Mass and Inertia Properties of V27 Hubs (Pitch Yaw Linkage Included) | | | | | |
|---|---|---|---|---|---|
| **Property** | **Hub #** | **Load Cell** | **Bifilar Pendulum** | **Modal Inversion**** | **Mass Line Inversion** |
| **Mass (kg)** | **1** | 481.7 | | 508.1 | 483.7 |
| | **2** | 474.0 | | | |
| **CGx (m)*** | **1** | | | -0.438 | -0.754 |
| **Cgy (m)*** | | | | 0.015 | 0.105 |
| **CGz (m)*** | | | | 0.005 | -0.143 |
| **Ixx (kg*m$^2$)** | | | 26.6 | 69.1 | 110.8 |
| **Iyy (kg*m$^2$)** | | | | 76.3 | 343.6 |
| **Izz (kg*m$^2$)** | | | | 86.2 | 151.6 |
| *** Origin Defined at Front Face of Hub Rotor About the Center Using Rotor Csys** | | | | | |
| **** Includes the Effective Mass of the Airbags** | | | | | |

As seen in the table, both the modal inversion and mass line inversion methods yield approximately the same mass as the load cell to within 5%. The CGs are similar between both methods, but there is an observable discrepancy between the two. The inertia for the bifilar pendulum is significantly lower than both methods, and the mass line inversion is noticeably higher than the modal inversion.

All four methods used to obtain the mass and inertia properties are discussed below to explain possible sources of error and to comment on their accuracy.

- The load cell used to measure the mass is a calibrated transducer with accuracy down to the tenth of a kilogram. These measurements are assumed accurate.
- Use of the bifilar pendulum assumes that the two straps are equal in length and hang perfectly vertical. Since visual inspection of the straps shows that neither of these assumptions was valid, the resulting term is likely to be inaccurate.
- The modal inversion was shown to have a high fit between the test data and the synthesized response. The highest percent error on any of the modes was 2%, also indicating a high level of correlation. The result for the mass is high due to the influence of the airbags, as the upper airbag plate is considered part of the system and is therefore added to the weight. The results seen for the CG appear reasonable; the Y and Z terms should be close to zero, as the hub is symmetrical about those two axes. The X term should be about half a meter, as the test origin was obviously away from the expected CG of the hub. The inertia terms about Y and Z are also fairly close, which is expected due to the symmetry of the hub.
- The mass line inversion was shown to have some oscillations, which indicated that the estimated results would therefore contain error. Although the results are fairly reasonable, they are high for all of the CG and inertia terms. Due to the hub's physical structure, impacting at some of the drive points was more challenging and poorer results were obtained.

**Summary and Conclusions**

The V27 hub was tested to obtain mass and inertia properties for use as part of SNL SWIFT. All aspects of this test were completed successfully.

Thank you for the opportunity to complete this project work for Sandia National Laboratories. Please contact David Cloutier or Tim Marinone if you have any questions about this report.

Sincerely,

Scanned signature - original on file ATA ENGINEERING INC

Tim Marinone
Engineer (858.480.2078; tim.marinone@ata-e.com)

Reviewed by:

Scanned signature - original on file ATA ENGINEERING INC

David Cloutier
Project Engineer (858.480.2083; david.cloutier@ata-e.com)

cc: David L. Hunt, Account Manager
(858.480.2095; david.hunt@ata-e.com)

July 18, 2013

Mr. Bruce LeBlanc
Sandia National Laboratories
P.O. Box 5800
Albuquerque, NM 87123

Subject: ATA Report No. 61178-R1, "Inertia Testing of SWIFT V27 Nacelles"

Dear Bruce:

This report documents ATA Engineering's inertia testing of two nacelles that are to be installed as part of Sandia National Laboratories' Scaled Wind Farm Technology (SWIFT). Testing was conducted December 17–21, 2012, and January 6–11, 2013. Mass, CG, and moment of inertia were obtained for both nacelles, and the testing procedure and results are documented below.

## Introduction

Sandia National Laboratories (SNL) is developing the Scaled Wind Farm Technology center to enable rapid, cost-efficient testing and development of transformative wind energy technology. ATA Engineering, Inc., (ATA) was contracted as part of this effort to dynamically characterize a number of components and assemblies to be used at SWIFT. This report documents the inertia testing for the Vestas 27 (V27) nacelles. The testing was successfully completed December 17–21, 2012, and January 6–11, 2013. Two nacelles were tested in a free-free configuration.

## Technical Approach

Two Vestas 27 (V27) nacelles were tested to obtain inertia properties. Each nacelle was lifted at four points with load cells in order to obtain the mass and CG of the structure, as shown in Figure 1. An effort was made to ensure that the nacelle was level with respect to the yaw bearing.

Figure 1. V27 nacelle suspended and attached to load cells to measure mass and CG (exterior of nacelle on left and interior of nacelle on right).

The nacelle was then placed on air springs (Firestone Airmount Isolators Model 19), which were used to simulate a free-free boundary condition, as shown in Figure 2. The nacelle was made level by adjusting the pressure of the various air springs.

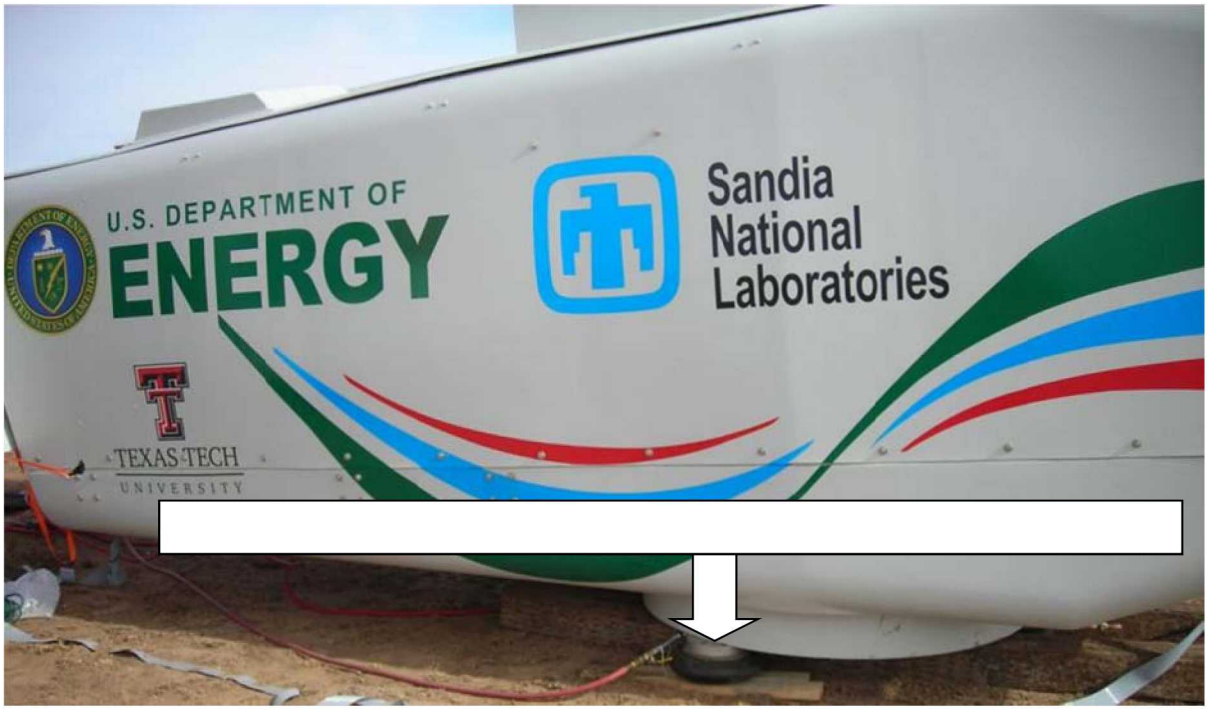


Figure 2. V27 nacelle mounted on air spring suspensions system.

ATA created a test model representative of the nacelle to develop a set of test measurement degrees of freedom (DOF). The test display model (TDM) is used for mode shape visualization and is shown in Figure 3. The coordinate system used for testing the nacelle is shown in Figure 4. All inertia and CG terms are defined about the indicated origin.

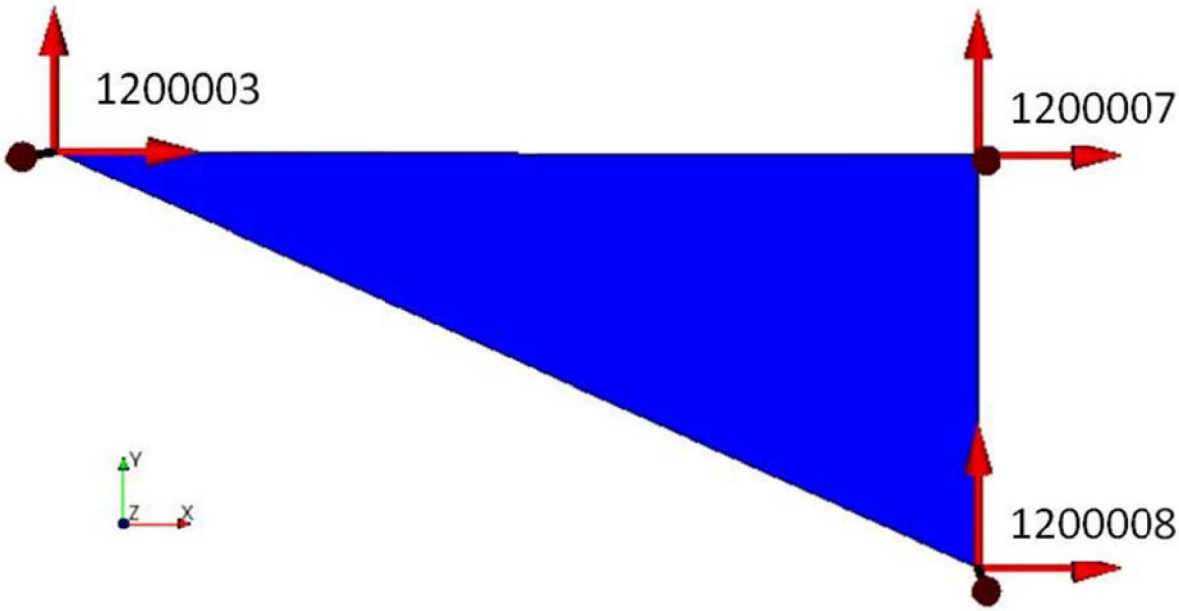


Figure 3. V27 nacelle and measurement locations for inertia testing.

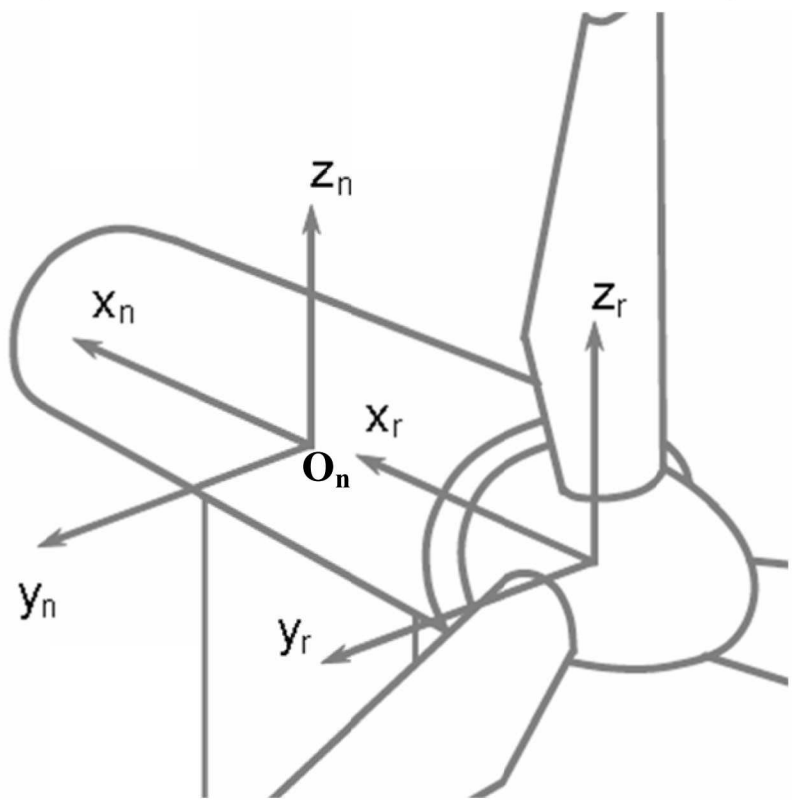


Figure 4. Coordinate system of nacelle with origin used for inertia calculations.

One method was used for calculating the inertia properties of the nacelles. This method, modal inversion involves obtaining high-quality rigid body mode shapes. This was performed by using

shakers to excite all six rigid body modes in the same data run. Seismic accelerometers (PCB 393B04) were mounted onto the nacelle frame as shown in Figure 5, while electrodynamic shakers were used to excite the nacelle as seen in Figure 6.

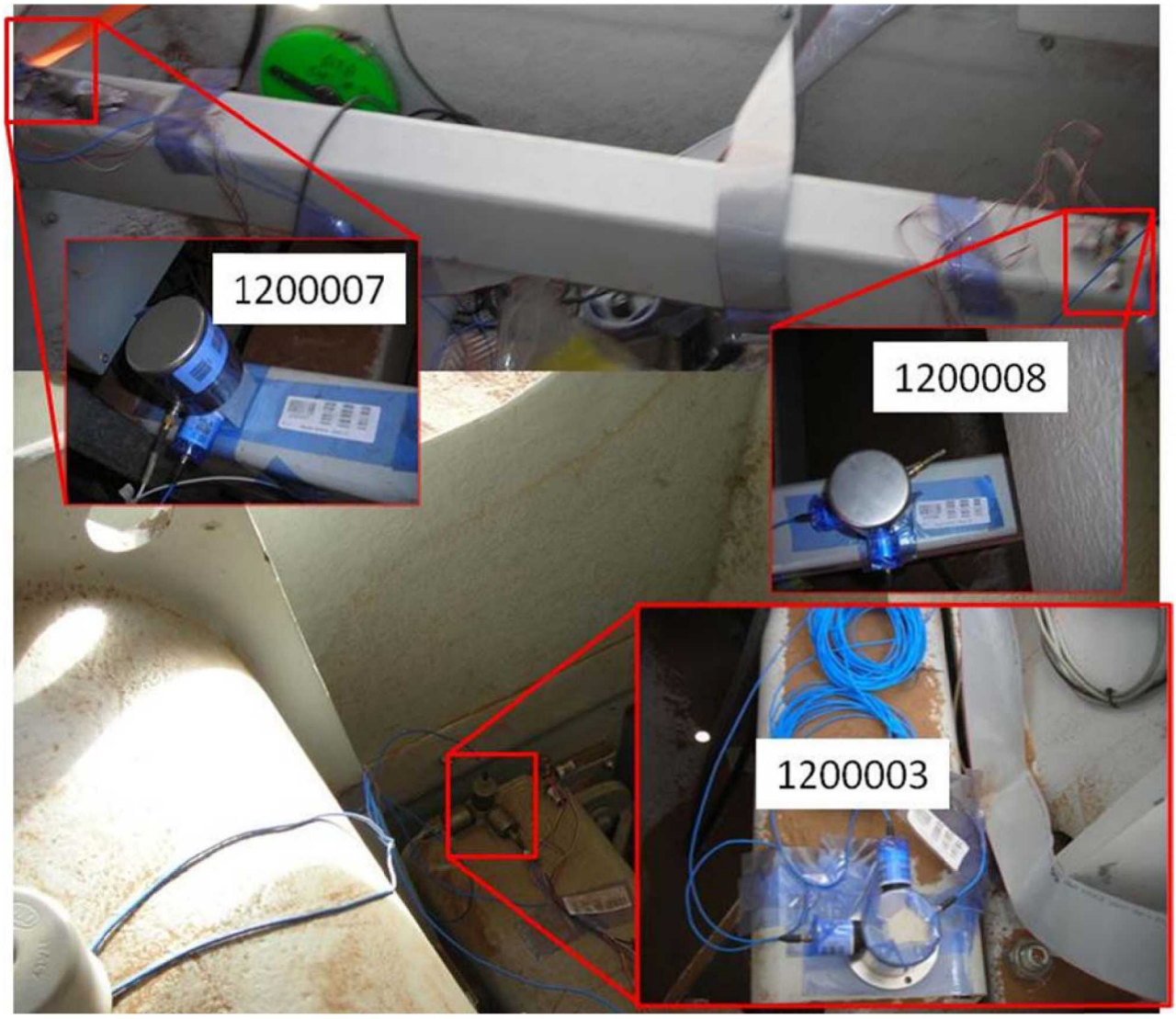


Figure 5. Location of accelerometers on V27 nacelle.

Figure 6. Shakers used to excite the V27 nacelle.

Figure 7 shows the power spectrum mode-indicator function (PSMIF) for the test run with shakers for both nacelles. The PSMIF is the summation of all FRF multiplied by each FRF conjugate and is an ideal function to visualize the overall response of the structure. As shown, all six rigid body modes can be seen in the peaks of the PSMIF for each run. To evaluate the quality of the rigid body modes obtained, the PSMIF was then synthesized using only the six rigid body modes. The synthesized PSMIF shows a high level of correlation with the test data. As a result, there is confidence that the extracted rigid body modes will accurately describe the inertia properties of the nacelles. There are significant differences between the PSMIFs of the two nacelles due to the change of both the structure and test setup. Because the synthesized PSMIF is accurate for both nacelles, however, the data obtained will be correct for both.

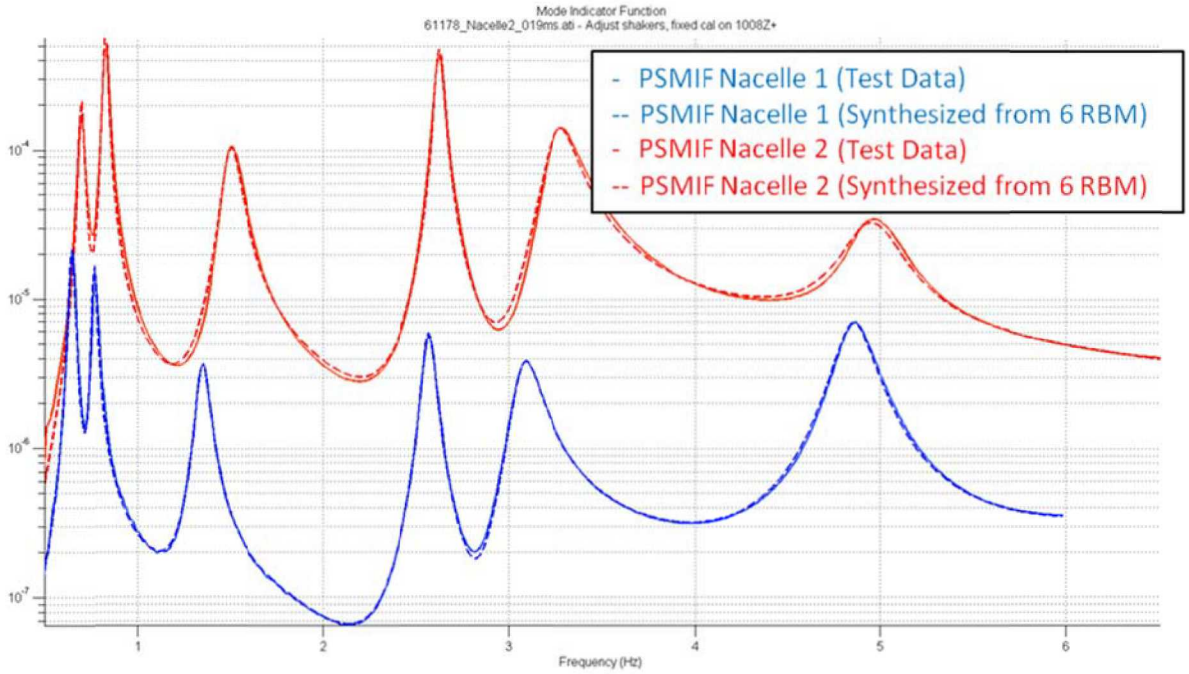


Figure 7. Test vs. synthesized PSMIF from shaker runs, showing all six rigid body modes.

The inertia results from modal inversion are shown in Table 1. The masses of the nacelles were also measured independently by a crane company during transportation, and these are included for completeness. The mass and CG properties of Nacelle 3 were also obtained, but modal testing was not performed on this nacelle.

Table 1. Final list of inertia properties for V27 nacelles.

| Mass and Inertia Properties of V27 Nacelles | | | | |
|---|---|---|---|---|
| **Property** | **Nacelle #** | **Crane** | **Load Cell** | **Modal Inversion** |
| **Mass (kg)** | **1** | 6804 | 7038 | 5570 |
| | **2** | 6577 | 6781 | 5551 |
| | **3** | 6668 | 7203 | |
| **CGx (m)*** | **1** | | 0.67 | 0.33 |
| | **2** | | 0.61 | 0.13 |
| | **3** | | 0.65 | |
| **Cgy (m)*** | **1** | | 0.09 | 0.08 |
| | **2** | | 0.07 | -0.09 |
| | **3** | | 0.09 | |
| **CGz (m)*** | **1** | | | 0.13 |
| | **2** | | | 0.13 |
| | **3** | | | |
| **Ixx (kg*m^2)** | **1** | | | 2465 |
| | **2** | | | 2422 |
| **Iyy (kg*m^2)** | **1** | | | 12292 |
| | **2** | | | 14296 |
| **Izz (kg*m^2)** | **1** | | | 4728 |
| | **2** | | | 7192 |

The two nacelles have fairly consistent properties, which is to be expected due to the assumed similarity in manufacture of the nacelles. The CG of the nacelles in the X direction (fore-aft) is forward of the origin. This is expected, as the nacelle should be balanced when the rotor is assembled—without the rotor, the nacelle will be significantly back-heavy. The CG about the Y direction (side-side) is relatively close to the origin, although there is a slight offset due to the generator being primarily located on one side of the nacelle.

Substantial rigging was used when the nacelles were being lifted by the crane, which accounts for some of the discrepancy in the masses obtained between the crane, load cell, and modal inversion methods. Additionally, oil and equipment were installed after the initial inertia testing, changing the mass and CG of the nacelle. The results obtained from the crane and the load cell are assumed to be more accurate than the modal inversion method, as the loads were obtained directly from the calibrated load cells in contrast to estimating them from the modal mass of the rigid body shapes. The error seen using modal inversion may be due to error in measurement, curve-fitting, or measurement of the accelerometer locations. However, the mass is within 20% of the load cell results, which indicates that the moment of inertia terms are reasonably accurate. Finally, the moment of inertia about the Y-axis is the largest, which is expected since the mass is most spread out about the Y-axis.

**Summary and Conclusions**

V27 nacelles were tested to obtain mass and inertia properties for use as part of SNL SWIFT. All aspects of this test were completed successfully.

Thank you for the opportunity to complete this project work for Sandia National Laboratories. Please contact David Cloutier or Tim Marinone if you have any questions about this report.

Sincerely,

Scanned signature - original on file ATA ENGINEERING INC

Timothy Marinone
Engineer (858.480.2078; tim.marinone@ata-e.com)

Reviewed by:

Scanned signature - original on file ATA ENGINEERING INC

David Cloutier
Project Engineer (858.480.2083; david.cloutier@ata-e.com)

cc: David L. Hunt, Account Manager
(858.480.2095; david.hunt@ata-e.com)

March 27, 2013

Mr. Bruce LeBlanc
Sandia National Laboratories
P.O. Box 5800
Albuquerque, NM 87123

Subject: ATA Report No. 61178, "Modal Survey of SWIFT V27 Towers"

Dear Bruce:

This report documents ATA Engineering's modal testing of two towers that are to be installed as part of the Sandia National Laboratories (SNL) Scaled Wind Farm Technology (SWIFT). Testing was conducted December 17–21, 2012, and January 7–9, 2013. Modal parameters were obtained for the towers, and the testing procedure and results are documented below.

## Introduction

Sandia National Laboratories (SNL) is developing the Scaled Wind Farm Technology (SWIFT) center to enable rapid, cost-efficient testing and development of transformative wind energy technology. ATA Engineering, Inc., (ATA) was contracted as part of this effort to dynamically characterize a number of components and assemblies to be used at SWIFT. This report documents the model survey for two Vestas 27 (V27) towers. The testing was successfully completed December 17–21, 2012, and January 7–9, 2013. The two towers were tested in a free-free configuration.

## Technical Approach

V27 towers were located on specialty characterization supports designed by ATA and Sandia, shown in Figure 1. The stands were located approximately at the nodes of the first bending mode (4.25 and 23.1 meters from the base of the tower). Airbags (Firestone Airmount Isolators Model 19) were supported by the stands and were used to simulate a free-free boundary condition. The airbags were pressurized to approximately 90 Psi at 23.1 meters from the tower base and to approximately 120 Psi at 4.25 meters from the tower base.

Figure 1. Overall view of tower on stands (left), individual stand (right), and tower lifted on airbags (bottom).

ATA created a test model representative of the tower to develop a set of test measurement degrees of freedom (DOF). The test display model (TDM) is used for mode shape visualization and is shown in Figure 2. Accelerometers (PCB T33B) were mounted tangential to the tower to spatially filter the response and minimize the response attributed to the breathing modes. Force was input into the structure by a calibrated modal impact hammer (PCB 086D20).

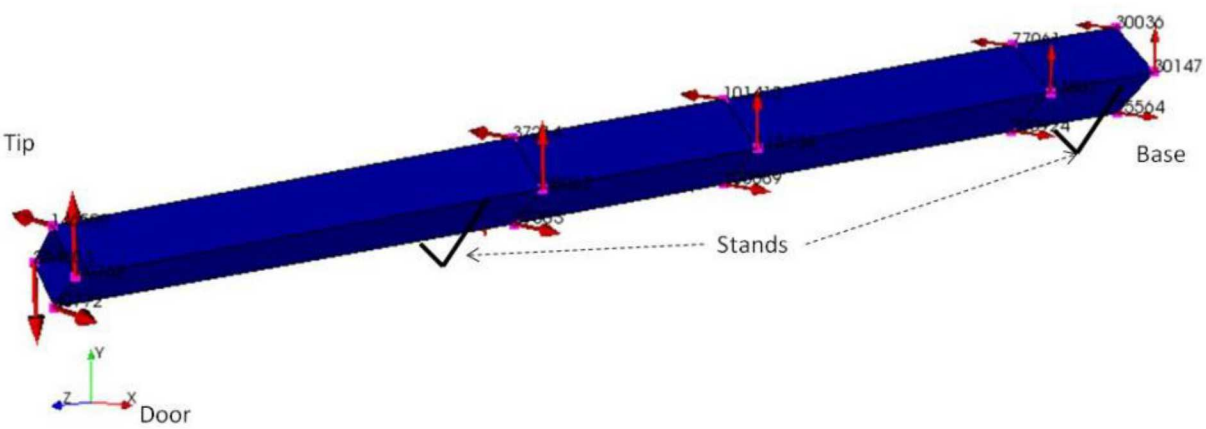


Figure 2. V27 tower and measurement locations for modal testing.

Due to the structure geometry and the orientation of the accelerometers, most of the impact locations were not drive points. Node 146589X at the tip, however, has a tab that allowed a drive point impact to be performed. The resulting FRF and coherence at that point are shown in Figure 3 for Tower 1. The coherence is generally high and distinct FRF peaks are seen, indicating high-quality measurements.

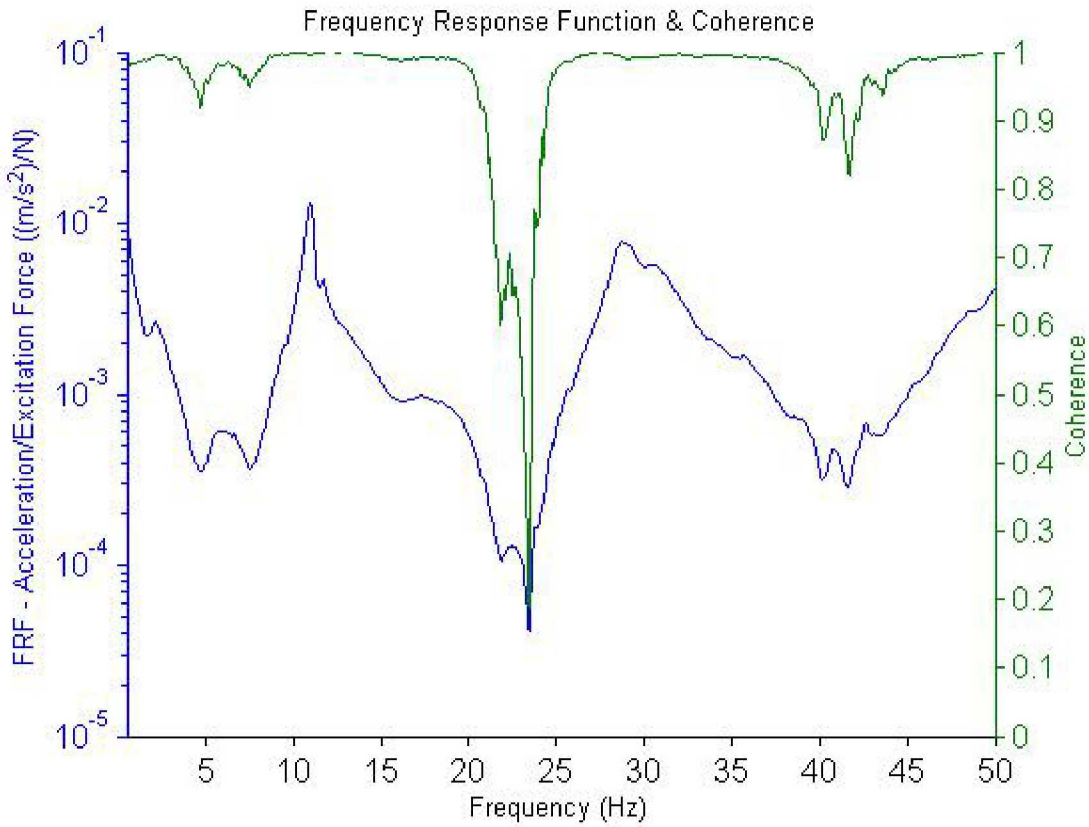


Figure 3. Drive point FRF and coherence at node 146589X for Tower 1.

The power spectrum mode-indicator function (PSMIF) is shown in Figure 4 for both towers on the air springs as well as Tower 1 without air springs. Because the PSMIF is the summation of all FRF multiplied by each FRF conjugate, it is an ideal function to view the overall response. While Tower 1 and Tower 2 on air springs show the same general trends, Tower 1 without air springs shows a clear change due to the different boundary condition.

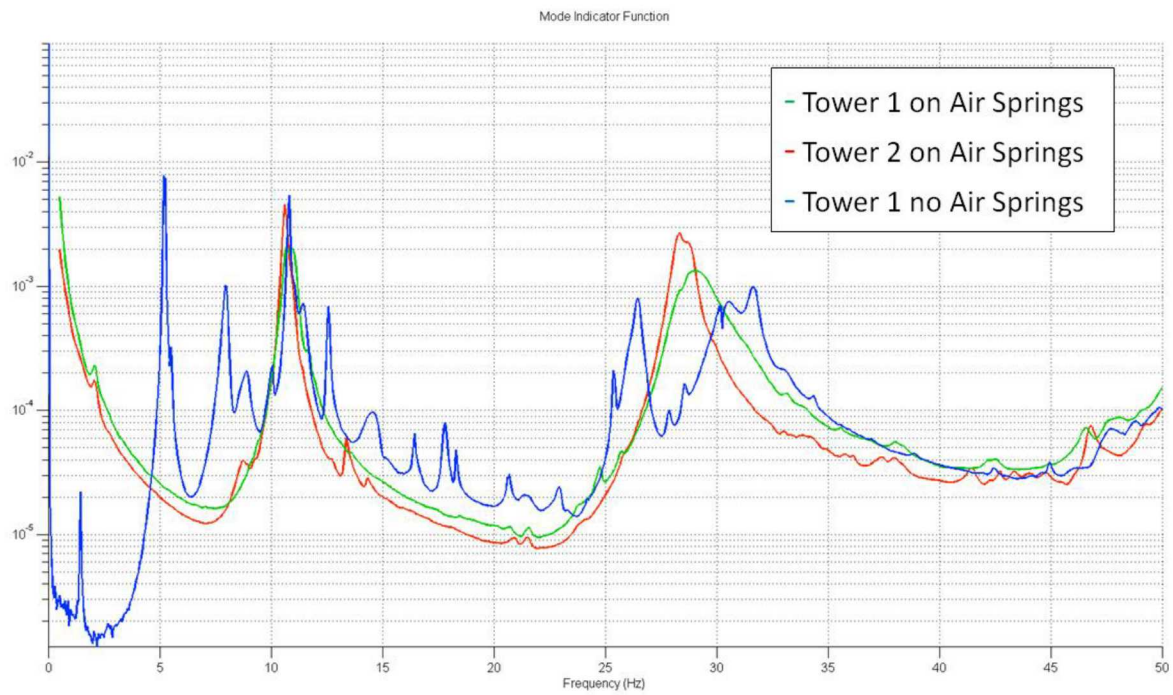


Figure 4. PSMIF for Towers 1 and 2 on air springs and Tower 1 without air springs.

The final list of mode shapes is included in Table 1. The first and second bending modes are of primary importance. Rigid body modes can be used to help correlate the model by determining the stiffness of the supports. Plots of the mode shapes can be seen in Appendix A.

The frequencies for Tower 1 and Tower 2 are within 5% of each other, indicating a high level of similarity between the two towers. Due to the orientation of each tower with respect to the air springs, the modes are not predominantly in the same axes. As also seen in the PSMIF comparison, Tower 1 has a higher level of damping than Tower 2 for all of the modes of interest. Finally, some of the modes were able to be extracted from Tower 1 without air springs.

Table 1. Final mode list for V27 towers in free-free configuration.

| | Tower 1 | | Tower 2 | | Tower 1 without Air Springs | |
|---|---|---|---|---|---|---|
| | Frequency (Hz) | Damping (% Crit) | Frequency (Hz) | Damping (% Crit) | Frequency (Hz) | Damping (% Crit) |
| First Bending Mode | 10.66 | 1.47 | 10.61 | 1.10 | 10.81 | 0.81 |
| | 10.88 | 2.47 | 10.69 | 1.92 | | |
| Second Bending Mode | 28.34 | 3.06 | 28.29 | 0.85 | 26.39 | 1.10 |
| | 29.10 | 2.24 | 28.80 | 1.09 | | |
| Rigid Body Mode | 2.12 | 6.86 | 2.08 | 5.48 | 5.21 | 0.49 |

The modal assurance criterion (MAC) shown in Figure 5 was computed between the two towers and also shows a high level of agreement between the modes of the towers. MAC was also computed between the test mode shapes and the FEM-predicted shapes, as shown in Figure 6. These values are not as high; this may be due to the effect of the support stands, which were not modeled in the FEM. Updating the FEM to account for the stiffness of the support stands would improve the MAC results.

**Test Self MAC Table**

| Test Shapes | | Test Shapes | 1 | 2 | 3 | 4 | 5 | 6 | 7 | 8 | 9 | 10 |
|---|---|---|---|---|---|---|---|---|---|---|---|---|
| | | MACtt | 2.1 | 10.7 | 10.9 | 28.3 | 29.1 | 2.1 | 10.6 | 10.7 | 28.3 | 28.8 |
| | 1 | 2.1 | 1.00 | | | | | 0.41 | | | | |
| | 2 | 10.7 | | 1.00 | | | | | | 0.93 | | |
| | 3 | 10.9 | | | 1.00 | | | | 0.57 | | | |
| | 4 | 28.3 | | | | 1.00 | | | | | | 0.91 |
| | 5 | 29.1 | | | | | 1.00 | | | | 0.91 | |
| | 6 | 2.1 | 0.41 | | | | | 1.00 | | | | |
| | 7 | 10.6 | | | 0.57 | | | | 1.00 | | | |
| | 8 | 10.7 | | 0.93 | | | | | | 1.00 | | |
| | 9 | 28.3 | | | | | 0.91 | | | | 1.00 | |
| | 10 | 28.8 | | | | 0.91 | | | | | | 1.00 |

Figure 5. Test self-MAC table of two towers in free-free configuration.

**FEM/Test Cross MAC Table**

| Test Shapes | | FEM shapes | 1 | 2 | 3 | 4 |
|---|---|---|---|---|---|---|
| | | MACtg | 11.3 | 11.3 | 29.8 | 29.9 |
| | 2 | 10.7 | 0.86 | | | |
| | 3 | 10.9 | | 0.90 | | |
| | 4 | 28.3 | | | 0.58 | |
| | 5 | 29.1 | | | | 0.45 |
| | 7 | 10.6 | 0.49 | 0.40 | | |
| | 8 | 10.7 | 0.71 | | | |
| | 9 | 28.3 | | | 0.24 | 0.39 |
| | 10 | 28.8 | | | 0.50 | 0.24 |

Figure 6. FEM and test cross-MAC table of two towers in free-free configuration.

## Summary and Conclusions

This report documents ATA Engineering's modal testing of two towers that are to be installed as part of the Sandia National Laboratories (SNL) Scaled Wind Farm Technology (SWIFT). Testing was conducted December 17–21, 2012, and January 7–9, 2013. Modal parameters were obtained for the towers, and the testing procedure and results were documented. Frequencies for both towers for the first and second bending modes were within 5% of each other, indicating a high level of similarity between the two towers.

Thank you for the opportunity to complete this project work for Sandia National Laboratories. Please contact David Cloutier or Tim Marinone if you have any questions about this report.

Sincerely,

Scanned signature - original on file ATA ENGINEERING INC

Timothy Marinone
Engineer (858.480.2078; tim.marinone@ata-e.com)

Reviewed by:

Scanned signature - original on file ATA ENGINEERING INC

David Cloutier
Project Engineer (858.480.2083; david.cloutier@ata-e.com)

cc: David L. Hunt, Account Manager
(858.480.2095; david.hunt@ata-e.com)

# Appendix A

# Test Mode Shapes

# Tower 1

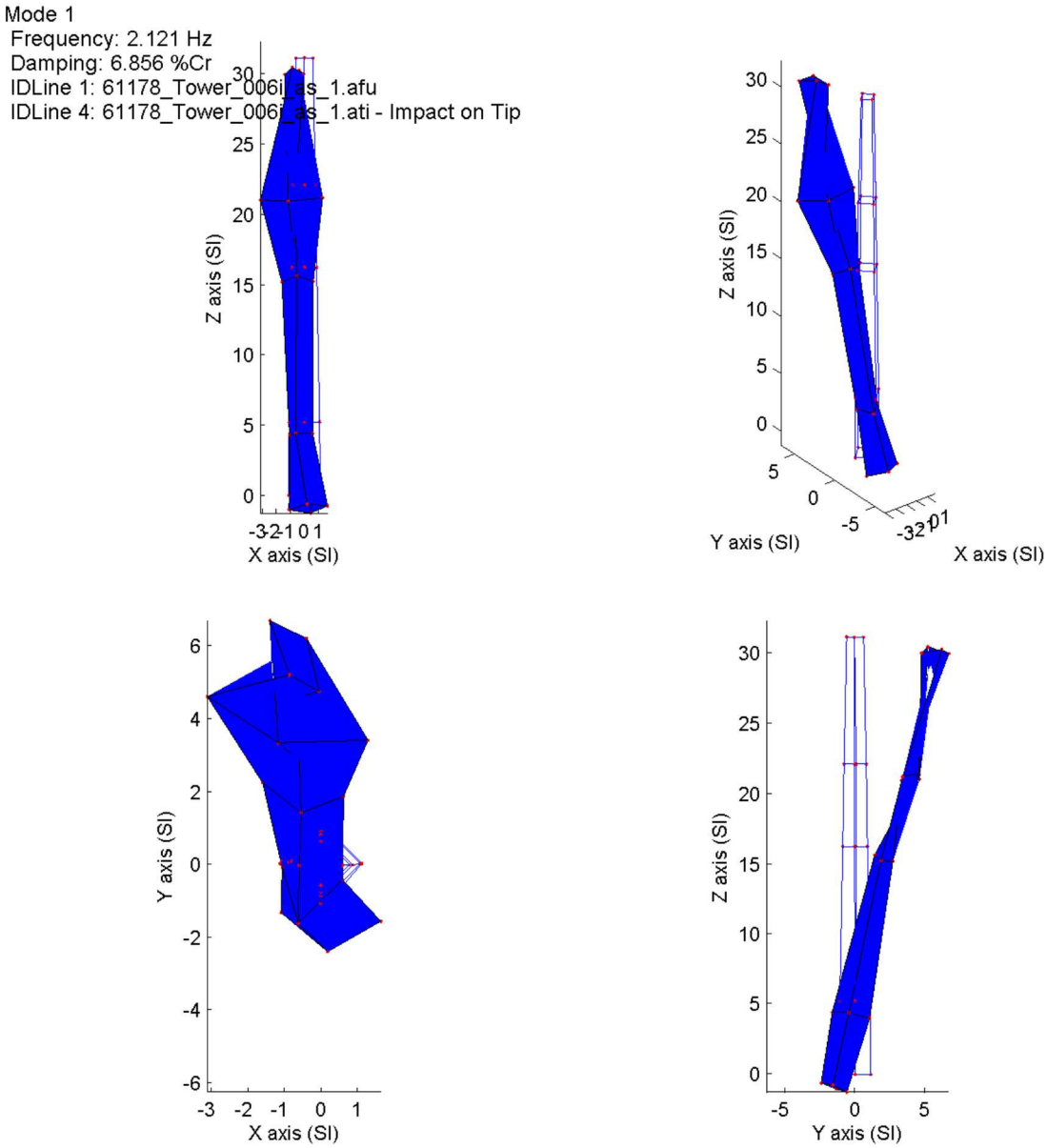
Mode 1
Frequency: 2.121 Hz
Damping: 6.856 %Cr
IDLine 1: 61178_Tower_006i_as_1.afu
IDLine 4: 61178_Tower_006i_as_1.ati - Impact on Tip
Z axis (SI)
X axis (SI)
Y axis (SI)

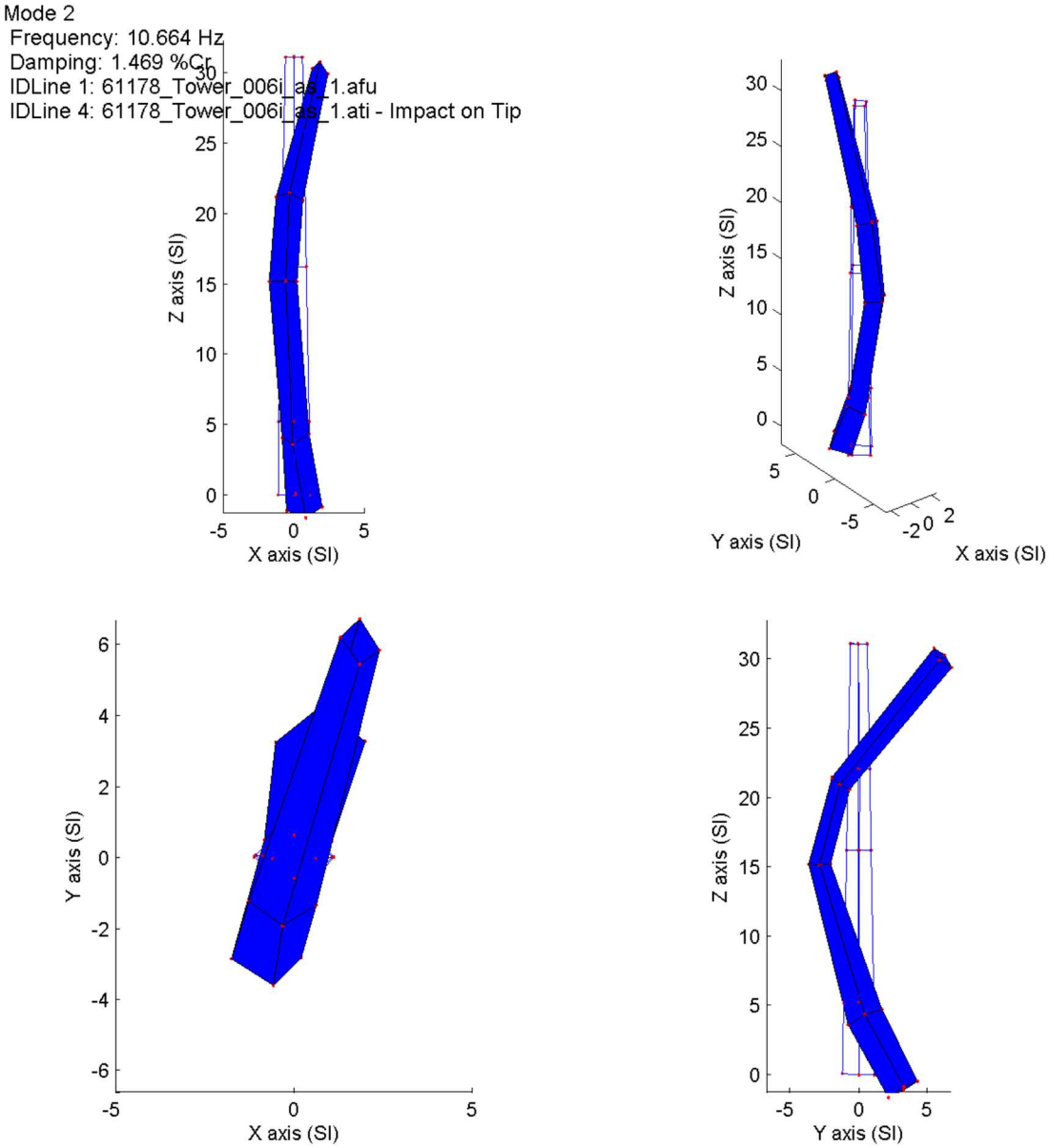
Mode 2
Frequency: 10.664 Hz
Damping: 1.469 %Cr
IDLine 1: 61178_Tower_006i_as_1.afu
IDLine 4: 61178_Tower_006i_as_1.ati - Impact on Tip
Z axis (SI)
X axis (SI)
Y axis (SI)

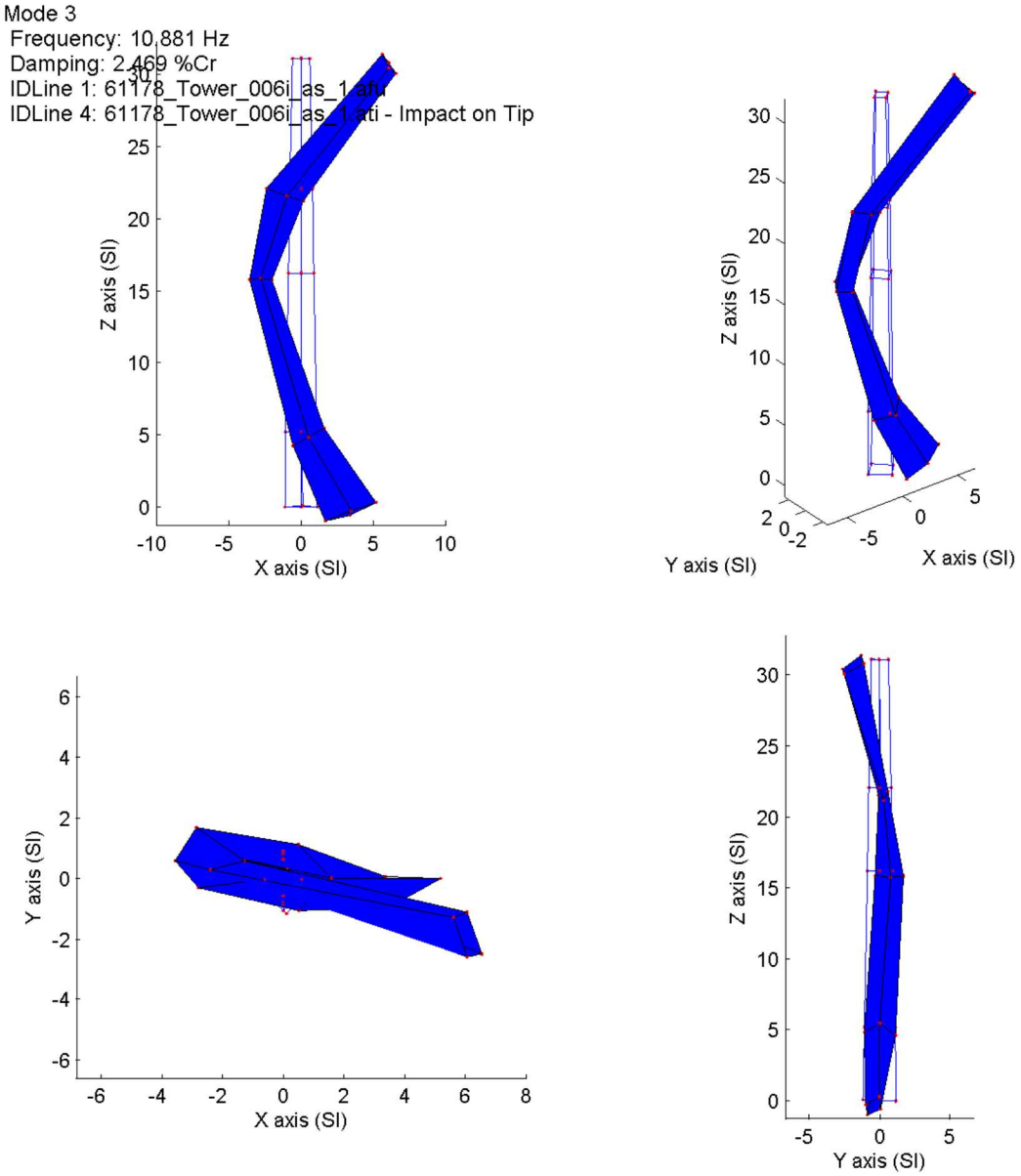
Mode 3
Frequency: 10.881 Hz
Damping: 2.469 %Cr
IDLine 1: 61178_Tower_006i_as_1 aft
IDLine 4: 61178_Tower_006i_as_1 ati - Impact on Tip
Z axis (SI)
X axis (SI)
Y axis (SI)

Mode 4
Frequency: 28.338 Hz
Damping: 3.060 %Cr
IDLine 1: 61178_Tower_006i_as_1.afu
IDLine 4: 61178_Tower_006i_as_1.ati - Impact on Tip

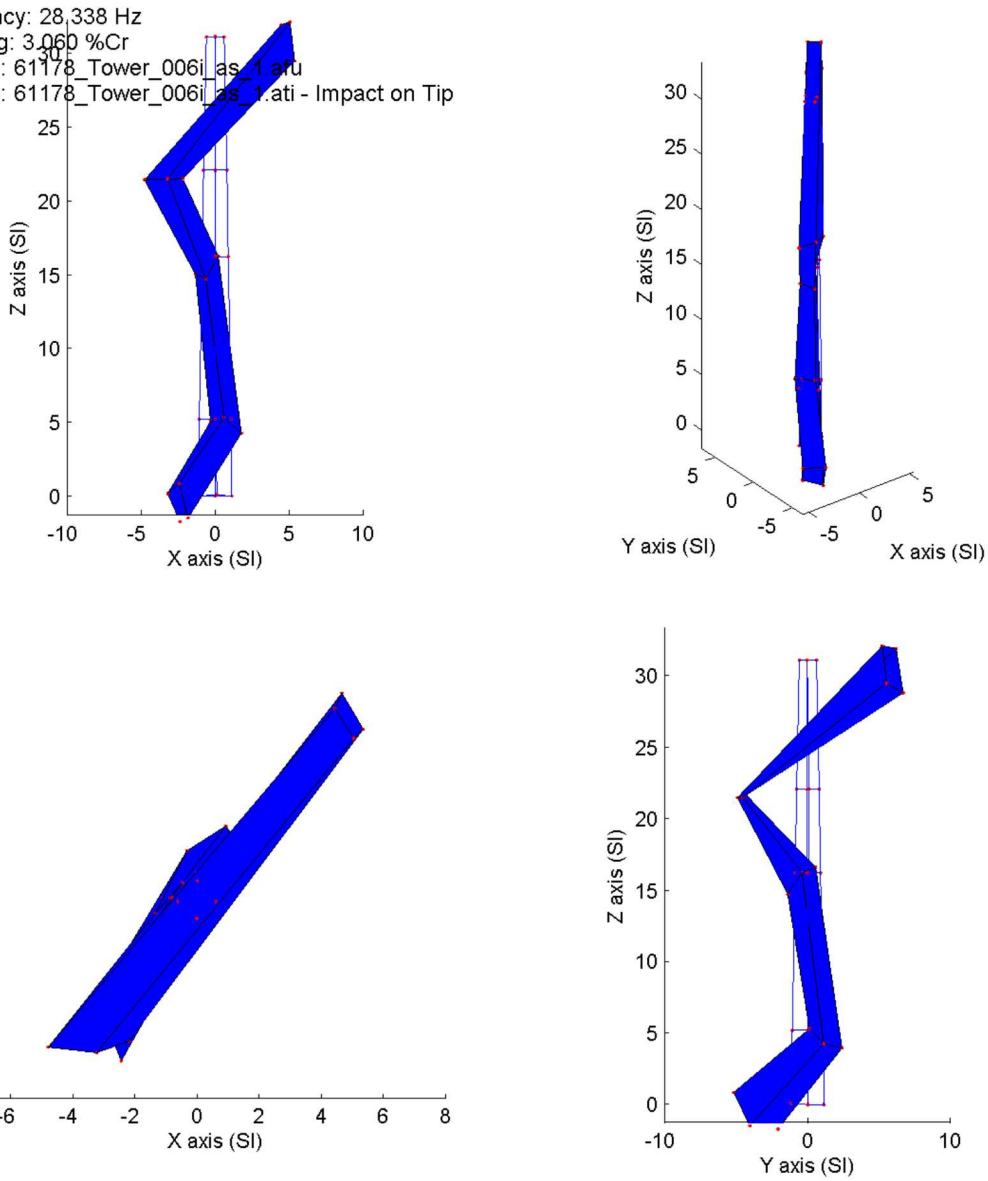

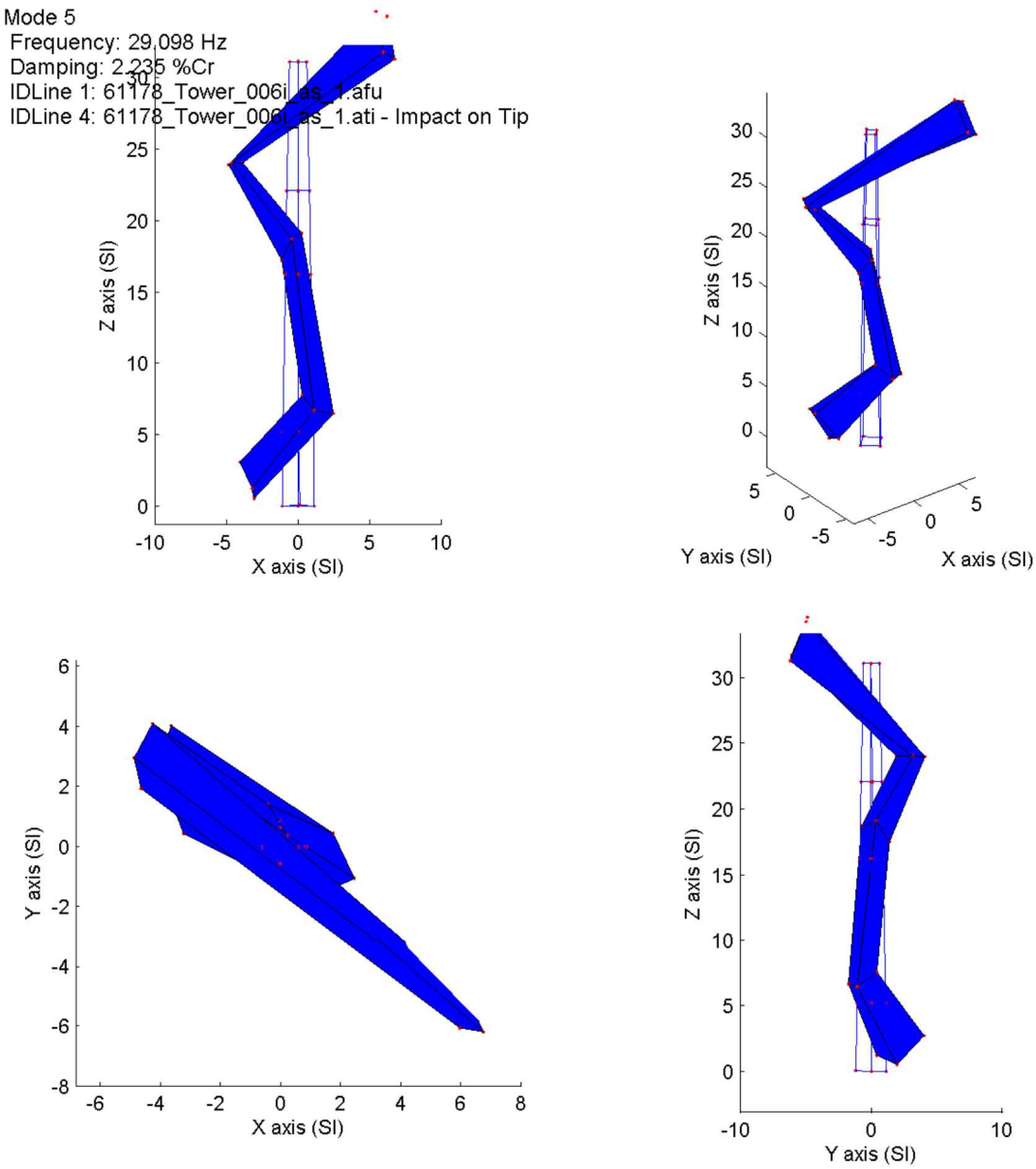
Mode 5
Frequency: 29.098 Hz
Damping: 2.235 %Cr
IDLine 1: 61178_Tower_006i_as_1.afu
IDLine 4: 61178_Tower_006i_as_1.ati - Impact on Tip
Z axis (SI)
X axis (SI)
Z axis (SI)
Y axis (SI)
X axis (SI)
Y axis (SI)
X axis (SI)
Z axis (SI)
Y axis (SI)

# Tower 2

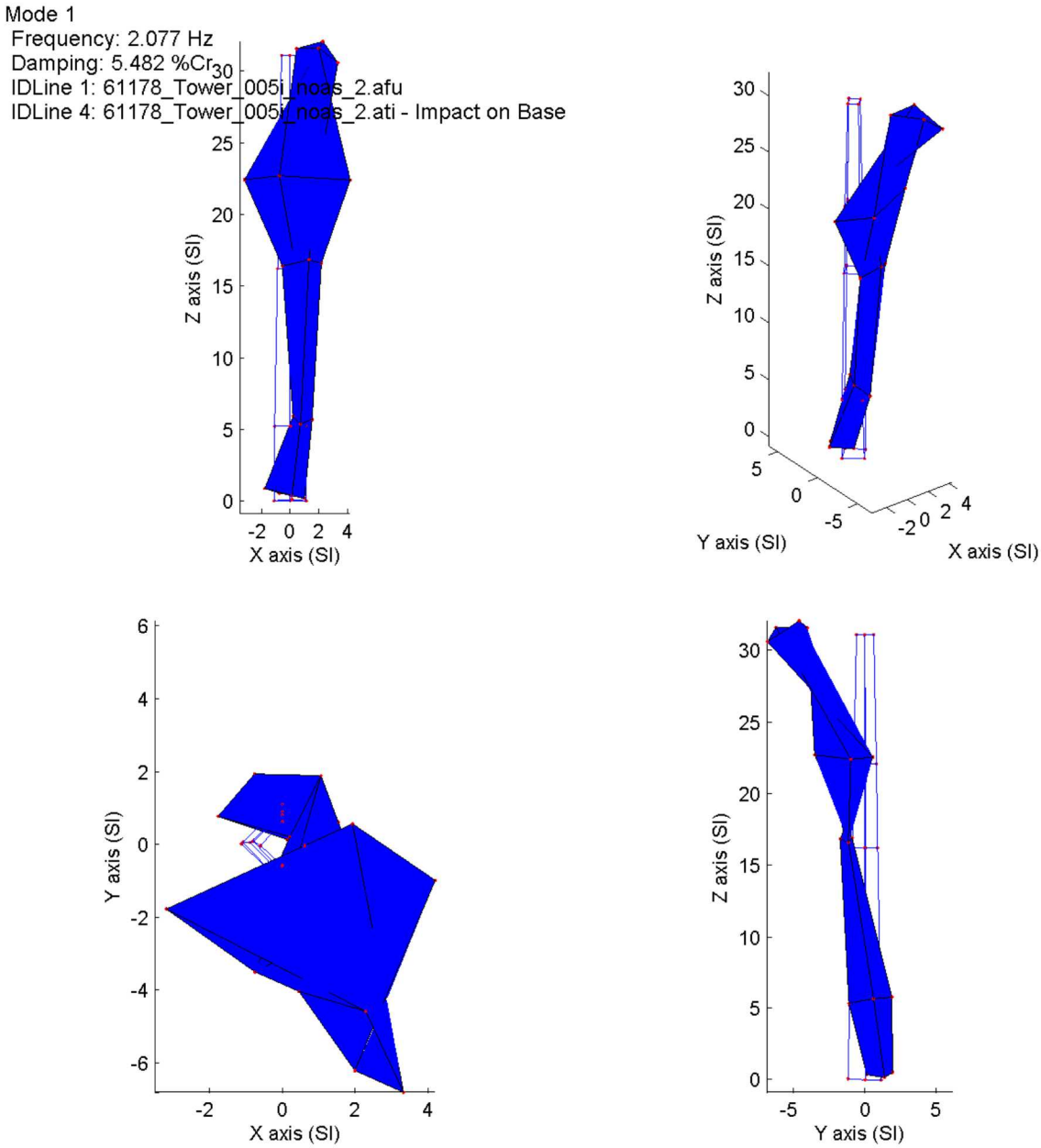
Mode 1
Frequency: 2.077 Hz
Damping: 5.482 %Cr
IDLine 1: 61178_Tower_005i_noas_2.afu
IDLine 4: 61178_Tower_005i_noas_2.ati - Impact on Base
Z axis (SI)
X axis (SI)
Y axis (SI)

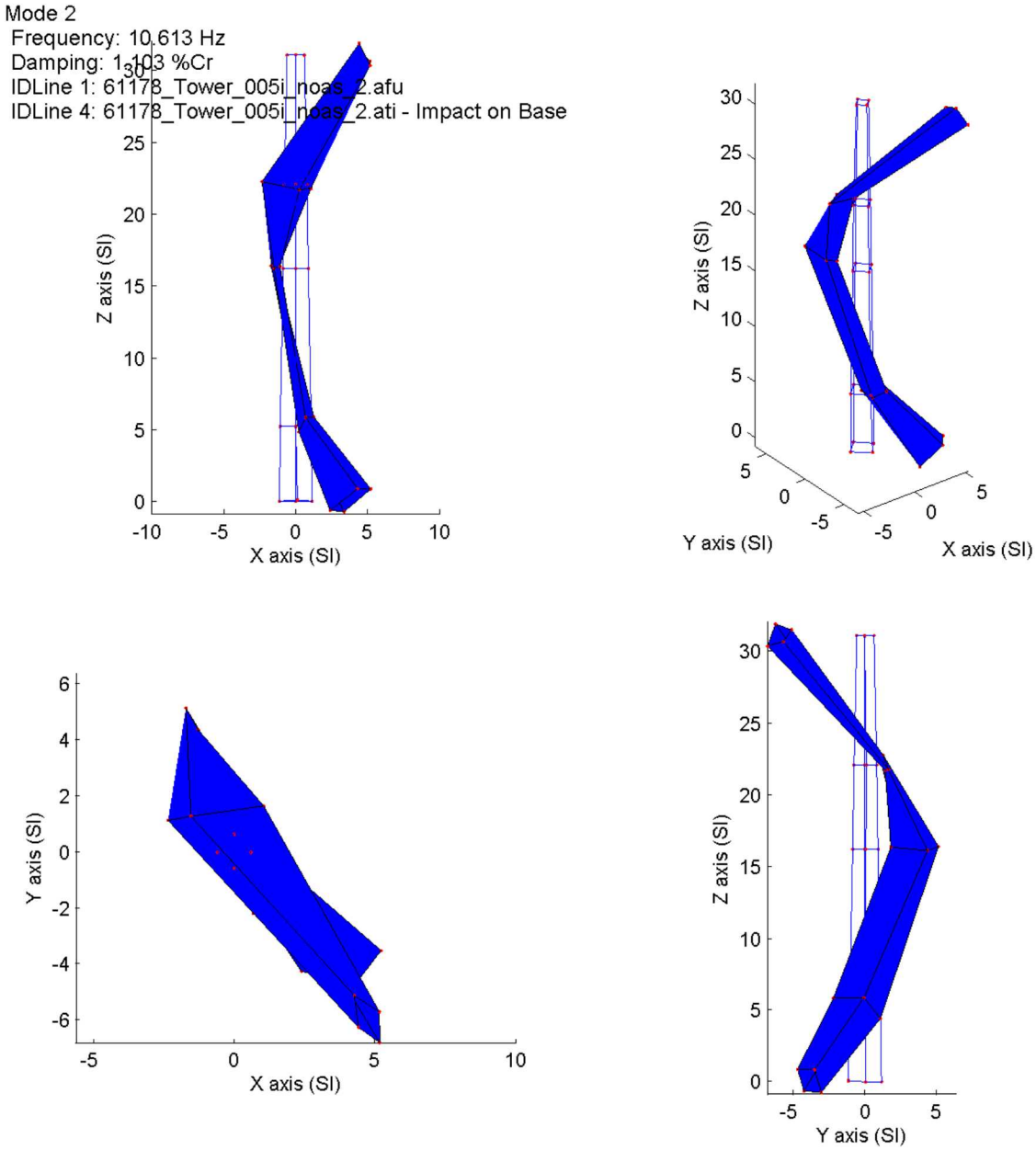
Mode 2
Frequency: 10.613 Hz
Damping: 1.103 %Cr
IDLine 1: 61178_Tower_005i_noas_2.afu
IDLine 4: 61178_Tower_005i_noas_2.ati - Impact on Base
Z axis (SI)
X axis (SI)
Y axis (SI)

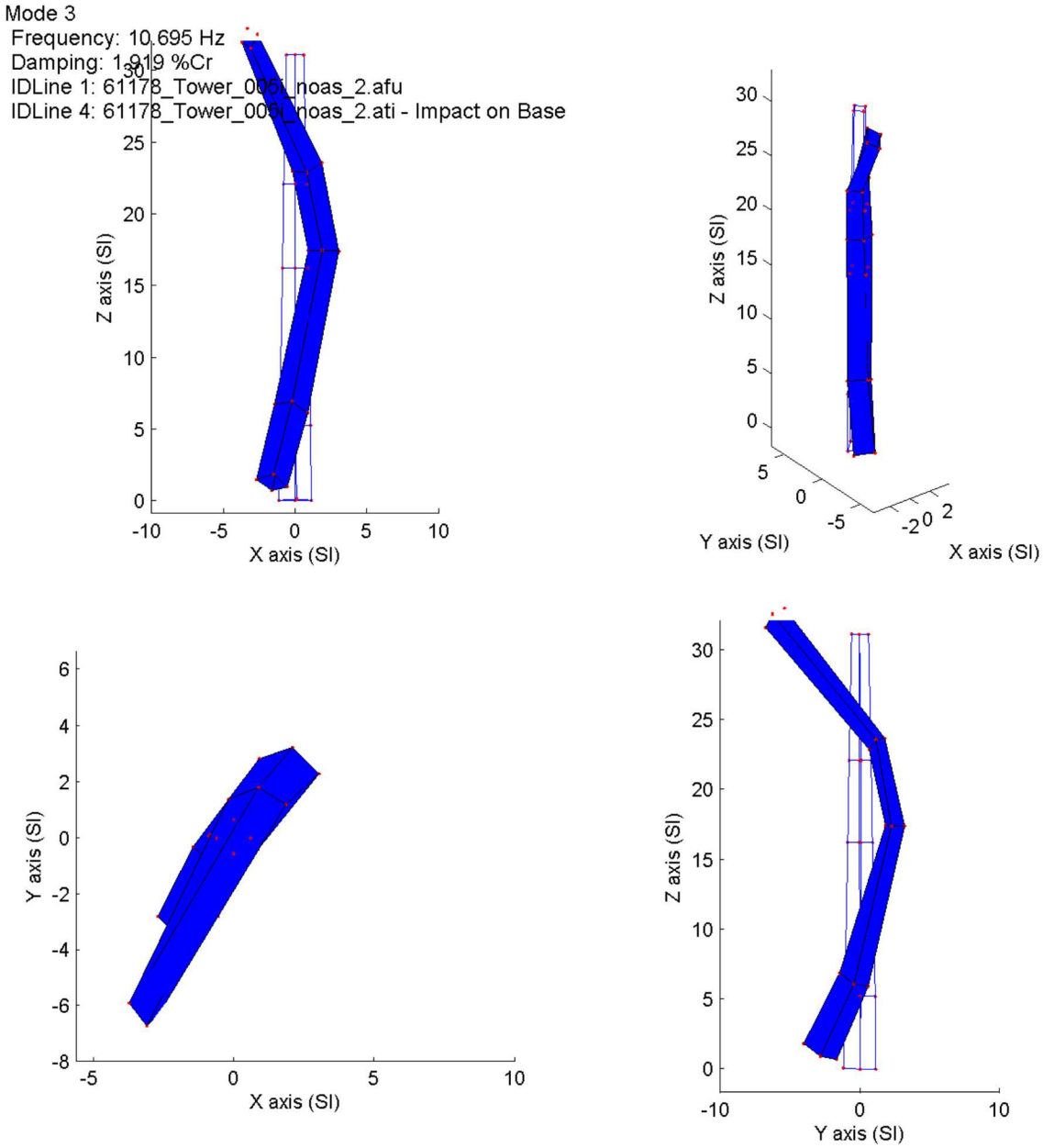
Mode 3
Frequency: 10.695 Hz
Damping: 1.919 %Cr
IDLine 1: 61178_Tower_005_noas_2.afu
IDLine 4: 61178_Tower_005_noas_2.ati - Impact on Base
Z axis (SI)
X axis (SI)
Z axis (SI)
Y axis (SI)
X axis (SI)
Y axis (SI)
X axis (SI)
Z axis (SI)
Y axis (SI)

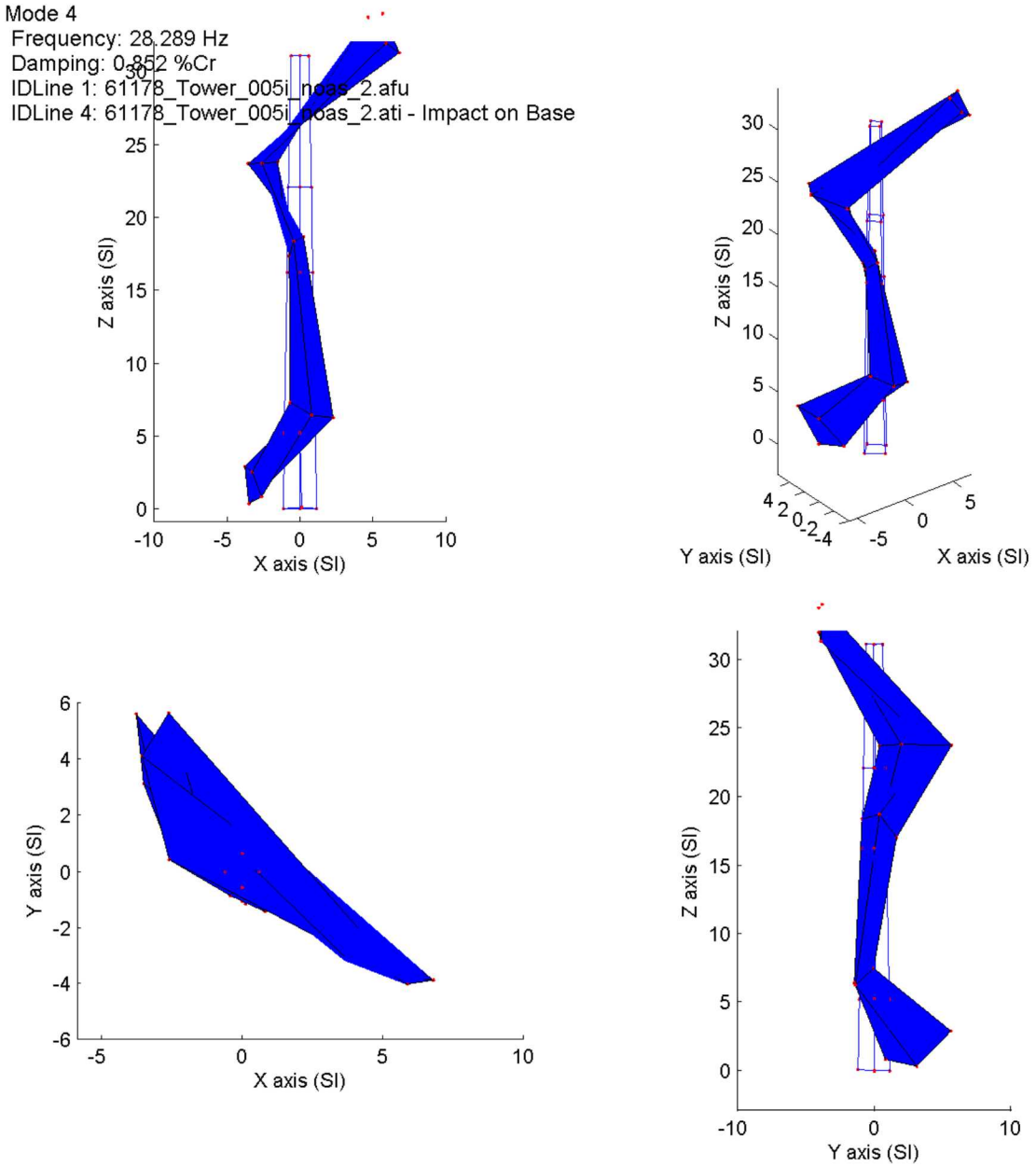
Mode 4
Frequency: 28.289 Hz
Damping: 0.852 %Cr
IDLine 1: 61178_Tower_005i_noas_2.afu
IDLine 4: 61178_Tower_005i_noas_2.ati - Impact on Base
Z axis (SI)
X axis (SI)
Y axis (SI)

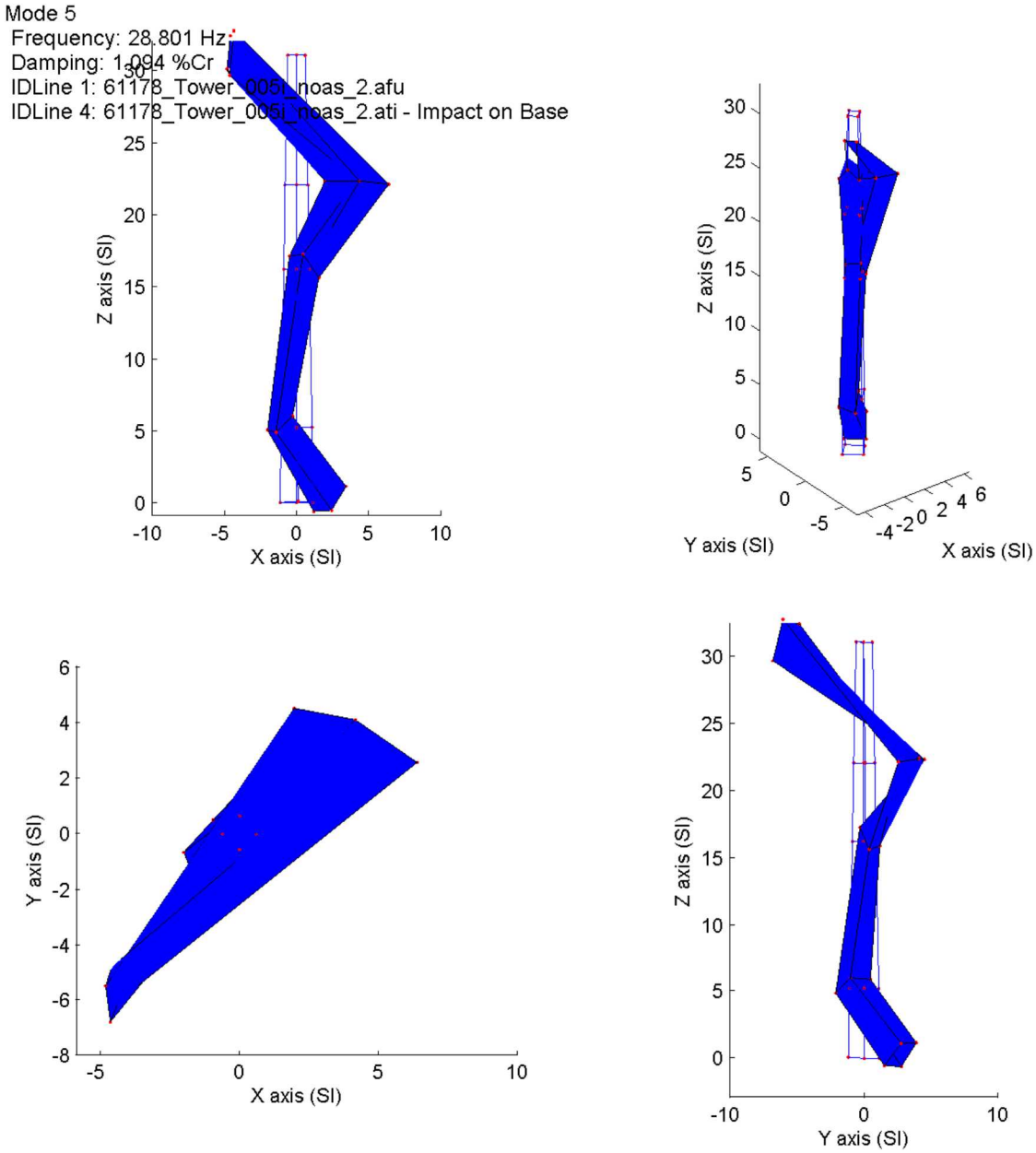
Mode 5
Frequency: 28.801 Hz
Damping: 1.094 %Cr
IDLine 1: 61178_Tower_005i_noas_2.afu
IDLine 4: 61178_Tower_005i_noas_2.ati - Impact on Base
Z axis (SI)
X axis (SI)
Y axis (SI)

July 18, 2013

Mr. Bruce LeBlanc
Sandia National Laboratories
P.O. Box 5800
Albuquerque, NM 87123

Subject: ATA Report No. 61178, "Modal Survey of SWIFT V27 Towers on Foundation"

Dear Bruce:

This report documents ATA Engineering's modal testing of two towers bolted to the foundation that are to be installed as part of Sandia National Laboratories' Scaled Wind Farm Technology (SWIFT). Testing was conducted February 7–13, 2013. Modal parameters were obtained for the towers, and the testing procedure and results are documented below.

## Introduction

Sandia National Laboratories (SNL) is developing the Scaled Wind Farm Technology center to enable rapid, cost-efficient testing and development of transformative wind energy technology. ATA Engineering, Inc., (ATA) was contracted as part of this effort to dynamically characterize a number of components and assemblies to be used at SWIFT. This report documents the model survey for two Vestas 27 (V27) towers on the concrete foundation. The testing was successfully completed February 7–13, 2013. The two towers were tested bolted to the concrete foundation.

## Technical Approach

V27 towers were bolted to the concrete foundation as shown in Figure 1.

Figure 1. Overall view of tower on foundation.

ATA created a test model representative of the tower to develop a set of test measurement degrees of freedom (DOF). The test display model (TDM), shown in Figure 2, is used for mode shape visualization. Accelerometers (PCB T33B) were mounted tangential to the tower to spatially filter the response and minimize the response attributed to the breathing modes. Force was input into the structure with a calibrated modal impact hammer (PCB 086D20). Seismic accelerometers (PCB

393B04) were located on the concrete foundation to obtain the motion of the foundation for use in determining the impedance of the structure. Seismic accelerometers were also located at the base of the tower in the vertical direction to determine the transfer function across the bolted interface.

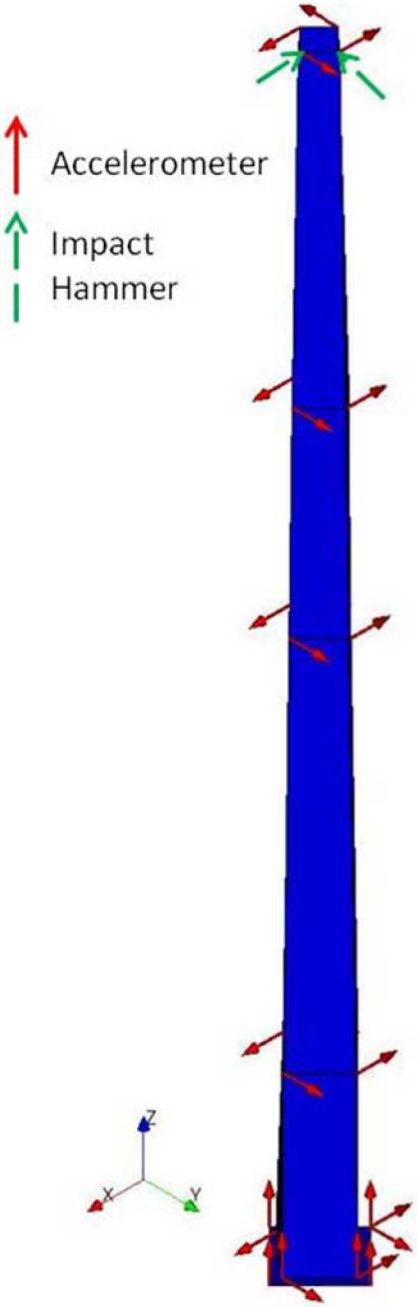


| Group Name | Node | X+ | Y+ | Z+ | Locations |
|---|---|---|---|---|---|
| Tower | 30018 | | Y- | | Base-6Clock |
| Tower | 30036 | X- | | Z+ | Base-9Clock |
| Tower | 30147 | | Y+ | Z+ | Base -12Clock |
| Tower | 33807 | | Y+ | | Platform1-12Clock |
| Tower | 37003 | X+ | | | 22Ft-3Clock |
| Tower | 37214 | X- | | | 22Ft-9Clock |
| Tower | 38067 | | Y+ | | 22Ft-12Clock |
| Tower | 40762 | | Y+ | | Tip-12Clock |
| Tower | 40772 | X+ | | | Tip-3Clock |
| Tower | 44049 | | Y- | | 22Ft-6Clock |
| Tower | 75564 | X+ | | | Base-3Clock |
| Tower | 77061 | X- | | | Platform1-9Clock |
| Tower | 100589 | X+ | | | Platform2-3Clock |
| Tower | 101415 | X- | | | Platform2-9Clock |
| Tower | 115734 | | Y+ | | Platform2-12Clock |
| Tower | 146589 | X- | | | Tip-9Clock |
| Tower | 200924 | X+ | | | Platform1-3Clock |
| Tower | 254503 | | Y- | | Tip-6Clock |
| Tower | 271687 | | Y- | | Platform2-6Clock |
| Tower | 281849 | | Y- | | Platform1-6Clock |
| Tower | 400001 | | | Z+ | Foundation-12Clock |
| Tower | 400004 | | | Z+ | Foundation-3Clock |
| Tower | 400003 | X- | Y+ | Z+ | Foundation-6Clock |
| Tower | 400002 | | | Z+ | Foundation-9Clock |

Figure 2. V27 tower and measurement locations for modal testing.

Due to the structure geometry and the orientation of the accelerometers, the impact locations were not drive points. The resulting FRF and coherence at node 146589X are shown in Figure 3 for Tower 1. The coherence is generally high and distinct FRF peaks are seen, indicating high-quality measurements.

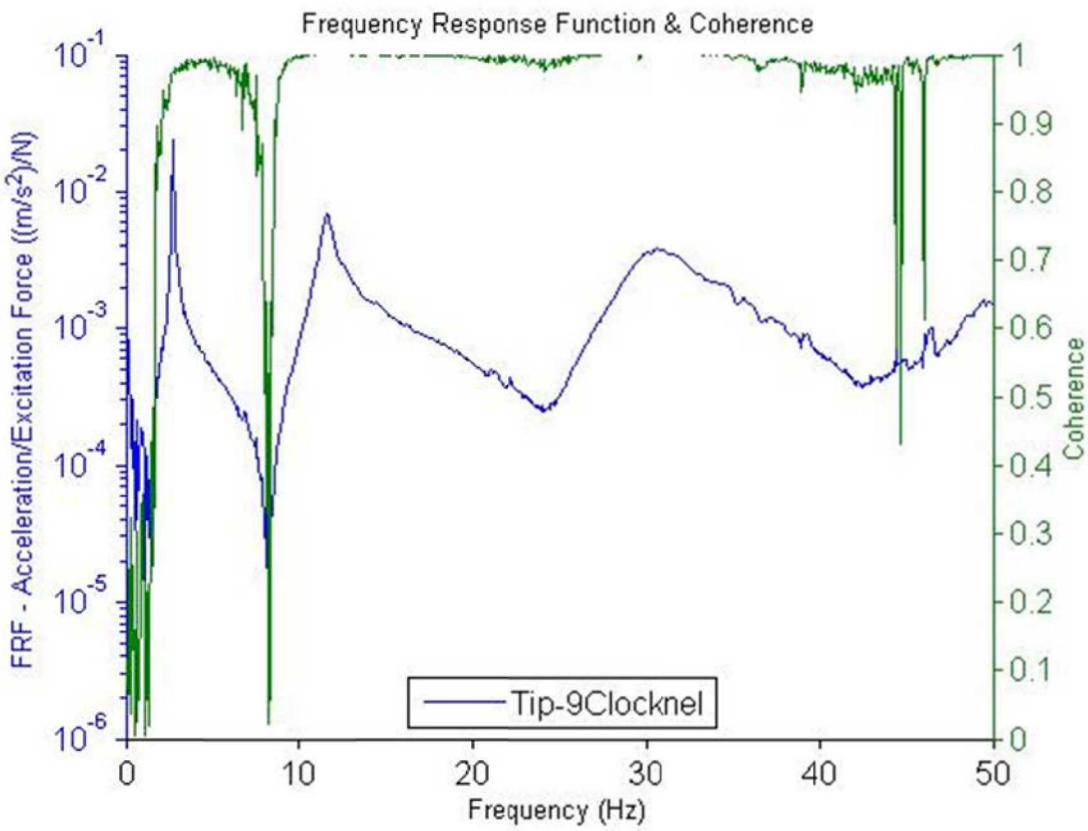


Figure 3. FRF and coherence at node 146589X due to impact at 254503X for Tower 1.

The power spectrum mode indicator function (PSMIF) is shown in Figure 4 for both towers. Because the PSMIF is the summation of all FRF multiplied by each FRF conjugate, it is an ideal function to view the overall response. The PSMIF for Towers 1 and 2 show the same general trends.

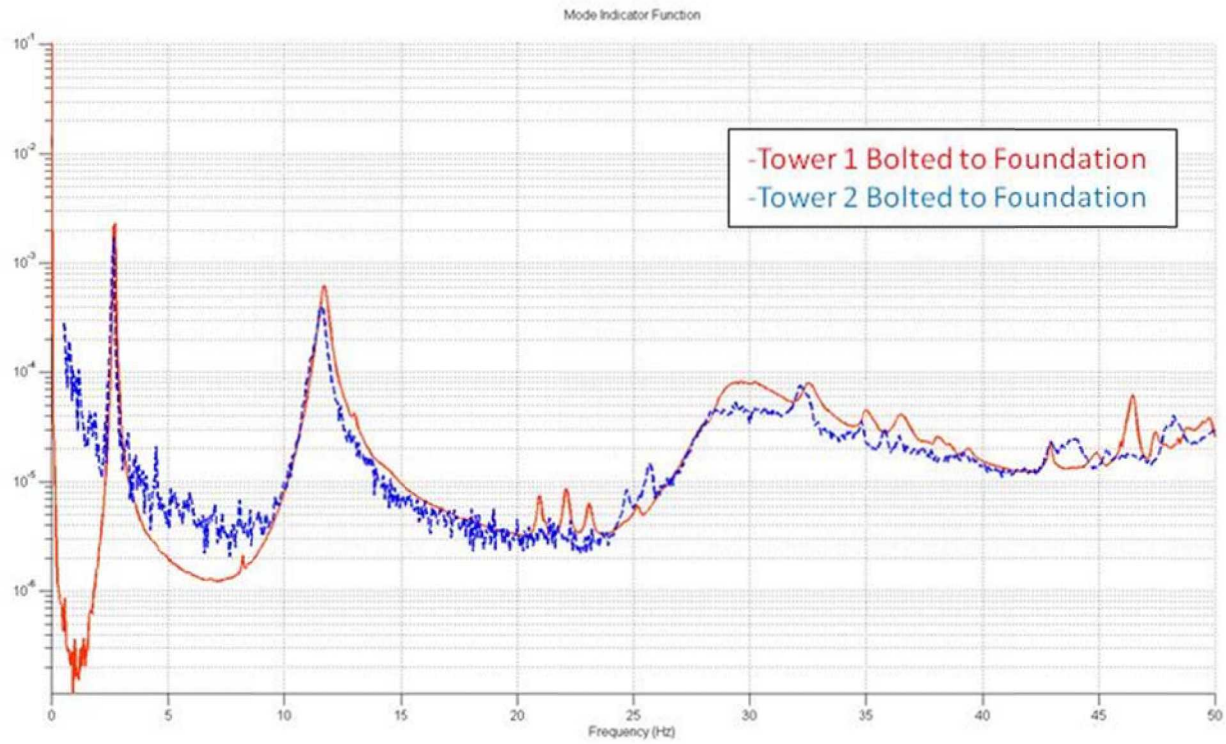


Figure 4. PSMIF for Towers 1 and 2 bolted to foundation.

As seen in Figure 4, the PSMIF of Tower 1 is significantly cleaner than the PSMIF of Tower 2. Unfortunately, a thunderstorm occurred during setup of Tower 2 and caused some of the channels to produce erroneous measurements. Due to time constraints for the installation of the nacelle by the crane company, it was not possible to troubleshoot and repair the channels with issues. Enough channels remained functional, however, to obtain good-quality measurements as long as the affected channels were removed.

The final list of mode shapes is included in Table 1. The first and second bending modes are of primary importance. Plots of the mode shapes can be seen in Appendix A.

The frequencies of Tower 1 and Tower 2 are within 5% of each other, indicating a high level of similarity between the two towers. The modal assurance criterion (MAC) was also computed between the two towers and shows a high level of agreement; the slightly lower values for the second bending mode are due to removing the affected channels from the mode shapes and not having sufficient high response measurements.

Table 1. Final mode list for V27 towers bolted to concrete foundation.

| | Axis of Motion | Tower 1 | | Tower 2 | | MAC |
|---|---|---|---|---|---|---|
| | | Frequency (Hz) | Damping (% Crit) | Frequency (Hz) | Damping (% Crit) | |
| First Bending Mode | Fore-Aft (X) | 2.70 | 0.56 | 2.61 | 0.82 | 0.95 |
| | Side-Side (Y) | 2.73 | 0.98 | 2.67 | 0.50 | 0.90 |
| Second Bending Mode | Fore-Aft (X) | 11.58 | 2.24 | 11.32 | 2.49 | 0.81 |
| | Side-Side (Y) | 11.71 | 1.76 | 11.58 | 1.57 | 0.84 |

In addition, SNL was interested in determining the stiffness between the foundation and tower due to the bolted interface. For this, the axial (Z-axis) accelerometer FRFs at the base of the tower and at the foundation are overlaid as shown in Figure 5.

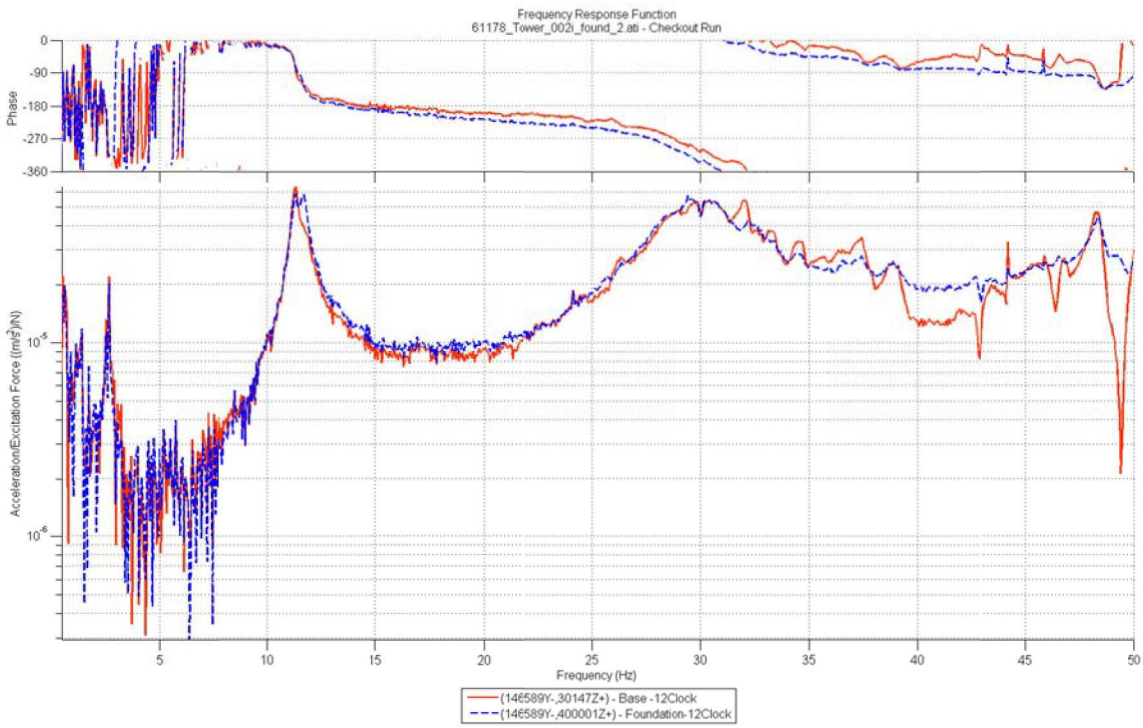


Figure 5. FRF comparison of base of tower and foundation.

The overlaid FRFs are almost identical, indicating that there is very minimal energy lost over the interface and therefore the interface is a very good approximation of a fixed boundary condition. There is significant motion in the foundation, however, indicating that the entire concrete foundation has relative motion with respect to ground.

**Summary and Conclusions**

This report has documented ATA Engineering's modal testing of two towers that are to be installed as part of the Sandia National Laboratories (SNL) Scaled Wind Farm Technology (SWIFT). Testing was conducted February 7–13, 2013. Modal parameters were obtained for the towers, and the testing procedure and results were documented. Frequencies for both towers for the first and second bending modes were within 5% of each other, indicating a high level of similarity between the two towers.

Thank you for the opportunity to complete this project work for Sandia National Laboratories. Please contact David Cloutier or Tim Marinone if you have any questions about this report.

Sincerely,

Scanned signature - original on file ATA ENGINEERING INC

Tim Marinone
Engineer (858.480.2078; tim.marinone@ata-e.com)

Reviewed by:

Scanned signature - original on file ATA ENGINEERING INC

David Cloutier
Project Engineer (858.480.2083; david.cloutier@ata-e.com)

cc: David L. Hunt, Account Manager
(858.480.2095; david.hunt@ata-e.com)

# Appendix A

# Test Mode Shapes

# Tower 1
# (Tower 2 Had Some Damaged Channels and Shapes Are Not Shown)

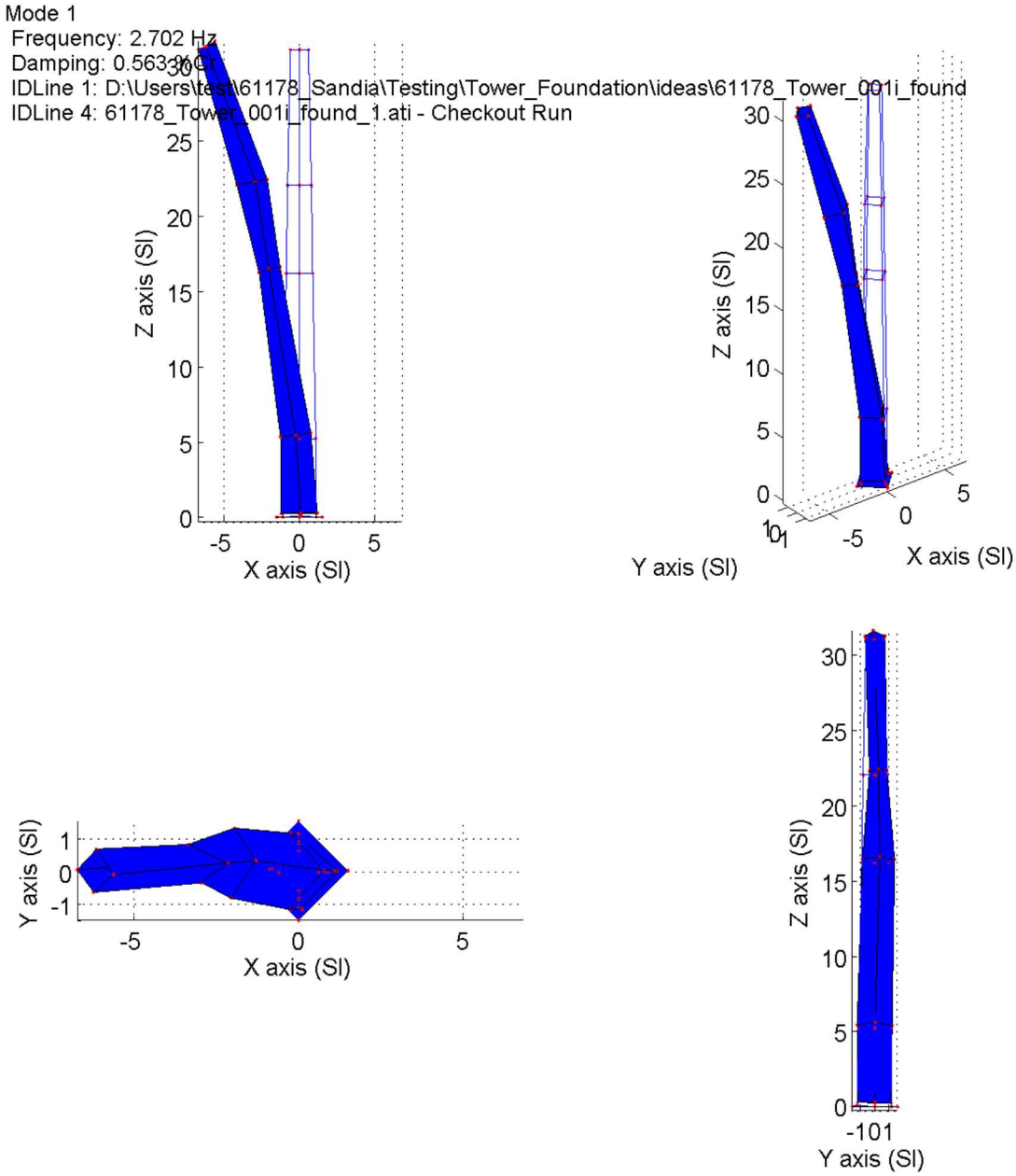

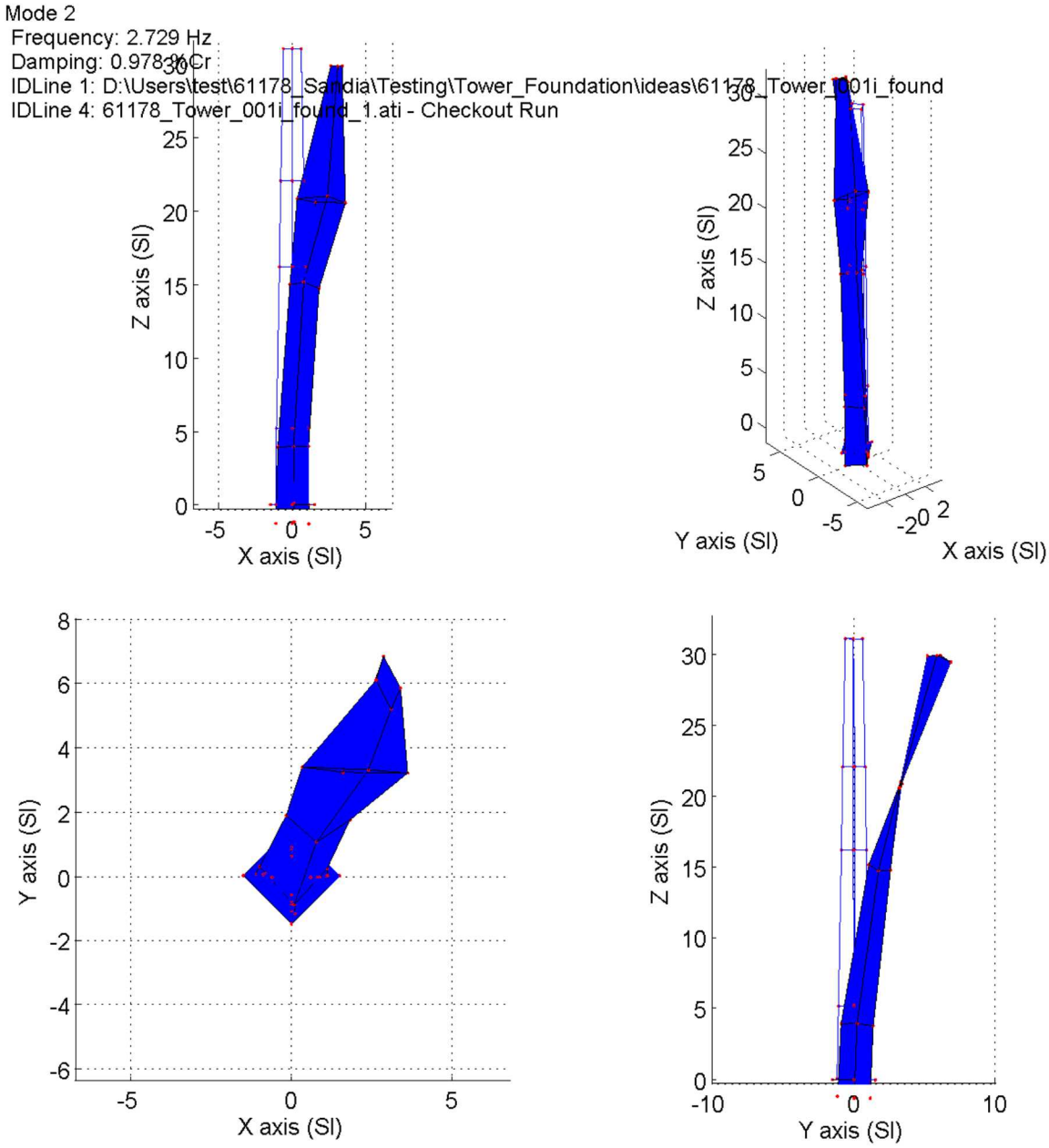
Mode 2
Frequency: 2.729 Hz
Damping: 0.9783%Cr
IDLine 1: D:\Users\test\61178_Sandia\Testing\Tower_Foundation\ideas\61178_Tower_001i_found
IDLine 4: 61178_Tower_001i_found_1.ati - Checkout Run
Z axis (SI)
X axis (SI)
Y axis (SI)

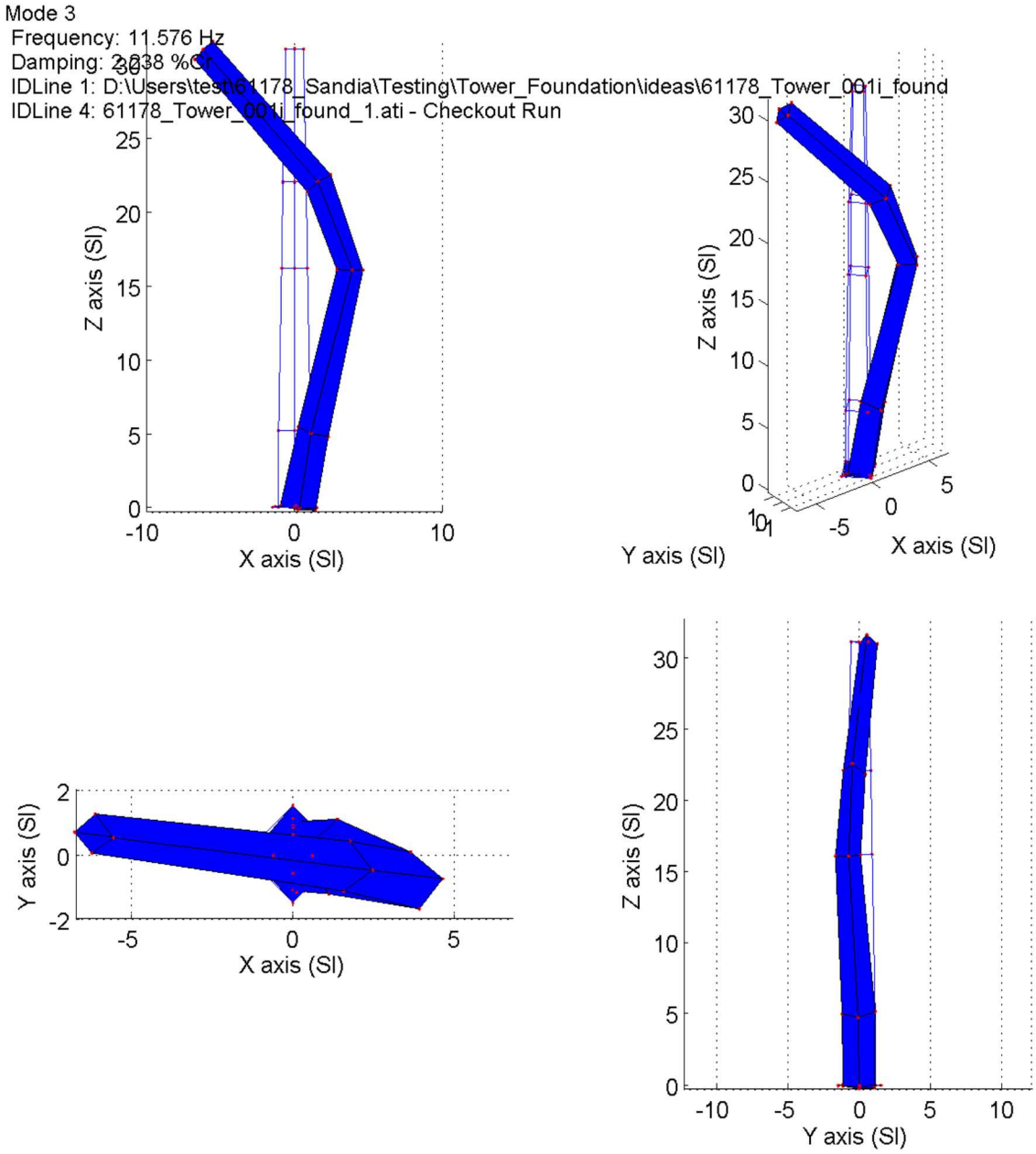
Mode 3
Frequency: 11.576 Hz
Damping: 2.238 %Cr
IDLine 1: D:\Users\test\61178_Sandia\Testing\Tower_Foundation\ideas\61178_Tower_001i_found
IDLine 4: 61178_Tower_001i_found_1.ati - Checkout Run
Z axis (SI)
X axis (SI)
Y axis (SI)

Mode 4
Frequency: 11.712 Hz
Damping: 1.761 %Cr
IDLine 1: D:\Users\test\61178_Sandia\Testing\Tower_Foundation\ideas\61178_Tower_001i_found
IDLine 4: 61178_Tower_001i_found_1.ati - Checkout Run

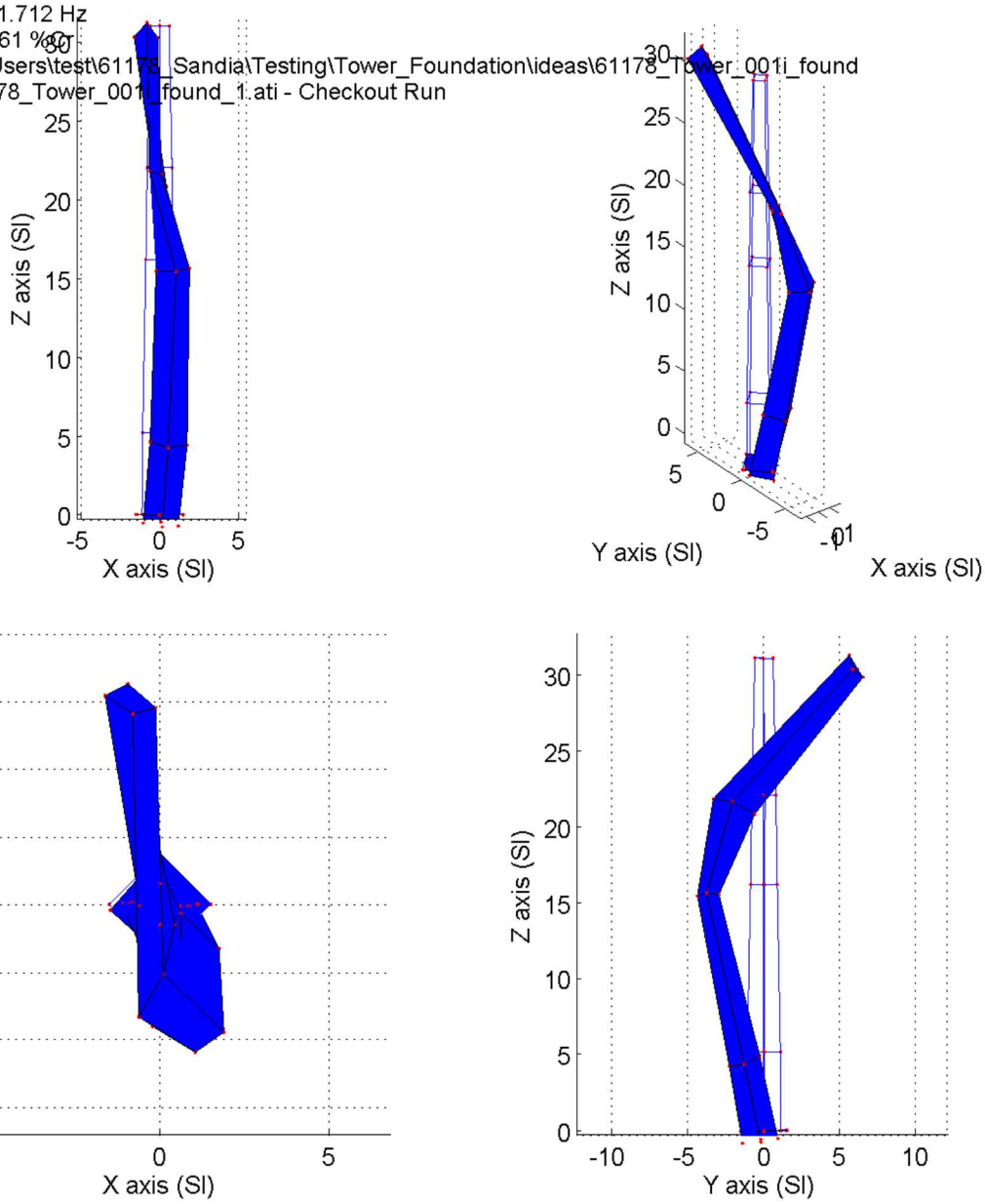

ATA Project No. 61178
Sandia National Laboratories RFQ No. 273252
July 18, 2013

# Final Report on SNL SWIFT V27 Full Wind Turbine Experimental and Operational Modal Analysis

Prepared for

Sandia National Laboratories
P.O. Box 5800
Albuquerque, New Mexico 87123

Prepared by

ATA Engineering, Inc.
11995 El Camino Real, Suite 200
San Diego, California 92130


Prepared by:

Scanned signature - original on file ATA ENGINEERING INC

Timothy Marinone
Engineer, Test

Reviewed by:

Scanned signature - original on file ATA ENGINEERING INC

David Cloutier
Project Engineer, Test


CONTACTS

| | |
|---|---|
| SNL: | |
| Bruce Leblanc | 505-844-1438 |
| John White | 505-284-5400 |
| Gil Sanchez | 505-284-4481 |
| ATA: | |
| Tim Marinone | 858-480-2076 |
| Dave Cloutier | 858-480-2083 |
| Ralph Brillhart | 858-480-2082 |
| Dave Hunt | 858-480-2095 |

**ABSTRACT**

This final report documents ATA Engineering, Inc.'s experimental and operational modal analysis of Sandia National Laboratories' Scaled Wind Farm Technology (SWIFT) Vestas 27 (V27) wind turbines. The modal survey was performed at SNL's SWIFT facility in Lubbock, Texas, on June 10 through June 16, 2013. Two wind turbines were tested: one turbine with a full set of instrumentation and a second turbine with a reduced set of instrumentation. All flexible bending modes below 15 Hz were identified as target modes. The modal survey was conducted with modal impact hammer test runs and with natural wind excitation, and all target modes were identified from the impact hammer excitation. The modal results of both turbines were compared to identify variation between the turbines.

This report documents one of several different tests performed to characterize various components and assemblies of the V27 wind turbines for the SWIFT project. Details of the other tests can be found in their respective reports.

TABLE OF CONTENTS

1. INTRODUCTION ..... 1
1.1. Test Objectives ..... 1
1.2. Test Performance and Results ..... 1
2. TEST CONFIGURATIONS AND PRETEST MODELING ..... 5
2.1. Test Article Description and Configuration ..... 5
2.2. Test Measurements and Geometry ..... 7
3. TEST DESCRIPTION ..... 10
3.1. Test Conduct ..... 10
3.1.1. Modal Survey ..... 10
3.1.2. Operational Modal Analysis ..... 12
3.2. Test Instrumentation ..... 13
3.2.1. Accelerometers ..... 14
3.2.2. Impact Hammer ..... 15
3.2.3. Data Measurement and Recording ..... 17
3.3. Test Performance ..... 19
3.3.1. Data Quality Assessment ..... 19
3.3.2. Modal Extraction from Frequency Response Functions ..... 20
3.3.3. Modal Extraction from Cross-Spectrum Functions ..... 21
3.3.4. Modal Assurance Criteria ..... 21
4. TEST RESULTS ..... 22
4.1. V27 Turbine Modal Test Results ..... 22
4.2. V27 Turbine Operational Modal Test Result ..... 25
5. CONCLUSIONS ..... 28
Appendix A On-Site Test Log and Run Log ..... A-1
Appendix B Nodes and Accelerometers Table ..... B-1
Appendix C Accelerometer Photos ..... C-1
Appendix D Impact Hammer Location Photos ..... D-1
Appendix E Modal Test Channel Table ..... E-1
Appendix F Test Mode Shapes ..... F-1
Appendix G Equipment Specifications ..... G-1

LIST OF TABLES

Table 1-1. Final modes, SNL1 and SNL2 V27 wind turbines. ..... 3
Table 1-2. Final modes, SNL1 V27 wind turbines—comparison of EMA and OMA..... 4
Table 2-1. Accelerometer locations (80 channels and 40 nodes, not including impact hammer)..... 9
Table 3-1. SNL V27 modal survey test run log. ..... 11
Table 4-1. SNL1 and SNL2 V27 turbine final global modes sorted by test frequency. ..... 23
Table 4-2. V27 final test modes (SNL1 at full instrumentation set): self-MAC..... 24
Table 4-3. SNL1 turbine EMA and OMA final global modes sorted by test frequency..... 26
Table 4-4. V27 final test modes (SNL1 at full instrumentation set): self-orthogonality. ..... 27

LIST OF FIGURES

Figure 2-1. Overall view of V27 turbine..... 6
Figure 2-2. V27 coordinate systems and measurement locations. ..... 8
Figure 3-1. Data acquisition equipment and analysis workstations. ..... 13
Figure 3-2. Instrumentation cabling was routed to gather boxes where DB-50 cables were then used to connect to the data acquisition system..... 14
Figure 3-3. Example accelerometer installation; note the barcode used for documenting the accelerometer location. ..... 15
Figure 3-4. PSD for input hammer, run 7. ..... 16
Figure 3-5. Data acquisition system schematic..... 18
Figure 3-6. FRF and coherence for impact hammer drive point 53557Y+, run 8. ..... 20
Figure 4-1. SNL1 and SNL2 PSMIF using common DOF set. ..... 23
Figure 4-2. Stabilization diagram for operational model analysis. ..... 25

## LIST OF ABBREVIATIONS

| | |
|---|---|
| ATA | - ATA Engineering, Inc. |
| ASD | - auto spectral density |
| CMIF | - complex mode-indicator function |
| CRS | - corrected root sum |
| DOF | - degree of freedom |
| EMA | experimental modal analysis |
| FEM | - finite element model |
| FRF | - frequency response functions |
| Hz | - hertz |
| ICP™[1] | - integrated circuit preamplifier |
| IMAT | - interface between MATLAB, analysis, and test |
| MAC | - modal assurance criteria |
| MMIF | - multivariate mode-indicator function |
| MPR | - multiple-point random |
| OMA | operational modal analysis |
| PCB | - PCB Electronics, Inc. |
| PSD | - power spectral density |
| PSMIF | - power spectrum mode-indicator function |
| SNL | - Sandia National Laboratories |
| SWIFT | - Scaled Wind Farm Technology |
| TEDS | - transducer electronic data sheet |
| TAM | - test analysis model |
| V27 | - Vestas 27 |

[1] ICP is a registered trademark of PCB Piezotronics, Inc.

# 1. INTRODUCTION

Sandia National Laboratories (SNL) is developing the Scaled Wind Farm Technology (SWIFT) center to enable rapid, cost-efficient testing and development of transformative wind energy technology. ATA Engineering, Inc., (ATA) was contracted as part of this effort to dynamically characterize a number of components and assemblies to be used at SWIFT. This report documents the experimental modal analysis (EMA) and operational modal analysis (OMA) for the Vestas 27 (V27) wind turbines. The modal survey was successfully completed June 10–16, 2013. Two turbines were tested: one with a full set of instrumentation (SNL1) and a second with a reduced set of instrumentation (SNL2). All turbines were tested bolted to the concrete foundation in their final configuration.

In preparation for the modal survey, SNL worked with ATA to develop a test display model (TDM) to be used in animating the modes obtained. A back-expansion matrix for visualization of the test mode shapes was also developed based on this TDM. ATA used this information to plan and conduct the modal survey.

ATA conducted the test using modal impact hammer and natural wind excitation methods. ATA provided the data collection equipment and instrumentation. All V27 turbine primary modes were identified up to 15 Hz, and these are presented in Table 1-1.

## 1.1. Test Objectives

The overall objective of the SNL V27 turbine modal survey was to obtain modal properties to use for correlation. The requirements to satisfy the overall objective were stated as follows:

1. Perform a pretest analysis, predicting the target mode shapes and frequencies.
    a. Develop a TAM for defining accelerometer locations and expanding out mode shapes.
    b. Identify modal survey excitation locations.
2. Develop a detailed test plan and procedure for conducting the modal survey. The frequency range of interest was 0–15 Hz for the V27 turbine bolted to the concrete foundation. All flexible bending and torsion modes below 15 Hz were identified as target modes.
3. Experimentally define the modal parameters (frequency, damping, and shape) for all target modes of the turbine.
4. Provide quick-look results on site during testing (including animated mode shapes and comparison with finite element predictions).
5. Deliver a final report detailing all tasks of the modal survey.

## 1.2. Test Performance and Results

In preparation for the modal survey, SNL provided ATA with the measurement geometry of the V27 turbine. ATA used this information to plan, prepare for, and perform the modal survey. ATA provided the necessary data collection equipment and instrumentation.

ATA completed the test using modal impact hammer and operational excitation methods. Global modes were extracted from the impact hammer data runs as well as the wind excitation data runs. All V27 turbine primary modes were identified up to 15 Hz, and they are presented in Table 1-1 for both SNL1 and SNL2 turbines. Table 1-2 lists the comparison of modes with artificial and natural excitation on SNL1.

Table 1-1. Final modes, SNL1 and SNL2 V27 wind turbines.

| | SNL1 | | SNL2 | | | | |
|---|---|---|---|---|---|---|---|
| Mode | Frequency (Hz) | Damping (% Crit.) | Frequency (Hz) | Damping (% Crit.) | Diff (%) | MAC | Description |
| 1 | 1.00 | 3.39 | 0.97 | 2.66 | 3% | 96 | 1st Tower Bending Edgewise |
| 2 | 1.01 | 3.82 | 0.99 | 2.95 | 2% | 83 | 1st Tower Bending Flapwise |
| 3 | 2.02 | 2.48 | 1.88 | 2.87 | 7% | 68 | 1st Blade Flapwise Bending - Asym |
| 4 | 2.04 | 2.51 | 2.00 | 2.36 | 2% | 50 | 1st Blade Flapwise Bending - Asym |
| 5 | 2.40 | 2.13 | 2.37 | 1.59 | 1% | 82 | 1st Blade Flapwise Bending - Sym |
| 6 | 3.65 | 1.45 | | | | | 1st Blade Edgewise Bending - Asym |
| 7 | 3.73 | 1.24 | 3.75 | 0.01 | 0% | 32 | 1st Blade Edgewise Bending - Asym |
| 8 | 5.33 | 1.35 | 5.05 | 1.96 | 5% | 76 | 2nd Blade Flapwise Bending - Asym |
| 9 | 5.36 | 1.46 | 5.34 | 1.26 | 0% | 68 | 2nd Blade Flapwise Bending - Asym |
| 10 | 6.67 | 1.20 | 6.70 | 0.98 | 0% | 88 | 2nd Blade Flapwise Bending - Sym |
| 11 | 7.83 | 1.38 | 7.76 | 1.18 | 1% | 90 | 2nd Tower Bending Flapwise |
| 12 | 7.97 | 1.19 | 7.99 | 1.52 | 0% | 85 | 2nd Tower Bending Edgewise |
| 13 | 8.43 | 1.32 | 8.34 | 0.80 | 1% | 89 | 1st Tower Torsion, 2nd Blade Edgewise Bending |
| 14 | 9.67 | 1.65 | 9.99 | 1.64 | -3% | 73 | 2nd Blade Edgewise Bending - Sym |
| 15 | 11.15 | 1.19 | 11.12 | 1.29 | 0% | 83 | 3rd Blade Flapwise Bending - Asym |
| 16 | 12.52 | 3.64 | | | | | 3rd Blade Flapwise Bending - Asym |
| 17 | 12.69 | 1.70 | 12.17 | 2.68 | 4% | 84 | 2nd Blade Edgewise Bending - Asym / 3rd Blade Flap - Asym |
| 18 | 13.45 | 1.06 | 13.22 | 1.11 | 2% | 71 | 2nd Blade Edgewise Bending - Asym |
| 19 | 13.66 | 1.08 | 13.82 | 1.98 | -1% | 66 | 2nd Blade Edgewise Bending - Asym / 3rd Blade Flap -Sym |
| 20 | 13.80 | 1.04 | | | | | 3rd Blade Flapwise Bending -Sym |

Table 1-2. Final modes, SNL1 V27 wind turbines—comparison of EMA and OMA.

| | SNL1 - EMA | | SNL1 - OMA | | | | |
|---|---|---|---|---|---|---|---|
| Mode | Frequency (Hz) | Damping (% Crit.) | Frequency (Hz) | Damping (% Crit.) | Diff (%) | MAC | Description |
| 1 | 1.00 | 3.39 | | | | | 1st Tower Bending Edgewise |
| 2 | 1.01 | 3.82 | 1.00 | 0.82 | 0% | 44 | 1st Tower Bending Flapwise |
| 3 | 2.02 | 2.48 | 1.98 | 2.24 | 2% | 63 | 1st Blade Flapwise Bending - Asym |
| 4 | 2.04 | 2.51 | 2.02 | 2.45 | 1% | 98 | 1st Blade Flapwise Bending - Asym |
| 5 | 2.40 | 2.13 | 2.37 | 1.77 | 1% | 100 | 1st Blade Flapwise Bending - Sym |
| 6 | 3.65 | 1.45 | | | | | 1st Blade Edgewise Bending - Asym |
| 7 | 3.73 | 1.24 | 3.61 | 0.95 | 3% | 42 | 1st Blade Edgewise Bending - Asym |
| 8 | 5.33 | 1.35 | 5.25 | 1.40 | 2% | 73 | 2nd Blade Flapwise Bending - Asym |
| 9 | 5.36 | 1.46 | 5.31 | 1.20 | 1% | 93 | 2nd Blade Flapwise Bending - Asym |
| 10 | 6.67 | 1.20 | 6.61 | 0.97 | 1% | 100 | 2nd Blade Flapwise Bending - Sym |
| 11 | 7.83 | 1.38 | | | | | 2nd Tower Bending Flapwise |
| 12 | 7.97 | 1.19 | | | | | 2nd Tower Bending Edgewise |
| 13 | 8.43 | 1.32 | | | | | 1st Tower Torsion, 2nd Blade Edgewise Bending |
| 14 | 9.67 | 1.65 | 9.37 | 2.07 | 3% | 94 | 2nd Blade Edgewise Bending - Sym |
| 15 | 11.15 | 1.19 | 11.00 | 1.31 | 1% | 99 | 3rd Blade Flapwise Bending - Asym |
| 16 | 12.52 | 3.64 | | | | | 3rd Blade Flapwise Bending - Asym |
| 17 | 12.69 | 1.70 | | | | | 2nd Blade Edgewise Bending - Asym / 3rd Blade Flap - Asym |
| 18 | 13.45 | 1.06 | | | | | 2nd Blade Edgewise Bending - Asym |
| 19 | 13.66 | 1.08 | | | | | 2nd Blade Edgewise Bending - Asym / 3rd Blade Flap -Sym |
| 20 | 13.80 | 1.04 | 13.49 | 1.32 | 0.01 | 92 | 3rd Blade Flapwise Bending -Sym |

# 2. TEST CONFIGURATIONS AND PRETEST MODELING

This section of the report describes the specific pretest activities for the V27 turbine experimental and operational modal analysis. The turbine is described along with pretest model preparation activities.

## 2.1. Test Article Description and Configuration

The Vestas 27 225 kW wind turbine has a 30 meter tower with 13 meter rotor blades. The V27 turbine is shown in Figure 2-1. The V27 was tested in a parked configuration to prevent the turbine from rotating during testing, and the turbine rotor was set to zero degrees to minimize the potential of damage due to wind.

Figure 2-1. Overall view of V27 turbine.

## 2.2. Test Measurements and Geometry

This section of the report provides information about the measurement locations used during the modal survey. Measurement locations were selected based on discussion with SNL engineers. ATA created a test model representative of the V27 turbine to develop a set of test measurement degrees of freedom (DOF).

The final set of measurement locations totaled 80 fixed DOF at 53 node locations. The geometry and nodes were defined using one global coordinate system and four local coordinate systems. The tower and foundation DOF were located in the global coordinate system; each blade and the nacelle were in their own local coordinate systems. Figure 2-2 shows the test display model and accelerometer locations, with each arrow in the figure representing an accelerometer. Table 2-1 lists the 80 test DOF at the 53 selected model node locations, along with a description of each. Photos of the accelerometers are included in Appendix C. In total, 81 channels counting the modal hammer were measured during impact testing. The same channels—with the exception of the modal hammer—were measured during operational testing. Due to time constraints, only a subset of channels was measured on the second turbine for comparing natural frequencies. This included all DOF measured on SNL1 except the blades. Additional biaxial accelerometers were installed on the blades at max chord on SNL2.

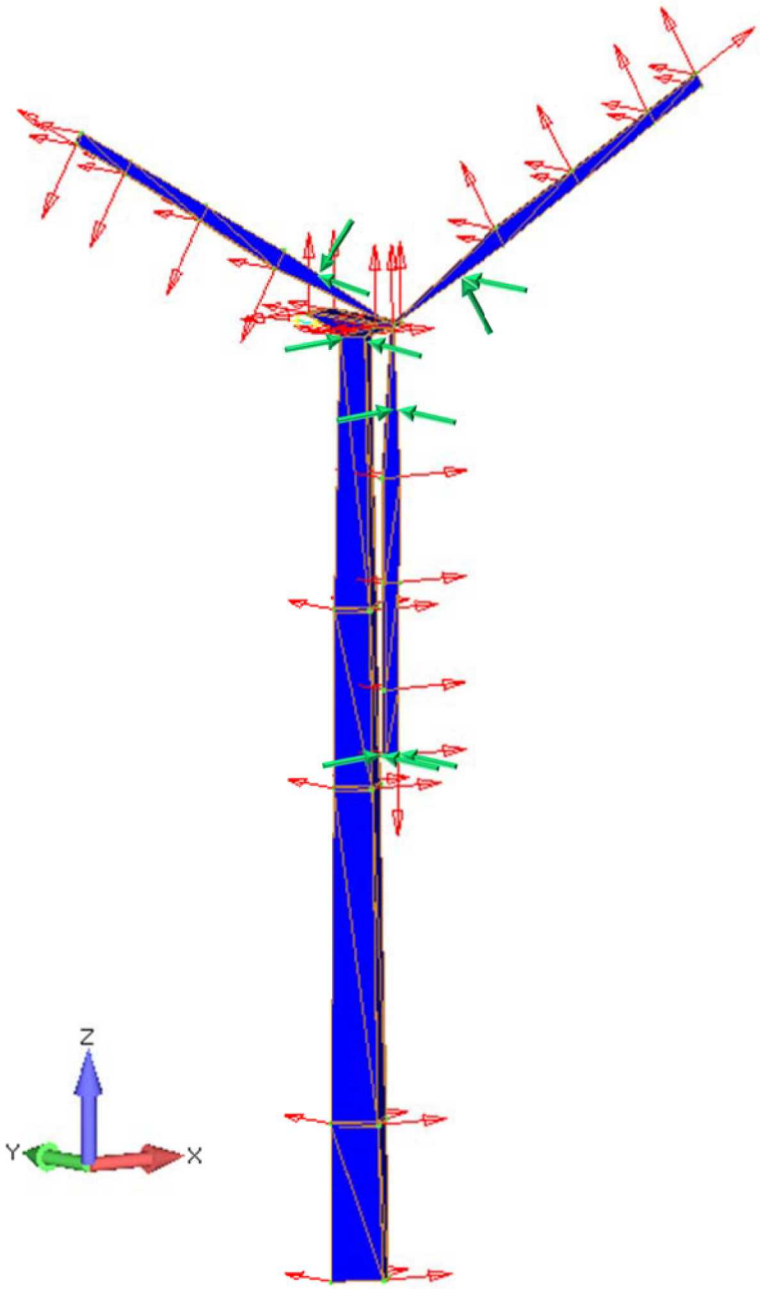


Figure 2-2. V27 coordinate systems and measurement locations.

Table 2-1. Accelerometer locations (80 channels and 40 nodes, not including impact hammer).

| Group Name | Node | X+ | Y+ | Z+ | Locations |
|---|---|---|---|---|---|
| Tower | 30018 | | Y- | | Base-6Clock |
| Tower | 30036 | X- | | | Base-9Clock |
| Tower | 30147 | | Y+ | | Base -12Clock |
| Tower | 33807 | | Y+ | | Platform1-12Clock |
| Tower | 37003 | X+ | | | 22Ft-3Clock |
| Tower | 37214 | X- | | | 22Ft-9Clock |
| Tower | 38067 | | Y+ | | 22Ft-12Clock |
| Tower | 40762 | | Y- | | Tip-12Clock |
| Tower | 40772 | X- | | | Tip-3Clock |
| Tower | 44049 | | Y+ | | 22Ft-6Clock |
| Tower | 75564 | X+ | | | Base-3Clock |
| Tower | 77061 | X- | | | Platform1-9Clock |
| Tower | 100589 | X+ | | | Platform2-3Clock |
| Tower | 101415 | X- | | | Platform2-9Clock |
| Tower | 115734 | | Y+ | | Platform2-12Clock |
| Tower | 146589 | X+ | | | Tip-9Clock |
| Tower | 200924 | X+ | | | Platform1-3Clock |
| Tower | 254503 | | Y+ | | Tip-6Clock |
| Tower | 271687 | | Y- | | Platform2-6Clock |
| Tower | 281849 | | Y- | | Platform1-6Clock |
| Blade 1 | 53502 | X- | Y+ | Z+ | B1-Trail-1(Tip) |
| Blade 1 | 53052 | X- | Y+ | | B1-Trail-3 |
| Blade 1 | 52208 | X- | Y+ | | B1-Trail-6 |
| Blade 1 | 51359 | X- | Y+ | | B1-Trail-9 |
| Blade 1 | 53537 | X- | | | B1-Lead-1(Tip) |
| Blade 1 | 53101 | X- | | | B1-Lead-3 |
| Blade 1 | 52290 | X- | | | B1-Lead-6 |
| Blade 1 | 51465 | X- | | | B1-Lead-9 |
| Blade 2 | 53527 | X- | Y+ | Z+ | B2-Trail-1(Tip) |
| Blade 2 | 53523 | X- | Y+ | | B2-Trail-3 |
| Blade 2 | 53517 | X- | Y+ | | B2-Trail-6 |
| Blade 2 | 53511 | X- | Y+ | | B2-Trail-9 |
| Blade 2 | 53528 | X- | | | B2-Lead-1(Tip) |
| Blade 2 | 53524 | X- | | | B2-Lead-3 |
| Blade 2 | 53518 | X- | | | B2-Lead-6 |
| Blade 2 | 53512 | X- | | | B2-Lead-9 |
| Blade 3 | 53580 | X- | Y+ | Z+ | B3-Trail-1(Tip) |
| Blade 3 | 53576 | X- | Y+ | | B3-Trail-3 |
| Blade 3 | 53570 | X- | Y+ | | B3-Trail-6 |
| Blade 3 | 53564 | X- | Y+ | | B3-Trail-9 |
| Blade 3 | 53581 | X- | | | B3-Lead-1(Tip) |
| Blade 3 | 53577 | X- | | | B3-Lead-3 |
| Blade 3 | 53571 | X- | | | B3-Lead-6 |
| Blade 3 | 53565 | X- | | | B3-Lead-9 |
| Tower | 400001 | | | Z+ | Found-12Clock |
| Tower | 400004 | | | Z+ | Found-3Clock |
| Tower | 400003 | X- | Y+ | Z+ | Found-6Clock |
| Tower | 400002 | | | Z+ | Found-9Clock |
| Nacelle | 120003 | X+ | Y- | Z+ | Nacelle Fwd Port |
| Nacelle | 120004 | X+ | Y- | Z+ | Nacelle Fwd Stbd |
| Nacelle | 120007 | X- | Y+ | Z+ | Nacelle Rear Port |
| Nacelle | 120008 | X- | Y+ | Z+ | Nacelle Rear Stbd |
| Hub | 130001 | X+ | Y+ | Z+ | Hub |

| # X Entries | #Y Entries | # Z Entries |
|---|---|---|
| 40 | 28 | 12 |
| | | |
| Total Number of Entries | | 80 |

# 3. TEST DESCRIPTION

The V27 turbine experimental modal survey involved applying and measuring external force excitations to the turbine and measuring the acceleration responses at the instrumented locations. This testing allowed the measurement of frequency response functions (FRF) between the instrumented response locations and the applied shaker input forces. The FRF characterize the dynamic behavior of the structure and can be used to identify the modal parameters (frequency, damping, and shape) of the turbine.

The V27 turbine operational modal testing involved measuring the acceleration responses at the instrumented locations due to the natural excitation of the wind. This testing allowed the measurement of cross-spectra functions between the instrumented response locations. The cross spectra characterize the dynamic behavior of the structure and can be used to identify the operational modal parameters (frequency, damping, and shape) of the turbine.

## 3.1. Test Conduct

The following sections provide the test conduct for the experimental and operational modal tests performed on the V27 turbines.

### 3.1.1. Modal Survey

The modal survey was performed on site at SNL's SWIFT facility in Lubbock, Texas, June 10–16, 2013. ATA was responsible for the installation and removal of all transducers and cabling necessary for the modal survey. All DOF locations on the turbine were measured and marked on the surface by ATA. The measurement locations matched those in the test display model, as selected for visualization of the primary modes. After all of the measurement locations were mapped on the turbine, the accelerometers and cables were installed.

Impact testing was performed using an instrumented modal impact hammer to excite the structure and perform the modal survey. The excitation locations for the V27 modal survey, selected based on prior test experience, were identified during the pretest analysis effort. The data acquisition system measured all data channels simultaneously, allowing all data to be taken in a single pass. A complete channel table list is provided in Appendix E.

In total, two runs were performed using impact excitation, while seven runs using natural excitation were recorded. These included checkout runs. The test run log is provided in Table 3-1 below. The text in the "Notes" column provides brief details on each run and any anomalies encountered. The final test mode shapes were extracted from runs 6 and 7 for SNL1 (natural and artificial excitation) and run 8 for SNL2 (artificial excitation only).

Table 3-1. SNL V27 modal survey test run log.

| 61178 SWIFT Full Turbine Test Run Log | | | | | | | | | |
|---|---|---|---|---|---|---|---|---|---|
| Run | Date | Start Time | Config† | Tower # | Exc. | File Name | Reference Channels | Freq Range (Hz) | Notes |
| **Day 1 - SNL 1** | | | | | | | | | |
| 1 | 6/10/2013 | 22:20 | pitch | 1 | o | 61178_Full_001o_pitch_1.ati | Chosen During Post-Processing | 0-30 | Checkout Run-Tower Only |
| 2 | 6/11/2013 | 10:19 | pitch | 1 | o | 61178_Full_002o_pitch_1.ati | Chosen During Post-Processing | 0-30 | Checkout Run - Tower and Blade 3 |
| 3 | 6/11/2013 | 10:50 | pitch | 1 | o | 61178_Full_003o_pitch_1.ati | Chosen During Post-Processing | 0-30 | Checkout Run - Tower and Blade 3 - Nacelle Orientation |
| **Day 2 - SNL 1** | | | | | | | | | |
| 4 | 6/12/2013 | 9:31 | pitch | 1 | o | 61178_Full_004o_pitch_1.ati | Chosen During Post-Processing | 0-30 | SNL1 Full |
| 5 | 6/12/2013 | 12:50 | pitch | 1 | o | 61178_Full_005o_pitch_1.ati | Chosen During Post-Processing | 0-30 | SNL1 Full |
| 6 | 6/12/2013 | 14:52 | pitch | 1 | o | 61178_Full_006o_pitch_1.ati | Chosen During Post-Processing | 0-30 | SNL1 Full - Fixed ATS |
| **Day 3 - SNL 1** | | | | | | | | | |
| 7 | 6/13/2013 | 7:13 | pitch | 1 | i | 61178_Full_007i_pitch_1.ati | 53517X-,53518Y+, 254503X+,40772Y+, | 0-30 | SNL1 Full - Fixed ATS- Impact |
| **Day 4 - SNL 2** | | | | | | | | | |
| 8 | 6/14/2013 | 6:22 | pitch | 2 | i | 61178_Full_008i_pitch_2.ati | 53517X-,53518Y+, 254503X+,40772Y+, | 0-30 | SNL2 Full - Impact |
| 9 | 6/14/2013 | 10:59 | pitch | 2 | o | 61178_Full_009o_pitch_2.ati | Chosen During Post-Processing | 0-30 | SNL2 Full - Operational |

| * EXCITATION TYPE | |
|---|---|
| i | modal impact |
| o | operational |

| + Config | |
|---|---|
| pitch | Pitched at 0 degrees, parked, facing east |

### 3.1.2. Operational Modal Analysis

Operational modal analysis is the principle of obtaining the experimental modal parameters of the test object (frequencies, damping and mode shapes) while the test object is in its natural "operating" configuration. This allows effects such as rotational stiffening to be included and may give a better understanding of the test object. Natural excitation due to ground vibration or wind may be used for this purpose when the operating configuration prohibits the use of artificial excitation (such as impact hammer or electrodynamic shaker) or when the structure is of sufficient size such that a large enough force cannot be input into the structure. In such cases, determining the input force caused by natural excitation is not possible, so the formulation of equations for determining the modal properties is different than in the classical experimental modal analysis.

The key summary equation is the cross-correlation function ($\Re$) evaluated at a time separation T:

$$\Re_{ijk}(T)=\sum_{r=1}^{n}\left[A_{ijk}^{r}\exp\left(-\zeta^{r}\omega_{\mathrm{n}}^{\mathrm{r}}T\right)\cos\left(\omega_{\mathrm{d}}^{\mathrm{r}}T\right)+B_{ijk}^{r}\exp\left(-\zeta^{r}\omega_{\mathrm{n}}^{\mathrm{r}}T\right)\sin\left(\omega_{\mathrm{d}}^{\mathrm{r}}T\right)\right] \qquad \text{Equation 3-1}$$

where

$A_{ijk}^{r}$ and $B_{ijk}^{r}$, shown below, independent of T, are functions of only the modal parameters,

| | |
|---|---|
| $\omega_{\mathrm{d}}^{\mathrm{r}}=\omega_{\mathrm{n}}^{\mathrm{r}}\left(1-\zeta^{r2}\right)^{1/2}$ | is the damped modal frequency; |
| $\omega_{n}^{r}$ | is the $r_{th}$ modal frequency; |
| $\zeta_r$ | is the $r_{th}$ modal damping ratio; |
| $m_r$ | is the $r_{th}$ modal mass; |
| n | is the number of modes; |
| $\psi_{ir}$ | is the $i_{th}$ component of mode shape r; and |
| t | is the time. |

Because this cross-correlation function is in the same form (damped sinusoidal) as the impulse response function assumed in classical modal analysis, the assorted modal parameter estimation methods can be used.

Further details on this technique can be found in the following references.


1. T.G. Carne, J.P. Lauffer, and A.J. Gomez, "Modal Testing of a Very Flexible 110 m Wind Turbine Structure," *Proceedings of the 6th International Modal Analysis Conference*, Kissimmee, Florida, 1988, pp. 848–855.
2. G.H. James, T.G. Carne, and A.R. Nord, "Modal Testing Using Natural Excitation," *Proceedings of the 10th International Modal Analysis Conference*, San Diego, California, 1992, pp.1209–16.
3. T.G. Carne and G.H. James, "The Inception of OMA in the Development of Modal Testing Technology for Wind Turbines," *Mechanical Systems and Signal Processing* 24, No.5 (2010): pp. 1213–26.

## 3.2. Test Instrumentation

Modal response data were measured using accelerometers mounted on the turbine. An impact hammer with an attached load cell was used to measure the amount of force applied to the turbine. ATA provided all instrumentation required to complete the test. This included the impact hammer transducer signal conditioning, data acquisition hardware, and data collection and analysis computers. SNL provided the lift and personnel responsible for moving the ATA engineer to the correct impact locations.

All of the accelerometer cabling was routed and plugged into gather boxes at a central location near the data acquisition system. A photograph of ATA's workstation is shown in Figure 3-1.

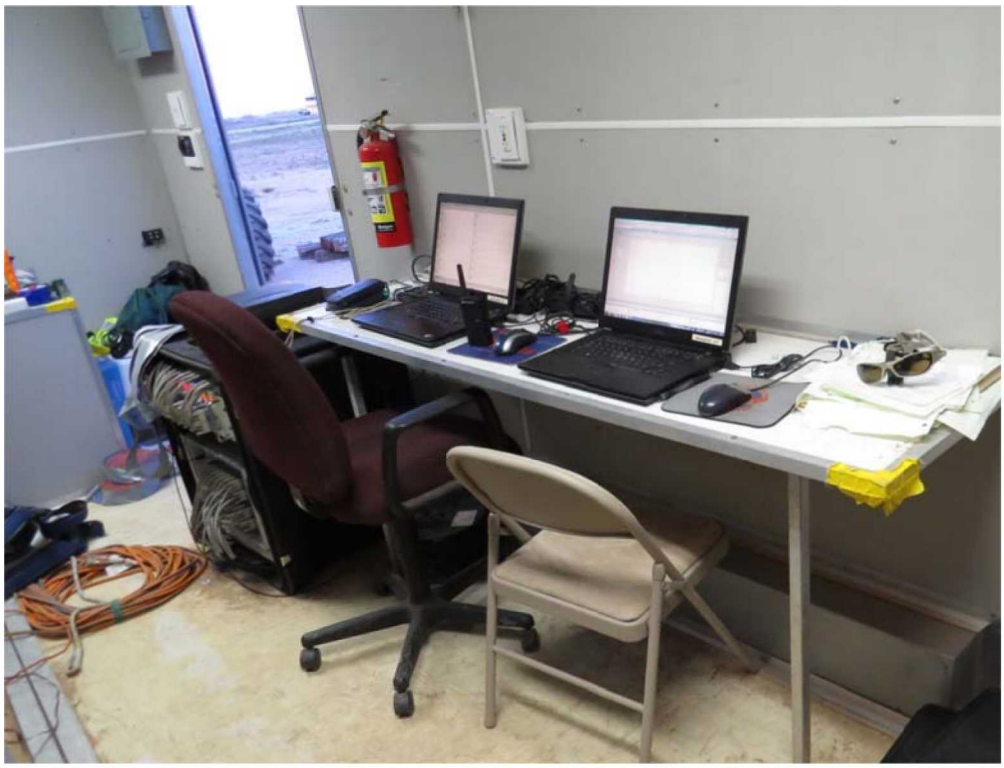

Figure 3-1. Data acquisition equipment and analysis workstations.

The DB-50 cables were then routed from the gather boxes to the data acquisition system. A photograph of the gather boxes and cabling is shown in Figure 3-2. All equipment specifications are provided in Appendix G.

Figure 3-2. Instrumentation cabling was routed to gather boxes where DB-50 cables were then used to connect to the data acquisition system.

### 3.2.1. Accelerometers

All of the accelerometers for the modal survey were defined to allow for ease of installation on the turbine. Local coordinate systems were defined for each of the blades and the nacelle. All accelerometers located on the tower were defined in the global coordinate system. Accelerometers were attached as needed to mounting blocks, allowing correct alignment to the proper displacement coordinate system. Cube blocks permitted the attachment of up to three accelerometers per block and allowed tangential measurements. Semicylindrical accelerometer mounting blocks and bubble levels were used to orient some accelerometers to their respective coordinate systems. The blocks also ensured that the accelerometers were electrically isolated from the turbine. ATA provided the blocks that were used to attach accelerometers to the turbine. Figure 3-3 shows an example of the accelerometer installation, including the cube and barcodes used to document the measurement location. Photos of all of the accelerometer locations are provided in Appendix C.

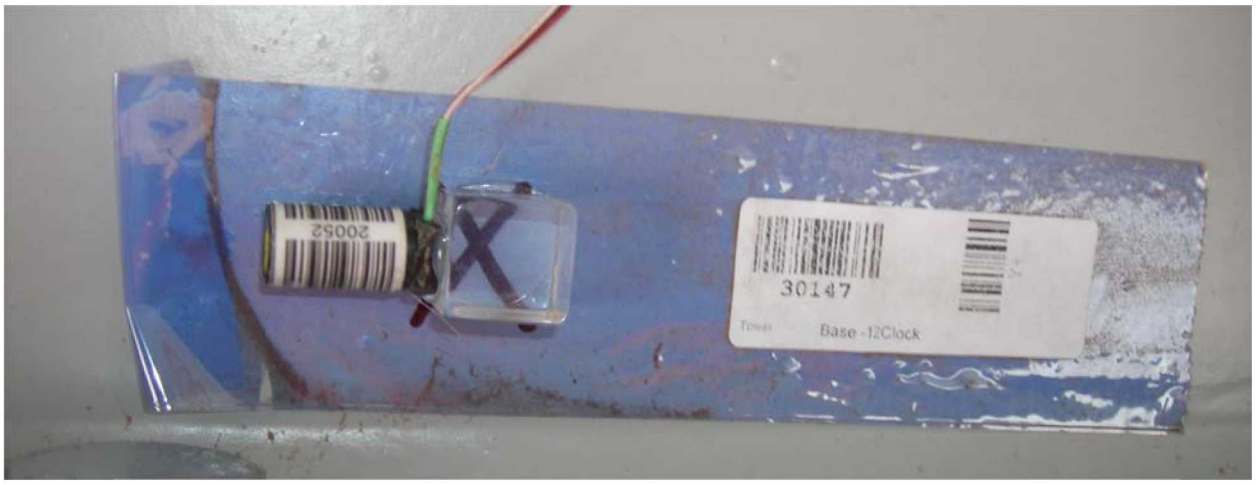


Figure 3-3. Example accelerometer installation; note the barcode used for documenting the accelerometer location.

Each accelerometer was labeled with a barcode that identified its serial number. These barcode labels were scanned with a special Palm™ handheld, which stored the information in its database. The Palm's database was then downloaded to a database on the acquisition computer, which was used to set up the channel table in the data acquisition system.

Acceleration values of 0.001 to 0.5 g (maximum) were anticipated for the modal survey. The accelerometers used for the modal survey were PCB model T333B piezoelectric, integrated circuit preamplifier (ICP®) type, capable of measuring accelerations accurately (± 5%) from 2 to 1,000 Hz. The transducers were powered by signal conditioning units supplied by ATA and included transducer electronic data sheet (TEDS) information, which allowed the amplifier to recognize each serial number for all of the accelerometers. Specification sheets for the accelerometers are included in Appendix G of this report. The calibrated sensitivities and calibration due dates for all accelerometers used for this test are included in Appendix E.

In addition, seismic accelerometers (PCB model 393B04) were used for determining the response of the concrete foundation as low acceleration and frequency values were expected at these locations. These transducers were also powered by signal conditioning units supplied by ATA.

Test instrumentation logs were prepared and maintained to show the location of each accelerometer, along with its serial number and sensitivity.

### 3.2.2. Impact Hammer

The impact hammer load cell transducer is a piezoelectric device (PCB model 086D50) that can measure up to 5000 pounds of force in the frequency range of 1 to 5000 Hz. The calibration values and due dates for the impact hammer used for this test are included in Appendix E. The hammer tip chosen (PCB model 084A31) was used due to the low-frequency bandwidth excitation. The auto power spectrum for a typical impact is shown in Figure 3-4.

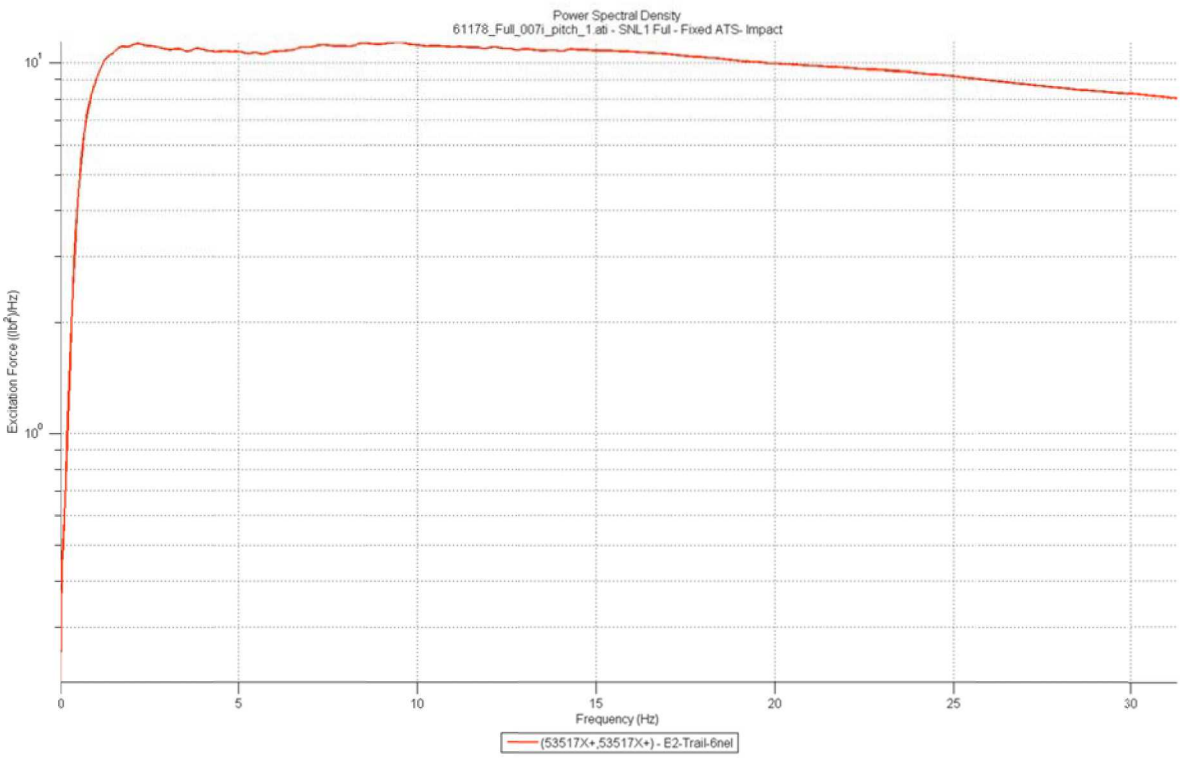


Figure 3-4. PSD for input hammer, run 7.

### 3.2.3. Data Measurement and Recording

All time history, auto spectrum, coherence, cross spectrum, and FRF data were stored on the hard disk of the data acquisition computer. All data were written to an external hard disk as a backup at the conclusion of each test day. After completion of the modal survey, the data were transferred onto the computer system at ATA's San Diego office, where the final data analysis was performed and the report written.

A schematic layout of the data collection system is shown in Figure 3-5. The system utilized a 128-channel VXI Technology digitizing front-end hardware system with 1432B analog-to-digital converter modules. The data acquisition chassis was then connected to the laptop computer through a FireWire interface card. All input forces and all response measurements were acquired simultaneously, which allowed all data to be collected in a single pass, thus reducing overall test time. The data acquisition computer was a laptop PC, and one additional computer at the test site was used for analysis and documentation. Brüel & Kjær I-deas® Test software and ATA's IMAT™ software were run on these computers to acquire and process the data. Processing included extracting the modal parameters from the FRF and evaluating the data quality and mode shapes. Further processing of the operational data was performed using ARTeMIS ® software.

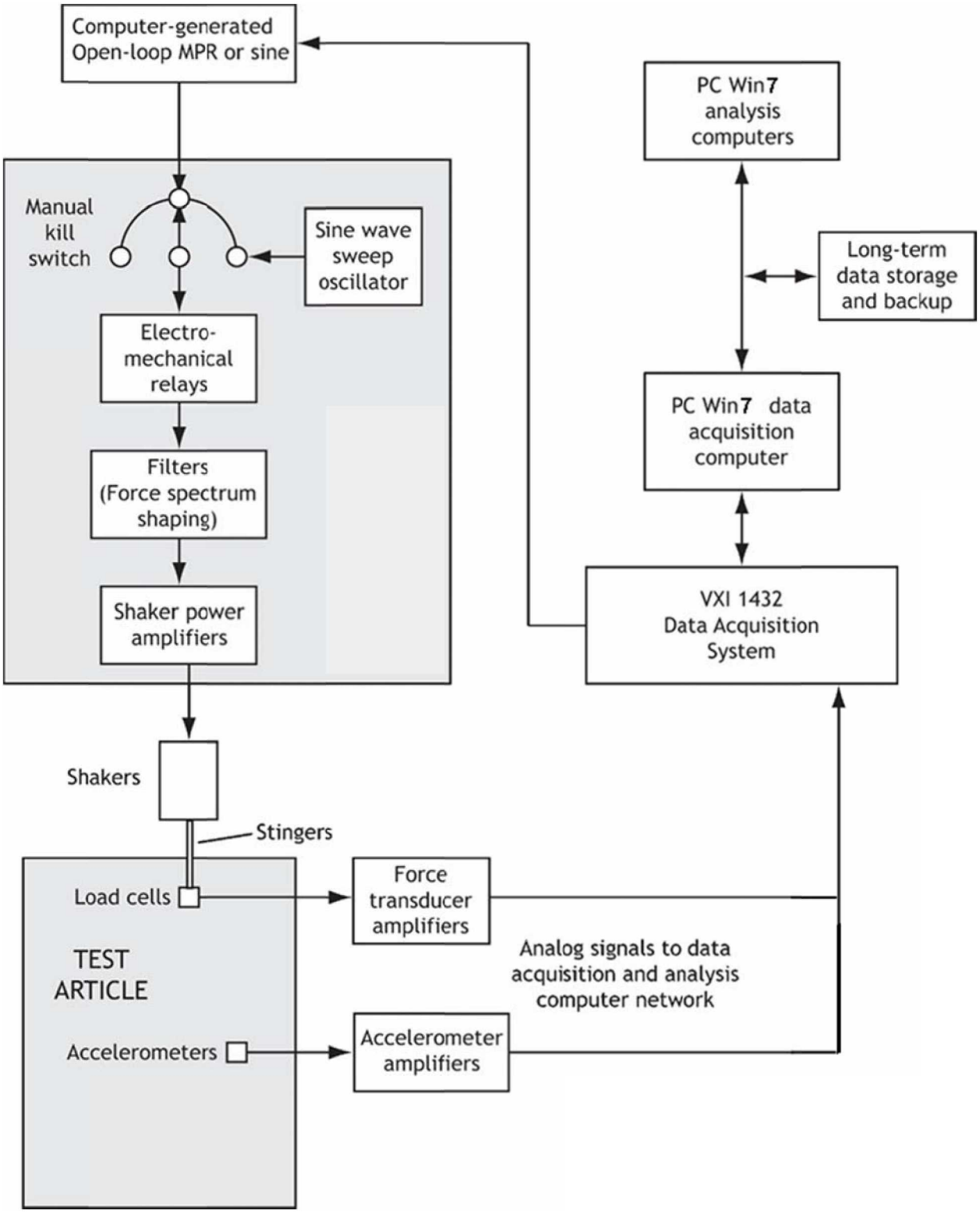


Figure 3-5. Data acquisition system schematic.

## 3.3. Test Performance

One computer was used acquire data, and the other on-site data processing computer was used for signal processing and to extract modal parameter information from the FRF data. The FRF data were processed to determine the resonant frequencies, mode shapes, and modal damping. Preliminary data analysis was performed as soon as the FRF were available for processing. This allowed for a quick study of the dynamic characteristics of the turbine. It also allowed the data quality to be verified through the use of coherence, complex mode-indicator functions (CMIF), multivariate mode-indicator functions (MMIF), power spectrum mode-indicator functions (PSMIF) and FRF quality. Quick processing of the data into mode shapes permitted the modal assurance criteria (MAC) and self-orthogonality to be computed between the test shapes, which helped to verify the independence of the extracted modes. Back-expansion of test shapes from the measured DOF to the full test display DOF allowed for visual verification that all target modes were identified. These preliminary data were shared with SNL engineers at the test site.

### 3.3.1. Data Quality Assessment

After acquisition, processing, and on-site analysis of the test data were completed, all of the data were reviewed by ATA and SNL engineers to ensure that the test objectives and the criteria for satisfaction of the test objectives had been attained.

During the data collection process, the response signals on the acquisition computer screen were monitored continuously, and the data quality was evaluated immediately after the collection of each data set by examining the force spectra (shown previously in Figure 3-4), coherence, reciprocity, and FRF quality.

Coherence functions that were computed during the acquisition process were all stored, along with the auto spectrum and FRF for each channel. In this manner, any questions about data quality could be assessed by reviewing specific coherence functions associated with a particular response measurement. Figure 3-6 shows an example of an impact excitation drive point FRF and coherence measurement.

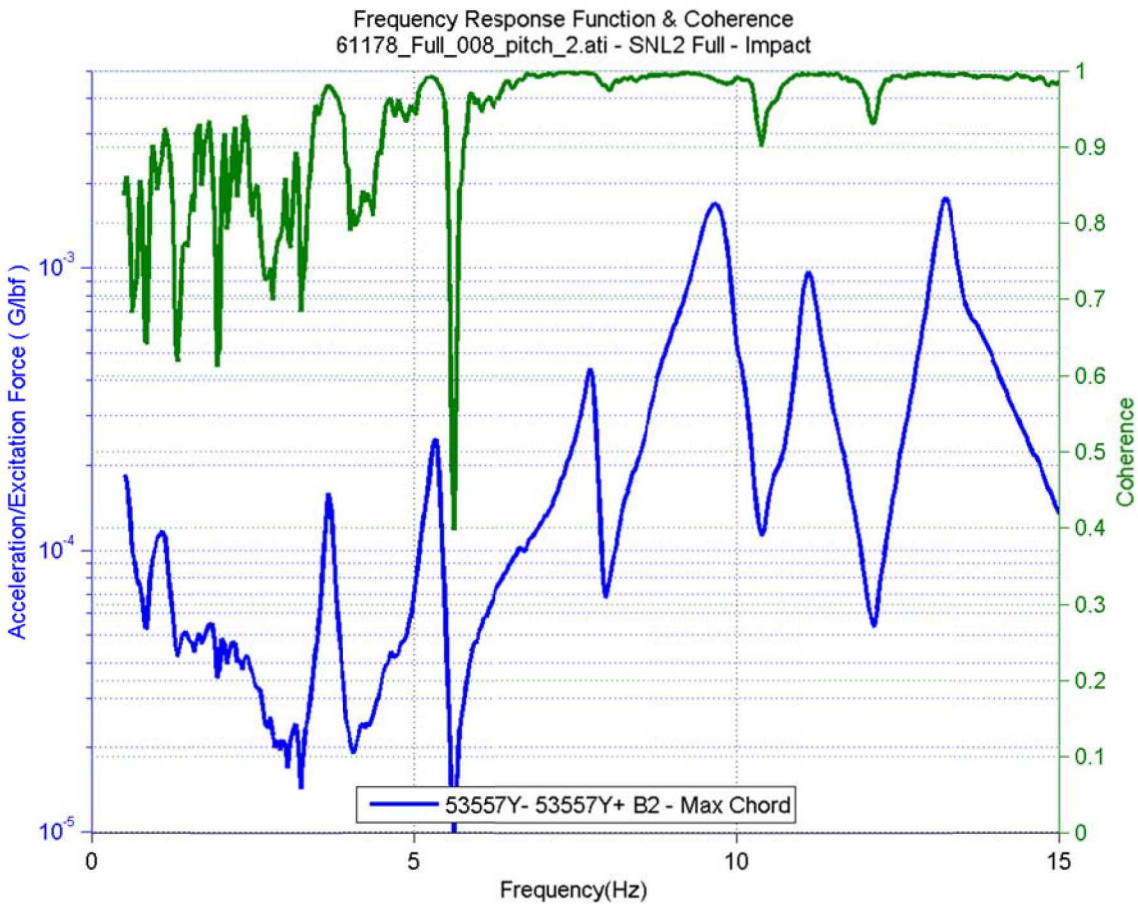


Figure 3-6. FRF and coherence for impact hammer drive point 53557Y+, run 8.

### 3.3.2. Modal Extraction from Frequency Response Functions

The first indications of resonance were determined by evaluating the FRF, in particular the drive point FRF. Peaks showing dynamic amplification were tagged for documentation. Natural frequencies were verified by looking at the minimums of the MIF and MMIF, maximums of the PSMIF, and peaks indicated by the FRF. All of the modal parameters were extracted from the FRF. These modal parameters include the natural frequency, damping, and corresponding mode shapes. The modal data extracted from the FRF were evaluated while the turbine was still available so that any modes that had not been clearly identified could be studied further. Data collected during MPR excitation were used to extract the final modal parameters.

The alias-free polyreference algorithm was the primary method used to extract the modal information from the test data. Real normal modes were computed directly from the test data. Damping was estimated using the same polyreference FRF curve-fitting algorithm that was used to extract the resonant frequencies. The alias-free polyreference technique in ATA's AFPoly™ IMAT toolkit employs a Laplace-domain curve-fitting algorithm capable of extracting lightly or highly damped modes in a single pass.

Data processing that was not completed during the test program was finalized at ATA following the test. Ongoing data analysis was performed at the test site as further testing was being performed. Final listings of modal frequencies, shapes, and damping estimates are provided in Section 4.

### 3.3.3. Modal Extraction from Cross-Spectrum Functions

Operational modal analysis was additionally performed using ARTeMIS® software. The Crystal Clear Stochastic Subspace Identification (CC-SSI) was the primary algorithm used to extract modal parameters; the CC-SSI relies on a linear least-squares estimation of the model using the raw measured time series.

### 3.3.4. Modal Assurance Criteria

Once test modes were extracted from the data, evaluation of the modes was performed on site. This approach helped to confirm that all primary (target) modes of interest had been characterized.

The MAC was computed for the test modes to obtain an indication of the independence of the modes as directly measured. The MAC is a scalar value between zero and one representing the correlation between two mode shapes. High correlation is indicated by a value near one. The MAC value between two mode shapes is computed using the following vector inner products.

$$MAC_{12} = \frac{\left|\{\Phi_1\}^H \{\Phi_2\}\right|^2}{\{\Phi_1\}^H \{\Phi_1\}\{\Phi_2\}^H \{\Phi_2\}} \qquad \text{Equation 3-2}$$

The vectors $\Phi_1$ and $\Phi_2$ are the mode shapes being compared.

Ideally, an acquired mode will be perfectly orthogonal with respect to all of the other modes, and the modal coefficients for each DOF will contain only the contribution of the mode of interest. However, there are various practical limitations in actual testing that render the attainment of perfect modal orthogonality nearly impossible, including the following:

1. Extremely high modal density (several modes close in frequency)
2. Any inaccuracy or insufficiency of the acquired data
3. The possibility of the exciter location being at or near a node point of the target mode
4. Any interference of uninstrumented and nonstructural component modes

# 4. TEST RESULTS

This section of the report documents the results of the V27 modal analysis due to artificial and natural excitation. The summary tables include the modal parameters identified from the experimental data. As discussed previously, the modes of interest were all the flexible bending and torsion modes below 15 Hz. Most of the parameter estimation effort was focused on identifying these modes. All flexible target modes were extracted successfully.

Test self-MAC calculations, along with visual inspection of the shapes, were used to verify the uniqueness of modes reported for each configuration. The MAC values presented were calculated using all of the test DOF.

A back-expansion matrix was used to fill in the unmeasured DOF at each test node to improve the ability to visualize the mode shapes. For example, an accelerometer measured DOF 1465X- and Y-, but not the accelerations in the corresponding Z direction. The back-expansion uses the TAM constraint matrix to interpolate these missing DOF for purposes of visualization only. The mode shapes presented in Appendix F include the back-expanded DOF. The MAC calculations did not use the back-expanded shapes.

## 4.1. V27 Turbine Modal Test Results

A single V27 turbine configuration was tested to obtain the modal and operational results: the V27 turbine bolted to the concrete foundation and rotor locked. All target modes of this configuration were identified. Impact hammer excitation was used during this testing, and all target modes of the SNL1 turbine were successfully extracted from impact hammer test run 7. The reduced instrumentation on SNL2 allowed a subset of the target modes to be identified from impact hammer test run 8. The test run number corresponds to the test run log presented in Table 3-1.

The list of modes, sorted by test mode shape frequency, is provided in Table 4-1. This table lists the shape description, test frequency, and damping for the two turbines tested. Additionally, the MAC between SNL1 and SNL2 is provided for each mode. As SNL2 had a significantly reduced instrumentation set, modes were compared to SNL1 using a combination of MAC, mode shape, and comparison of PSMIF using a common sensor set, as shown in Figure 4-1. Because the PSMIF is the summation of all FRF multiplied by each FRF conjugate, it is an ideal function to allow a global study of response. The PSMIF plotted in Figure 4-1 are summed for a common set of references and responses. Differences in the PSMIF between SNL1 and SNL2 are likely due to minor differences in construction and components of the turbine, as well as slight differences in rotor orientation. However, all but two modes are within a 5% difference. Mode shape plots for SNL1 are provided in Appendix F.

Table 4-1. SNL1 and SNL2 V27 turbine final global modes sorted by test frequency.

| | SNL1 | | SNL2 | | | | |
|---|---|---|---|---|---|---|---|
| Mode | Frequency (Hz) | Damping (% Crit.) | Frequency (Hz) | Damping (% Crit.) | Diff (%) | MAC | Description |
| 1 | 1.00 | 3.39 | 0.97 | 2.66 | 3% | 96 | 1st Tower Bending Edgewise |
| 2 | 1.01 | 3.82 | 0.99 | 2.95 | 2% | 83 | 1st Tower Bending Flapwise |
| 3 | 2.02 | 2.48 | 1.88 | 2.87 | 7% | 68 | 1st Blade Flapwise Bending - Asym |
| 4 | 2.04 | 2.51 | 2.00 | 2.36 | 2% | 50 | 1st Blade Flapwise Bending - Asym |
| 5 | 2.40 | 2.13 | 2.37 | 1.59 | 1% | 82 | 1st Blade Flapwise Bending - Sym |
| 6 | 3.65 | 1.45 | | | | | 1st Blade Edgewise Bending - Asym |
| 7 | 3.73 | 1.24 | 3.75 | 0.01 | 0% | 32 | 1st Blade Edgewise Bending - Asym |
| 8 | 5.33 | 1.35 | 5.05 | 1.96 | 5% | 76 | 2nd Blade Flapwise Bending - Asym |
| 9 | 5.36 | 1.46 | 5.34 | 1.26 | 0% | 68 | 2nd Blade Flapwise Bending - Asym |
| 10 | 6.67 | 1.20 | 6.70 | 0.98 | 0% | 88 | 2nd Blade Flapwise Bending - Sym |
| 11 | 7.83 | 1.38 | 7.76 | 1.18 | 1% | 90 | 2nd Tower Bending Flapwise |
| 12 | 7.97 | 1.19 | 7.99 | 1.52 | 0% | 85 | 2nd Tower Bending Edgewise |
| 13 | 8.43 | 1.32 | 8.34 | 0.80 | 1% | 89 | 1st Tower Torsion, 2nd Blade Edgewise Bending |
| 14 | 9.67 | 1.65 | 9.99 | 1.64 | -3% | 73 | 2nd Blade Edgewise Bending - Sym |
| 15 | 11.15 | 1.19 | 11.12 | 1.29 | 0% | 83 | 3rd Blade Flapwise Bending - Asym |
| 16 | 12.52 | 3.64 | | | | | 3rd Blade Flapwise Bending - Asym |
| 17 | 12.69 | 1.70 | 12.17 | 2.68 | 4% | 84 | 2nd Blade Edgewise Bending - Asym / 3rd Blade Flap - Asym |
| 18 | 13.45 | 1.06 | 13.22 | 1.11 | 2% | 71 | 2nd Blade Edgewise Bending - Asym |
| 19 | 13.66 | 1.08 | 13.82 | 1.98 | -1% | 66 | 2nd Blade Edgewise Bending - Asym / 3rd Blade Flap -Sym |
| 20 | 13.80 | 1.04 | | | | | 3rd Blade Flapwise Bending -Sym |

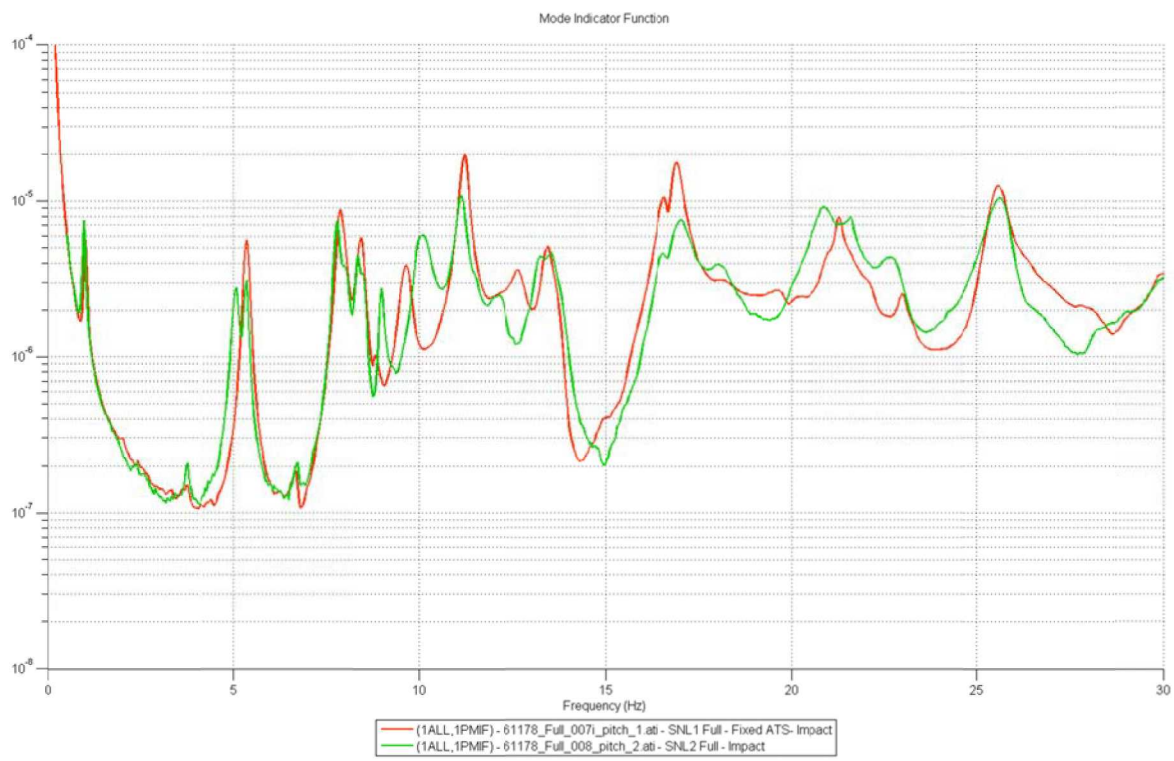


Figure 4-1. SNL1 and SNL2 PSMIF using common DOF set.

The self-MAC matrix for the V27 final modes is provided in Table 4-2 for the full set of instrumentation turbine (SNL1). Any significant off-diagonal terms observed in the self-MAC were verified to be independent through visualization of the mode shape.

Table 4-2. V27 final test modes (SNL1 at full instrumentation set): self-MAC.

| Test Self MAC Table | | | | | | | | | | | | | | |
|---|---|---|---|---|---|---|---|---|---|---|---|---|---|---|
| SNL1 EMA Test Shapes | | | | | | | | | | | | | | |
| | | | 1 | 2 | 3 | 4 | 5 | 6 | 7 | 8 | 9 | 10 | 11 | 12 |
| | | MACtt | 1.0 | 1.0 | 2.0 | 2.0 | 2.4 | 3.6 | 3.7 | 5.3 | 5.4 | 6.7 | 7.8 | 8.0 |
| SNL1 EMA Test Shape | 1 | 1.0 | 1.00 | 0.07 | | | 0.11 | | 0.13 | | | | | 0.12 |
| | 2 | 1.0 | 0.07 | 1.00 | | 0.07 | 0.24 | | | | | 0.06 | 0.10 | |
| | 3 | 2.0 | | | 1.00 | 0.27 | 0.07 | | 0.06 | | 0.44 | 0.07 | | 0.07 |
| | 4 | 2.0 | | 0.07 | 0.27 | 1.00 | | | | 0.31 | 0.40 | | 0.29 | 0.11 |
| | 5 | 2.4 | 0.11 | 0.24 | 0.07 | | 1.00 | | | | | 0.55 | 0.10 | |
| | 6 | 3.6 | | | | | | 1.00 | 0.14 | | | | 0.08 | |
| | 7 | 3.7 | 0.13 | | 0.06 | | | 0.14 | 1.00 | | | | | |
| | 8 | 5.3 | | | | 0.31 | | | | 1.00 | 0.05 | | 0.50 | 0.05 |
| | 9 | 5.4 | | | 0.44 | 0.40 | | | | 0.05 | 1.00 | | 0.27 | 0.16 |
| | 10 | 6.7 | | 0.06 | 0.07 | | 0.55 | | | | | 1.00 | 0.13 | |
| | 11 | 7.8 | | 0.10 | | 0.29 | 0.10 | 0.08 | | 0.50 | 0.27 | 0.13 | 1.00 | 0.16 |
| | 12 | 8.0 | 0.12 | | 0.07 | 0.11 | | | | 0.05 | 0.16 | | 0.16 | 1.00 |
| | 13 | 8.4 | | | 0.19 | | | | 0.06 | 0.30 | 0.17 | | | |
| | 14 | 9.7 | | | | | | | | | | | | 0.07 |
| | 15 | 11.1 | | 0.06 | 0.08 | 0.36 | | 0.09 | | 0.31 | 0.42 | | 0.62 | 0.19 |
| | 16 | 12.5 | | | 0.27 | | 0.07 | | | 0.06 | 0.37 | 0.13 | | |
| | 17 | 12.7 | | | 0.14 | | 0.09 | 0.07 | | 0.30 | 0.07 | 0.13 | 0.14 | |
| | 18 | 13.5 | | | | 0.09 | | 0.24 | 0.20 | 0.06 | 0.14 | | | |
| | 19 | 13.7 | | 0.13 | | | 0.22 | | | 0.05 | | 0.44 | 0.19 | |
| | 20 | 13.8 | | 0.11 | | | 0.27 | | | | | 0.54 | 0.13 | |

## 4.2. V27 Turbine Operational Modal Test Result

Operational modal analysis was performed on the SNL1 V27 turbine. Approximately two hours of natural wind excitation data were recorded in run 6, which was used for OMA. The CC-SSI algorithm in ARTeMIS was used to extract modes in the operational data. The stabilization diagram for the final set of OMA modes is shown in Figure 4-2.

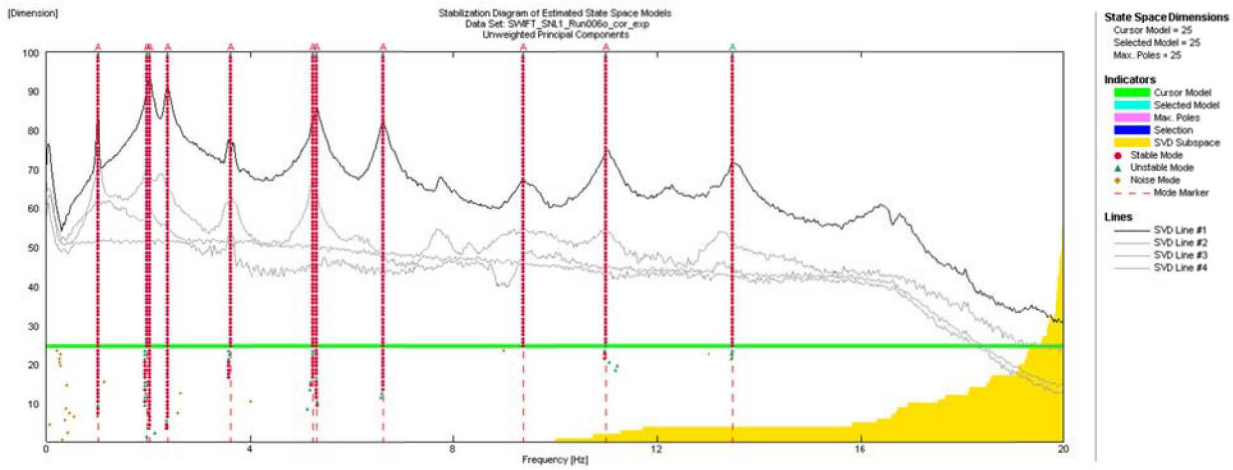


Figure 4-2. Stabilization diagram for operational model analysis.

The list of modes, sorted by test mode shape frequency, is provided in Table 4-3. This table lists the shape description, test frequency, and damping for SNL1, comparing the EMA results to OMA. Additionally, the MAC between EMA and OMA is provided for each mode. Modes were compared using a combination of MAC and visualization of the mode shape. Mode shape plots are provided in Appendix F.

Table 4-3. SNL1 turbine EMA and OMA final global modes sorted by test frequency.

| | SNL1 - EMA | | SNL1 - OMA | | | | |
|---|---|---|---|---|---|---|---|
| Mode | Frequency (Hz) | Damping (% Crit.) | Frequency (Hz) | Damping (% Crit.) | Diff (%) | MAC | Description |
| 1 | 1.00 | 3.39 | | | | | 1st Tower Bending Edgewise |
| 2 | 1.01 | 3.82 | 1.00 | 0.82 | 0% | 44 | 1st Tower Bending Flapwise |
| 3 | 2.02 | 2.48 | 1.98 | 2.24 | 2% | 63 | 1st Blade Flapwise Bending - Asym |
| 4 | 2.04 | 2.51 | 2.02 | 2.45 | 1% | 98 | 1st Blade Flapwise Bending - Asym |
| 5 | 2.40 | 2.13 | 2.37 | 1.77 | 1% | 100 | 1st Blade Flapwise Bending - Sym |
| 6 | 3.65 | 1.45 | | | | | 1st Blade Edgewise Bending - Asym |
| 7 | 3.73 | 1.24 | 3.61 | 0.95 | 3% | 42 | 1st Blade Edgewise Bending - Asym |
| 8 | 5.33 | 1.35 | 5.25 | 1.40 | 2% | 73 | 2nd Blade Flapwise Bending - Asym |
| 9 | 5.36 | 1.46 | 5.31 | 1.20 | 1% | 93 | 2nd Blade Flapwise Bending - Asym |
| 10 | 6.67 | 1.20 | 6.61 | 0.97 | 1% | 100 | 2nd Blade Flapwise Bending - Sym |
| 11 | 7.83 | 1.38 | | | | | 2nd Tower Bending Flapwise |
| 12 | 7.97 | 1.19 | | | | | 2nd Tower Bending Edgewise |
| 13 | 8.43 | 1.32 | | | | | 1st Tower Torsion, 2nd Blade Edgewise Bending |
| 14 | 9.67 | 1.65 | 9.37 | 2.07 | 3% | 94 | 2nd Blade Edgewise Bending - Sym |
| 15 | 11.15 | 1.19 | 11.00 | 1.31 | 1% | 99 | 3rd Blade Flapwise Bending - Asym |
| 16 | 12.52 | 3.64 | | | | | 3rd Blade Flapwise Bending - Asym |
| 17 | 12.69 | 1.70 | | | | | 2nd Blade Edgewise Bending - Asym / 3rd Blade Flap - Asym |
| 18 | 13.45 | 1.06 | | | | | 2nd Blade Edgewise Bending - Asym |
| 19 | 13.66 | 1.08 | | | | | 2nd Blade Edgewise Bending - Asym / 3rd Blade Flap -Sym |
| 20 | 13.80 | 1.04 | 13.49 | 1.32 | 1% | 92 | 3rd Blade Flapwise Bending -Sym |

The cross-MAC matrices for the V27 EMA to OMA modes are provided in Table 4-2. While some values of matched modes were fairly low, every mode pair was verified through comparison of the visualized mode shapes.

Table 4-4. V27 final test modes (SNL1 at full instrumentation set): self-orthogonality.

| | | | Test Cross MAC Table | | | | | | | | | | | |
|---|---|---|---|---|---|---|---|---|---|---|---|---|---|---|
| | | | SNL1 OMA Shapes | | | | | | | | | | | |
| | | | 1 | 2 | 3 | 4 | 5 | 6 | 7 | 8 | 9 | 10 | 11 | Test |
| | | MACtg | 1.0 | 2.0 | 2.0 | 2.4 | 3.6 | 5.2 | 5.3 | 6.6 | 9.4 | 11.0 | 13.5 | CRS |
| SNL1 EMA Shapes | 1 | 1.0 | 0.26 | | | | | | | | | | | 0.28 |
| | 2 | 1.0 | 0.44 | | | 0.23 | | | | | | | | 0.40 |
| | 3 | 2.0 | | 0.63 | 0.38 | | | 0.25 | 0.30 | | | | | 0.92 |
| | 4 | 2.0 | | | 0.98 | | | | 0.49 | | | 0.34 | | 0.97 |
| | 5 | 2.4 | 0.45 | | | 1.00 | | | | 0.53 | | | 0.27 | 0.98 |
| | 6 | 3.6 | | | | | 0.25 | | | | | | | 0.21 |
| | 7 | 3.7 | | | | | 0.42 | | | | | | | 0.32 |
| | 8 | 5.3 | | 0.30 | 0.24 | | | 0.73 | 0.22 | | | 0.26 | | 0.96 |
| | 9 | 5.4 | | | 0.45 | | | | 0.93 | | | 0.44 | | 0.98 |
| | 10 | 6.7 | | | | 0.55 | | | | 1.00 | | | 0.57 | 0.98 |
| | 11 | 7.8 | | | 0.26 | | | | 0.44 | | | 0.57 | | 0.66 |
| | 12 | 8.0 | | | | | | | | | | | | |
| | 13 | 8.4 | | 0.25 | | | | 0.54 | | | | | | 0.51 |
| | 14 | 9.7 | | | | | | | | | 0.94 | | | 0.86 |
| | 15 | 11.1 | | | 0.35 | | | | 0.55 | | | 0.99 | | 0.94 |
| | 16 | 12.5 | | | | | | 0.31 | 0.24 | | | 0.21 | | 0.45 |
| | 17 | 12.7 | | 0.22 | | | | 0.44 | | | | | 0.25 | 0.37 |
| | 18 | 13.5 | | | | | | | | | | | | |
| | 19 | 13.7 | | | | 0.21 | | | | 0.44 | | | 0.76 | 0.58 |
| | 20 | 13.8 | | | | 0.26 | | | | 0.54 | | | 0.92 | 0.79 |
| | FEM | CRS | 0.81 | 0.92 | 0.98 | 0.98 | 0.95 | 0.97 | 0.99 | 0.99 | 0.95 | 0.98 | 0.96 | |

## 5. CONCLUSIONS

A modal survey was successfully performed on two V27 turbines. A global modal survey for a single test configuration was conducted, and all primary flexible target modes were identified. ATA was responsible for test setup, data acquisition, data analysis, and instrumentation and hardware removal from the V27 turbines following the test. All phases of the test program were completed June 10–16, 2013.

Modal parameters were extracted from modal impact hammer and wind excitation runs, and the uniqueness of the final mode shapes was verified through visual inspection and the test self-MAC. The self-MAC demonstrated that the extracted flexible mode shapes were unique, and all target modes were clearly identified with shape visualization.

# Appendix A

## On-Site Test Log and Run Log

**61178 SWIFT Full Turbine Test Run Log**

| Run | Date | Start Time | Config† | Tower # | Exc. | File Name | Reference Channels | Freq Range (Hz) | Notes |
|---|---|---|---|---|---|---|---|---|---|
| **Day 1 - SNL 1** | | | | | | | | | |
| 1 | 6/10/2013 | 22:20 | pitch | 1 | o | 61178_Full_001o_pitch_1.ati | Chosen During Post-Processing | 0-30 | Checkout Run-Tower Only |
| 2 | 6/11/2013 | 10:19 | pitch | 1 | o | 61178_Full_002o_pitch_1.ati | Chosen During Post-Processing | 0-30 | Checkout Run - Tower and Blade 3 |
| 3 | 6/11/2013 | 10:50 | pitch | 1 | o | 61178_Full_003o_pitch_1.ati | Chosen During Post-Processing | 0-30 | Checkout Run - Tower and Blade 3 - Nacelle Orientation |
| **Day 2 - SNL 1** | | | | | | | | | |
| 4 | 6/12/2013 | 9:31 | pitch | 1 | o | 61178_Full_004o_pitch_1.ati | Chosen During Post-Processing | 0-30 | SNL1 Full |
| 5 | 6/12/2013 | 12:50 | pitch | 1 | o | 61178_Full_005o_pitch_1.ati | Chosen During Post-Processing | 0-30 | SNL1 Full |
| 6 | 6/12/2013 | 14:52 | pitch | 1 | o | 61178_Full_006o_pitch_1.ati | Chosen During Post-Processing | 0-30 | SNL1 Full - Fixed ATS |
| **Day 3 - SNL 1** | | | | | | | | | |
| 7 | 6/13/2013 | 7:13 | pitch | 1 | i | 61178_Full_007i_pitch_1.ati | 53517X-,53518Y+, 254503X+,40772Y+, | 0-30 | SNL1 Full - Fixed ATS- Impact |
| **Day 4 - SNL 2** | | | | | | | | | |
| 8 | 6/14/2013 | 6:22 | pitch | 2 | i | 61178_Full_008i_pitch_2.ati | 53517X-,53518Y+, 254503X+,40772Y+, | 0-30 | SNL2 Full - Impact |
| 9 | 6/14/2013 | 10:59 | pitch | 2 | o | 61178_Full_009o_pitch_2.ati | Chosen During Post-Processing | 0-30 | SNL2 Full - Operational |

| * EXCITATION TYPE | |
|---|---|
| i | modal impact |
| o | operational |

| + Config | |
|---|---|
| pitch | Pitched at 0 degrees, parked, facing east |

# Appendix B

## Nodes and Accelerometers Table

| Group Name | Node | X+ | Y+ | Z+ | Locations |
|---|---|---|---|---|---|
| Tower | 30018 | | Y- | | Base-6Clock |
| Tower | 30036 | X- | | | Base-9Clock |
| Tower | 30147 | | Y+ | | Base -12Clock |
| Tower | 33807 | | Y+ | | Platform1-12Clock |
| Tower | 37003 | X+ | | | 22Ft-3Clock |
| Tower | 37214 | X- | | | 22Ft-9Clock |
| Tower | 38067 | | Y+ | | 22Ft-12Clock |
| Tower | 40762 | | Y- | | Tip-12Clock |
| Tower | 40772 | X- | | | Tip-3Clock |
| Tower | 44049 | | Y+ | | 22Ft-6Clock |
| Tower | 75564 | X+ | | | Base-3Clock |
| Tower | 77061 | X- | | | Platform1-9Clock |
| Tower | 100589 | X+ | | | Platform2-3Clock |
| Tower | 101415 | X- | | | Platform2-9Clock |
| Tower | 115734 | | Y+ | | Platform2-12Clock |
| Tower | 146589 | X+ | | | Tip-9Clock |
| Tower | 200924 | X+ | | | Platform1-3Clock |
| Tower | 254503 | | Y+ | | Tip-6Clock |
| Tower | 271687 | | Y- | | Platform2-6Clock |
| Tower | 281849 | | Y- | | Platform1-6Clock |
| Blade 1 | 53502 | X- | Y+ | Z+ | B1-Trail-1(Tip) |
| Blade 1 | 53052 | X- | Y+ | | B1-Trail-3 |
| Blade 1 | 52208 | X- | Y+ | | B1-Trail-6 |
| Blade 1 | 51359 | X- | Y+ | | B1-Trail-9 |
| Blade 1 | 53537 | X- | | | B1-Lead-1(Tip) |
| Blade 1 | 53101 | X- | | | B1-Lead-3 |
| Blade 1 | 52290 | X- | | | B1-Lead-6 |
| Blade 1 | 51465 | X- | | | B1-Lead-9 |
| Blade 2 | 53527 | X- | Y+ | Z+ | B2-Trail-1(Tip) |
| Blade 2 | 53523 | X- | Y+ | | B2-Trail-3 |
| Blade 2 | 53517 | X- | Y+ | | B2-Trail-6 |
| Blade 2 | 53511 | X- | Y+ | | B2-Trail-9 |
| Blade 2 | 53528 | X- | | | B2-Lead-1(Tip) |
| Blade 2 | 53524 | X- | | | B2-Lead-3 |
| Blade 2 | 53518 | X- | | | B2-Lead-6 |
| Blade 2 | 53512 | X- | | | B2-Lead-9 |
| Blade 3 | 53580 | X- | Y+ | Z+ | B3-Trail-1(Tip) |
| Blade 3 | 53576 | X- | Y+ | | B3-Trail-3 |
| Blade 3 | 53570 | X- | Y+ | | B3-Trail-6 |
| Blade 3 | 53564 | X- | Y+ | | B3-Trail-9 |
| Blade 3 | 53581 | X- | | | B3-Lead-1(Tip) |
| Blade 3 | 53577 | X- | | | B3-Lead-3 |
| Blade 3 | 53571 | X- | | | B3-Lead-6 |
| Blade 3 | 53565 | X- | | | B3-Lead-9 |
| Tower | 400001 | | | Z+ | Found-12Clock |
| Tower | 400004 | | | Z+ | Found-3Clock |
| Tower | 400003 | X- | Y+ | Z+ | Found-6Clock |
| Tower | 400002 | | | Z+ | Found-9Clock |
| Nacelle | 120003 | X+ | Y- | Z+ | Nacelle Fwd Port |
| Nacelle | 120004 | X+ | Y- | Z+ | Nacelle Fwd Stbd |
| Nacelle | 120007 | X- | Y+ | Z+ | Nacelle Rear Port |
| Nacelle | 120008 | X- | Y+ | Z+ | Nacelle Rear Stbd |
| Hub | 130001 | X+ | Y+ | Z+ | Hub |

| # X Entries | #Y Entries | # Z Entries |
|---|---|---|
| 40 | 28 | 12 |
| | | |
| Total Number of Entries | | 80 |

# Appendix C

# Accelerometer Photos

The accelerometers shown are located on SNL1. SNL2 consisted of a subset of nodes and pictures are not shown for brevity. Due to time constraints, not all accelerometers were photographed.

Tower

| | |
|---|---|
| | |
| Node: 30018 Group: Tower Dir: Y- | Node: 30036 Group: Tower Dir: X- |
| | Missing |
| Node: 30147 Group: Tower Dir: Y+ | Node: 33807 Group: Tower Dir: Y+ |

| | |
|---|---|
| | Missing |
| Node: 37003 Group: Tower Dir: X+ | Node: 37214 Group: Tower Dir: X- |
| Missing | |
| Node: 38067 Group: Tower Dir: Y+ | Node: 40762 Group: Tower Dir: Y- |
| | Missing |
| Node: 40772 Group: Tower Dir: X- | Node: 44049 Group: Tower Dir: Y+ |

| | |
|---|---|
| 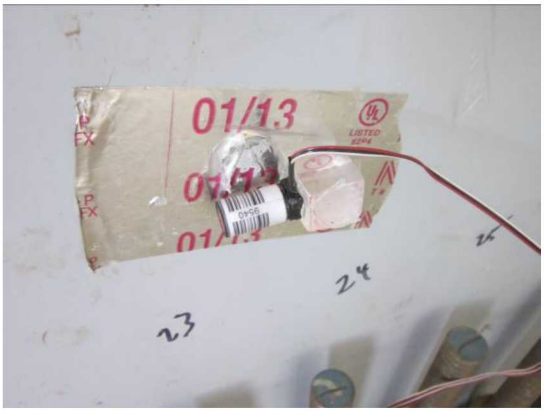 | Missing |
| Node: 75564 Group: Tower Dir: X+ | Node: 77061 Group: Tower Dir: X- |
| | Missing |
| Node: 100589 Group: Tower Dir: X+ | Node: 101415 Group: Tower Dir: X- |
| Missing | |
| Node: 115734 Group: Tower Dir: Y+ | Node: 146589 Group: Tower Dir: X+ |

| | |
|---|---|
| 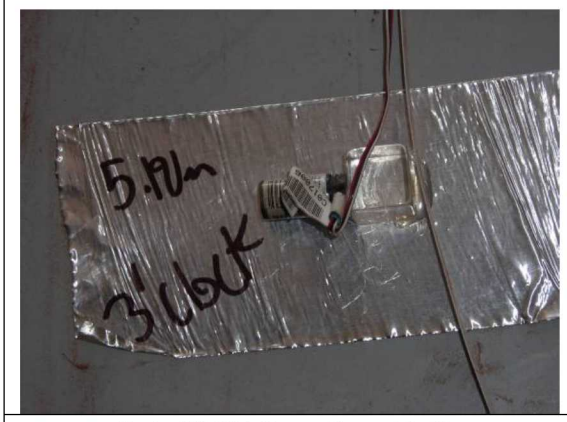 | |
| Node: 200924 Group: Tower Dir: X+ | Node: 254503 Group: Tower Dir: Y+ |
| Missing | |
| Node: 271687 Group: Tower Dir: Y- | Node: 281849 Group: Tower Dir: Y- |

Blade 1

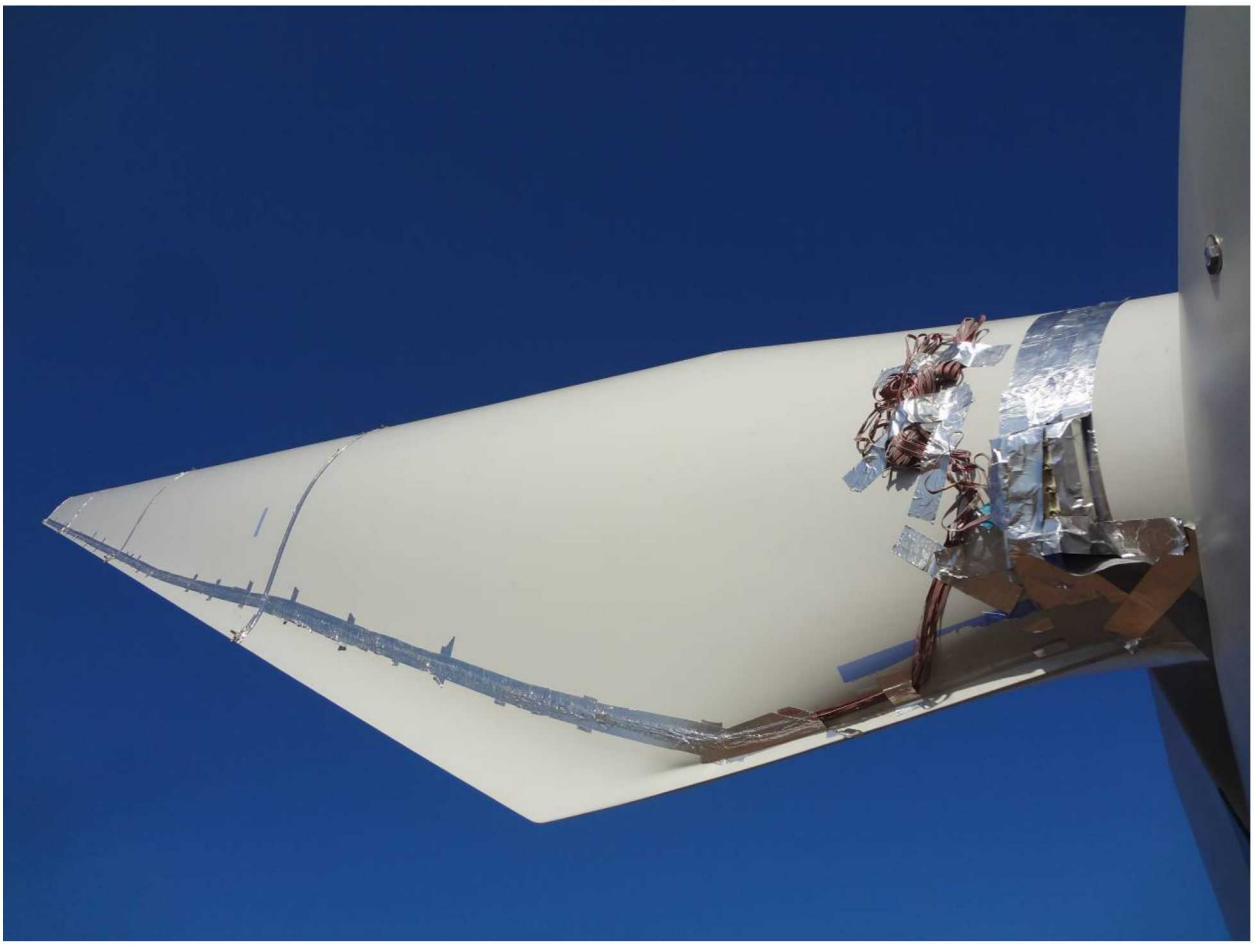

| | |
|---|---|
| | |
| Node: 53502 Group: Blade 1 Dir: X- Y+ Z+ | Node: 53052 Group: Blade 1 Dir: X- Y+ |

| | |
|---|---|
| | Missing |
| Node: 52208 Group: Blade 1 Dir: X- Y+ | Node: 51359 Group: Blade 1 Dir: X- Y+ |
| Missing | |
| Node: 53537 Group: Blade 1 Dir: X- | Node: 53101 Group: Blade 1 Dir: X- |
| | Missing |
| Node: 52290 Group: Blade 1 Dir: X- | Node: 51465 Group: Blade 1 Dir: X- |

Blade 2

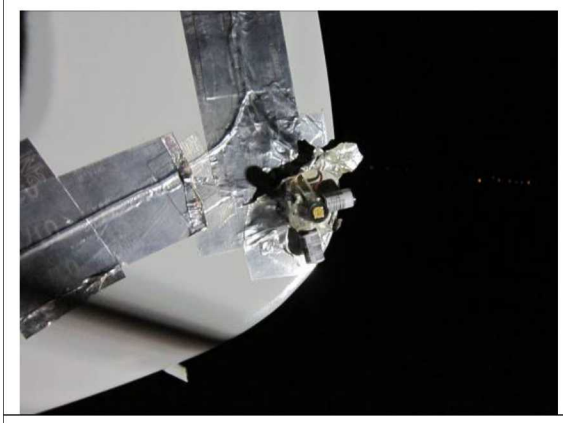

Node: 53527 Group: Blade 2 Dir: X- Y+ Z+

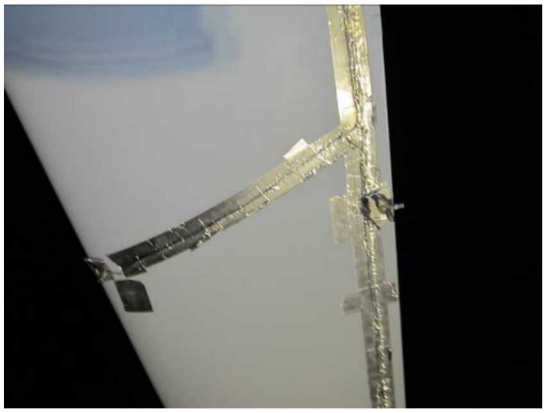

Node: 53523 Group: Blade 2 Dir: X- Y+

| | |
|---|---|
| | Missing |
| Node: 53517 Group: Blade 2 Dir: X- Y+ | Node: 53511 Group: Blade 2 Dir: X- Y+ |
| 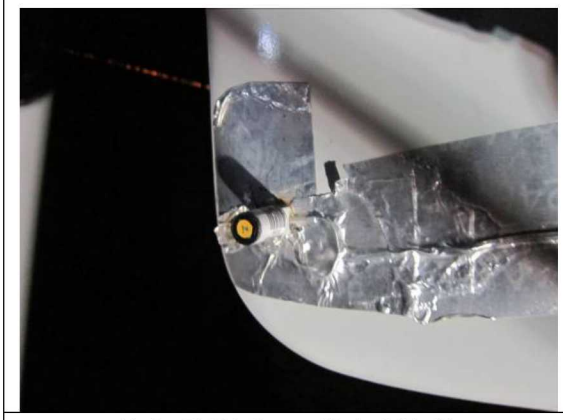 | 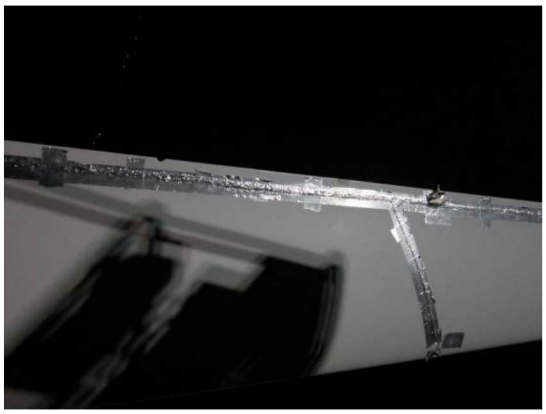 |
| Node: 53528 Group: Blade 2 Dir: X- | Node: 53524 Group: Blade 2 Dir: X- |
| | Missing |
| Node: 53518 Group: Blade 2 Dir: X- | Node: 53512 Group: Blade 2 Dir: X- |

# Blade 3

Node: 53580 Group: Blade 3 Dir: X- Y+ Z+

Node: 53576 Group: Blade 3 Dir: X- Y+

Node: 53570 Group: Blade 3 Dir: X- Y+

Node: 53564 Group: Blade 3 Dir: X- Y+

Node: 53581 Group: Blade 3 Dir: X-

Node: 53577 Group: Blade 3 Dir: X-

| | |
|---|---|
| | 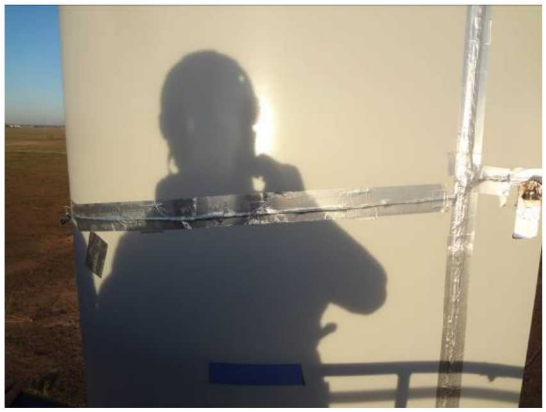 |
| Node: 53571 Group: Blade 3 Dir: X- | Node: 53565 Group: Blade 3 Dir: X- |

Tower Foundation

| | |
|---|---|
| Missing | Missing |
| Node: 400001 Group: Tower Dir: Z+ | Node: 400004 Group: Tower Dir: Z+ |
| | Missing |
| Node: 400003 Group: Tower Dir: X- Y+ Z+ | Node: 400002 Group: Tower Dir: Z+ |

## Nacelle

| | |
|---|---|
| | |
| Node: 120003 Group: Nacelle Dir: X+ Y- Z+ | Node: 120004 Group: Nacelle Dir: X+ Y- Z+ |
| | 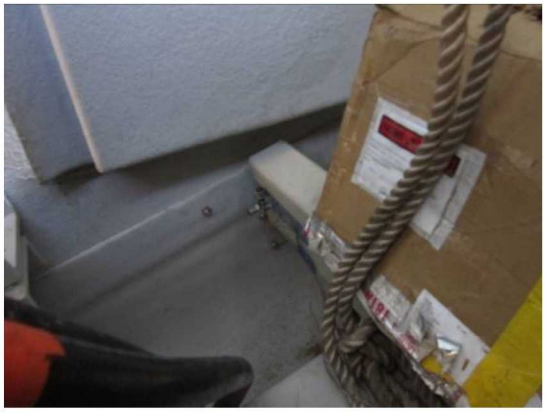 |
| Node: 120007 Group: Nacelle Dir: X- Y+ Z+ | Node: 120008 Group: Nacelle Dir: X- Y+ Z+ |

Hub

Missing

Node: 130001 Group: Hub Dir: X+ Y+ Z+

# Appendix D

## Impact Hammer Location Photos

All impact locations shown are for SNL1. The same impact locations were used for SNL2 but are not shown. In addition, not all of the impact locations were photographed due to time constraints.

Hammer Location - 40772Y+

Hammer Location - 254503X+

Hammer Location - 53571Y +

Hammer Location - 53570X +

Hammer Location - 52208X+

Hammer Location - 52290Y+

Hammer Location - 53527X-

# Appendix E

# Modal Test Channel Table

Channels with the calibration due date highlighted in red are accelerometers whose calibration had expired by the time testing occurred due to the delay in the test schedule; these accelerometers were calibrated post test to verify the change in sensitivity.

## SNL1 Channel Table

| CH | SN | Node | DIR | Data Type | EU | Cal mV/EU | Channel Description | Cal Due Date | Cal mV/EU | Cal Due Data | Cal Difference (%) |
|---|---|---|---|---|---|---|---|---|---|---|---|
| 1 | 9404 | 120003 | X+ | 12 | 11 | 92.5641 | Nacelle Fwd Port | 11-Mar-14 | 93.312 | 02-Jul-14 | 0.80% |
| 2 | 9474 | 120003 | Z+ | 12 | 11 | 103.5122 | Nacelle Fwd Port | 11-Mar-14 | 103.8189 | 02-Jul-14 | 0.30% |
| 4 | 28935 | 120004 | Z+ | 12 | 11 | 83.9087 | Nacelle Fwd Stbd | 11-Mar-14 | 83.7327 | 02-Jul-14 | -0.21% |
| 5 | 31738 | 120004 | X+ | 12 | 11 | 91.0143 | Nacelle Fwd Stbd | 11-Mar-14 | 91.7879 | 02-Jul-14 | 0.85% |
| 6 | 9400 | 120004 | Y- | 12 | 11 | 101.4538 | Nacelle Fwd Stbd | 11-Mar-14 | 101.4385 | 02-Jul-14 | -0.02% |
| 7 | 9199 | 120008 | Z+ | 12 | 11 | 98.5099 | Nacelle Rear Stbd | 11-Mar-14 | 98.7142 | 02-Jul-14 | 0.21% |
| 8 | 9539 | 120008 | Y+ | 12 | 11 | 102.7979 | Nacelle Rear Stbd | 11-Mar-14 | 102.7655 | 02-Jul-14 | -0.03% |
| 9 | 40625 | 120008 | X- | 12 | 11 | 87.2808 | Nacelle Rear Stbd | 11-Mar-14 | 86.9669 | 02-Jul-14 | -0.36% |
| 10 | 9544 | 120007 | Z+ | 12 | 11 | 109.6148 | Nacelle Rear Port | 11-Mar-14 | 109.5254 | 02-Jul-14 | -0.08% |
| 11 | 33000 | 120007 | Y+ | 12 | 11 | 86.4976 | Nacelle Rear Port | 11-Mar-14 | 86.1469 | 02-Jul-14 | -0.41% |
| 12 | 9725 | 120007 | X- | 12 | 11 | 95.2249 | Nacelle Rear Port | 11-Mar-14 | 93.7956 | 02-Jul-14 | -1.51% |
| 13 | 9550 | 120003 | Y- | 12 | 11 | 99.7771 | Nacelle Fwd Port | 11-Mar-14 | 99.6785 | 02-Jul-14 | -0.10% |
| 17 | 9698 | 254503 | Y+ | 12 | 11 | 80.2236 | Tip-6Clock | 11-Mar-14 | 80.1898 | 02-Jul-14 | -0.04% |
| 18 | 32132 | 40772 | X- | 12 | 11 | 86.9648 | Tip-3Clock | 11-Mar-14 | 86.6188 | 02-Jul-14 | -0.40% |
| 19 | 10283 | 40762 | Y- | 12 | 11 | 82.8392 | Tip-12Clock | 11-Mar-14 | 82.6561 | 02-Jul-14 | -0.22% |
| 20 | 28936 | 146589 | X+ | 12 | 11 | 92.2927 | Tip-9Clock | 11-Mar-14 | 92.5145 | 02-Jul-14 | 0.24% |
| 21 | 28915 | 38067 | Y+ | 12 | 11 | 90.892 | 22Ft-12Clock | 05-Apr-13 | 90.4587 | 02-Jul-14 | -0.48% |
| 22 | 9712 | 37214 | X- | 12 | 11 | 98.8333 | 22Ft-9Clock | 05-Apr-13 | 98.0181 | 02-Jul-14 | -0.83% |
| 23 | 9707 | 44049 | Y+ | 12 | 11 | 95.3371 | 22Ft-6Clock | 11-Mar-14 | 95.6783 | 02-Jul-14 | 0.36% |
| 24 | 10339 | 37003 | X+ | 12 | 11 | 93.555 | 22Ft-3Clock | 05-Apr-13 | 92.6879 | 02-Jul-14 | -0.93% |
| 25 | 32977 | 130001 | Z+ | 12 | 11 | 85.5774 | Hub | 11-Mar-14 | 86.1093 | 02-Jul-14 | 0.62% |
| 26 | 9198 | 130001 | X+ | 12 | 11 | 90.7648 | Hub | 11-Mar-14 | 89.3579 | 02-Jul-14 | -1.56% |
| 27 | 9391 | 130001 | Y+ | 12 | 11 | 106.3255 | Hub | 11-Mar-14 | 104.5697 | 02-Jul-14 | -1.67% |
| 33 | 9424 | 52290 | X- | 12 | 11 | 97.5336 | B1-Lead-6 | 17-Aug-13 | 97.6056 | 02-Jul-14 | 0.07% |
| 34 | 10322 | 52208 | Y+ | 12 | 11 | 80.0196 | B1-Trail-6 | 17-Aug-13 | 80.1374 | 02-Jul-14 | 0.15% |
| 35 | 9715 | 52208 | X- | 12 | 11 | 98.4429 | B1-Trail-6 | 17-Aug-13 | 98.2345 | 02-Jul-14 | -0.21% |
| 36 | 26725 | 53502 | Z+ | 12 | 11 | 85.6211 | B1-Trail-1(Tip) | 17-Aug-13 | 86.4841 | 02-Jul-14 | 1.00% |
| 37 | 9212 | 53502 | Y+ | 12 | 11 | 96.3224 | B1-Trail-1(Tip) | 17-Aug-13 | 96.9419 | 02-Jul-14 | 0.64% |
| 38 | 20663 | 53502 | X- | 12 | 11 | 90.8111 | B1-Trail-1(Tip) | 17-Aug-13 | 91.2451 | 02-Jul-14 | 0.48% |
| 39 | 27440 | 51465 | X- | 12 | 11 | 85.8724 | B1-Lead-9 | 17-Aug-13 | 86.3842 | 02-Jul-14 | 0.59% |
| 40 | 28966 | 51359 | X- | 12 | 11 | 93.9675 | B1-Trail-9 | 17-Aug-13 | 94.5122 | 02-Jul-14 | 0.58% |
| 41 | 10334 | 51359 | Y+ | 12 | 11 | 97.9161 | B1-Trail-9 | 17-Aug-13 | 97.3391 | 02-Jul-14 | -0.59% |
| 42 | 9385 | 53052 | Y+ | 12 | 11 | 100.0472 | B1-Trail-3 | 17-Aug-13 | 100.5384 | 02-Jul-14 | 0.49% |
| 43 | 9660 | 53052 | X- | 12 | 11 | 108.1925 | B1-Trail-3 | 17-Aug-13 | 108.7976 | 02-Jul-14 | 0.56% |
| 44 | 10292 | 53101 | X- | 12 | 11 | 108.8477 | B1-Lead-3 | 17-Aug-13 | 108.9221 | 02-Jul-14 | 0.07% |
| 45 | 9654 | 53537 | X- | 12 | 11 | 102.3447 | B1-Lead-1(Tip) | 17-Aug-13 | 102.6406 | 02-Jul-14 | 0.29% |
| 49 | 9502 | 53580 | Z+ | 12 | 11 | 93.0965 | B3-Trail-1(Tip) | 19-Feb-14 | 93.2148 | 02-Jul-14 | 0.13% |
| 50 | 51313 | 53580 | X- | 12 | 11 | 96.9 | B3-Trail-1(Tip) | 23-Jan-14 | 95.5764 | 02-Jul-14 | -1.38% |
| 51 | 32996 | 53580 | Y+ | 12 | 11 | 82.4021 | B3-Trail-1(Tip) | 19-Feb-14 | 82.0684 | 02-Jul-14 | -0.41% |
| 53 | 40608 | 53570 | X- | 12 | 11 | 85.1676 | B3-Trail-6 | 17-Aug-13 | 85.4554 | 02-Jul-14 | 0.34% |

# SNL1 Channel Table (Continued)

| CH | SN | Node | DIR | Data Type | EU | Cal mV/EU | Channel Description | Cal Due Date | Cal mV/EU | Cal Due Data | Cal Difference (%) |
|---|---|---|---|---|---|---|---|---|---|---|---|
| 54 | 32126 | 53570 | Y+ | 12 | 11 | 86.8008 | B3-Trail-6 | 17-Aug-13 | 87.6591 | 02-Jul-14 | 0.98% |
| 55 | 9713 | 53564 | X- | 12 | 11 | 97.7486 | B3-Trail-9 | 17-Aug-13 | 98.0196 | 02-Jul-14 | 0.28% |
| 56 | 28961 | 53564 | Y+ | 12 | 11 | 89.368 | B3-Trail-9 | 17-Aug-13 | 90.0076 | 02-Jul-14 | 0.71% |
| 57 | 9382 | 53565 | X- | 12 | 11 | 88.8745 | B3-Lead-9 | 17-Aug-13 | 89.0346 | 02-Jul-14 | 0.18% |
| 59 | 9500 | 53576 | Y+ | 12 | 11 | 93.1801 | B3-Trail-3 | 17-Aug-13 | 92.3453 | 02-Jul-14 | -0.90% |
| 60 | 9645 | 53576 | X- | 12 | 11 | 100.7877 | B3-Trail-3 | 17-Aug-13 | 101.9524 | 02-Jul-14 | 1.15% |
| 61 | 10326 | 53577 | X- | 12 | 11 | 111.3768 | B3-Lead-3 | 17-Aug-13 | 111.3494 | 02-Jul-14 | -0.02% |
| 65 | 9554 | 53517 | X- | 12 | 11 | 85.1508 | B2-Trail-6 | 17-Aug-13 | 85.2857 | 02-Jul-14 | 0.16% |
| 66 | 9689 | 53518 | X- | 12 | 11 | 85.3983 | B2-Lead-6 | 17-Aug-13 | 85.0062 | 02-Jul-14 | -0.46% |
| 67 | 9509 | 53517 | Y+ | 12 | 11 | 110.356 | B2-Trail-6 | 17-Aug-13 | 110.2212 | 02-Jul-14 | -0.12% |
| 68 | 28933 | 53512 | X- | 12 | 11 | 89.6398 | B2-Lead-9 | 17-Aug-13 | 89.7219 | 02-Jul-14 | 0.09% |
| 69 | 32990 | 53511 | X- | 12 | 11 | 94.8144 | B2-Trail-9 | 17-Aug-13 | 94.8144 | 17-Aug-13 | 0.00% |
| 70 | 9451 | 53511 | Y+ | 12 | 11 | 98.4928 | B2-Trail-9 | 17-Aug-13 | 98.8939 | 02-Jul-14 | 0.41% |
| 71 | 10298 | 53528 | X- | 12 | 11 | 86.3401 | B2-Lead-1(Tip) | 17-Aug-13 | 86.6556 | 02-Jul-14 | 0.36% |
| 72 | 9593 | 53524 | X- | 12 | 11 | 96.2132 | B2-Lead-3 | 17-Aug-13 | 97.1602 | 02-Jul-14 | 0.98% |
| 73 | 9735 | 53523 | X- | 12 | 11 | 111.4605 | B2-Trail-3 | 17-Aug-13 | 112.0681 | 02-Jul-14 | 0.54% |
| 74 | 9410 | 53523 | Y+ | 12 | 11 | 101.5418 | B2-Trail-3 | 17-Aug-13 | 102.1072 | 02-Jul-14 | 0.56% |
| 75 | 9658 | 53527 | Z+ | 12 | 11 | 83.4838 | B2-Trail-1(Tip) | 17-Aug-13 | 83.8357 | 02-Jul-14 | 0.42% |
| 76 | 9630 | 53527 | Y+ | 12 | 11 | 90.8782 | B2-Trail-1(Tip) | 17-Aug-13 | 90.8249 | 02-Jul-14 | -0.06% |
| 77 | 9687 | 53527 | X- | 12 | 11 | 80.239 | B2-Trail-1(Tip) | 17-Aug-13 | 79.9969 | 02-Jul-14 | -0.30% |
| 78 | H21234SS | 53517 | X+ | 13 | 7 | 0.968 | B2-Trail-6 | 26-Jan-14 | 0.968 | 26-Jan-14 | 0.00% |
| 81 | 26738 | 75564 | x+ | 12 | 11 | 85.022 | Base-3Clock | 11-Mar-14 | 84.9971 | 02-Jul-14 | -0.03% |
| 82 | 36860 | 30036 | x- | 12 | 11 | 88.0891 | Base-9Clock | 11-Mar-14 | 88.272 | 02-Jul-14 | 0.21% |
| 83 | 9601 | 30147 | y+ | 12 | 11 | 96.5654 | Base -12Clock | 11-Mar-14 | 96.692 | 02-Jul-14 | 0.13% |
| 84 | 9494 | 30018 | Y- | 12 | 11 | 102.3094 | Base-6Clock | 11-Mar-14 | 102.2488 | 02-Jul-14 | -0.06% |
| 85 | 40621 | 200924 | X+ | 12 | 11 | 86.1792 | Platform1-3Clock | 05-Apr-13 | 85.3712 | 02-Jul-14 | -0.94% |
| 86 | 9383 | 33807 | Y+ | 12 | 11 | 105.9951 | Platform1-12Clock | 05-Apr-13 | 105.2722 | 02-Jul-14 | -0.68% |
| 87 | 9479 | 281849 | Y- | 12 | 11 | 103.1655 | Platform1-6Clock | 05-Apr-13 | 102.0558 | 02-Jul-14 | -1.08% |
| 88 | 32981 | 77061 | X- | 12 | 11 | 82.6019 | Platform1-9Clock | 05-Apr-13 | 82.5109 | 02-Jul-14 | -0.11% |
| 89 | 10294 | 100589 | X+ | 12 | 11 | 83.2345 | Platform2-3Clock | 05-Apr-13 | 82.0825 | 02-Jul-14 | -1.39% |
| 90 | 9629 | 271687 | Y- | 12 | 11 | 105.1793 | Platform2-6Clock | 05-Apr-13 | 104.0629 | 02-Jul-14 | -1.07% |
| 91 | 9436 | 115734 | Y+ | 12 | 11 | 95.0544 | Platform2-12Clock | 05-Apr-13 | 94.4506 | 02-Jul-14 | -0.64% |
| 92 | 9403 | 101415 | X- | 12 | 11 | 102.8616 | Platform2-9Clock | 05-Apr-13 | 101.765 | 02-Jul-14 | -1.07% |
| 97 | 36796A | 400001 | Z+ | 12 | 11 | 1001 | Found-12Clock | 11-Dec-13 | 1001 | 11-Dec-13 | 0.00% |
| 98 | 36919 | 400002 | Z+ | 12 | 11 | 1019 | Found-9Clock | 11-Dec-13 | 1019 | 11-Dec-13 | 0.00% |
| 99 | 36795A | 400003 | X- | 12 | 11 | 1005 | Found-6Clock | 11-Dec-13 | 1005 | 11-Dec-13 | 0.00% |
| 100 | 36782 | 400003 | Y+ | 12 | 11 | 1005 | Found-6Clock | 11-Dec-13 | 1005 | 11-Dec-13 | 0.00% |
| 101 | 36783 | 400003 | Z+ | 12 | 11 | 987 | Found-6Clock | 11-Dec-13 | 987 | 11-Dec-13 | 0.00% |
| 102 | 36908 | 400004 | Z+ | 12 | 11 | 1006 | Found-3Clock | 11-Dec-13 | 1006 | 11-Dec-13 | 0.00% |

# SNL2 Channel Table

| CH | SN | Node | DIR | Data Type | EU | Cal mV/EU | Channel Description | Cal Due Date | Cal mV/EU | Cal Due Data | Cal Difference (%) |
|---|---|---|---|---|---|---|---|---|---|---|---|
| 1 | 20662 | 101415 | X- | 12 | 11 | 90.4674 | Platform2-9 | 05-Apr-13 | 90.1026 | 02-Jul-14 | 0.40% |
| 2 | 9223 | 200924 | X- | 12 | 11 | 89.8244 | Platform1-1 | 05-Apr-13 | 89.0494 | 02-Jul-14 | 0.87% |
| 3 | 32938 | 115734 | Y+ | 12 | 11 | 93.4313 | Platform2-1 | 05-Apr-13 | 93.1916 | 02-Jul-14 | 0.26% |
| 4 | 32124 | 100589 | X+ | 12 | 11 | 86.4926 | Platform2-1 | 05-Apr-13 | 86.109 | 02-Jul-14 | 0.44% |
| 5 | 31843 | 33807 | Y+ | 12 | 11 | 93.07 | Platform1-1 | 05-Apr-13 | 93.1891 | 02-Jul-14 | -0.13% |
| 6 | 9133 | 77061 | X- | 12 | 11 | 83.4079 | Platform1-9 | 05-Apr-13 | 81.494 | 02-Jul-14 | 2.32% |
| 7 | 9429* | 281849 | Y- | 12 | 11 | 104.4135 | Platform1-6 | 05-Apr-13 | 104.4135 | 05-Apr-13 | 0.00% |
| 8 | 9443 | 271687 | Y- | 12 | 11 | 90.0314 | Platform2-6 | 11-Mar-14 | 88.9742 | 02-Jul-14 | 1.18% |
| 9 | 9749 | 30147 | Y+ | 12 | 11 | 96.1607 | Base -12Clo | 05-Apr-13 | 95.1542 | 02-Jul-14 | 1.05% |
| 10 | 9540 | 75564 | X+ | 12 | 11 | 95.2859 | Base-3Cloc | 05-Apr-13 | 93.7499 | 02-Jul-14 | 1.63% |
| 11 | 9476 | 30018 | Y- | 12 | 11 | 93.9078 | Base-6Cloc | 05-Apr-13 | 91.2129 | 02-Jul-14 | 2.91% |
| 12 | 9441 | 30036 | X- | 12 | 11 | 100.507 | Base-9Cloc | 05-Apr-13 | 99.7337 | 02-Jul-14 | 0.77% |
| 17 | 20653 | 146589 | X- | 12 | 11 | 83.012 | Tip-9Clock | 22-May-14 | 83.4691 | 02-Jul-14 | -0.55% |
| 18 | 9697 | 254503 | Y- | 12 | 11 | 90.1052 | Tip-6Clock | 22-May-14 | 90.3954 | 02-Jul-14 | -0.32% |
| 19 | 27441 | 40772 | X+ | 12 | 11 | 87.7906 | Tip-3Clock | 22-May-14 | 88.3991 | 02-Jul-14 | -0.69% |
| 20 | 28951 | 40762 | Y+ | 12 | 11 | 91.7495 | Tip-12Clock | 22-May-14 | 92.274 | 02-Jul-14 | -0.57% |
| 21 | 28962 | 38067 | Y+ | 12 | 11 | 90.9492 | 22Ft-12Cloc | 05-Apr-13 | 90.6833 | 02-Jul-14 | 0.29% |
| 22 | 20645 | 44049 | Y- | 12 | 11 | 87.7401 | 22Ft-6Clock | 22-May-14 | 87.2311 | 02-Jul-14 | 0.58% |
| 23 | 10328 | 37003 | X+ | 12 | 11 | 98.5028 | 22Ft-3Clock | 22-May-14 | 99.3399 | 02-Jul-14 | -0.85% |
| 24 | 9204 | 37214 | X- | 12 | 11 | 95.0249 | 22Ft-9Clock | 05-Apr-13 | 91.6084 | 02-Jul-14 | 3.66% |
| 25 | 26737 | 130001 | X+ | 12 | 11 | 87.9272 | Hub | 22-May-14 | 91.4395 | 02-Jul-14 | -3.92% |
| 26 | 26755 | 130001 | Y+ | 12 | 11 | 81.6396 | Hub | 22-May-14 | 82.098 | 02-Jul-14 | -0.56% |
| 27 | 28982 | 130001 | Z+ | 12 | 11 | 89.6069 | Hub | 22-May-14 | 90.3467 | 02-Jul-14 | -0.82% |
| 33 | 9428 | 120003 | Y- | 12 | 11 | 98.6329 | Nacelle Fw | 22-May-14 | 98.7104 | 02-Jul-14 | -0.08% |
| 34 | 32906 | 120003 | X+ | 12 | 11 | 89.4542 | Nacelle Fw | 22-May-14 | 90.037 | 02-Jul-14 | -0.65% |
| 35 | 32954 | 120003 | Z+ | 12 | 11 | 89.8832 | Nacelle Fw | 22-May-14 | 90.4687 | 02-Jul-14 | -0.65% |
| 36 | 27281 | 120004 | Z+ | 12 | 11 | 91.4956 | Nacelle Fw | 22-May-14 | 91.9866 | 02-Jul-14 | -0.54% |
| 37 | 32953 | 120004 | X+ | 12 | 11 | 90.6442 | Nacelle Fw | 22-May-14 | 90.3667 | 02-Jul-14 | 0.31% |
| 38 | 32923 | 120004 | Y- | 12 | 11 | 87.0084 | Nacelle Fw | 22-May-14 | 87.7216 | 02-Jul-14 | -0.82% |
| 39 | 9604 | 120007 | X- | 12 | 11 | 102.5048 | Nacelle Re | 22-May-14 | 102.4261 | 02-Jul-14 | 0.08% |
| 40 | 33013 | 120007 | Z+ | 12 | 11 | 86.4967 | Nacelle Re | 22-May-14 | 86.1979 | 02-Jul-14 | 0.35% |
| 41 | 26788 | 120007 | Y+ | 12 | 11 | 87.957 | Nacelle Re | 22-May-14 | 87.8589 | 02-Jul-14 | 0.11% |
| 42 | 9661 | 120008 | X- | 12 | 11 | 100.0978 | Nacelle Re | 22-May-14 | 100.052 | 02-Jul-14 | 0.05% |
| 43 | 32978 | 120008 | Y+ | 12 | 11 | 84.2131 | Nacelle Re | 22-May-14 | 84.0927 | 02-Jul-14 | 0.14% |
| 44 | 26794 | 120008 | Z+ | 12 | 11 | 85.3962 | Nacelle Re | 22-May-14 | 86.6612 | 02-Jul-14 | -1.47% |
| 49 | 36796A | 400001 | Z+ | 12 | 11 | 1001 | Found-12Cl | 11-Dec-13 | 1001 | 11-Dec-13 | 0.00% |
| 50 | 36919 | 400002 | Z+ | 12 | 11 | 1019 | Found-9Clo | 11-Dec-13 | 1019 | 11-Dec-13 | 0.00% |
| 51 | 36795A | 400003 | X- | 12 | 11 | 1005 | Found-6Clo | 11-Dec-13 | 1005 | 11-Dec-13 | 0.00% |
| 52 | 36782 | 400003 | Y+ | 12 | 11 | 1005 | Found-6Clo | 11-Dec-13 | 1005 | 11-Dec-13 | 0.00% |
| 53 | 36783 | 400003 | Z+ | 12 | 11 | 987 | Found-6Clo | 11-Dec-13 | 987 | 11-Dec-13 | 0.00% |
| 54 | 36908 | 400004 | Z+ | 12 | 11 | 1006 | Found-3Clo | 11-Dec-13 | 1006 | 11-Dec-13 | 0.00% |
| 65 | H21234SS | 53504 | X- | 13 | 7 | 0.968 | Hammer | 26-Jan-14 | 0.968 | 26-Jan-14 | 0.00% |
| 66 | 10292 | 53504 | X- | 12 | 11 | 108.8477 | B3 - Max Ch | 17-Aug-13 | 108.9221 | 02-Jul-14 | -0.07% |
| 67 | 9424 | 53504 | Y+ | 12 | 11 | 97.5336 | B3 - Max Ch | 17-Aug-13 | 97.6056 | 02-Jul-14 | -0.07% |
| 69 | 9715 | 53557 | X- | 12 | 11 | 98.4429 | B2 - Max Ch | 17-Aug-13 | 98.2345 | 02-Jul-14 | 0.21% |
| 71 | 10322 | 53557 | Y+ | 12 | 11 | 80.0196 | B2 - Max Ch | 17-Aug-13 | 80.1374 | 02-Jul-14 | -0.15% |
| 72 | 9654 | 50095 | Y+ | 12 | 11 | 102.3447 | B1 - Max Ch | 17-Aug-13 | 102.6406 | 02-Jul-14 | -0.29% |
| 73 | 20663 | 50095 | X- | 12 | 11 | 90.8111 | B1 - Max Ch | 17-Aug-13 | 91.2451 | 02-Jul-14 | -0.48% |

* SN 9429 taken out of service due to bad pin connection

# Appendix F

# Test Mode Shapes

# Experimental Modal Analysis Shapes
# SNL1 – Run 7

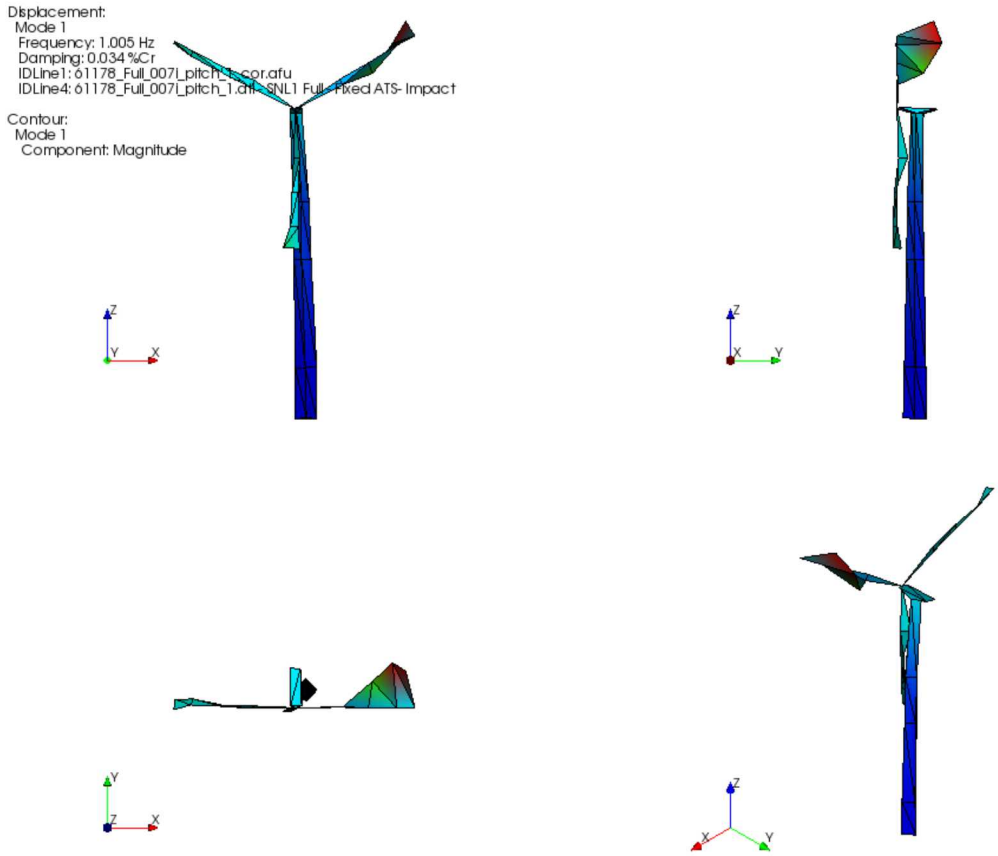

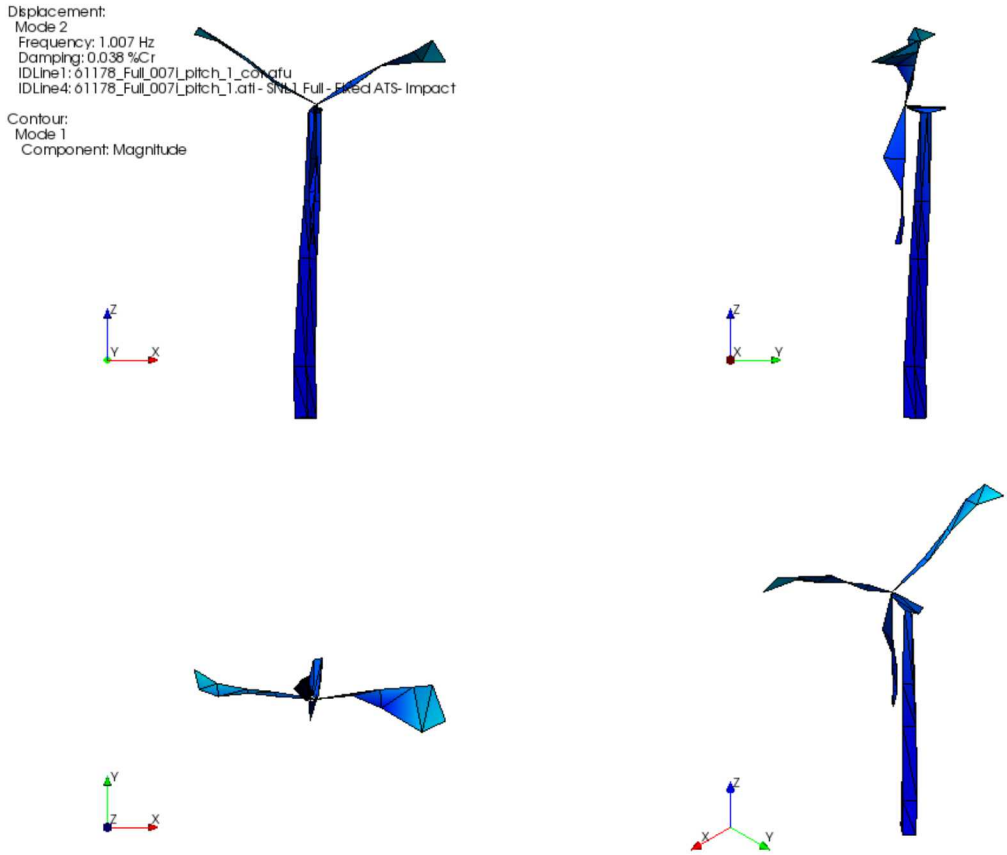
Displacement:
Mode 2
Frequency: 1.007 Hz
Damping: 0.038 %Cr
IDLine1: 61178_Full_007I_pitch_1_cor.qfu
IDLine4: 61178_Full_007I_pitch_1.atl - SNL1_Full - Fixed ATS- Impact
Contour:
Mode 1
Component: Magnitude

Displacement:
Mode 3
Frequency: 2.017 Hz
Damping: 0.025 %Cr
IDLine1: 61178_Full_007I_pitch_1_sor.afu
IDLine4: 61178_Full_007I_pitch_1.afl - SNL1 Full - Fixed ATS- Impact
Contour:
Mode 1
Component: Magnitude

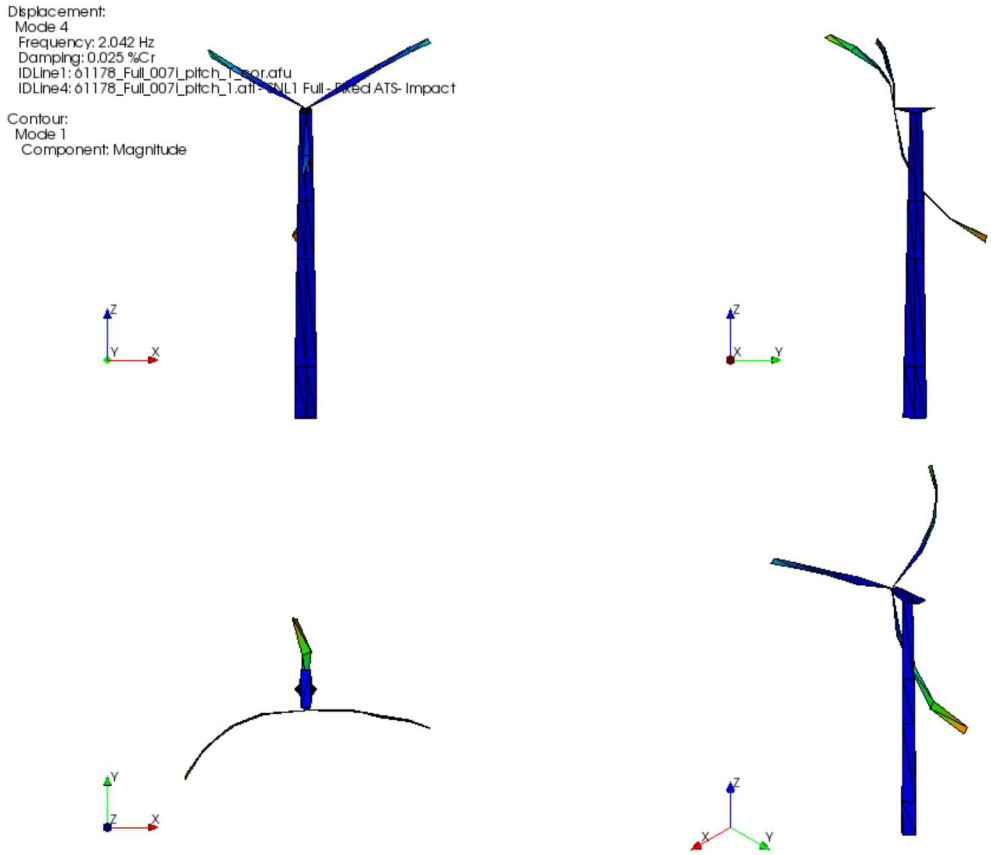
Displacement:
Mode 4
Frequency: 2.042 Hz
Damping: 0.025 %Cr
IDLine1: 61178_Full_007I_pitch_1_cor.afu
IDLine4: 61178_Full_007I_pitch_1.afl - SNL1 Full - Fixed ATS- Impact
Contour:
Mode 1
Component: Magnitude

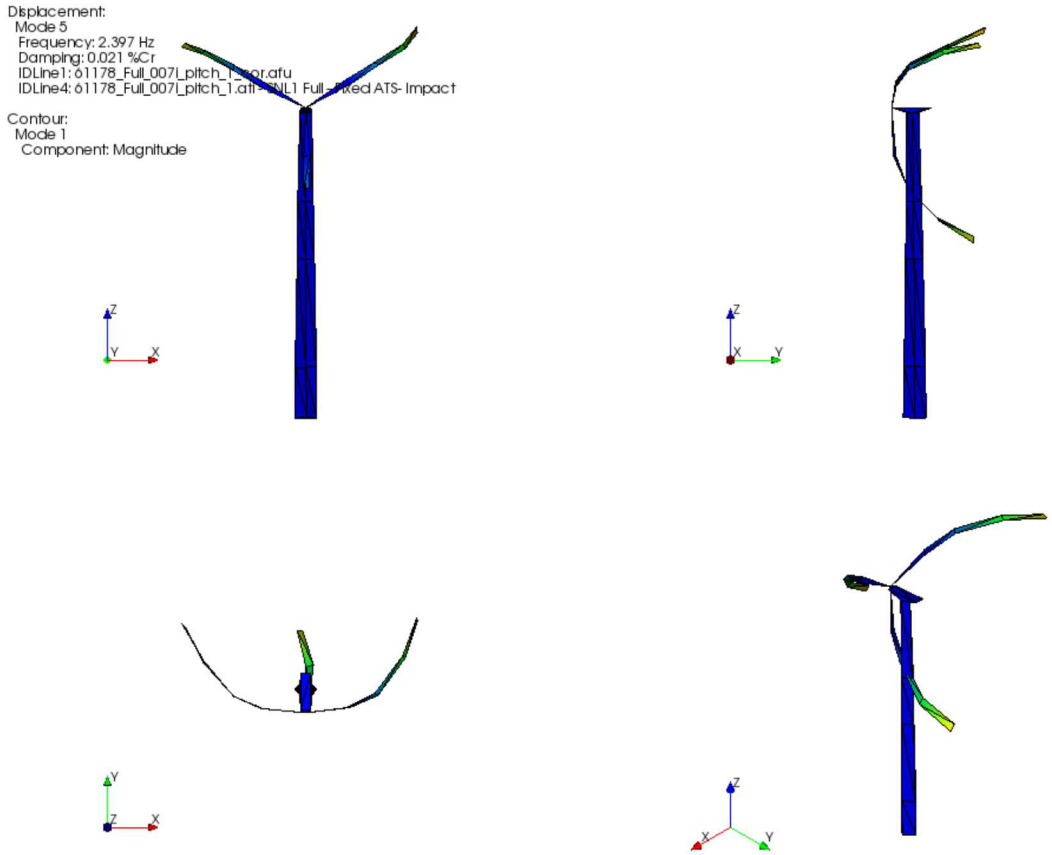
Displacement:
Mode 5
Frequency: 2.397 Hz
Damping: 0.021 %Cr
IDLine1: 61178_Full_007I_pitch_1_cor.afu
IDLine4: 61178_Full_007I_pitch_1.afi - SNL1 Full - Fixed ATS- Impact
Contour:
Mode 1
Component: Magnitude
Z
Y
X
Z
X
Y
Y
Z
X
Z
X
Y

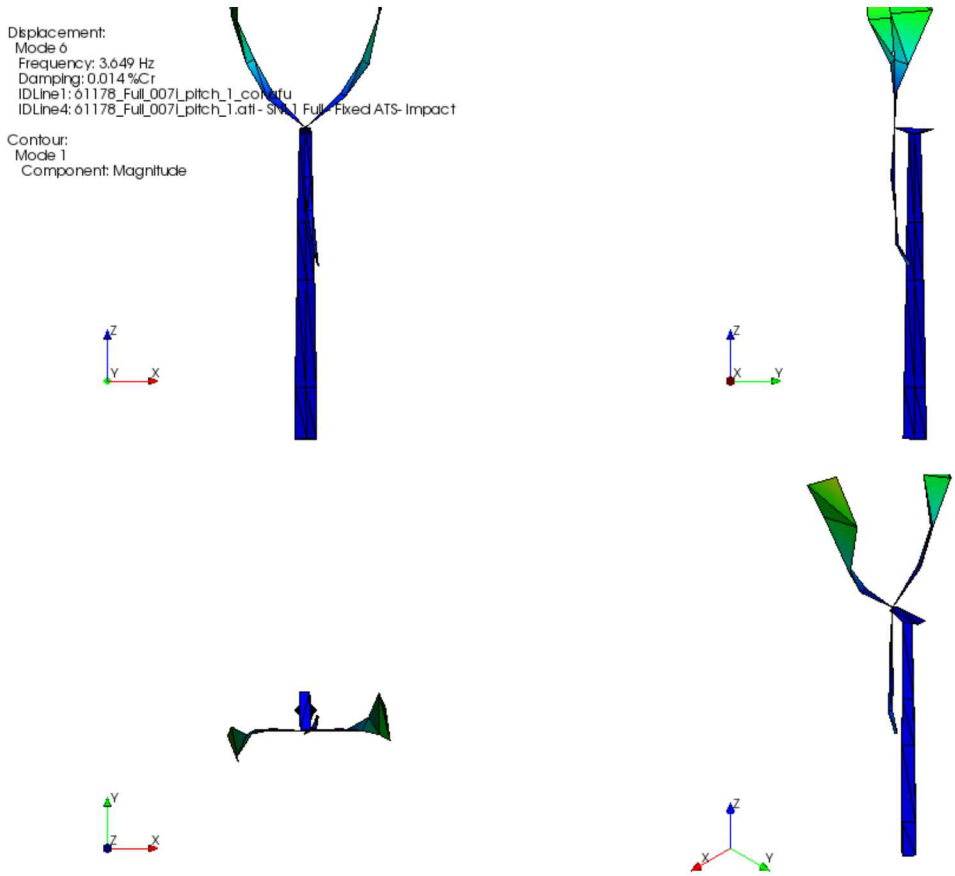
Displacement:
Mode 6
Frequency: 3.649 Hz
Damping: 0.014 %Cr
IDLine1: 61178_Full_007I_pitch_1_co
IDLine4: 61178_Full_007I_pitch_1.atl - SW1 Full - Fixed ATS- Impact
Contour:
Mode 1
Component: Magnitude

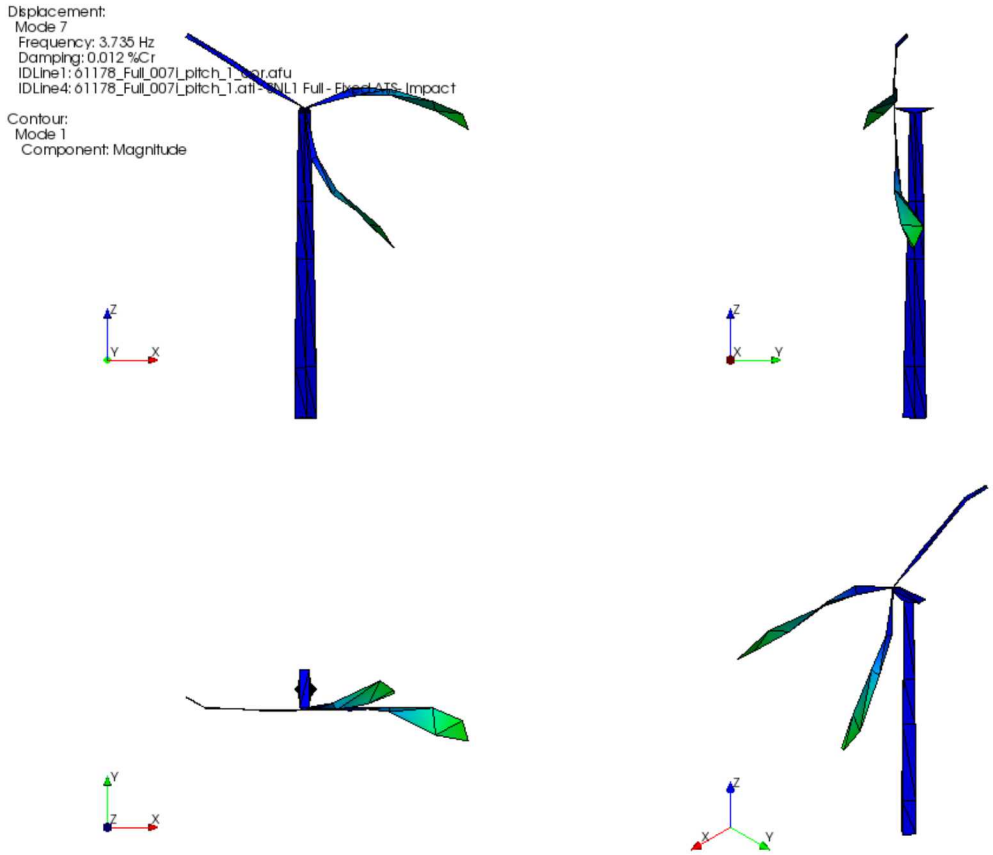
Displacement:
Mode 7
Frequency: 3.735 Hz
Damping: 0.012 %Cr
IDLine1: 61178_Full_007I_pitch_1_cor.afu
IDLine4: 61178_Full_007I_pitch_1.afl - SNL1 Full - FixedLATS, Impact
Contour:
Mode 1
Component: Magnitude

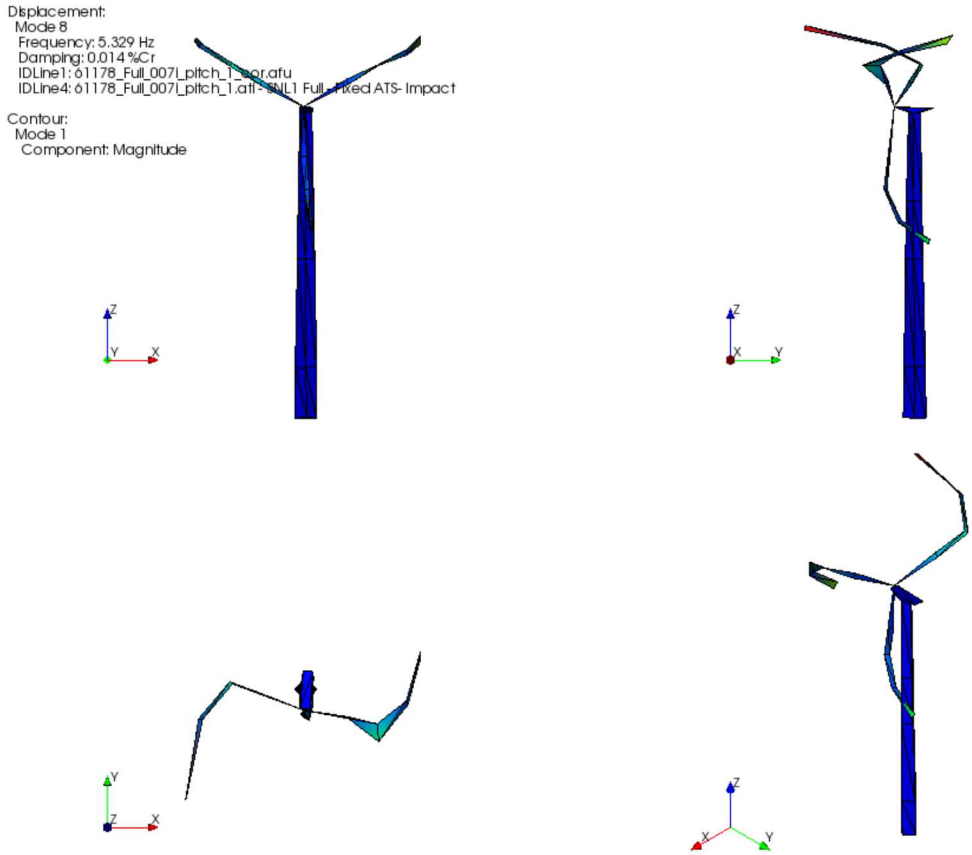
Displacement:
Mode 8
Frequency: 5.329 Hz
Damping: 0.014 %Cr
IDLine1: 61178_Full_007I_pitch_1_cor.afu
IDLine4: 61178_Full_007I_pitch_1.atf - SNL1 Full - Fixed ATS- Impact
Contour:
Mode 1
Component: Magnitude

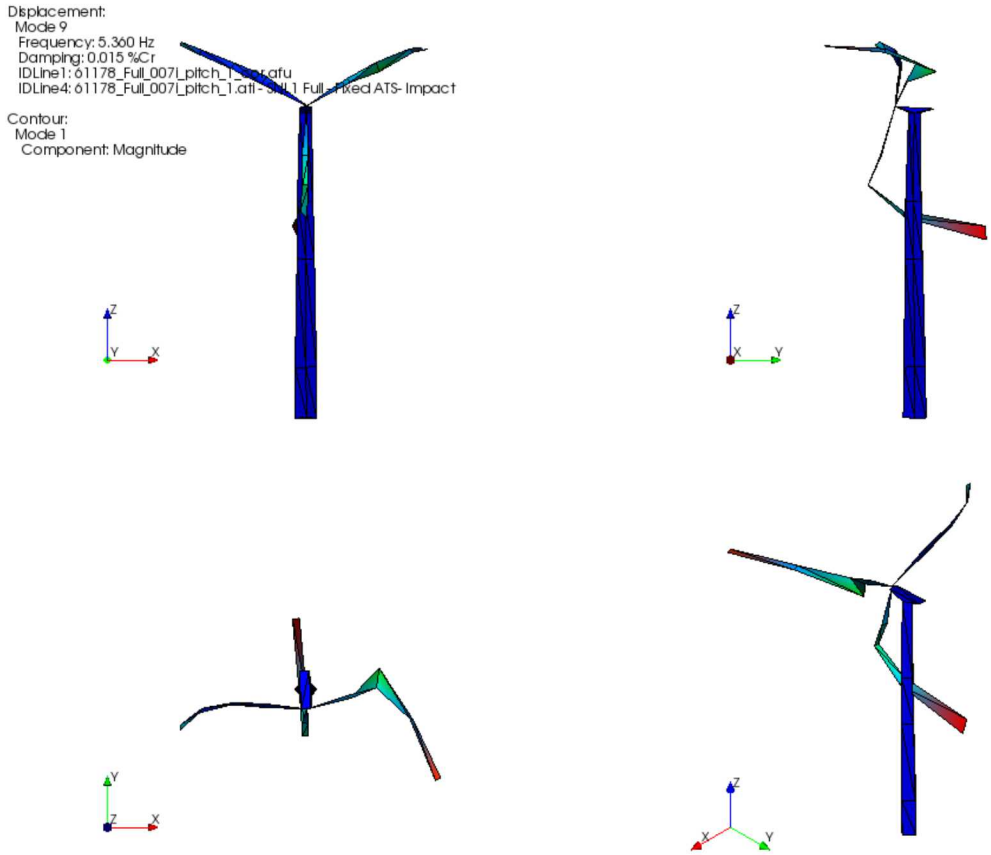
Displacement:
Mode 9
Frequency: 5.360 Hz
Damping: 0.015 %Cr
IDLine1: 61178_Full_007l_pitch_1.afu
IDLine4: 61178_Full_007l_pitch_1.afl - SWL 1 Full - Fixed ATS- Impact
Contour:
Mode 1
Component: Magnitude

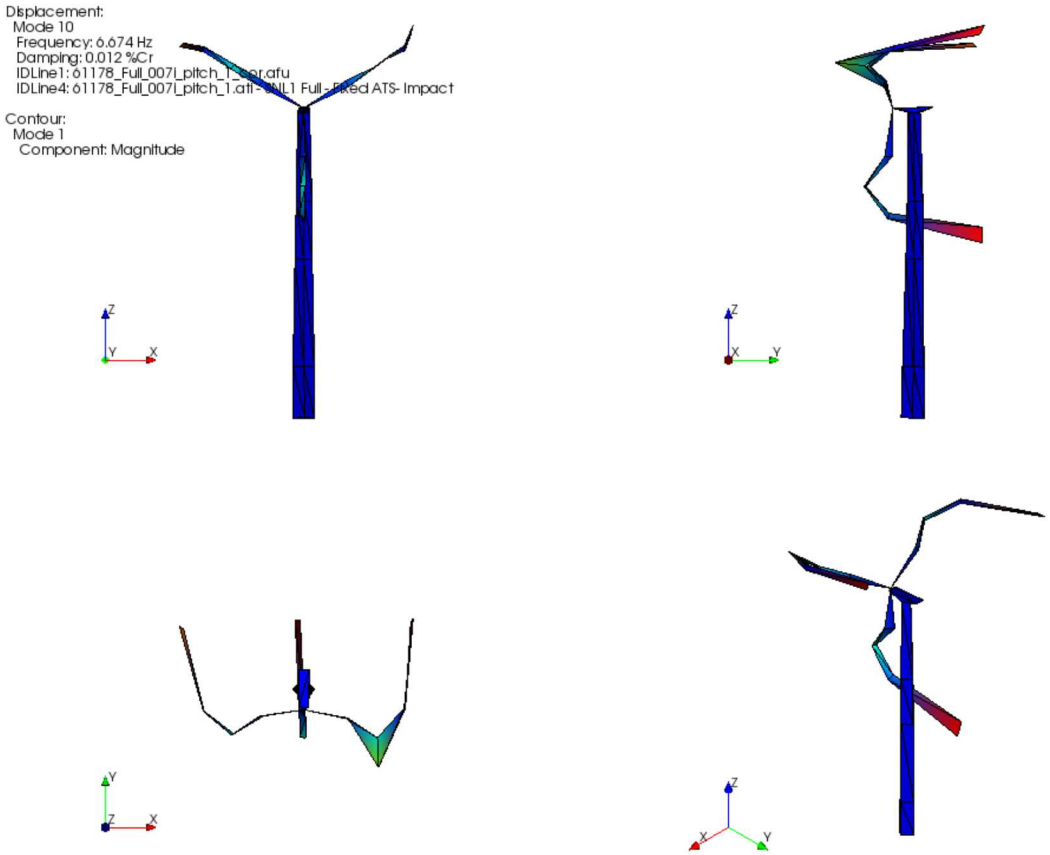
Displacement:
Mode 10
Frequency: 6.674 Hz
Damping: 0.012 %Cr
IDLine1: 61178_Full_007I_pitch_1_ser.afu
IDLine4: 61178_Full_007I_pitch_1.afl - SNL1 Full - Fixed ATS- Impact
Contour:
Mode 1
Component: Magnitude

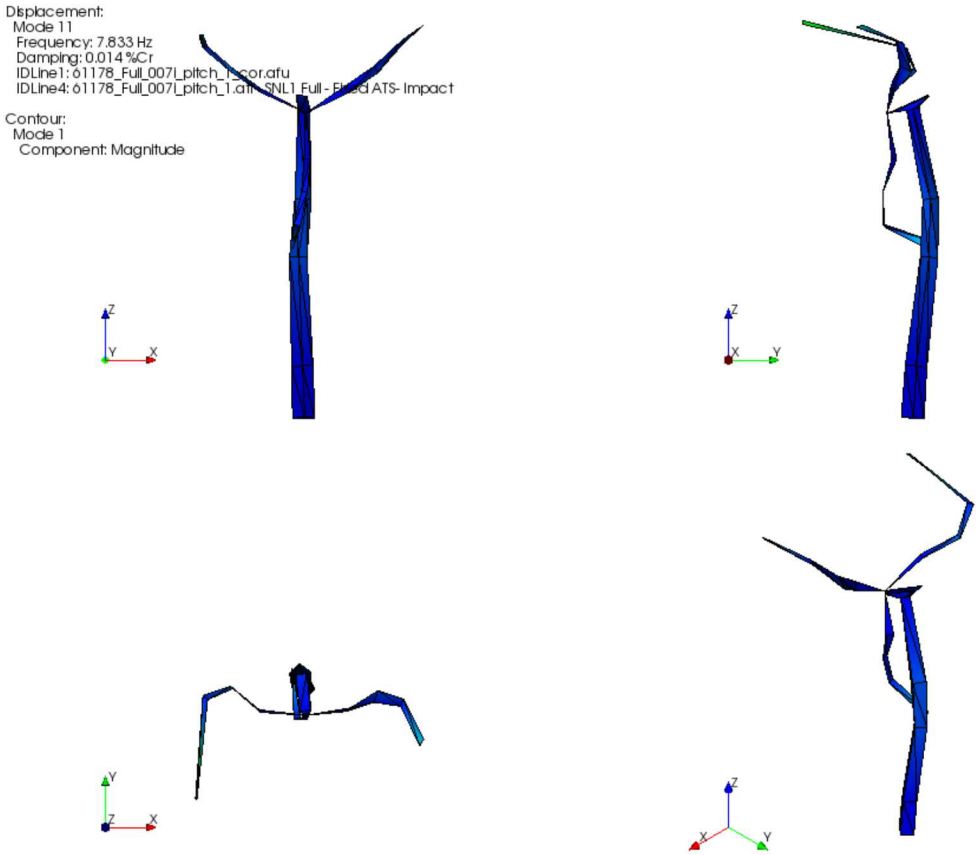
Displacement:
Mode 11
Frequency: 7.833 Hz
Damping: 0.014 %Cr
IDLine1: 61178_Full_007I_pitch_1_cor.afu
IDLine4: 61178_Full_007I_pitch_1.afu SNL1_Full - Fixed ATS- Impact
Contour:
Mode 1
Component: Magnitude

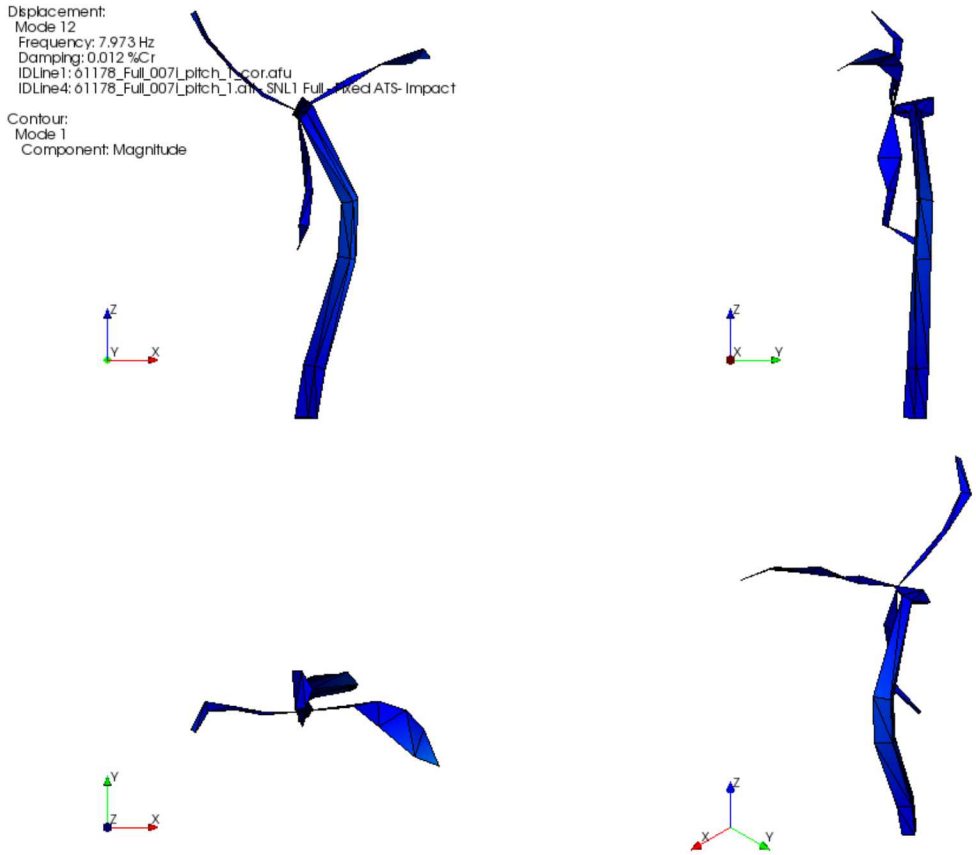
Displacement:
Mode 12
Frequency: 7.973 Hz
Damping: 0.012 %Cr
IDLine1: 61178_Full_007I_pitch_1_cor.afu
IDLine4: 61178_Full_007I_pitch_1.afu SNL1 Full Fixed ATS- Impact
Contour:
Mode 1
Component: Magnitude

Displacement:
Mode 13
Frequency: 8.429 Hz
Damping: 0.013 %Cr
IDLine1: 61178_Full_007l_pitch_1_cor.afu
IDLine4: 61178_Full_007l_pitch_1.afu - SNL1 Full - Fixed ATS- Impact
Contour:
Mode 1
Component: Magnitude

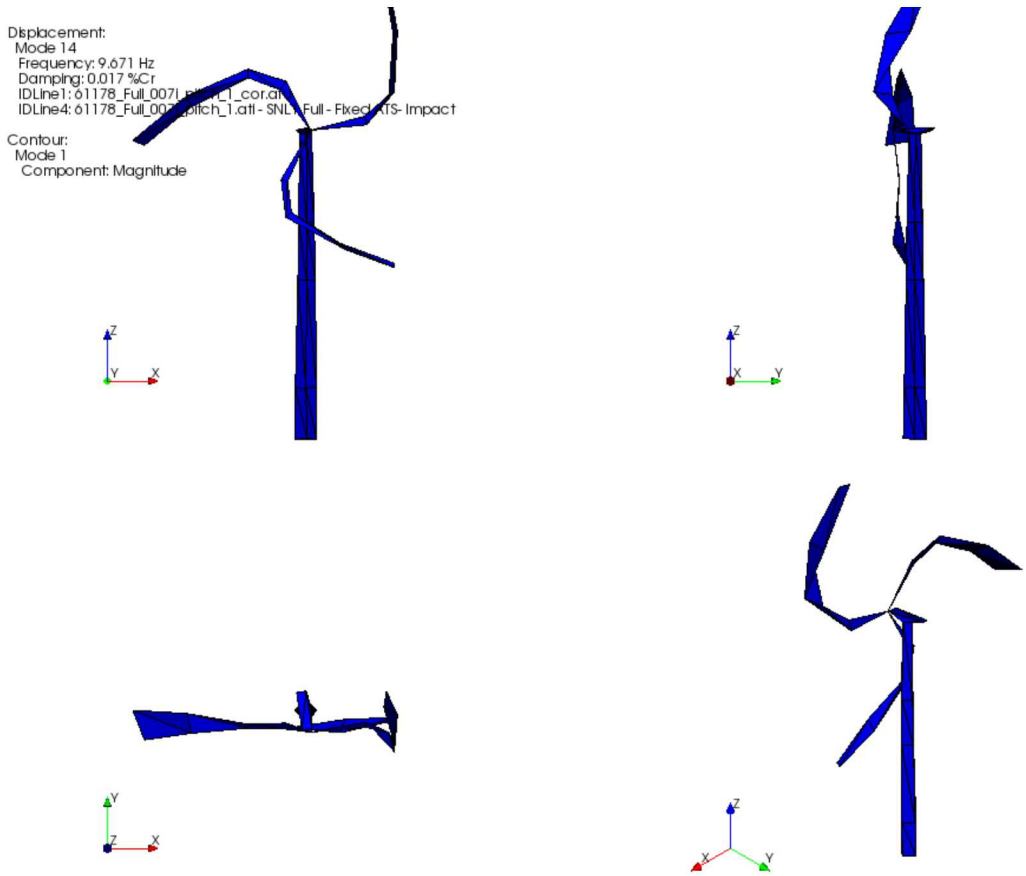
Displacement:
Mode 14
Frequency: 9.671 Hz
Damping: 0.017 %Cr
IDLine1: 61178_Full_007
_1_cor.at
IDLine4: 61178_Full_00
pitch_1.att - SNL
Full - Fixed
TS- Impact
Contour:
Mode 1
Component: Magnitude
Z
Y
X
Z
X
Y
Y
Z
X
Z
X
Y

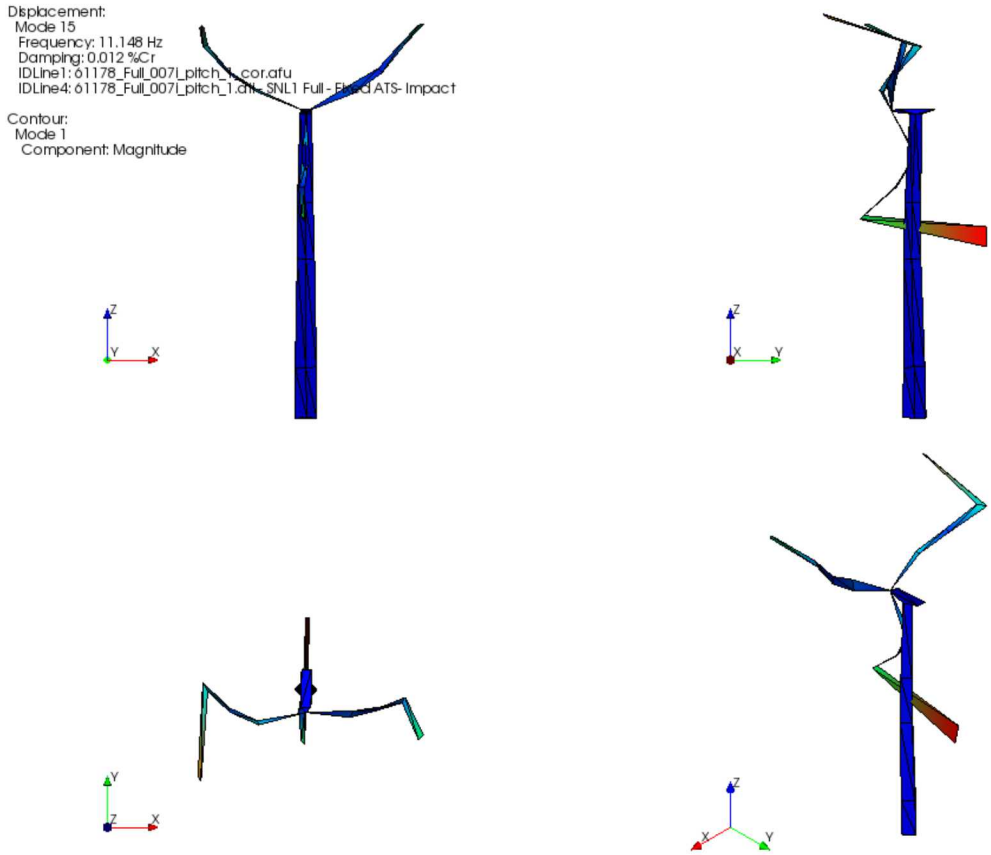
Displacement:
Mode 15
Frequency: 11.148 Hz
Damping: 0.012 %Cr
IDLine1: 61178_Full_007I_pitch_1_cor.afu
IDLine4: 61178_Full_007I_pitch_1.afu - SNL1 Full - Fixed ATS- Impact
Contour:
Mode 1
Component: Magnitude

Displacement:
Mode 16
Frequency: 12.522 Hz
Damping: 0.036 %Cr
IDLine1: 61178_Full_007l_pitch_1_coor.afu
IDLine4: 61178_Full_007l_pitch_1.atl - SNL1 Full - Fixed ATS- Impact
Contour:
Mode 1
Component: Magnitude

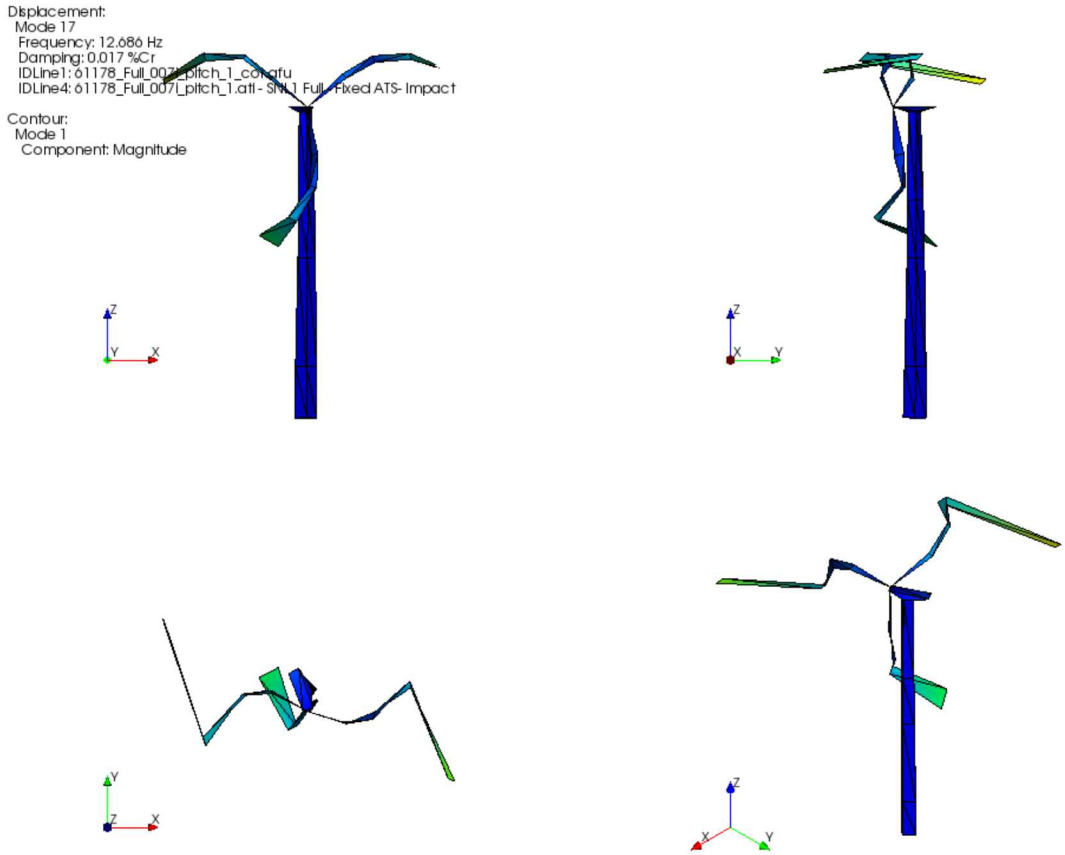
Displacement:
Mode 17
Frequency: 12.686 Hz
Damping: 0.017 %Cr
IDLine1: 61178_Full_007I_pitch_1_cor.afu
IDLine4: 61178_Full_007I_pitch_1.atl - SNL1 Full - Fixed ATS- Impact
Contour:
Mode 1
Component: Magnitude
Z
Y
X
Z
X
Y
Y
Z
X
Z
X
Y

Displacement:
Mode 18
Frequency: 13.454 Hz
Damping: 0.011 %Cr
Contour:
Mode 1
Component: Magnitude

Displacement:
Mode 19
Frequency: 13.660 Hz
Damping: 0.011 %Cr
IDLine1: 61178_Full_007I_pitch_1_cor.afu
IDLine4: 61178_Full_007I_pitch_1_atl - SNL1 Full - Fixed ATS- Impact
Contour:
Mode 1
Component: Magnitude

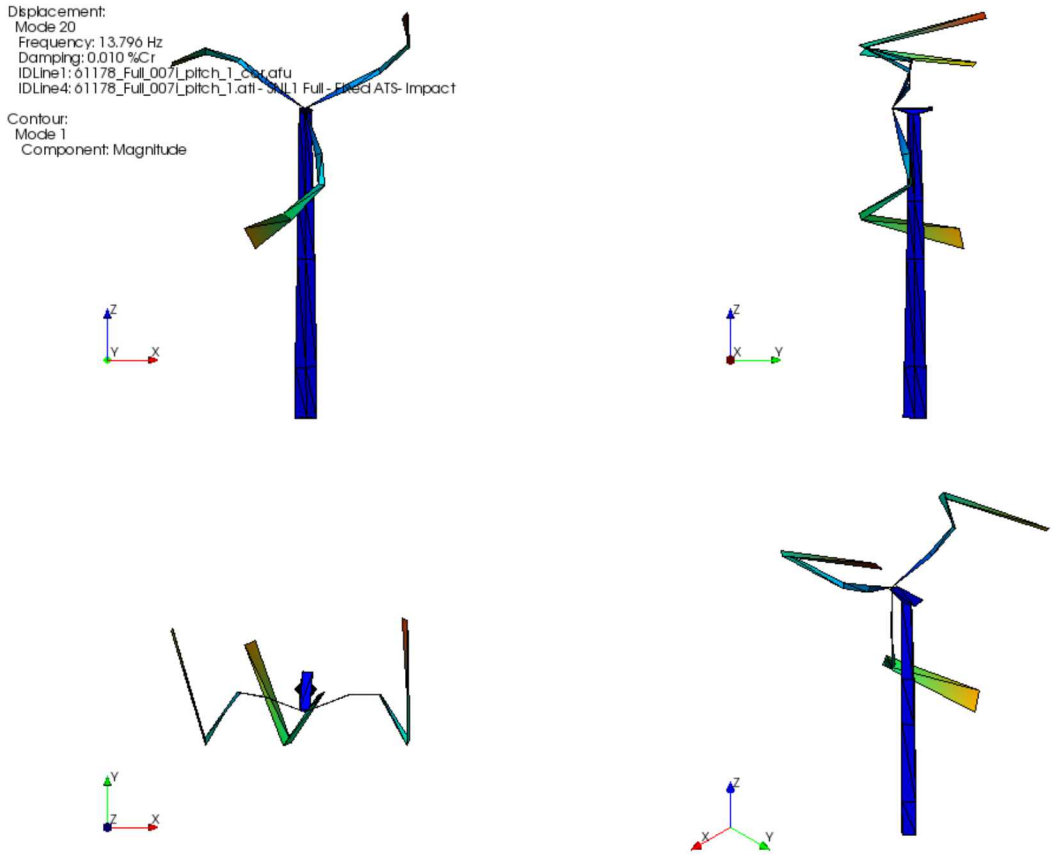
Displacement:
Mode 20
Frequency: 13.796 Hz
Damping: 0.010 %Cr
IDLine1: 61178_Full_007l_pitch_1_
IDLine4: 61178_Full_007l_pitch_1.atl - SNL1 Full - Fixed ATS- Impact
Contour:
Mode 1
Component: Magnitude

# Operational Modal Analysis Shapes
# SNL1 – Run6

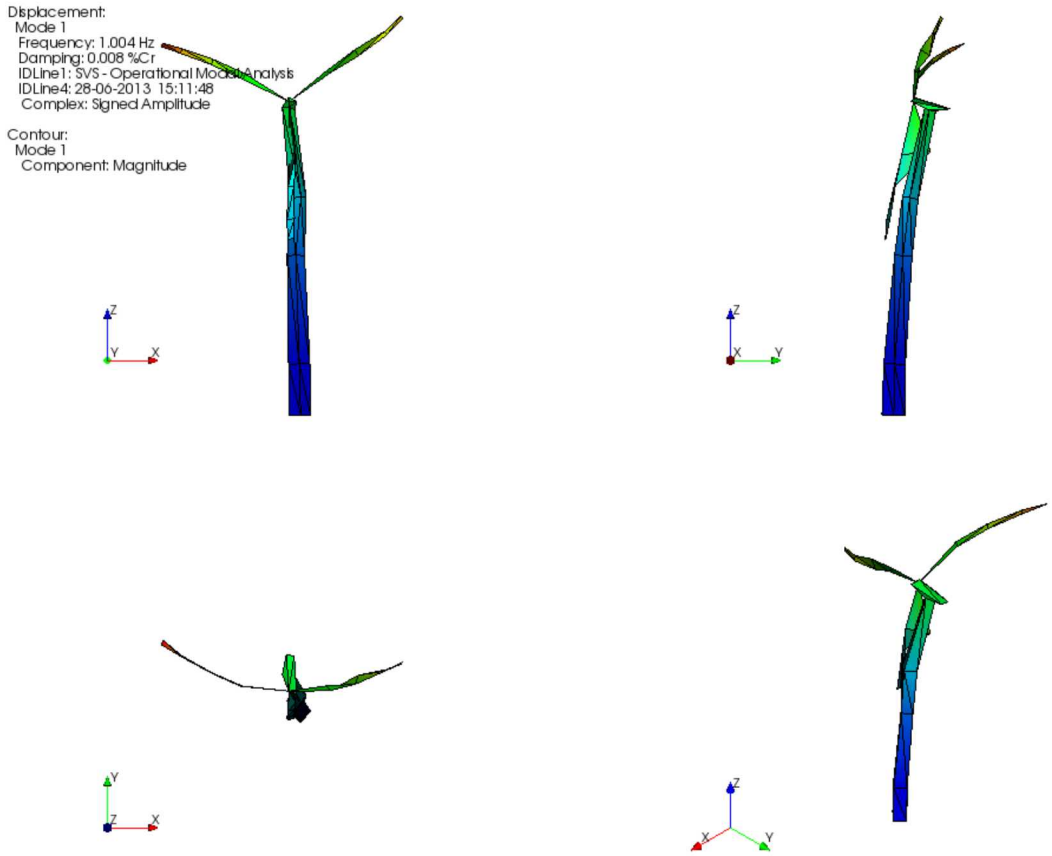

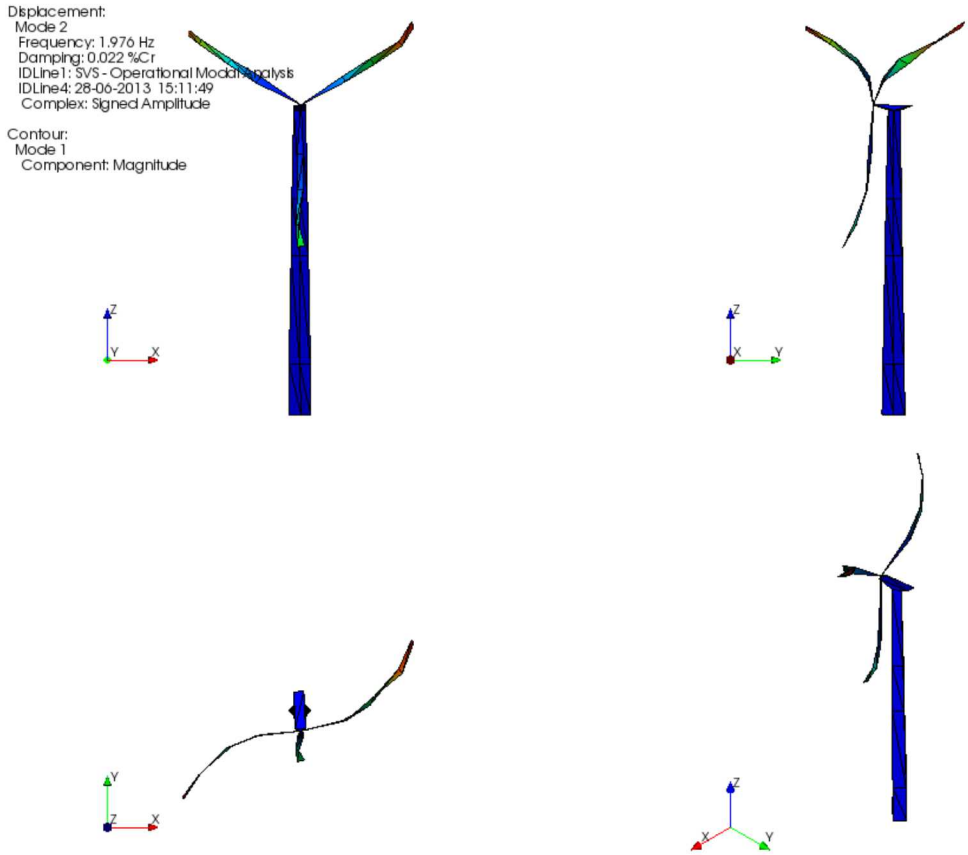
Displacement:
Mode 2
Frequency: 1.976 Hz
Damping: 0.022 %Cr
IDLine1: SVS - Operational Modal Analysis
IDLine4: 28-06-2013 15:11:49
Complex: Signed Amplitude
Contour:
Mode 1
Component: Magnitude

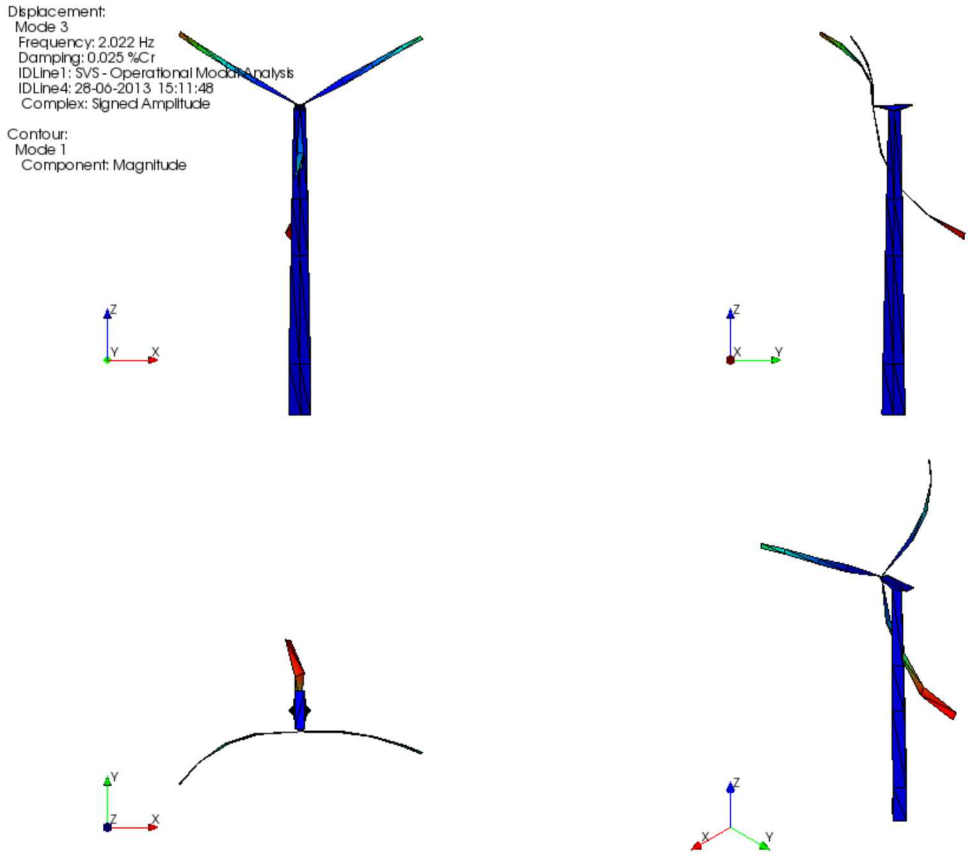
Displacement:
Mode 3
Frequency: 2.022 Hz
Damping: 0.025 %Cr
IDLine1: SVS - Operational Modal Analysis
IDLine4: 28-06-2013 15:11:48
Complex: Signed Amplitude
Contour:
Mode 1
Component: Magnitude

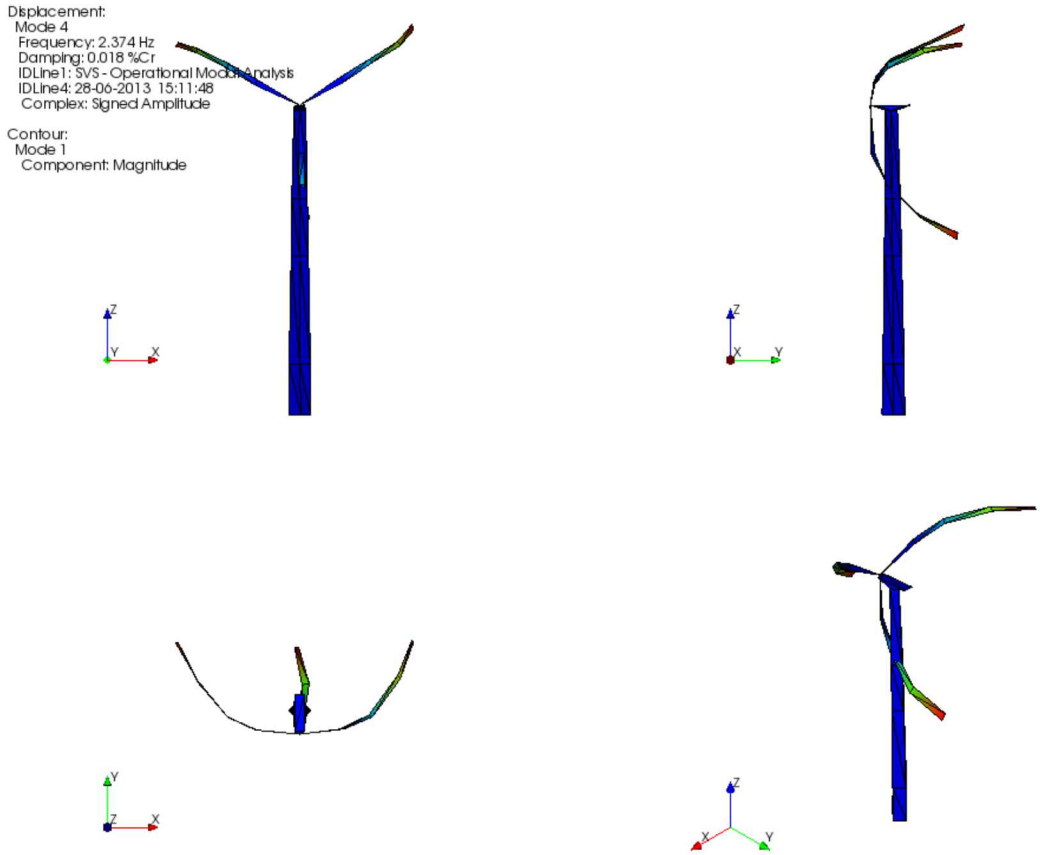
Displacement:
Mode 4
Frequency: 2.374 Hz
Damping: 0.018 %Cr
IDLine1: SVS - Operational Modal Analysis
IDLine4: 28-06-2013 15:11:48
Complex: Signed Amplitude
Contour:
Mode 1
Component: Magnitude

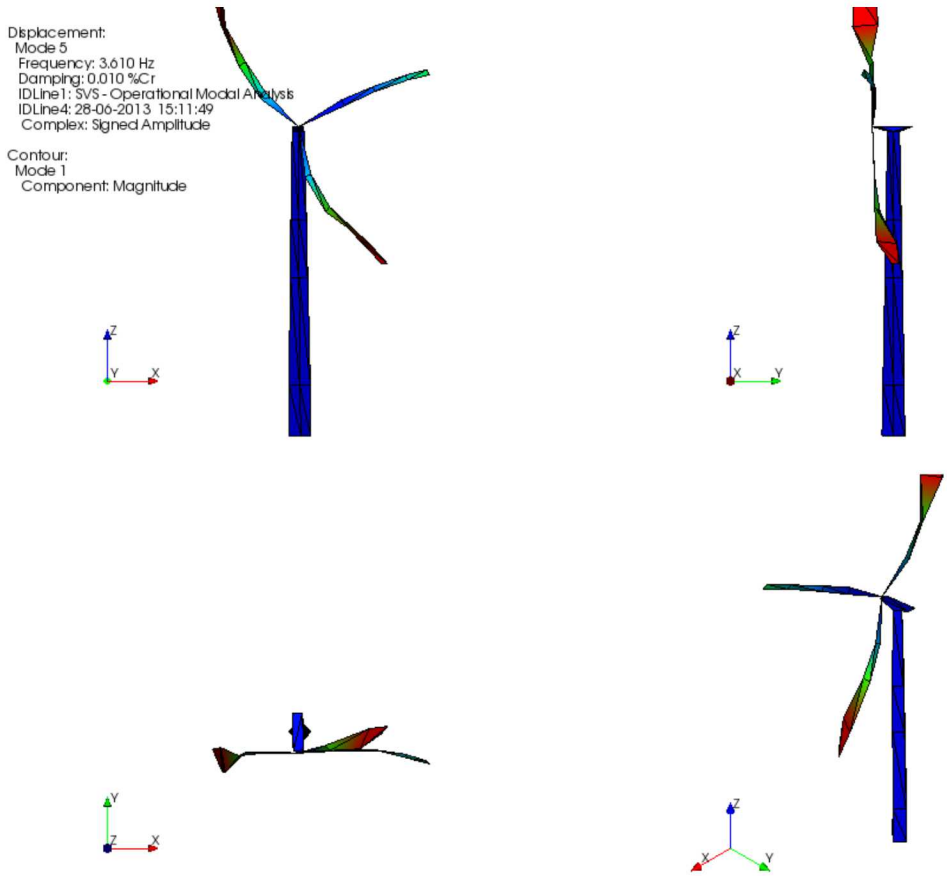
Displacement:
Mode 5
Frequency: 3.610 Hz
Damping: 0.010 %Cr
IDLine1: SVS - Operational Modal Analysis
IDLine4: 28-06-2013 15:11:49
Complex: Signed Amplitude
Contour:
Mode 1
Component: Magnitude

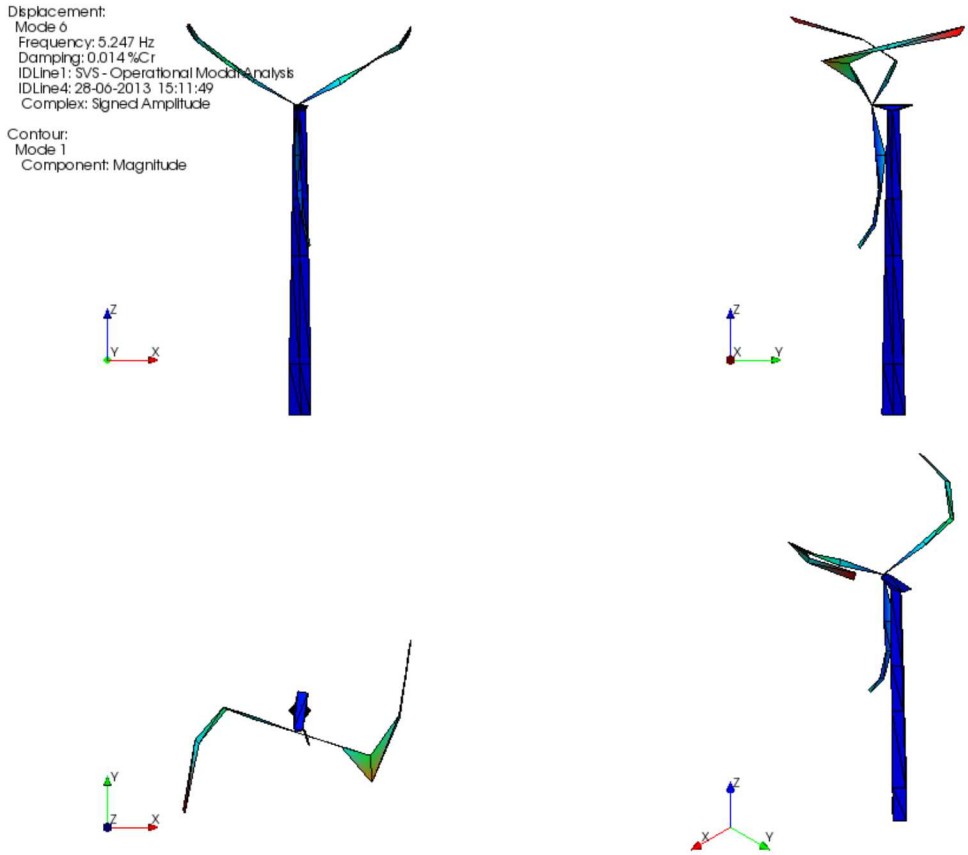
Displacement:
Mode 6
Frequency: 5.247 Hz
Damping: 0.014 %Cr
IDLine1: SVS - Operational Modal Analysis
IDLine4: 28-06-2013 15:11:49
Complex: Signed Amplitude
Contour:
Mode 1
Component: Magnitude

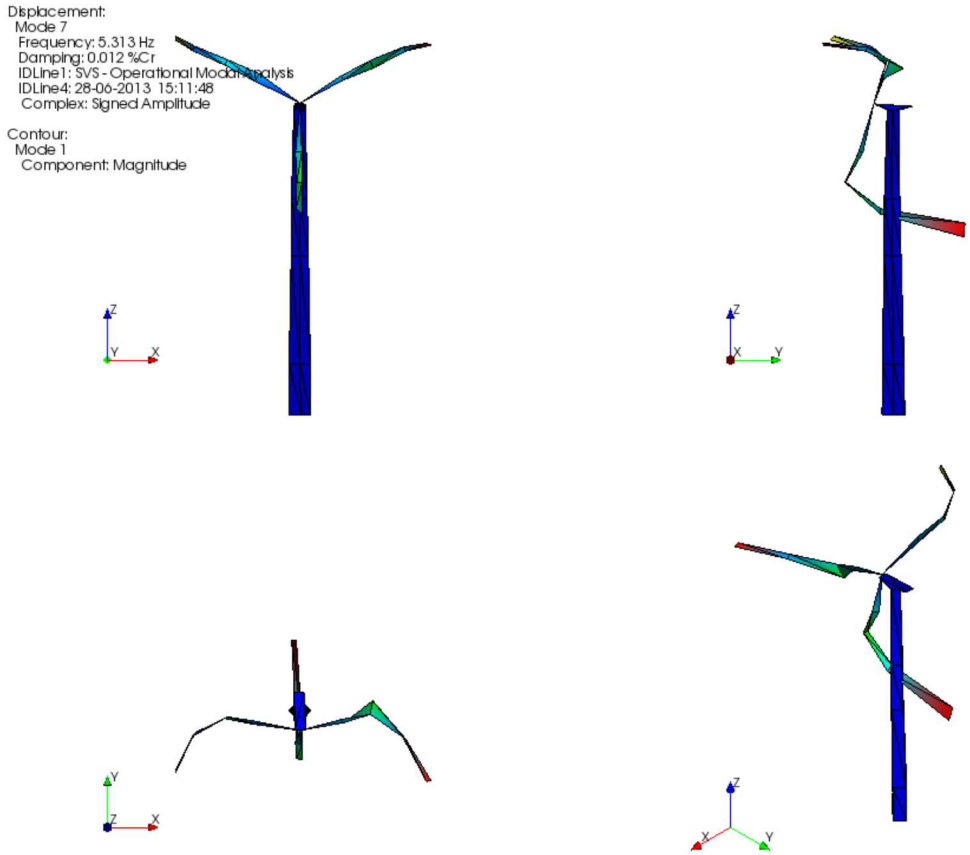
Displacement:
Mode 7
Frequency: 5.313 Hz
Damping: 0.012 %Cr
IDLine1: SVS - Operational Modal Analysis
IDLine4: 28-06-2013 15:11:48
Complex: Signed Amplitude
Contour:
Mode 1
Component: Magnitude

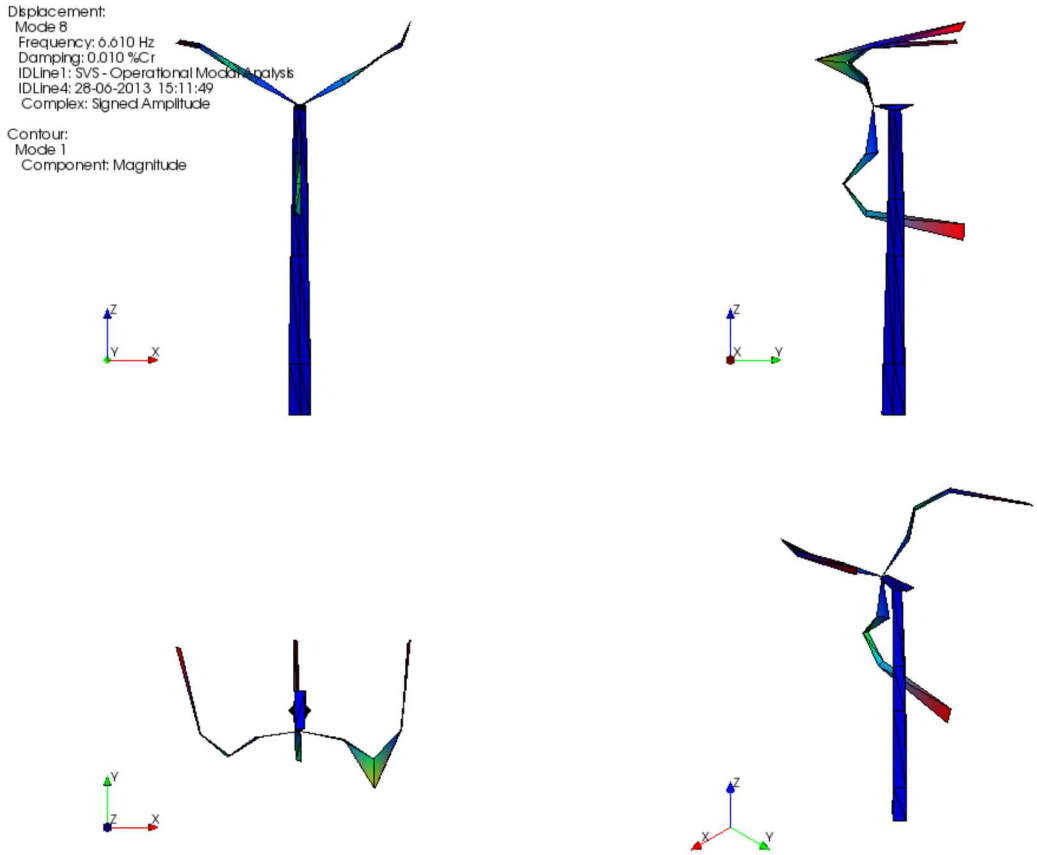
Displacement:
Mode 8
Frequency: 6.610 Hz
Damping: 0.010 %Cr
IDLine1: SVS - Operational Modal Analysis
IDLine4: 28-06-2013 15:11:49
Complex: Signed Amplitude
Contour:
Mode 1
Component: Magnitude

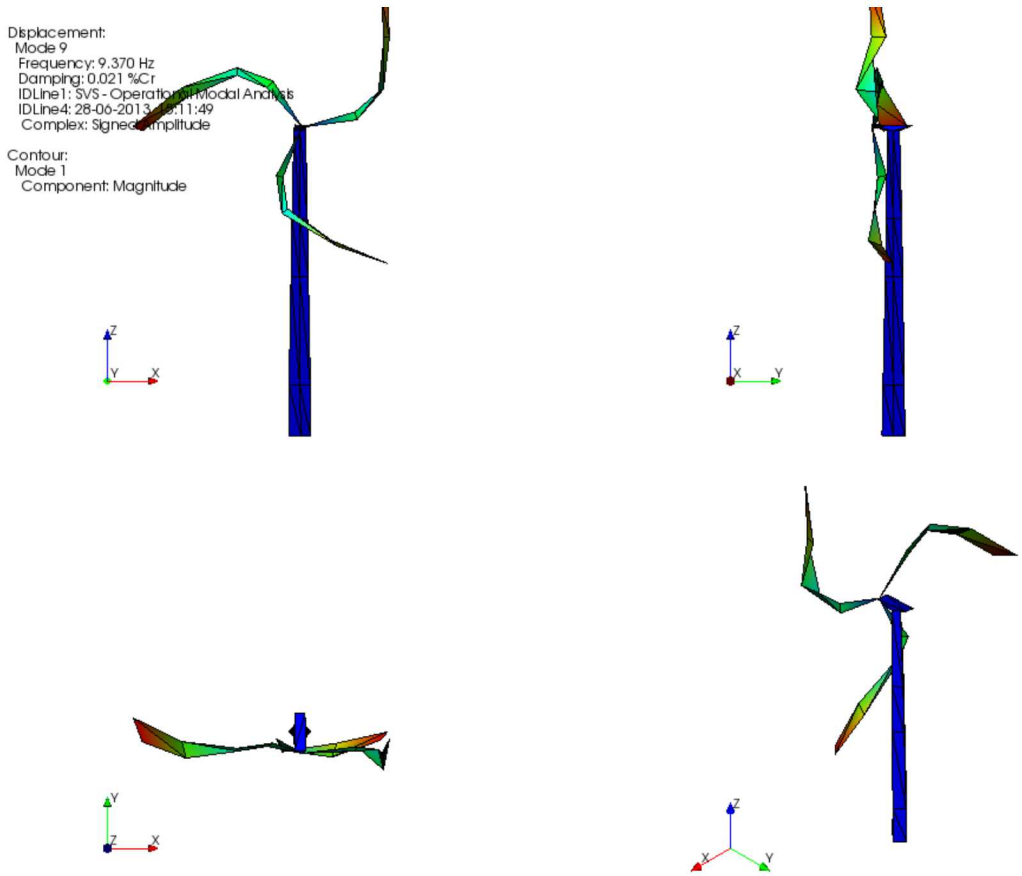
Displacement:
Mode 9
Frequency: 9.370 Hz
Damping: 0.021 %Cr
IDLine1: SVS - Operational Modal Analysis
IDLine4: 28-06-2013 11:49
Complex: Signed Amplitude
Contour:
Mode 1
Component: Magnitude
Z
Y
X

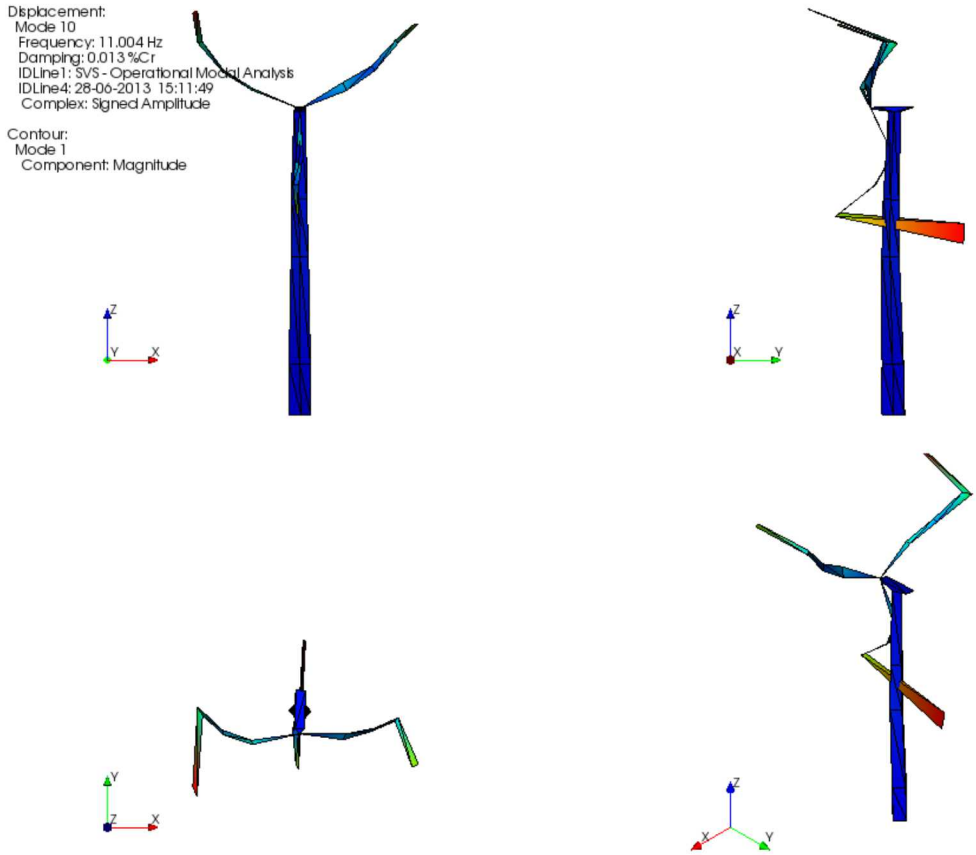
Displacement:
Mode 10
Frequency: 11.004 Hz
Damping: 0.013 %Cr
IDLine1: SVS - Operational Modal Analysis
IDLine4: 28-06-2013 15:11:49
Complex: Signed Amplitude
Contour:
Mode 1
Component: Magnitude

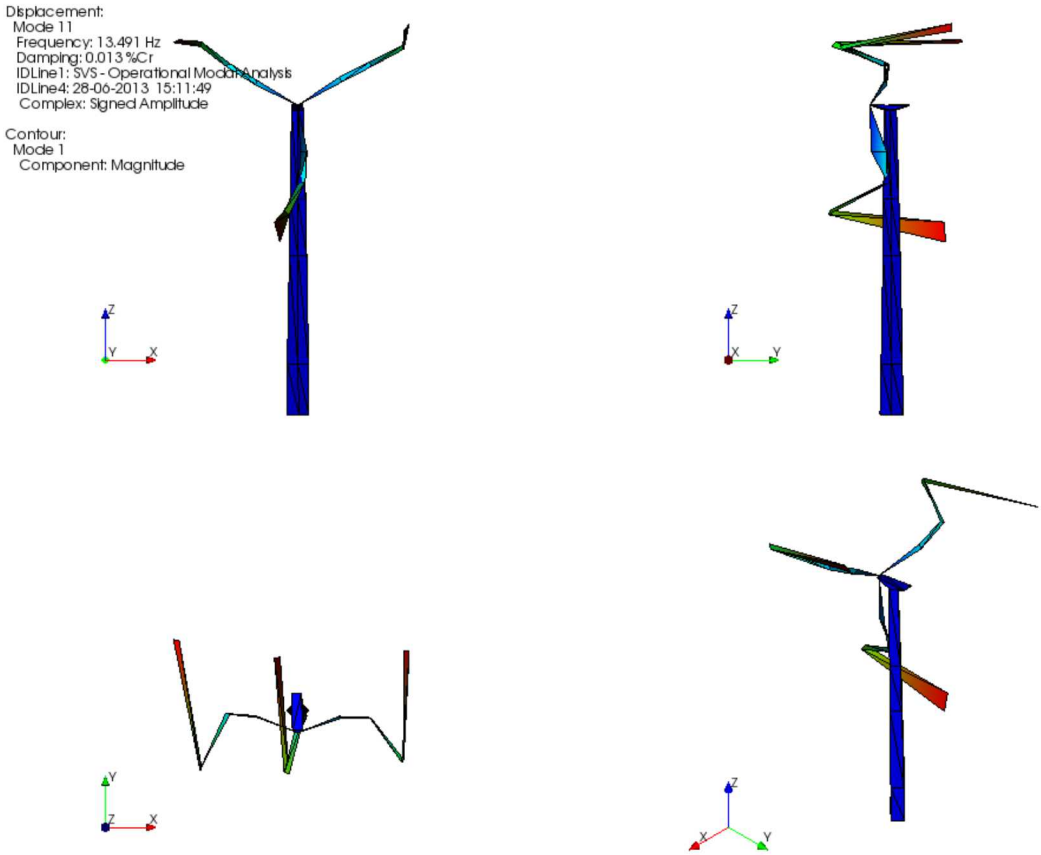
Displacement:
Mode 11
Frequency: 13.491 Hz
Damping: 0.013 %Cr
IDLine1: SVS - Operational Modal Analysis
IDLine4: 28-06-2013 15:11:49
Complex: Signed Amplitude
Contour:
Mode 1
Component: Magnitude

# Appendix G

# Equipment Specifications

## Accelerometers

PCB PIEZOTRONICS INC.

**Model 333B**

**Product Type:** Accelerometer

Modal array, ceramic shear ICP® accel., 100 mV/g, 2 to 1000 Hz, 3-pin socket connector mounting

There is no product photo available at this time.

| PERFORMANCE | ENGLISH | SI | |
|---|---|---|---|
| Sensitivity (±20 %) | 100 mV/g | 10.2 mV/(m/s²) | |
| Measurement Range | ±50 g pk | ±490 m/s² pk | |
| Frequency Range (±5 %) | 2 to 1000 Hz | 2 to 1000 Hz | |
| Resonant Frequency | 5 kHz | 5 kHz | |
| Phase Response (±5 °) | 2 to 1000 Hz | 2 to 1000 Hz | |
| Broadband Resolution (1 to 10000 Hz) | 0.00007 g rms | 0.0007 m/s² rms | [1] |
| Non-Linearity | 1 % | 1 % | [2] |
| Transverse Sensitivity | 5 % | 5 % | [3] |
| **ENVIRONMENTAL** | | | |
| Overload Limit (Shock) | ±3500 g pk | ±34300 m/s² pk | |
| Temperature Range | 0 to 150 °F | -18 to +66 °C | |
| Temperature Response | 0.15 %/°F | 0.27 %/°C | [1] |
| **ELECTRICAL** | | | |
| Excitation Voltage | 18 to 30 VDC | 18 to 30 VDC | |
| Constant Current Excitation | 2 to 20 mA | 2 to 20 mA | |
| Output Impedance | 100 ohms | 100 ohms | |
| Output Bias Voltage | 8 to 12 VDC | 8 to 12 VDC | |
| Discharge Time Constant | 0.7 to 1.3 sec | 0.7 to 1.3 sec | |
| Settling Time (within 10% of bias) | <5 sec | <5 sec | |
| Spectral Noise (1 Hz) | 20 g/ Hz | 196 ( m/s²)/ Hz | [1] |
| Spectral Noise (10 Hz) | 4.3 g/ Hz | 42.1 ( m/s²)/ Hz | [1] |
| Spectral Noise (100 Hz) | 1.3 g/ Hz | 12.8 ( m/s²)/ Hz | [1] |
| Spectral Noise (1 kHz) | 0.6 g/ Hz | 5.9 ( m/s²)/ Hz | [1] |
| **PHYSICAL** | | | |
| Sensing Element | Ceramic | Ceramic | |
| Sensing Geometry | Shear | Shear | |
| Housing Material | Polymer | Polymer | |
| Sealing | Hermetic | Hermetic | |
| Size (Height x Diameter) | 0.84 in x 0.48 in | 21.4 mm x 12.2 mm | |
| Weight | 0.2 oz | 5.6 gm | [1] |
| Electrical Connector | 3-Pin Socket | 3-Pin Socket | |

**SUPPLIED ACCESSORIES:**

Model ACS-2 NIST Traceable single point (100 Hz) sensitivity. (1)

**OPTIONAL VERSIONS**

**T** - TEDS Capable of Digital Memory and Communication Compliant with IEEE P1451.4

**TLA** - TEDS LMS International - Free Format

**TLB** - TEDS LMS International - Automotive Format

**TLC** - TEDS LMS International - Aeronautical Format

*All specifications are at room temperature unless otherwise specified.*

**NOTES:**

[1] Typical.

[2] Zero-based, least-squares, straight line method.

[3] Transverse sensitivity is typically <= 3%.

**In the interest of constant product improvement,**
**we reserve the right to change specifications without notices.**

| Model Number 393B04 | ACCELEROMETER, ICP®, SEISMIC | Revision E ECN #: 29253 |
|---|---|---|

| | ENGLISH | SI | |
|---|---|---|---|
| **Performance** | | | |
| Sensitivity (±10 %) | 1000 mV/g | 102 mV/(m/s²) | |
| Measurement Range | ±5 g pk | ±49 m/s² pk | |
| Frequency Range (±5 %) | 0.06 to 450 Hz | 0.06 to 450 Hz | |
| Frequency Range (±10 %) | 0.05 to 750 Hz | 0.05 to 750 Hz | |
| Frequency Range (±3 dB) | 0.02 to 1700 Hz | 0.02 to 1700 Hz | |
| Resonant Frequency | ≥2.5 kHz | ≥2.5 kHz | |
| Broadband Resolution (1 to 10000 Hz) | 0.000003 g rms | 0.00003 m/s² rms | [1] |
| Non-Linearity | ≤1 % | ≤1 % | [2] |
| Transverse Sensitivity | ≤5 % | ≤5 % | [3] |
| **Environmental** | | | |
| Overload Limit (Shock) | ±300 g pk | ±2950 m/s² pk | |
| Temperature Range | 0 to +176 °F | -18 to +80 °C | |
| Base Strain Sensitivity | ≤0.0005 g/με | ≤0.005 (m/s²)/με | [1] |
| **Electrical** | | | |
| Excitation Voltage | 18 to 30 VDC | 18 to 30 VDC | |
| Constant Current Excitation | 2 to 10 mA | 2 to 10 mA | |
| Output Impedance | <500 Ohm | <500 Ohm | |
| Output Bias Voltage | 7 to 12 VDC | 7 to 12 VDC | |
| Discharge Time Constant | 5 to 15 sec | 5 to 15 sec | |
| Settling Time | <100 sec | <100 sec | |
| Spectral Noise (1 Hz) | 0.30 μg/√Hz | 2.9 (μm/sec²)/√Hz | [1] |
| Spectral Noise (10 Hz) | 0.10 μg/√Hz | 1.0 (μm/sec²)/√Hz | [1] |
| Spectral Noise (100 Hz) | 0.04 μg/√Hz | 0.4 (μm/sec²)/√Hz | [1] |
| Spectral Noise (1 kHz) | 0.04 μg/√Hz | 0.4 (μm/sec²)/√Hz | [1] |
| **Physical** | | | |
| Sensing Element | Ceramic | Ceramic | |
| Sensing Geometry | Flexural | Flexural | |
| Housing Material | Titanium | Titanium | |
| Sealing | Hermetic | Hermetic | |
| Size (Diameter x Height) | 0.99 in x 1.22 in | 25 mm x 31 mm | |
| Weight | 1.8 oz | 50 gm | [1] |
| Electrical Connector | 10-32 Coaxial Jack | 10-32 Coaxial Jack | |
| Electrical Connection Position | Top | Top | |
| Mounting Thread | 10-32 Female | 10-32 Female | |

CE[4]

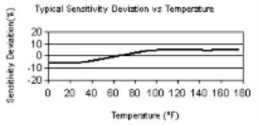


*All specifications are at room temperature unless otherwise specified.*
In the interest of constant product improvement, we reserve the right to change specifications without notice.
ICP® is a registered trademark of PCB group, Inc.

**Optional Versions** (Optional versions have identical specifications and accessories as listed for standard model except where noted below. More than one option maybe used.)

**T** - TEDS Capable of Digital Memory and Communication Compliant with IEEE P1451.4

| | | |
|---|---|---|
| Output Bias Voltage | 7.5 to 13 VDC | 7.5 to 13 VDC |
| Excitation Voltage | 20 to 30 VDC | 20 to 30 VDC |

**TLA** - TEDS LMS International - Free Format
**TLB** - TEDS LMS International - Automotive Format
**TLC** - TEDS LMS International - Aeronautical Format
**TLD** - TEDS Capable of Digital Memory and Communication Compliant with IEEE 1451.4

| | | |
|---|---|---|
| Excitation Voltage | 20 to 30 VDC | 20 to 30 VDC |
| Output Bias Voltage | 7.5 to 13 VDC | 7.5 to 13 VDC |

**W** - Water Resistant Cable

| | | |
|---|---|---|
| Electrical Connector | Sealed Integral Cable | Sealed Integral Cable |
| Electrical Connection Position | Top | Top |

**Notes**
[1] Typical.
[2] Zero-based, least-squares, straight line method.
[3] Transverse sensitivity is typically <= 3%.
[4] See PCB Declaration of Conformance PS023 for details.

**Supplied Accessories**
081B05 Mounting Stud (10-32 to 10-32) (1)
ACS-1 NIST traceable frequency response (10 Hz to upper 5% point). (1)
ACS-4 Single axis, low frequency phase and amplitude response cal from 0.5 to 10 Hz (1)
M081B05 Mounting Stud 10-32 to M6 X 0.75 (1)

| Entered: BLS | Engineer: BAM | Sales: BLS | | Spec Number: |
|---|---|---|---|---|
| Date: 08/18/2008 | Date: 08/15/2008 | Date: 09/08/2008 | | **17026** |

PCB PIEZOTRONICS VIBRATION DIVISION
3425 Walden Avenue
Depew, NY 14043
UNITED STATES
Phone: 800-828-8840
Fax: 716-684-0987
E-mail: info@pcb.com
Web site: www.pcb.com

## Impact Hammer

| Model Number 086D50 | IMPACT HAMMER, ICP® | Revision F ECN #: 32971 |
|---|---|---|

| Performance | ENGLISH | SI | |
|---|---|---|---|
| Sensitivity (±15 %) | 1 mV/lbf | 0.23 mV/N | |
| Measurement Range | ±5000 lbf pk | ±22240 N pk | |
| Resonant Frequency | ≥5 kHz | ≥5 kHz | |
| Non-Linearity | ≤1 % | ≤1 % | |
| **Electrical** | | | |
| Excitation Voltage | 20 to 30 VDC | 20 to 30 VDC | |
| Constant Current Excitation | 2 to 20 mA | 2 to 20 mA | |
| Output Impedance | <100 Ohm | <100 Ohm | [1] |
| Output Bias Voltage | 8 to 14 VDC | 8 to 14 VDC | |
| Discharge Time Constant | ≥2000 sec | ≥2000 sec | [1] |
| **Physical** | | | |
| Sensing Element | Quartz | Quartz | |
| Sealing | Hermetic | Hermetic | |
| Hammer Mass | 12.1 lb | 5.5 Kg | |
| Head Diameter | 3.0 in | 7.6 cm | |
| Tip Diameter | 3.0 in | 7.6 cm | |
| Hammer Length | 35 in | 89 cm | |
| Electrical Connection Position | Bottom of Handle | Bottom of Handle | |
| Electrical Connector | BNC Jack | BNC Jack | |

*All specifications are at room temperature unless otherwise specified.*
In the interest of constant product improvement, we reserve the right to change specifications without notice.
ICP® is a registered trademark of PCB group, Inc.

**Optional Versions** (Optional versions have identical specifications and accessories as listed for standard model except where noted below. More than one option maybe used.)

**T** - TEDS Capable of Digital Memory and Communication Compliant with IEEE P1451.4

| | | |
|---|---|---|
| Output Bias Voltage | 8.5 to 15 VDC | 8.5 to 15 VDC |

**Notes**

[1] Typical.

**Supplied Accessories**

084A31 Tip - soft plastic, brown (1)
084A32 Tip - hard plastic, red (1)
HCS-2 Calibration of Series 086 instrumented impact hammers (1)

| Entered: LLH | Engineer: BAM | Sales: WDC | Approved: LLH | Spec Number: |
|---|---|---|---|---|
| Date: 05/20/2010 | Date: 05/12/2010 | Date: 05/12/2010 | Date: 05/20/2010 | **12993** |

PCB PIEZOTRONICS VIBRATION DIVISION
3425 Walden Avenue
Depew, NY 14043
UNITED STATES
Phone: 800-828-8840
Fax: 716-684-0987
E-mail: info@pcb.com
Web site: www.pcb.com

| Model Number 086D20 | IMPACT HAMMER, ICP® | Revision G ECN #: 32971 |
|---|---|---|

| Performance | ENGLISH | SI | |
|---|---|---|---|
| Sensitivity (±15 %) | 1 mV/lbf | 0.23 mV/N | |
| Measurement Range | ±5000 lbf pk | ±22240 N pk | |
| Resonant Frequency | ≥12 kHz | ≥12 kHz | |
| Non-Linearity | ≤1 % | ≤1 % | |
| **Electrical** | | | |
| Excitation Voltage | 20 to 30 VDC | 20 to 30 VDC | |
| Constant Current Excitation | 2 to 20 mA | 2 to 20 mA | |
| Output Impedance | <100 Ohm | <100 Ohm | [1] |
| Output Bias Voltage | 8 to 14 VDC | 8 to 14 VDC | |
| Discharge Time Constant | ≥1400 sec | ≥1400 sec | [1] |
| **Physical** | | | |
| Sensing Element | Quartz | Quartz | |
| Sealing | Hermetic | Hermetic | |
| Hammer Mass | 2.4 lb | 1.1 Kg | |
| Head Diameter | 2.0 in | 5.1 cm | |
| Tip Diameter | 2.0 in | 5.1 cm | |
| Hammer Length | 14.5 in | 37 cm | |
| Electrical Connection Position | Bottom of Handle | Bottom of Handle | |
| Electrical Connector | BNC Jack | BNC Jack | |

*All specifications are at room temperature unless otherwise specified.*
In the interest of constant product improvement, we reserve the right to change specifications without notice.
ICP® is a registered trademark of PCB group, Inc.

**Optional Versions** (Optional versions have identical specifications and accessories as listed for standard model except where noted below. More than one option maybe used.)
**T** - TEDS Capable of Digital Memory and Communication Compliant with IEEE P1451.4
**TLD** - TEDS Capable of Digital Memory and Communication Compliant with IEEE 1451.4

| | | |
|---|---|---|
| Output Bias Voltage | 8.5 to 15 VDC | 8.5 to 15 VDC |

**Notes**
[1] Typical.

**Supplied Accessories**
084A60 Tip - super soft plastic, gray (1)
084A61 Tip - soft plastic, brown (1)
084A62 Tip - medium plastic, red (1)
084A63 Tip - hard plastic, black (1)
HCS-2 Calibration of Series 086 instrumented impact hammers (1)

| Entered: LLH | Engineer: BAM | Sales: WDC | Approved: LLH | Spec Number: |
|---|---|---|---|---|
| Date: 05/20/2010 | Date: 05/12/2010 | Date: 05/12/2010 | Date: 05/20/2010 | **12923** |

PCB PIEZOTRONICS VIBRATION DIVISION
3425 Walden Avenue
Depew, NY 14043
UNITED STATES
Phone: 800-828-8840
Fax: 716-684-0987
E-mail: info@pcb.com
Web site: www.pcb.com

## Signal Conditioner

Model Number
**442B119**

### 16 CHANNEL ICP® SENSOR SIGNAL CONDITIONER

Revision: -B-
ECN #: ECN-64

| | | | |
|---|---|---|---|
| **PERFORMANCE** | | | |
| Frequency Response (±5% Amplitude) | Hz | 0.125 to 30k | |
| Frequency Response (±5° Phase) | Hz | 0.3 to 10k | |
| Broadband Noise (1 to 27.5k Hz) | μVrms | <100 | |
| Signal Gain (±1%) | V/V | x1 | |
| Sensor Excitation Voltage (±0.5) | VDC | 22 | |
| Constant Current Sensor Excitation | mA | 2 to 10 (Preset @ 4mA) | |
| Ouput Range | Vpk | ±10 | |
| Output Impedance (±10%) | Ω | 1000 | |
| Typical Spectral Noise | $\mu Vrms/Hz^{1/2}$ | 15 @ 1 Hz<br>5 @ 10 Hz<br>0.4 @ 100 Hz<br>0.2 @ 1,000 Hz | |
| **DIGITAL COMMUNICATION** | | | |
| Module Control | Type | Via PCB 440 Series RS-485 Backplane Network | |
| TEDS Sensor Control | Type | IEEE P1451.4 | |
| **ENVIRONMENTAL** | | | |
| Operating Temperature Range | °F (°C) | 32 to 120 (0 to 50) | |
| **ELECTRICAL** | | | |
| Power Consumption | mAmps @ 28VDC<br>mAmps @ 5VDC<br>mAmps @ 15VDC<br>mAmps @ -15VDC | 94<br>165<br>85<br>60 | [1] |
| **MECHANICAL** | | | |
| Input Connector | Type | DB-50 Female | |
| Output Connector | Type | Quad Agilent E1432 Compatible | |
| Size (H x W) | inches (mm) | 5.05 x 1.8 (128,3 x 45,7) | [2] |
| Mass | lb (kg) | 0.69 (0,31) | |

**NOTES:**
[1] All Power Consumption Values Rated At Factory Set 4mA Constant Current Sensor Excitation
[2] Conforms to PCB 440 Series Modular System Form Factor (Single Slot)

**SUPPLIED ACCESSORIES:**
PCB 440 Series Control Software

*All specifications are at room temperature unless otherwise specified.*

ICP® is a registered trademark of PCB Group, Inc.
*In the interest of constant product improvement, specifications may change without notice.*

| Engineer: | Sales: | Approved: | Spec Number: |
|---|---|---|---|
| Date: | Date: | Date: | PS-0010 |

THE MODAL SHOP
TMS
A PCB GROUP CO.
*3149 East Kemper Rd*
*Cincinnati, OH 45241*
*800-860-4867* *Fax (513)458-2172* *sales@modalshop.com*
ENG-F011REV. NR 1/19/Y2K

## Data Acquisition

**High-speed Digitizers**
**VT1432B**

- 8 input ranges including a 100mV range allows use of low sensitivity transducers
- True balanced differential inputs
- On-board user-programmable DSP greatly improves total system performance
- User programmable digital anti-alias filters, with API controllable FIR and Bessel filter
- FIR digital anti-alias filter provides linear phase response for accurate single and cross channel measurements
- Multiple breakout box options with built-in signal conditioning including charge inputs, simplify tests and reduce cost
- Optional arbitrary source or dual input tachometer
- 32 MB on card FIFO memory plus optional local bus allows data records up to 146 GB with the VT2216A VXI data disk, and larger data files to external SCSI disks

**16-CHANNEL 102.4KSA/S 24-BIT DIGITIZER PLUS DSP**

## Agilent E1434A 4-Channel 65kSa/s Arbitrary Source

The Agilent Technologies E1434A four-channel arbitrary source is a C-size, one-slot, VXI module that provides stimulus for mechanical, acoustical, and electrical testing. Its versatile waveform types, performance, and tight integration with the E1432A and E1433A digitizers make it the ideal source for multi-channel measurements. Built-in sine and random noise waveforms save development time and offload computation and data movement chores from the host computer.

A single-channel version of the E1434A is available as an internal option (1D4) to the E1432A and E1433A digitizers.

▼ **More info on this product**

Downloads
Table 1